MTR 01W0000024

98-206

MITRE TECHNICAL REPORT

Analysis of Potential MVDDS Interference to DBS in the 12.2–12.7 GHz Band

RECEIVED

APR 23 2001

FEDERAL COMMUNICATIONS COMMISSION
OFFICE OF THE SECRETARY

April 2001

© 2001 The MITRE Corporation. All Rights Reserved.

MITRE

MTR 01W0000024

MITRE TECHNICAL REPORT

Analysis of Potential MVDDS Interference to DBS in the 12.2–12.7 GHz Band

April 2001

Sponsor: Federal Communications Commission **Project No.:** 1201FCC2-01
Contract No.: FCC-2

This is the copyright work of The MITRE Corporation and was produced for the U.S. Government, the Federal Communications Commission, and is subject to Federal Acquisition Regulation Clause 52.227-14, Rights in Data-General, Alt. III (JUN 1987) and Alt. IV (JUN 1987). No other use other than that granted to the U.S. Government, or to those acting on behalf of the U.S. Government, under that Clause is authorized without the express written permission of The MITRE Corporation. For further information, please contact The MITRE Corporation, Contracts Office, 1820 Dolley Madison Blvd., McLean, VA 22102, (703) 883-6000.

© 2001 The MITRE Corporation. All Rights Reserved.

MITRE

The contents of this document reflect the views of The MITRE Corporation and do not necessarily reflect the views of the Federal Communications Commission. The FCC does not make any warranty or guarantee, expressed or implied, concerning the content or accuracy of these views.

MITRE Project Approval:

D. James Chadwick

Director, Communications, Navigation, and Surveillance Division

Abstract

The frequency band between 12.2 and 12.7 gigahertz (GHz) is allocated to Fixed and Broadcasting-Satellite radio services on a co-primary basis. In the United States, this band is widely used for direct broadcast satellite (DBS) services. Terrestrial radiocommunication services are also permitted, provided that these do not interfere with the satellite services. In 1999, Broadwave USA, a subsidiary of Northpoint Technologies, filed a petition with the Federal Communications Commission (FCC) seeking an authorization to operate terrestrial stations delivering Multichannel Video Distribution and Data Service (MVDDS) in the 12.2–12.7 GHz band. Since that time, numerous concerns have been raised about the extent and impact of potential interference of MVDDS transmissions on the existing DBS service. This report provides a thorough assessment of MVDDS interference into DBS receivers. It is based on a comprehensive analysis that included extensive laboratory and field measurements. The analysis also made use of modeling and simulation techniques to validate published and measured performance results. Special attention was given to the degradation of system availability in the presence of rain losses. The report also discusses possible interference-mitigation approaches, recommends a process for licensing MVDDS transmitters, and addresses key policy issues.

KEYWORDS: Spectrum sharing, MVDDS, DBS, interference, broadcast satellite, EchoStar, DIRECTV, Dish TV, Northpoint, video quality.

Table of Contents

Section	Page
1. Introduction	**1-1**
1.1 Background	1-1
1.2 MITRE's Tasking	1-1
1.3 Approach	1-2
1.3.1 Equipment Measurements Task	1-2
1.3.2 Satellite Receiver Susceptibility Simulation	1-3
1.3.3 Propagation and Rain Modeling	1-3
1.3.4 Interference Predictions	1-3
1.4 Simplifying Assumptions	1-4
2. Interference Mechanisms	**2-1**
2.1 Direct-Coupled Interference	2-2
2.1.1 Assumptions	2-2
2.1.2 Notation	2-2
2.1.3 Algorithm	2-5
2.2 Rain Scatter Interference	2-8
3. Receiver Susceptibility	**3-1**
3.1 Theoretical Analysis and Predictions	3-1
3.1.1 Simulation Model Description	3-1
3.1.2 DBS Transmitter	3-2
3.1.3 Satellite Channel	3-2
3.1.4 DBS Receiver Model	3-3
3.1.5 MVDDS Interferer	3-4
3.1.6 Simulation Validation	3-4
3.1.7 Simulation Results	3-7
3.1.8 EchoStar Simulated Performance	3-7
3.1.9 DirectTV Simulated Performance	3-8
3.1.10 Simulation Summary	3-9
3.1.11 Theoretical Explanation	3-9
3.2 Testing of DBS Set-Top Boxes in the Presence of Northpoint MVDDS Interference	3-12
3.2.1 Overview of Test Configuration for Receiver Degradation Measures	3-12
3.2.2 Standard for Signal Quality Measurement	3-12
3.2.3 DBS Signal Quality 6 in the Presence of Northpoint MVDDS Interference Using 12 GHz RF Output with Simulated Adjacent Channels	3-13
3.3 Selection of Threshold Values from Theoretical and Measured Results	3-15

3.3.1 Threshold for Noise Dominated Cases 3-15
3.3.2 Threshold Values for MVDDS Interference Dominated Cases 3-18

4. Antenna Patterns 4-1
4.1 MVDDS Antenna Patterns 4-1
4.1.1 Small Sectoral Horns 4-2
4.1.2 Large Sectoral Horns 4-4
4.2 DBS Antenna Patterns 4-6
4.2.1 DIRECTV 18-inch Reflector 4-6
4.2.2 DIRECTV 24” x 18” Reflector with Single Feed 4-8
4.2.3 DIRECTV 24 by 18-inch Reflector with Dual Feed 4-10
4.2.4 Fortel 4-13
4.2.5 Boresight Gain Summary 4-15
4.3 Polarization 4-16
4.3.1 The Transmitted Wave 4-16
4.3.2 Receive Antenna Response 4-17
4.3.3 Combined TX and RX 4-17
4.3.4 Polarization Model 4-19

5. Interference Assessment 5-1
5.1 Interference Predictions 5-1
5.1.1 Ranges of Parametric Values Used in the Simulations 5-2
5.1.2 Discussion of Results 5-6
5.2 Criteria for Sharing 5-11
5.2.1 Possible Sharing Criteria 5-11
5.2.2 Minimum *C*/*I* Criteria 5-12
5.2.3 Maximum Interference Level Criteria 5-16

6. Conclusions and Recommendations 6-1
6.1 Feasibility of MVDDS/DBS Bandsharing 6-1
6.2 Potential Interference-Mitigation Techniques 6-1
6.2.1 Selection of MVDDS Operational Parameters 6-2
6.2.2 Possible MVDDS System-Design Changes 6-3
6.2.3 Possible Corrective Measures at DBS Receiver Locations 6-4
6.3 Policy Issues and Recommendations 6-5

List of References RE-1

Appendix A. Testing of DBS Set-Top Boxes in the Presence of Northpoint MVDDS Interference A-1
A.1 Overview of Test Configuration for Receiver Degradation Measures A-1
A.2 Details of the Test Configuration A-2

A.2.1 Audiovisual (A/V) Signal Quality Determination A-3
A.3 Power Measurement for DBS, MVDDS, and Noise Signals A-4
A.3.1 Signal/Noise Power Measurements Using the Agilent 8564EC A-Spectrum Analyzer A-4
A.4 Notes on Interference Testing A-6
A.4.1 Test Objectives A-6
A.4.2 DBS Equipment A-6
A.4.3 MVDDS Equipment A-7
A.4.4 Signal Quality Level 6 A-8
A.4.5 Elimination of Drive Power as Testing Variable A-9
A.4.6 Selection of Programming A-10
A.4.7 Determination of Transponder Transmitting a Particular Television Channel A-11
A.5 DBS A/V Quality 6 in the Presence of Northpoint MVDDS Interference Using 70 MHz IF Output Translated to L Band with Simulated Adjacent Channels A-11
A.5.1 Test Configuration A-11
A.5.2 Test Results A-12
A.6 DBS A/V Quality 6 in the Presence of Northpoint MVDDS Interference Using RF Output with Simulated Adjacent Channels A-14
A.6.1 Test Configuration A-14
A.6.2 Test Results A-16
A.7 DBS A/V Quality 6 in the Presence of Northpoint MVDDS Interference Using RF Output with +7 MHz Offset and Simulated Adjacent Channels A-18
A.7.1 Test Configuration A-18
A.7.2 Test Results A-20
A.8 DBS A/V Quality 6 in the Presence of Northpoint MVDDS Interference Using Open Air RF Transmission A-21
A.8.1 Test Configuration A-21
A.8.2 Test Results A-23
A.8.3 Notes on Open Air Testing A-24
A.9 Summary of Results A-25

Appendix B. Interference Predictions for Selected Scenarios B-1

Glossary GL-1

List of Figures

Figure	Page
2-1. Rain Model Results for Representative DBS Locations	2-2
3-1. Top Level Simulation Model	3-1
3-2. DBS Transmitter Model	3-2
3-3. Satellite Channel Model	3-3
3-4. Satellite Filter Characteristics	3-3
3-5. DBS Receiver Model	3-4
3-6. EchoStar and DIRECTV Theoretical Performance	3-6
3-7. EchoStar Simulation Results with Interference	3-8
3-8. DIRECTV Simulation Results with Interference	3-8
3-9. Probability Density Functions of Received QPSK Signal	3-9
3-10. Probability Density Functions of Noise and Interference	3-11
3-11. QPSK BER as Computed from Numerical Integration of Probability Density Functions	3-11
3-12. Functional Overview of DBS Video Test Configuration	3-12
3-13. Carrier-to-Noise-Plus-Interference Required to Degrade DIRECTV to Signal Quality 6 Vs. Interference-to-Noise Power Ratio; 12 GHz RF Output	3-14
3-14. Carrier-to-Noise-Plus-Interference Required to Degrade Dish TV to Signal Quality 6 Vs. Interference-to-Noise Power Ratio; 12 GHz RF Output	3-15
3-15. Threshold Improvement	3-19
3-16. Laboratory Data and Threshold Model for DIRECTV	3-20
3-17. Laboratory Data and Threshold Model for Dish TV	3-21

3-18. Data and Threshold Model for 7 MHz Offset 3-22

4-1. Small Sectoral Horn on Spherical Scanner 4-2

4-2. Azimuthal Radiation Patterns of Small Sectoral Horns 4-3

4-3. Elevation Radiation Pattern of Northpoint Small Sectoral Horn 4-3

4-4. Large Sectoral Horn on Spherical Scanner 4-4

4-5. Azimuthal Radiation Patterns of Large Sectoral Horns 4-5

4-6. Elevation Radiation Pattern of Large Northpoint Sectoral Horn 4-5

4-7. DIRECTV 18-inch Reflector on Spherical Scanner 4-6

4-8. Azimuthal Radiation Pattern of DIRECTV 18-inch Reflector 4-7

4-9. Elevation Radiation Pattern of DIRECTV 18-inch Reflector 4-7

4-10. RHCP Radiation Pattern of DIRECTV 18-inch Reflector 4-8

4-11. Azimuthal Radiation Pattern of DIRECTV 24-by-18-inch Reflector with Single Feed 4-9

4-12. Elevation Radiation Pattern of DIRECTV 24-by-18-inch Reflector with Single Feed 4-9

4-13. RHCP Radiation Pattern of DIRECTV 24 by 18-inch Reflector with Single Feed 4-10

4-14. DIRECTV 24-by-18-inch Reflector with Dual Feed on Spherical Scanner 4-11

4-15. Azimuth Radiation Pattern of DIRECTV 24-by-18-inch Reflector with Dual Feed 4-11

4-16. Elevation Radiation Pattern of DIRECTV 24-by-18-inch Reflector with Dual Feed 4-12

4-17. RHCP Radiation Pattern of DIRECTV 24-by-18-inch Reflector with Dual Feed 4-13

4-18. Azimuth Radiation Pattern of Fortel Flat Panel Antenna 4-14

4-19. Elevation Radiation Pattern of Fortel Flat Panel Antenna 4-14

4-20. RHCP Radiation Pattern of Fortel Flat Panel Antenna 4-15

4-21. True Gain Product 4-20

4-22. MITRE Model for Gain Product 4-21

4-23. Dominant Mode Model for Gain Product 4-22

5-1. Interference Impact Predictions for Benchmark Case 5-3

5-2. Percentage of Increase of Unavailability for DBS System 5-13

5-3. Increase in Time of Unavailability for DBS System 5-14

5-4. Total Percentage of Time of Unavailability in an Average Year for DBS System 5-15

5-5. Total Unavailability for Washington, DC 5-18

5-6. Total Unavailability in Hours for Washington, DC 5-20

5-7. Increase in Unavailability 5-21

5-8. Relative Increase in Unavailability 5-22

5-9. Total Unavailability, Fargo 5-23

5-10. Unavailability in Hours, Fargo 5-24

5-11. Unavailability Increase, Fargo 5-25

5-12. Relative Increase in Unavailability, Fargo 5-26

5-13. Unavailability (%) for Miami, FL 5-27

5-14. Unavailability (Hours) for Miami, FL 5-28

5-15. Increase in Unavailability (Hours) for Miami, FL 5-29

5-16. Relative Increase in Unavailability (%) for Miami, FL 5-30

5-17. Total Unavailability (%) for QEF in Washington, DC 5-31

5-18. Total Unavailability (Hours) for QEF in Washington, DC 5-32

5-19. Unavailability Increase (Hours) for QEF in Washington, DC 5-33

5-20. Relative Increase in Unavailability (%) for QEF in Washington, DC 5-34

A-1. Functional Overview of DBS Video Test Configuration A-1

A-2. Details of the Test Configuration for DBS Video Testing A-2

A-3. Notional Depiction of DBS Effective Bandwidth A-6

A-4. Set-Top Boxes Used in Receiver Testing A-7

A-5. Northpoint MVDDS Single Channel Transmitter A-8

A-6. Comparison of 2 Different Drive Powers for DIRECTV A-10

A-7. Comparison of 2 Different Drive Powers for Dish TV A-10

A-8. Configuration for Northpoint Transmitter IF Output with Adjacent Channels A-11

A-9. Single Channel MVDDS IF Interference Plus Adjacent Ahannels Generated from Arbitrary Waveform Synthesizers A-12

A-10. Carrier-to-Noise-Plus-Interference Required to Degrade DIRECTV to A/V Quality 6 Vs. Noise-to-Interference Power Ratio; 70 MHz IF A-13

A-11. Carrier-to-Noise-Plus-Interference Required to Degrade Dish TV to A/A Quality 6 Vs. Noise-to-Interference Power Ratio; 70 MHz IF A-14

A-12. Interference Test Configuration Using Northpoint Transmitter with LNB A-15

A-13. Single Channel MVDDS Downcoverted RF Interference Alus Adjacent Channels Generated from Arbitrary Waveform Synthesizers A-16

A-14. Carrier-to-Noise-Plus-Interference Required to Degrade DIRECTV to A/V Quality 6 Vs. Noise-to-Interference Power Ratio; 12 GHz RF Output A-17

A-15. Carrier-to-Noise-Plus-Interference Required to Degrade Dish TV to A/A Quality 6 Vs. Noise-to-Interference Power Ratio; 12 GHz RF Output A-18

A-16. Interference Test Configuration Using Northpoint Transmitter with A7 MHz Offset and LNB Downconverter A-19

A-17. Single Channel MVDDS (with 7 MHz Offset With Aespect to DBS Channelization) Downcoverted RF Interference Plus One Adjacent Channel Generated from Arbitrary Waveform Synthesizer A-20

A-18. Carrier-to-Noise-Plus-Interference Required to Degrade DIRECTV to A/V Quality 6 Vs. Noise-to-Interference Power Ratio; Northpoint MVDDS 12 GHz RF Output, + 7 MHz Offset from DBS Channelization A-21

A-19. Configuration for Open Range Testing of Northpoint AVDDS Interference to DBS Systems A-22

A-20. Single Channel MVDDS Open Range Transmission Aoupled into Spillover Region of a DBS Receive Dish A-23

A-21. Carrier-to-Noise-Plus-Interference Required to Degrade DIRECTV to A/V Quality 6 Vs. Noise-to-Interference Power Ratio; Northpoint MVDDS 12 GHz RF Output, Open Range A-24

List of Tables

Table	Page
3-1. Transmitter Model Parameters	3-2
3-2. Calculation of (C/N) to (Eb/N_0) Conversion Factors	3-5
3-3. Simulation Results Summary	3-9
3-4. DBS Signal Quality Criteria	3-13
3-5. Summary of Eb/No for QEF Performance (dB)	3-17
3-6. Summary of C/N Values (dB)	3-18
3-7. System Model Threshold Improvement Factors	3-23
4-1. Boresight Gain Summary	4-16
5-1. EIRP-to-Threshold Ratios (dBW) and Unavailabilities for VQ6	5-5
5-2. Example of Minimum $[CI_{MV}]_0$ to Satisfy the Requirement $V \leq 10$ (%)	5-16
5-3. Satellite Summary	5-19
A-1. DBS A/V Quality Criteria	A-3
A-2. Spectrum Analyzer Settings	A-4
A-3. Power Occupied Bandwidth of DBS Signal	A-4

Executive Summary

The frequency band between 12.2 and 12.7 gigahertz (GHz) is allocated to the Fixed and Broadcasting-Satellite radio services on a co-primary basis. International Telecommunications Union (ITU) Footnote S5.490 permits the operation of stations that provide "terrestrial radiocommunication services" in the same band, subject to the restriction that they "shall not cause harmful interference to the space services operating in conformity with the broadcasting satellite Plan for Region 2 contained in Appendix S30." CFR 47, Part 100 codifies U.S. regulations for Direct Broadcast Satellite (DBS) service in this band.

In 1999, Broadwave USA, a subsidiary of Northpoint Technologies, Inc., filed a petition with the Federal Communications Commission (FCC) seeking an authorization to operate terrestrial stations delivering Multichannel Video Distribution and Data Service (MVDDS) in the 12.2–12.7 GHz band. Subsequently, two other companies, PDC Broadband Corporation and Satellite Receivers, Ltd. filed similar applications with the FCC.

The FCC issued a Notice of Proposed Rulemaking on 24 November 1998, and a First Report and Order (R&O) and a Further Notice of Proposed Rulemaking (NPRM) as ET Docket 98-206 on 8 December 2000. These documents address the issues associated with permitting MVDDS in the band, and conclude that sharing the band between MVDDS and DBS systems is possible, subject to certain precautions that must be taken to prevent interference to DBS systems.

The FCC's Fiscal Year (FY) 2001 budget authorization contains a requirement that the FCC select an independent engineering firm to perform an analysis to determine whether these two services can share the band without harmful interference to DBS systems. The FCC selected The MITRE Corporation to perform this work. The 19 January 2001 Statement of Work for the project says that "The objective of the tasks is to perform a technical demonstration or analysis of any terrestrial service technology proposed by any entity that has filed an application to provide terrestrial service in the direct broadcast satellite frequency band to determine whether the terrestrial service technology proposed to be provided by that entity will cause harmful interference to any direct broadcast satellite service."

MITRE's effort was divided into tasks in the following areas:

- Equipment measurements
- Satellite receiver simulation
- Propagation and rain-attenuation modeling
- Interference predictions

All measurements for the project were conducted at MITRE's laboratories in Bedford, Massachusetts. MITRE measured the radiation patterns of three DBS antennas and two MVDDS antennas in its anechoic chamber, which has been extensively used to make measurements of critical defense systems for several years. DBS receiver susceptibility to MVDDS interference was measured in the laboratory by connecting an MVDDS transmitter to a DBS receiver through an attenuator, and varying the MVDDS signal level to generate a set of susceptibility curves. The DBS receiver was operating with a live signal from the satellite at the time of these measurements. Limited field measurements of the MVDDS signal level at the terminals of the DBS antenna were also made for a variety of DBS antenna orientations. Appendix A contains a detailed description of measurement procedures.

MITRE's Fort Monmouth, New Jersey laboratory used the Signal Processing Workstation (SPW™) software package to model the DBS/MVDDS interference environment in order to provide an independent verification of the laboratory measurements. Runs were made for the combinations of code rate, interleaver length and Reed-Solomon error correction that are in use by DBS vendors. The simulations produced results that were consistent with those derived from the laboratory and field measurements. Details of the simulation can be found in Section 3.1.

The primary propagation mechanism of interest in this analysis is the attenuation of DBS signals by rain, which is the most significant variable in the computation of downlink availability. The amount of attenuation is a function of rain rate, which varies with geographic location. Section 2 provides a discussion of the rain model used in this analysis.

To quantify the effect that MVDDS systems would have on DBS reception, a model was developed that incorporates the measured and simulated susceptibility data, the rain attenuation statistics, and the equipment parameters of the two systems. This model was run for ten locations throughout the contiguous United States to assess the impact of MVDDS operations on DBS reception. The locations were selected to cover the full range of climatic regions and DBS elevation angles. The model produced plots showing areas where the interference-impact criterion (change in unavailability) was exceeded. From these plots, it was possible to determine the feasibility of MVDDS deployment in the band.

Conclusions

The analysis and testing performed by MITRE and described elsewhere in this report have demonstrated that:

- MVDDS sharing of the 12.2–12.7 GHz band currently reserved for DBS poses a significant interference threat to DBS operation in many realistic operational situations.

- However, a wide variety of mitigation techniques exists that, if properly applied under appropriate circumstances, can greatly reduce, or eliminate, the geographical extent of the regions of potential MVDDS interference impact upon DBS.
- MVDDS/DBS bandsharing appears feasible if and only if suitable mitigation measures are applied. Different combinations of measures are likely to prove "best" for different locales and situations.

The question remains: do the potential costs of applying the necessary mitigatory measures, together with the impact of the residual MVDDS-to-DBS interference that might remain after applying such measures, outweigh the benefits that would accrue from allowing MVDDS to coexist with DBS in this band? To facilitate the FCC's decision, we have assessed the probable effectiveness of available mitigation techniques in reducing the potential impact and geographical extent of MVDDS interference upon DBS operations.

Techniques for preventing or reducing MVDDS interference in DBS receivers fall into three general categories:

- Selection of MVDDS operational parameters
- Possible MVDDS system-design changes
- Corrective measures at DBS receiver locations

Mitigatory techniques in each of these three categories are discussed in detail in Section 6.2. The most important operational parameters that can be adjusted to control interference in existing MVDDS system designs are transmitter power, frequency offset, tower height, elevation tilt, and azimuthal orientation.

- *Keeping MVDDS transmitter power as low as possible* without sacrificing coverage requirements is the most basic and obvious means for controlling interference to DBS.
- The use of a *7-MHz frequency offset* between the MVDDS and DBS carriers has been shown through MITRE's testing to reduce effective interference levels by 1.7 dB, and noticeably shrinks the areas in which DBS receivers are potentially affected by MVDDS interference.
- *Increasing the MVDDS transmitting antenna height* reduces the sizes of the areas susceptible to a given level of interference. However, the simulations of pages B-11 through B-15 indicate that substantial benefits may not accrue unless the tower height is at least 100, or perhaps even 200, meters above the level of the DBS receiving antennas in the surrounding area.
- *Adjusting the elevation tilt* of the MVDDS transmitting antenna may not be particularly effective. Tilting the antenna up 5° reduces the interference-impact area

but shrinks the MVDDS coverage area in roughly the same proportion. This presumably means that more MVDDS towers (creating additional interference-impact areas) would be needed to cover a given geographical region than if the antennas had not been tilted.

- *Pointing the MVDDS transmitting antennas* ***away from*** *the satellites*, rather than toward them as generally envisioned, could have beneficial effects in many situations. These are indicated by the simulation results of pages B-21 and B-23, and by the outputs of several other simulations in which easterly and northerly MVDDS transmitter boresight azimuths were used. When the satellites are generally to the south and their elevation angle is reasonably high, as in Denver, dramatic improvements in interference protection appear possible when the MVDDS transmitting antenna points north. When satellite elevation angles are somewhat lower (as in Seattle) the geometry is somewhat less favorable, but north-pointing seems to yield significant benefits in all locales where it has been simulated. Further testing to validate this concept is recommended.

Potential MVDDS design changes that might reduce the interference impact on DBS downlinks include real-time power control, multiple narrow transmitting-antenna beams, the use of circular polarization, and increasing the size of MVDDS receiving antennas.

- *Real-time power control*, which would reduce MVDDS transmitter power as necessary to protect DBS downlinks from degradation during rain, has sometimes been proposed as a technique for controlling MVDDS-to-DBS interference.

- The use of *multiple MVDDS transmitting-antenna beams*, each having a much narrower azimuthal beamwidth than the existing sectoral horns, might provide much better flexibility than the present antenna design in directing the interference-impact regions away from areas containing DBS subscribers.

- *Circularly polarized MVDDS transmitting antennas*, if they used the same system of alternate senses for adjacent channels that is employed by DBS, might pose a considerably smaller interference threat than the currently planned exclusive use of horizontal polarization, for reasons explained in Section 6.2.2.

- *Larger MVDDS receiving antennas*, recently suggested by Pegasus, would increase their achievable gains and hence the G/T ratios of MVDDS receivers. This in turn would allow an MVDDS system to cover an identical service area with a smaller output power and hence with smaller resultant interference-impact regions.

Corrective measures that can be applied at DBS receiver installations include relocation and retrofitting of existing DBS antennas, the use of alternative antenna designs, and the replacement of older DBS set-top boxes.

- *Relocation of DBS receiving* antennas to put nearby buildings between them and nearby MVDDS interferers, while still leaving desired satellites in view, is a well-known corrective measure that would undoubtedly be effective in many situations.
- The use of absorptive or reflective *clip-on shielding for existing DBS antennas*, to block any direct lines of sight that might exist between their LNBs (antenna feeds) and potentially interfering MVDDS transmitting antennas, is a technique that worked quite well during MITRE's open-air testing.
- *DBS receiving-antenna replacement* is a relatively expensive but potentially effective mitigatory technique. For example, the simulation of page B-30 has shown the potential benefits of using single-feed 24"x18" antennas instead of the more commonly used 18" dishes.
- *Replacement of older DBS set-top boxes* may prove to be a useful mitigation technique if more recent models are more resistant to in-band interference.

Recommendations

If licensing of new MVDDS services is to be successful, while preventing significant interference to DBS services, a number of policy issues need to be considered and resolved. These resolutions naturally lead to a licensing and deployment process for new MVDDS services. In Section 6.3, MITRE recommends a procedure for coordinating MVDDS applications to minimize interference to DBS systems.

A number of additional policy issues should also be considered. These issues and questions are discussed below, along with MITRE's recommendation to the FCC.

- Should future DBS customers be protected and for how long?
  Recommendation: Yes, future DBS customers should be protected for as long as the MVDDS transmitter operates. The MVDDS service provider would need to measure *C/I* values and provide mitigation solutions to these new customers in the interference-mitigation region.
- Test results and analyses have been based on known MVDDS waveforms. Should new waveforms be allowed?
  Recommendation: New waveforms create an unknown vulnerability. MITRE recommends that these not be licensed without further study.
- Should the evaluation of sharing consider any DBS satellite in the geostationary arc, or should only existing U.S. satellites be considered? What about new U.S. satellites?
  Recommendation: DBS receivers operating with new and different satellites could be at risk in unforeseen ways. MITRE recommends that any satellites not addressed in the current report be studied further.

- If changes and improvements are made to any DBS system waveform, how should this impact policy?
  Recommendation: Results in this report are based on specific systems with known parameters. MITRE recommends that any new DBS waveforms be subject to further study.

- Should DBS satellites with weak coverage be protected? If so, how weak can these be and at what level should they be protected? (See examples in Section 5.2.3 and elsewhere.) What is the maximum baseline and degraded unavailability that should be allowed?
  Recommendation: Only DBS satellites with baseline unavailabilities of 100 hours/year or less, when operating without MVDDS interference into a DBS antenna with *G/T* of 11.2 dB/K, should be protected. DBS receivers operating with satellites that do not meet this criterion should not be protected from MVDDS interference when operating with such satellites.

- How should the advent of new DBS antennas affect the policy for MVDDS licensing?
  Recommendation: DBS antennas with *G/T* performance below 11.2 dB/K could seriously degrade DBS availability in rain. If the MVDDS service provider opts to mitigate MVDDS interference with the use of a different antenna, the replacement antenna should have a *G/T* at least as great as that of the original antenna.

- Should other causes of unavailability (besides rain and MVDDS interference) be included in the total budget?
  Recommendation: Other sources of outage should be considered, if they are significant and if their effect is known and documented. Sun-transit outages are an example.

- MVDDS antenna backlobes can interfere with a DBS antenna main beam. This would typically occur close to the MVDDS transmitter, generally north of the antenna. These regions are typically very small. Should very small regions of interference be exempted because of their small size?
  Recommendation: These small regions should not be exempted. All regions of the interference-mitigation region should be considered, regardless of size.

- Should MVDDS mitigation be based solely on customer complaints?
  Recommendation: MITRE believes that DBS customers may not know what is causing a particular outage, or the reason for its duration. Consequently, mitigation should not await DBS customer complaints. MITRE believes that mitigation should be done proactively, regardless of the presence or absence of such complaints.

- How much time should the MVDDS service provider be allowed in order to implement mitigation to the DBS receivers?

Recommendation: To the maximum extent possible, mitigation should be accomplished prior to a license being granted for MVDDS operation.

MITRE believes that with implementation of the licensing process described in Section 6.3 and the other policy recommendations outlined above, spectrum sharing between DBS and MVDDS services in the 12.2–12.7 GHz band is feasible. However, MITRE recognizes that it is the FCC that must ultimately resolve the various policy issues and the approach to licensing new MVDDS services.

Section 1

Introduction

1.1 Background

The frequency band between 12.2 and 12.7 gigahertz (GHz) is allocated to the Fixed and Broadcasting-Satellite radio services on a co-primary basis. The International Rules for assigning frequencies in this band are contained in the International Telecommunications Union (ITU) Radio Regulations, Volume 2, Appendix S30. In Region 2, which includes the United States (U.S.), ITU Footnote S5.490 permits the operation of stations that provide "terrestrial radiocommunication services," subject to the restriction that they "shall not cause harmful interference to the space services operating in conformity with the broadcasting satellite Plan for Region 2 contained in Appendix S30." CFR 47, Part 100 codifies U.S. regulations for Direct Broadcast Satellite (DBS).

In 1999, Broadwave USA, a subsidiary of Northpoint Technologies, Inc., filed a petition with the Federal Communications Commission (FCC) seeking an authorization to operate terrestrial stations delivering Multichannel Video Distribution and Data Service (MVDDS) in the 12.2 to 12.7 GHz band. Subsequently, two other companies, PDC Broadband Corporation and Satellite Receivers, Ltd. filed applications with the FCC to provide MVDDS in this band.

The FCC issued a Notice of Proposed Rulemaking on November 24, 1998, and a First Report and Order (R&O) and a Further Notice of Proposed Rulemaking (NPRM) as ET Docket 98-206 on December 8, 2000. These documents address the issues associated with permitting MVDDS in the band, and conclude that sharing the band between MVDDS and DBS systems is possible, subject to certain precautions that must be taken to prevent interference to DBS systems.

The FCC's Fiscal Year (FY) 2001 budget authorization contains a requirement that the FCC select an independent engineering firm to perform an analysis to determine whether these two services can share the band without any interference to DBS systems. The FCC selected The MITRE Corporation to perform this work.

1.2 MITRE's Tasking

The FCC provided MITRE with the following task description as part of the Statement of Work (FCC, 19 January 2001) for the project:

> **Caveats**. The Contractor shall carry out all the tasks as an independent technical consultant. In particular, the Contractor shall ensure that the personnel performing

the tasks do not have any financial or other material interests in any party to the technical demonstration.

Objective. The objective of the tasks is to perform a technical demonstration or analysis of any terrestrial service technology proposed by any entity that has filed an application to provide terrestrial service in the direct broadcast satellite frequency band to determine whether the terrestrial service technology proposed to be provided by that entity will cause harmful interference to any direct broadcast satellite service.

Specific Tasks. The contractor shall perform the following tasks, as a minimum:

1. Contact the appropriate parties in each of the relevant companies to obtain any technical information, equipment, and/or specifications needed for the demonstration or analysis.
2. Develop a work plan to perform all demonstrations or analyses needed to comply with the statutory requirements.
3. Prepare progress reports on the status of the demonstration or analysis.
4. Prepare a Final Report that fully describes the demonstration or analysis and provides conclusions. The Final Report must include relevant supporting information regarding the data, equipment, specifications and analyses used, discuss how demonstrations or analyses were performed, and provide the basis upon which conclusions were reached. The Final Report will be made available by the FCC for public comment.

1.3 Approach

MITRE assigned a Program Manager to the project, who was responsible for all aspects of the work. Four Technical Leads were assigned to manage tasks in the following areas:

- Equipment Measurements (antennas, MVDDS transmitter, DBS receivers, field measurements)
- Satellite Receiver Simulation (with a simulated MVDDS signal as an interference source)
- Propagation and Rain Attenuation Modeling
- Interference Predictions

1.3.1 Equipment Measurements Task

All measurements for the project were conducted at MITRE's laboratories located in Bedford, MA. MITRE measured the gain, polarization and phase of three DBS antenna and

one MVDDS antenna in its anechoic chamber, which has been extensively used to make measurements of critical defense systems for several years. DBS receiver susceptibility to MVDDS interference was measured in the laboratory by connecting an MVDDS transmitter to a DBS receiver through an attenuator, and varying the MVDDS signal level to generate a set of susceptibility curves. The DBS receiver was operating with a live signal from the satellite at the time of these measurements. Data was taken under two MVDDS frequency conditions: (1) MVDDS transmitter operating at the same frequency as the DBS signal; and (2) the MVDDS transmitter off-tuned by 7 megahertz (MHz). Limited field measurements of the MVDDS signal level at the terminals of the DBS antenna were also made for a variety of DBS antenna orientations. The laboratory and field measurements yielded consistent results. Details of the measurement setups, techniques and results can be found in Sections 3.2–3.3 (DBS receiver) and Section 4 (antennas).

1.3.2 Satellite Receiver Susceptibility Simulation

MITRE's Fort Monmouth, NJ laboratory has a capability to simulate virtually any electronic architecture using the Signal Processing Workstation (SPW™) software package. SPW was configured to model the DBS/MVDDS interference environment in order to provide an independent verification of the laboratory measurements. Runs were made for all combinations of code rate, interleaver length and Reed-Solomon error correction that are in use by DBS vendors. The simulations produced results that were consistent with those derived from the laboratory and field measurements. Details of the simulation can be found in Section 3.1.

1.3.3 Propagation and Rain Modeling

The primary propagation mechanism of interest in this analysis is the attenuation of DBS signals by rain. This is because it is the most significant variable in the computation of link availability. DBS signals become more susceptible to MVDDS interference when it is raining because the desired signal is attenuated. The amount of attenuation is a function of rain rate, which varies with geographic location. Section 2 provides a discussion of the selection of a rain model for this analysis.

1.3.4 Interference Predictions

In order to quantify the effect that MVDDS systems would have on DBS reception, a model was developed that incorporated the measure susceptibility data, the rain attenuation statistics and the equipment parameters of the two systems. This model was run for several locations throughout the 50 States to assess the impact of MVDDS operations on DBS reception. The locations were selected to cover the full range of DBS antenna elevation angles, DBS satellite orbit longitudes and rain regions. The model produced plots showing areas where the DBS interference criterion (change in availability) was exceeded. From

these plots, it was possible to determine the feasibility of MVDDS deployment in the band. Section 5.1 describes the model and interprets the plots, which are contained in Appendix B.

1.4 Simplifying Assumptions

The following parameters or conditions were not considered in MITRE's analysis. They were either determined to have a negligible effect on the results, or they were noted as being specific to a site and thus not analytically tractable for purposes of this study.

Items with negligible effects include:

- DBS sun transit effects
- Rain fading effects on the DBS *uplink*
- DBS transponder intermodulation effects
- DBS outages caused by hardware or software failures
- Interference from systems other than MVDDS and DBS
- Interference from multiple MVDDS systems at the same location (since a given DBS antenna will seldom be susceptible, while pointed in a given direction, to two different MVDDS antennas serving different areas)

Site-specific and analytically intractable items include:

- Rain effects on the MVDDS signal
- Foliage attenuation of MVDDS and DBS signals
- Shadowing of MVDDS and DBS signals by buildings and terrain
- Scattering and reflection of the MVDDS signal from buildings and terrain
- Manufacturing, installation and maintenance tolerances affecting DBS and MVDDS antenna performance (except that a 0.5 decibel [dB] DBS antenna pointing error *was* considered in link calculations)
- Snow, ice, and wind effects on antenna performance
- DBS power reduction resulting from spacecraft system aging

Section 2

Interference Mechanisms

The primary propagation characteristic of interest for the interference analysis is the attenuation of satellite signals due to rain. The reason the rain attenuation is important is because it is the leading variable factor in the computation of link availability. Also, the satellite signals become more susceptible to MVDDS interference during rain because of the reduced signal level caused by the rain fade.

Several possible models could be used to represent the attenuation effects of rain. Of these, the model described in ITU-R P.618-6 was used. This model was chosen because an ITU-R model has been widely used by the proponents in evaluating possible MVDDS interference (DIRECTV, 2000; Combs, 2001). The FCC in its First Report and Order and Further Notice of Proposed Rule Making also used the ITU-R model (FCC, 2001). To achieve the best possible accuracy, the latest version of the model was used, version 6.

For use in this study, the ITU-R P.618-6 rain attenuation model was implemented in MATLAB and integrated with the other analysis algorithms. MATLAB routines were created for both "forward" and "reverse" calculations. In effect, the "forward" method facilitates calculating the rain attenuation for a given unavailability, while the "reverse" method calculates the outage probability for a given rain attenuation. The "forward" calculation is useful for computing the link unavailability for a given link budget, while the "reverse" calculation is useful for generating *C*/*I* contours for specific outage probabilities. The "reverse" calculation is based on a simple sequential search of probabilities, looking for the desired rain attenuation.

Figure 2-1 depicts the rain model results for representative DBS locations used in FCC 00-418 (ITU, 1999b). In this figure, rain attenuation is plotted as a function of the probability that the given attenuation is exceeded.

The method used within the rain models uses the rainfall for an average year. It should be noted that there is often large seasonal and year-to-year variability in the actual rainfall experienced. Further, local rain rate characteristics, if available, may provide for more accurate rain attenuation estimates. Hence, the use of these models provides only a reference for evaluation.

Of lesser importance than the rain attenuation, but also a factor that needs to be considered, is the attenuation of satellite signals due to atmospheric gases. The atmospheric attenuation is approximated by all the proponents in this proceeding as 0.2 dB for DBS signals in the DBS frequency band (DIRECTV, 2000; Combs, 2001), and is computed from (ITU, 1999a). Although there is some variability of the atmospheric attenuation with earth station elevation angle, this is a reasonable approximation.

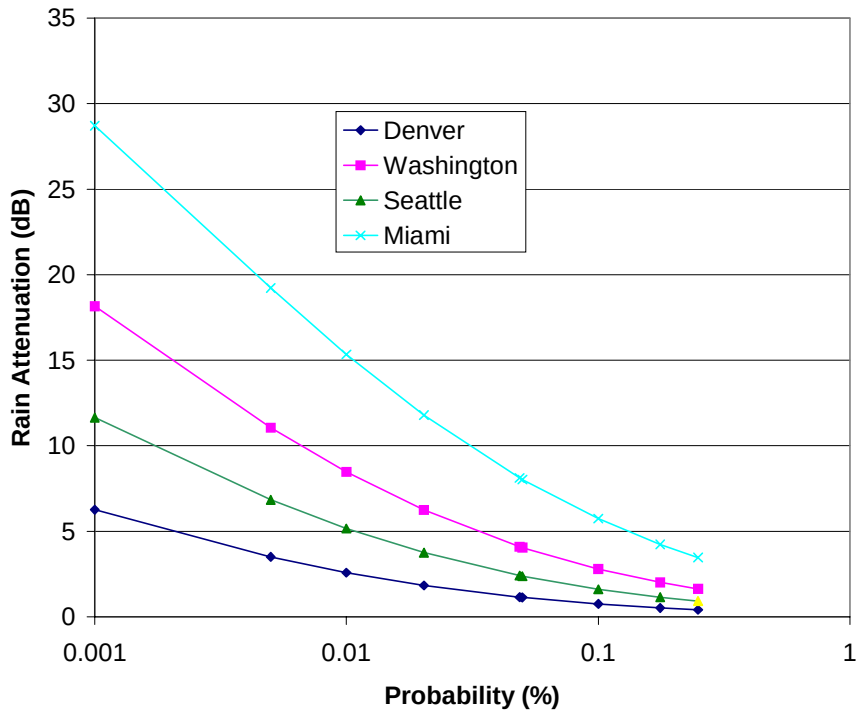

Figure 2-1. Rain Model Results for Representative DBS Locations

2.1 Direct-Coupled Interference

The following procedures provide estimates of the contours of constant DBS-downlink unavailability and related parameters resulting from MVDDS interference.

2.1.1 Assumptions

- Link outages due to DBS uplink rain fading are not considered.
- The calculated *C*/*I* is performed by not fading the MVDDS signal with rain.
- The rain loss (attenuation) exceeded 0.01% of time in an average year, $A_{0.01}$, is modeled according to the ITU-R Recommendation P. 618-6.

2.1.2 Notation

A (dB)	rain loss
A_{eRm} (dB)	effective rain margin in the presence of MVDDS interference
A_{Rm} (dB)	rain margin

$A_{0.01}$ (dB)	rain loss (attenuation) exceeded 0.01% of time in an average year
B_D (deg)	latitude of the DBS rx
CI_B (dB)	C/I for DBS adjacent satellite interference
CI_M (dB)	rainy-sky C/I for MVDDS interference
CI_{MV} (dB)	value of CI_M when I_M effects a change in the rain margin from A_{Rm} to A_{eRm}
CN_A (dB)	C/N for DBS rx when rain loss is equal to A
CN_{AeRm} (dB)	value of CN_A when $A = A_{eRm}$
CN_{ARm} (dB)	value of CN_A when $A = A_{Rm}$
CN_C (dB)	C/N for cross-polarization interference
CN_0 (dB)	C/N for DBS rx when $A = 0$ (i.e., clear-sky)
CNI_{sys} (dB)	C/N plus I of the system
CNI_{Th} (dB)	required C/N plus I operating threshold of DBS rx
CN_U (dB)	C/N for DBS feeder uplink
$E_d = 0.9$	dissipation efficiency of the antenna
e_d (deg)	elevation angle of the DBS rx antenna towards the satellite
$E_i = 0.778$	illumination efficiency of the antenna
$EIRP_{sat}$ (dBW)	effective isotropically radiated power (EIRP) of satellite towards DBS rx
f_{MHz} (MHz)	DBS operating frequency
$F_t = 8$ (dB)	noise figure of tuner with cable attached
$G_{Hr}(\theta_i, \phi_i)$ (dB)	gain of DBS rx antenna horizontal polarization in direction (θ_i, ϕ_i) towards the MVDDS tx
$G_{Ht}(\theta_t, \phi_t)$ (dB)	gain of MVDDS tx antenna horizontal polarization in direction (θ_t, ϕ_t) towards the DBS rx
$G_l = 50$ (dB)	gain of LNB
$G_{Lr}(\theta_r, \phi_r)$ (dB)	gain of DBS rx antenna left hand circular polarization in direction (θ_r, ϕ_r) towards the satellite
$G_{Vr}(\theta_i, \phi_i)$ (dB)	gain of DBS rx antenna vertical polarization in direction (θ_i, ϕ_i) towards the MVDDS tx

G_{Vt} (θ_t, ϕ_t) (dB)	gain of MVDDS tx antenna vertical polarization in direction (θ_t, ϕ_t) towards the DBS rx
I_M (dBW)	DBS received power of MVDDS interference
k (dB)	Boltzman constant
L_a (dB)	DBS rx – satellite path atmospheric absorption
L_{Mfree} (dB)	DBS rx – MVDDS tx path loss (free-space path loss)
L_{pt} (dB)	DBS rx antenna – satellite pointing loss
L_{Sfree} (dB)	DBS rx – satellite path loss (free-space path loss)
mf_{Th} (dB)	MVDDS interference calibration factor related to DBS rx threshold
P_M (dBW)	radiated power of MVDDS tx
p_{Rm} (%)	percentage time of DBS outage due to rain (associated with rain margin A_{Rm})
p_{total} (%)	total percentage time of DBS downlink outage (due to rain plus MVDDS interference)
Q (kilometer [km])	distance between DBS rx and DBS satellite
R_M (km)	distance between MVDDS tx and the geographical grid point under consideration
SAV (%)	system availability
T_A (°K)	system temperature in presence of rain loss A
T_a = 290 (°K)	temperature of atmosphere
T_b = 50 (°K)	temperature of the background (antenna sidelobes)
T_p = 300 (°K)	physical temperature of the antenna
T_r = 260 (°K)	temperature of the rain
T_s = 4 (°K)	noise temperature of sky the antenna is looking at
T_0 (°K)	clear-sky system temperature
T_1 = 80 °K	noise temperature of LNB
U_0 (min)	time of DBS service outage per year in the absence of MVDDS interference
U_{total} (min)	total time of DBS service outage per year in the presence of MVDDS

ΔU (min)	time of DBS service outage increase per year due to the presence of MVDDS
V (%)	percentage increase of DBS downlink outage time due to MVDDS interference
W_D (Hz)	bandwidth of DBS
W_M (Hz)	bandwidth of MVDDS
W_n (Hz)	DBS noise bandwidth
$X7$ (dB)	MVDDS interference 7 MHz offset calibration factor

2.1.3 Algorithm

The rationale of adopting antenna gains in specific polarization senses will be discussed in Section 4.5. The sequence of computation is described in the following:

Step 1: Calculate the DBS satellite to DBS rx (earth station) free space path loss

$$L_{Sfree} = 32.44 + 20 \log (f_{MHz}) + 20 \log Q$$

Step 2: Calculate the system temperature T_A in rain loss of A

(1) Effective noise temperature of the *LNB*

$$T_{eff} = T_1 + T_a \, (10^{F_l/10} - 1) / 10^{G_l/10}$$

(2) Noise temperature after atmospheric attenuation

$$T_{net} = T_s \, 10^{-L_a/10} + (1 - 10^{-L_a/10}) \, T_a$$

(3) Noise temperature after rain attenuation

$$T_{net} = T_{net} \, 10^{-A/10} + (1 - 10^{-A/10}) \, T_r$$

(4) Noise temperature with illumination inefficiencies

$$T_{net} = T_{net} \, E_i + (1 - E_i) \, T_b$$

(5) Noise temperature with dissipation inefficiencies

$$T_{net} = T_{net} \, E_d + (1 - E_d) \, T_p$$

(6) Resulting noise temperature of the system at the input to the LNB

$$T_A = T_{net} + T_{eff} \qquad (°K)$$

Step 3: Calculate the C/N value associated with rain loss A

$$CN_A = EIRP_{sat} - L_{Sfree} - L_{pt} - L_a + [G/T_A] - k - 10 \log W_n - A$$

where $[G/T_A] = G_{Lr} \, (\theta_r, \phi_r) - 10 \log T_A$.

Note: clear-sky corresponds to $A = 0$. The clear-sky CN_0 and clear-sky system temperature T_0 are also determined in this step.

Step 4: System carrier-to-noise plus interference power ratio is a function of A and is evaluated according to the following expression:

$$CNI_{sys}(A) = -10 \log \left\{ 10^{-CN_A/10} + 10^{-CI_B/10} + 10^{-CN_U/10} + 10^{-CN_C/10} + 10^{-(CI_M + mf_{Th} + X7)/10} \right\}$$

here CI_M is set to a large value, say 90 dB, in the absence of MVDDS.

(See Section 3.3.2 for rationale of including mf_{Th} and X7 as calibration factors.)

Step 5: The rain margin A_{Rm} is the value of A that drives the difference between CNI_{sys} (A) and CNI_{Th} to zero, i.e.,

$$CNI_{sys}(A_{Rm}) = CNI_{Th} \quad .$$

Note: A_{Rm} is determined through an iterative process over the value of A within Step 2 and Step 5. The value of CN_{ARm} (i.e., value of CN_A with $A=A_{Rm}$) is also recorded in this step.

Step 6: The p_{Rm} (%) time of an average year associated with the rain margin A_{Rm} is determined from the ITU-R Recommendation P.618-6 via the following expression:

$$A_{Rm} = A_{0.01} \left(\frac{p_{Rm}}{0.01} \right)^{-(0.655 + 0.033 \ln p_{Rm} - 0.045 \ln A_{0.01} - \beta(1 - p_{Rm}) \sin e_d)}$$

where $\beta = 0$ if $p_{Rm} \geq 1(\%)$ or $|B_D| \geq 36°$,

$\beta = -0.005\,(|B_D| - 36°)$ if $p_{Rm} < 1(\%)$ and $|B_D| < 36°$ and $e_d \geq 25°$,

$\beta = -0.005\,(|B_D| - 36°) + 1.8 - 4.25 \sin e_d$ otherwise.

Note: p_{Rm} can also be interpreted as the percentage time of DBS-downlink outage due to rain.

Step 7: Calculate the system availability (%)

$$SAV = 100 - p_{Rm} \qquad (\%).$$

Step 8: Calculate the time of system service outage per average year associated with p_{Rm}:

$$U_0 = 365 * 24 * 60 * \frac{p_{Rm}}{100} \quad \text{minutes.}$$

Step 9: If the MVDDS interference increases the service outage time by V(%) of U_0:

1. The increase of service outage time per average year is:

$$\Delta U = U_0 * \frac{V}{100} \qquad \text{minutes.}$$

2. The total time of service outage per average year is:

$$U_{total} = U_0 * \left(1 + \frac{V}{100}\right) \quad \text{minutes.}$$

3. The total percentage time of service outage thus becomes:

$$p_{total} = \frac{U_{total}}{365 * 24 * 60} * 100 = p_{Rm} * (1 + \frac{V}{100}) \qquad (\%)$$

Step 10: Apply P.618-6 again to determine the "effective rain margin," A_{eRm}, associated with p_{total}

$$A_{eRm} = A_{0.01} \left(\frac{p_{total}}{0.01} \right)^{-(0.655 + 0.033 \ln p_{total} - 0.045 \ln A_{0.01} - \beta(1 - p_{total}) \sin e_d)}$$

Step 11: Determine the value of CN_A when $A = A_{eRm}$

$$CN_{AeRm} = CN_0 - A_{eRm} - 10 \log \left(\frac{T_{AeRm}}{T_0} \right)$$

where T_{AeRm} is the value of T_A with $A = A_{eRm}$.

Step 12: Thus CI_{MV} : the value of carrier-to-MVDDS interference power ratio (CI_M) needed to effect a change of the rain margin from A_{Rm} to A_{eRm} is given by:

$$CI_{MV} = -10 \log \left\{ 10^{-CN_{ARm}/10} - 10^{-CN_{AeRm}/10} \right\} - (mf_{Th} + X7)$$

Step 13: The value of CI_M in general is calculated, at each grid point position, as:

$$CI_M = EIRP_{sat} - L_{Sfree} - L_{pt} - A_{Rm} - L_a + G_{Lr}(\theta_r, \phi_r) - P_M + L_{Mfree} -$$

$$10 \log \left\{ 10^{[G_{Ht}(\theta_t,\varphi_t) + G_{Hr}(\theta_i,\varphi_i)]/10} + 10^{[G_{Vt}(\theta_t,\varphi_t) + G_{Vr}(\theta_i,\varphi_i)]/10} \right\} + \max \left\{ 0, 10 \log \left(\frac{W_M}{W_D} \right) \right\}$$

where $L_{Mfree} = 32.44 + 20 \log (f_{MHz}) + 20 \log R_M$.

Note: The geographical area of interest (neighborhood extending from the MVDDS tx to the possible DBS rx locations) is divided by grids with the grid points identified.

Step 14: Record the calculated values of CI_M on the respective grid point positions.

Step 15: Extract the contour of $CI_M = CI_{MV}$ that associates with the V (%) outage increase due to MVDDS.

Step 16: To obtain contour of constant V, the following calculations are performed:

1. At each grid point position, based on the computed CI_M value, determine the corresponding value of V by reversing the procedure that has been adopted to evaluate CI_{MV}.

2. Record these derived values of V on the respective geographical grid positions.
3. Extract the contour of V equal to the constant value specified.

Step 17: Similar procedures are followed to obtain the contours of constant ΔU and constant U_{total}, respectively.

Step 18: To obtain contour of constant clear-air CI_M, the following calculations are performed:

1. At each grid point position, $(CI_M)_0$ (i.e., the value of CI_M with A_{Rm} set to zero) is calculated based on the expression of CI_M mentioned above.
2. Record the calculated values of $(CI_M)_0$ on the respective grid point positions.
3. Extract the contour of $(CI_M)_0$ equal to the constant value specified.

2.2 Rain Scatter Interference

In this section we consider the effect of rain scatter induced interference. Rain scatter interference occurs when energy that is transmitted from the MVDDS terrestrial terminal into a rain cell is scattered by the rain cell and the scattered energy is received by the DBS earth station. The necessary conditions for this interference to occur are that the main beams of the terrestrial terminal and the DBS earth station antenna patterns must create a common volume in which there is rain.

Preliminary analyses indicate that rain scattered interference is most likely to occur when the DBS antenna has a low look angle and the DBS beam goes through the main beam of the MVDDS transmit pattern at a point relatively close to the MVDDS transmitter. This implies a geometry such that the DBS antenna would be northeast or northwest of the MVDDS transmitter, and pointed nearly at the transmit antenna. It appears that, as long as the MVDDS transmitter has an EIRP no greater than 14 dBm, then regions of interference on the ground will be relatively small. For a 14 dBm EIRP, we expect the region of interference to be only tens of meters in diameter.

Section 3

Receiver Susceptibility

3.1 Theoretical Analysis and Predictions

In this section, the results of the simulation analysis used to quantify the degradation of the Direct Broadcast Satellite (DBS) service due to the Multichannel Video Distribution and Data Service (MVDDS) system are presented. This section is organized as follows: Sections 3.1.1-3.1.5 present an overview and a description of the simulation model and lists the system assumptions. The model validation is presented in Section 3.1.6. Sections 3.1.7-3.1.10 present a summary of the simulation results.

3.1.1 Simulation Model Description

A simulation model of the DIRECTV and EchoStar waveforms was developed using the Signal Processing Workstation (SPW) modeling tool. SPW is a powerful software package used for developing models of advanced waveforms. The high-level simulation model used for this analysis is depicted in Figure 3-1 below. The model consists of four primary blocks, as illustrated in Figure 3-1, namely, the DBS transmitter, a satellite channel, the DBS receiver, and the MVDDS interferer. Each of these four blocks is discussed individually in the following paragraphs. The details of each of these components were extracted from references (European Telecommunication Standard [ETS], 1994; Barker, 31 January 2001; ITU, 2001).

It should also be noted that simulations were not performed at quasi-error free bit error rate (BER) (assumed to be 10^{-10}) due to unreasonably long simulation runtimes. Instead, simulations were performed down to approximately 10^{-6} or 10^{-7}, and the results were extrapolated to compute the BER at 10^{-10}. Given the steepness of the curves, this should provide a relatively accurate estimate.

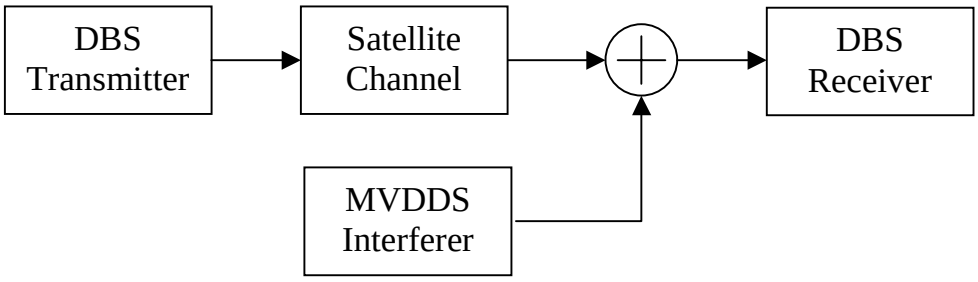

Figure 3-1. Top Level Simulation Model

3.1.2 DBS Transmitter

The DBS transmitter model is depicted in Figure 3-2. The model consists of a standard, concatenated Reed Solomon and convolutional encoder. A convolutional interleaver is inserted between the two encoders to disperse burst errors generated at the output of the Viterbi decoder. The encoded bits are sent into a quadrature phase shift keying (QPSK) modulator followed by a square-root raised cosine filter. The specific details of the code rates, interleaver sizes, and filter bandwidths are highlighted in Table 3-1.

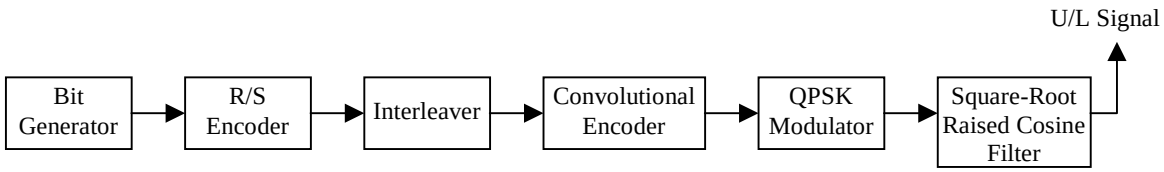

Figure 3-2. DBS Transmitter Model

Table 3-1. Transmitter Model Parameters

Parameter	EchoStar	DIRECTV
Reed Solomon Code Rate	188/204	130/146
Convolutional Code Rate	3/4	6/7
Viterbi Decoder	Soft, 3-bit	Soft, 3-bit
Interleaver	12x17 Convolutional - Forney	146x13 Convolutional - Ramsey Type II
Square Root Raised Cosine Filter Rolloff Rate	0.2	0.2

3.1.3 Satellite Channel

The satellite channel consists of an input multiplexer (IMUX) filter, memoryless nonlinearity, and an output multiplexer (OMUX) filter as depicted in Figure 3-3. The IMUX and OMUX filters are based on the Input and Output Multiplexer data found in reference (ETS, 1994) and are depicted in Figure 3-4. The amplitude modulation (AM)/AM and AM/phase modulation (PM) characteristics are based on a standard SPW satellite traveling wave tube amplifier (TWTA) model and are also depicted in the figure.

Figure 3-3. Satellite Channel Model

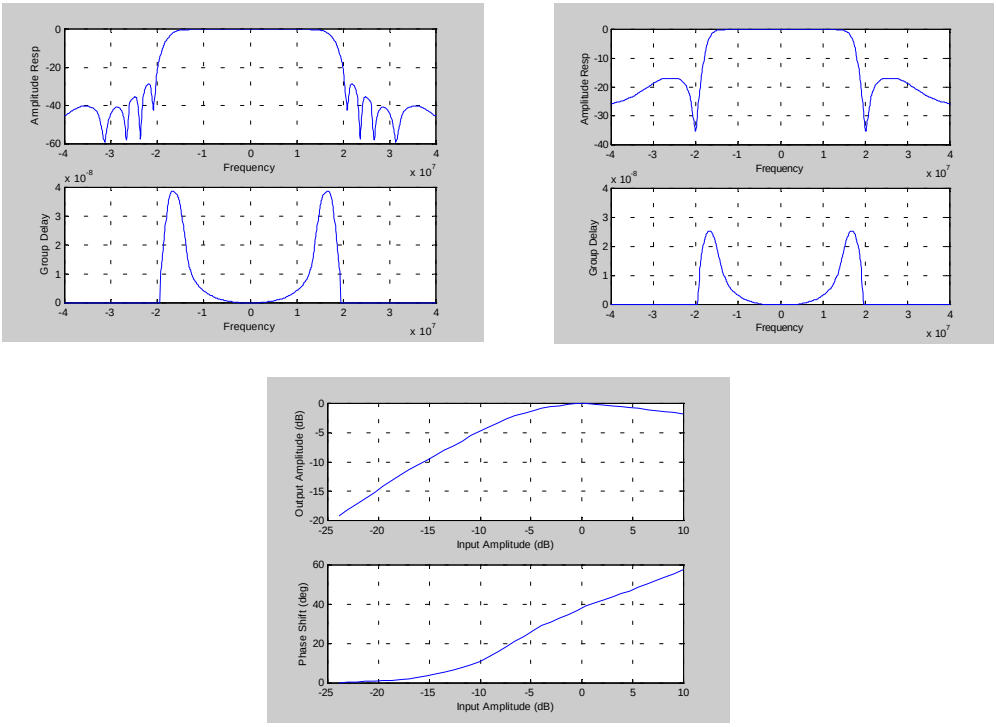

Figure 3-4. Satellite Filter Characteristics

3.1.4 DBS Receiver Model

The model for the DBS receiver is depicted in Figure 3-5. The block diagram shows that the downlink signal is first summed with additive white Gaussian noise to achieve a specified *C*/*N* ratio, followed by a square-root raised cosine receive filter with the identical properties as the transmit filter. The filtered signal is then demodulated through a static phase rotation. The received phase was determined through an offline cross correlation between the received signal and the original signal. Explicit carrier recovery was not modeled since this analysis is intended to assess the steady state performance of the waveform. If a carrier-tracking loop was explicitly included in the model, this would unavoidably inject a component of phase jitter into the received signal. The effects of carrier-tracking phase jitter, as well as other sources of phase jitter are accounted for in a more controlled fashion by injecting a fixed 2

degrees root mean square (RMS) phase noise prior to the demodulator. This phase noise is intended to account for phase noise accumulated in the transmitter, satellite channel, and receiver.

The demodulated signal is then sent through a 3-bit soft decision Viterbi decoder, deinterleaver and a Reed Solomon decoder. Bit error rate monitors were placed at the output of the Viterbi and Reed Solomon decoders to measure the bit error rate at the output of both decoders.

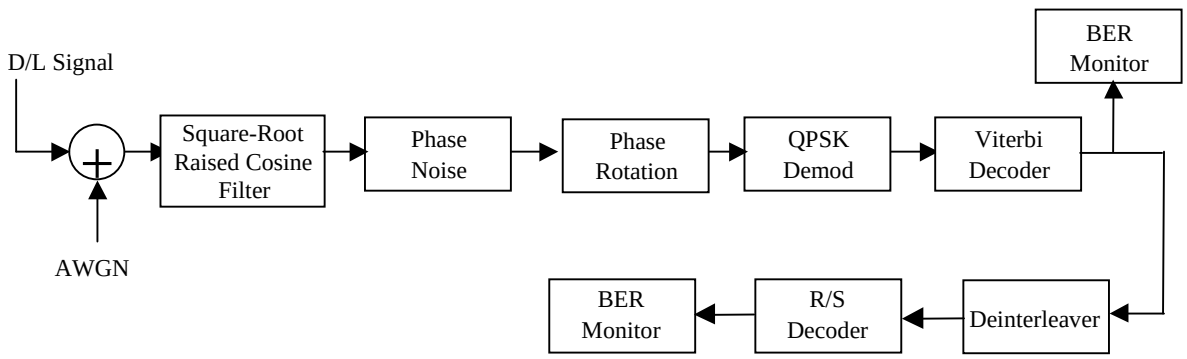

Figure 3-5. DBS Receiver Model

3.1.5 MVDDS Interferer

The MVDDS interfering signal was modeled identically as the DBS waveform described above. In order to improve the simulation run time efficiency, the convolutional encoding and Reed-Solomon encoding in the interfering waveform were excluded. We believe that the coders have no statistical significance on the effects of the interferer. The interfering signal was thus simply modeled as a QPSK modulated signal passed through a square-root raised cosine filter.

3.1.6 Simulation Validation

This section discusses the model validation. Simulation results are compared with theoretical results, laboratory measurements, and ITU documentation of EchoStar (Dish Network) and DIRECTV requirements. However, the results provided by each of these sources were expressed in terms of *C*/*N* ratio where the noise power was computed using different bandwidths. Consequently, a direct comparison of *C*/*N* results is not valid and will lead to incorrect conclusions. To make an accurate comparison, all *C*/*N* values were first converted to E_b/N_0 using the following equation, and the values computed in Table 3-2.

$$\left(\frac{Eb}{N_0}\right)=\left(\frac{C}{N}\right)\left(\frac{Bandwidth}{Uncoded\ Data\ Rate}\right)$$

Table 3-2. Calculation of (C/N) to (Eb/N_0) Conversion Factors

		DIRECTV 6/7	EchoStar 3/4	Comments
1	**Conv Code Rate**	0.857	0.750	
2	**RS Code Rate**	0.890	0.922	130/146 for DIRECTV and 188/204 for EchoStar
3	**Framing Efficiency (Eta)**	0.993	0.928	Portion of the uncoded data rate that is available for information (accounts for bits used to accomplish framing, etc.)
4	**Information Bit Rate (Rb)**	30.320	27.650	See References (Barker, 31 January 2001; ITU, 2000)
5	**Channel Symbol Rate (Rs)**	20.001	21.554	Row 4/ (2*Row 1*Row 2* Row 3)
6	**ITU BW Factor**	1.200	1.280	See References (Barker, 31 January 2001; ITU, 2000)
7	**Uncoded data rate (Rb/Eta)**	30.531	29.795	Data rate at the input of the convolutional coder Row 4/ Row 3
8	**BW (Lab)**	20.000	20.00	Measured
9	**BW (ITU Meas)**	24.002	27.589	Row 5 * Row 6
10	**BW (Sim)**	20.001	21.554	Row 5
11	**Uncoded Data Rate/Lab BW (dB)**	1.837	1.731	Row 7/Row 8
12	**Uncoded Data Rate/ITU Meas BW (dB)**	1.045	0.334	Row 7/Row 9
13	**Uncoded Data Rate/Sim BW (dB)**	1.837	1.406	Row 7/Row 10

Figures 3-6(a) and (b) illustrate the theoretical simulated performance of the EchoStar and DIRECTV modems with and without convolutional coding. The simulated performance of both systems is observed to agree quite closely with the theoretical bounds also depicted within the figures. Figure 3-6(c) depicts the modem performance with concatenated convolutional and Reed Solomon coding. Simulated performance was always well within the theoretical bound and the two agree very well at low BER values, although the curves do diverge at high BER as expected.

Figure 3-6(d) presents the performance of the DBS waveforms through the satellite channel without interference. Reference (ETS, 1994) indicates that the required E_b/N_0 for quasi-error free (QEF) performance, assumed to be a BER of 10^{-10}, for the EchoStar (3/4 rate) and DIRECTV (6/7 rate) modem is 5.5 dB and 6.2 dB respectively. These numbers include 0.8 dB of modem implementation loss, but do not include any losses introduced at the satellite. Reference (ITU, 2000) indicates that the worst case implementation loss from the satellite channel is an additional 1.0 dB. Combining the satellite implementation losses with the modem performance, results in a required E_b/N_0 of 6.5 dB and 7.2 dB respectively for the EchoStar and DIRECTV waveforms. One can see that in both instances, the

simulated performance without interference is within or at this bound (see Figure 3-6(d)). Note that these implementation losses are quoted worst case and that performance variations will occur, so the deviation between worst case and simulated is expected.

The simulation results also compare reasonably well with the minimum required *C*/*N* ratios cited in reference (Barker, 31 January 2001). The document indicates a required *C*/*N* for QEF operation of 6.1 dB and 7.6 dB for the EchoStar and DIRECTV systems respectively. Using the conversion factors computed in Table 3-2 for ITU-defined bandwidths (Row 12), these *C*/*N* requirements equate to an E_b/N_0 of 5.8 dB and 6.6 dB. As can be seen from Figure 3-6(d), the simulation results agree within tenths of a dB for both systems.

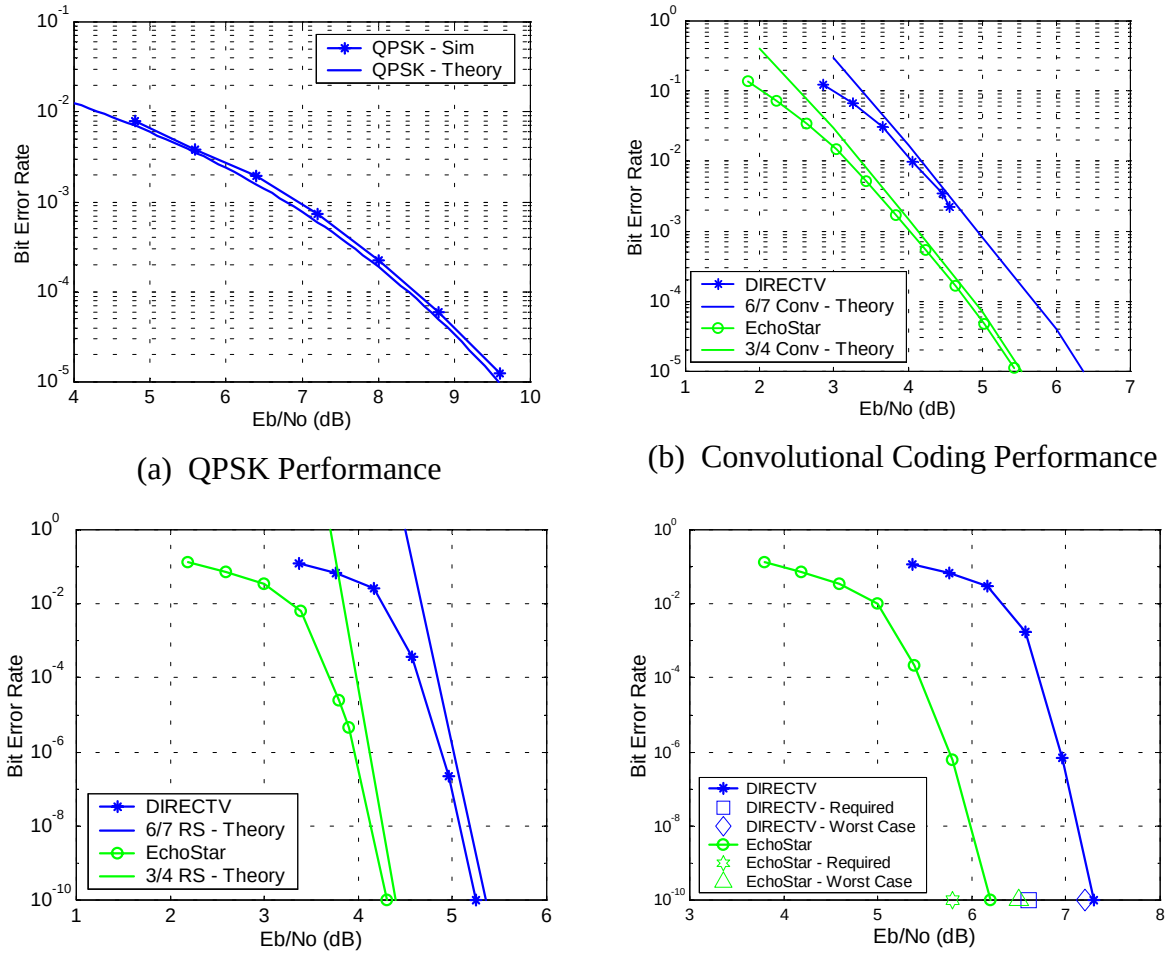

(a) QPSK Performance

(b) Convolutional Coding Performance

(c) Concatenated Coding

(d) Performance through Satellite Channel

Figure 3-6. EchoStar and DIRECTV Theoretical Performance

3.1.7 Simulation Results

Simulations were performed for two different sets of waveform characteristics as indicated in the simulation model section. Each set of simulations showed the same basic trends and conclusions. These results are discussed below.

3.1.8 EchoStar Simulated Performance

The BER results for the EchoStar waveform (3/4 convolutional coding, 188/204 RS coding) in the presence of various levels of interference are shown in Figure 3-7(a). Without interference, the system is able to achieve QEF operation at an E_b/N_0 of approximately 6.2 dB. The same curve was also generated in the presence of three levels of interference. For N/I ratios of 10, 5, and 0 dB, the performance was degraded by 0.4, 1.0, and 2.4 dB respectively.

These same results are also plotted in Figure 3-7(b) against $C/(N+I)$, where the noise power was computed over the simulation bandwidth (channel symbol rate). Again, comparing these C/N results with other sources that assume different bandwidth definitions is invalid. One should use the conversion factors shown in Table 3-2 to convert C/N to E_b/N_0 before attempting any such comparison. Note that the required $C/(N+I)$ is about 0.5 dB less when the noise and interference powers are equal. To accommodate this, the $C/(N+I)$ threshold value should be thought of as a function of the N/I ratio. See Section 3.3 for a further discussion of the threshold used in the system analysis tool.

The results indicate that performance improves as the ratio of N/I is decreased. A common assumption in many interference link budgets is that noise and interference are additive; that is, they are equally detrimental to system performance. If that were true, the BER would depend only on the total $(N+I)$ power, and the BER versus $C/(N+I)$ curves would be identical regardless of N/I ratio. Instead, it is observed that the performance curves improve as the N/I ratio decreased. For example, assume that the signal power is 1 watt and the $(N+I)$ power is 0.25 watts. The resulting BER with noise power of 0.25 watts and interference power of 0 watts ($C/(N+I)$ = 6 dB) is worse than the BER with noise power of 0.125 watts and interference power of 0.125 watts ($C/(N+I)$ = 6 dB). The conclusion is that for these signal, noise, and interference characteristics, the noise is more detrimental to system performance than interference. It is thus actually conservative to replace the interferer by an Additive White Gaussian Noise (AWGN) source of equal average power in system performance calculations. This basic conclusion was also verified with theoretical calculations; see the theoretical explanation provided in Section 3.1.11.

It should also be noted that additional simulations were performed to examine the impact of phase noise and traveling wave tube (TWT) backoff since the specific values for these parameters were unknown. Simulation results were not sensitive to these factors, and the trends/conclusions discussed above remain valid.

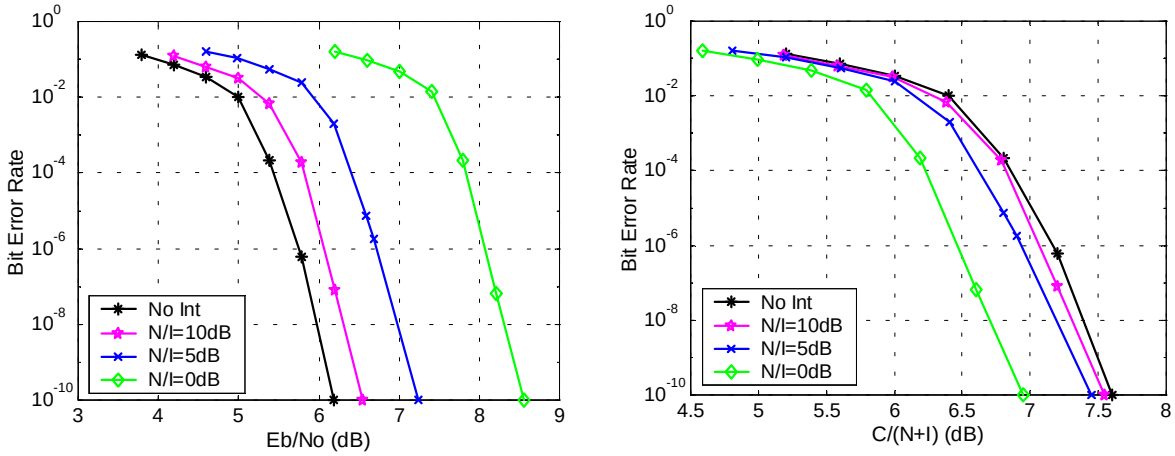

(a) (b)

Figure 3-7. EchoStar Simulation Results with Interference

3.1.9 DirectTV Simulated Performance

The trends for the DIRECTV simulation performance are similar to those shown for EchoStar. The common conclusion is that interference is less detrimental than noise. The results of the DIRECTV simulations are shown in Figure 3-8 below. As before, $C/(N+I)$ and E_b/N_0 are related by the conversion factors shown in Table 3-2. Again, we see that the required $C/(N+I)$ is about 0.8 dB lower for an N/I of 0 dB.

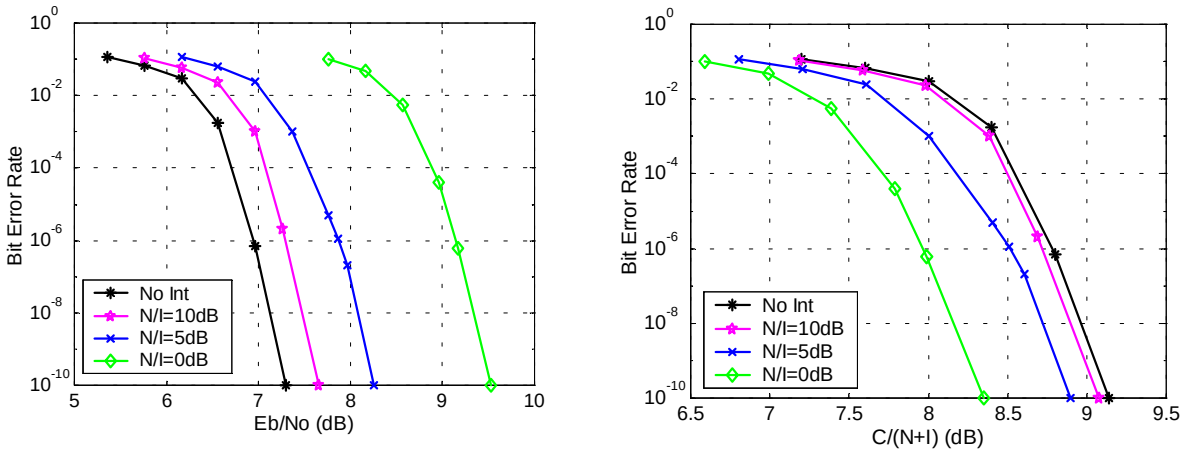

(a) (b)

Figure 3-8. DIRECTV Simulation Results with Interference

3.1.10 Simulation Summary

A summary of the results for the EchoStar and DIRECTV is provided in Table 3-3. The table lists the $C/(N+I)$ required to obtain QEF performance at the output of the Reed Solomon decoder for various levels of N/I (noise power is computed over the symbol rate bandwidth). The table indicates an 0.65 dB (EchoStar) and 0.79 dB (DIRECTV) improvement in the required $C/(N+I)$ as the N/I is decreased from ∞ to 0 dB.

Table 3-3. Simulation Results Summary

N/I	**Required *C/(N+I)* for QEF**	
	EchoStar	DIRECTV
∞	7.60 dB	9.14 dB
10	7.55 dB	9.08 dB
5	7.45 dB	8.90 dB
0	6.95 dB	8.35 dB

3.1.11 Theoretical Explanation

The results obtained with the waveform simulations described above can also be explained with theoretical calculations. Assume a QPSK signal in the presence of AWGN where the 00 symbol has been transmitted. The probability density function of the received signal is a two dimensional Gaussian distribution centered around the intended 00 symbol (see Figure 3-9). The relative width, or variance, of this distribution is determined by the C/N ratio.

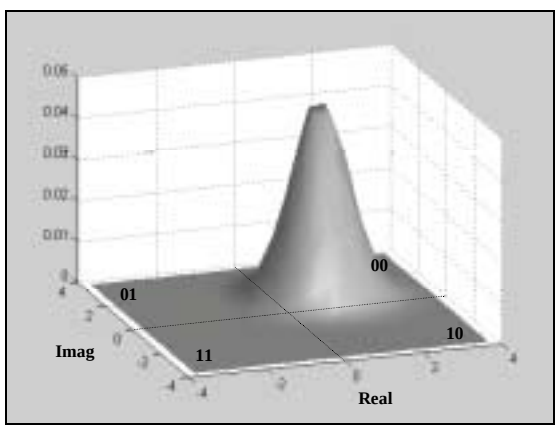

Figure 3-9. Probability Density Functions of Received QPSK Signal

To calculate BER, one would simply calculate the probability that the noise has pushed the received signal into an incorrect quadrant. This is accomplished by integrating the probability density function over the 01, 10, and 11 quadrants:

$$BER = \iint_{Quad01} f_{xy}\, dx\, dy + \iint_{Quad10} f_{xy}\, dx\, dy + 2 \iint_{Quad11} f_{xy}\, dx\, dy$$

NOTE: Because the symbol 00 was transmitted in this example, one bit error would be incurred if the received symbol were a 01 or 10, and two bit errors would be incurred if the received symbol were a 11. Hence, the coefficient for the third integral is a two.

Since interference has different statistical properties than AWGN, this integration will yield different results for noise and interference scenarios. Take the example shown in Figure 3-10. The density functions are compared for noise only (noise power = P_T, interference power = 0), interference only (noise power = 0, interference power = P_T), and half noise/half interference (noise power = $P_T/2$, interference power = $P_T/2$). In all three cases, the total power of noise + interference remains constant. However, the statistical properties of the degrading signal have been altered significantly. In fact, the QPSK interference (which has an equal probability of being in one of four different states) tends to concentrate the density function. Consequently, the probability of obtaining a high enough value to cause an error decreases. This is shown in Figure 3-11, which illustrates the BER obtained by integrating the density functions in Figure 3-10.

Note that the noise only BER is 10^{-5} at a S/N ratio of 12.6 dB (Eb/N_0 of 9.6 dB) as expected. It is also clear that the noise only scenario demonstrates worse performance than the half noise/half interference scenario (assuming total noise + interference power remains constant). That is, noise is more detrimental to system performance than this type of interference. This corroborates the trends that were observed in the waveform simulations, although the degree of improvement will depend on many other factors such as satellite distortions, coding, etc.

Probability density function
(Noise Only)

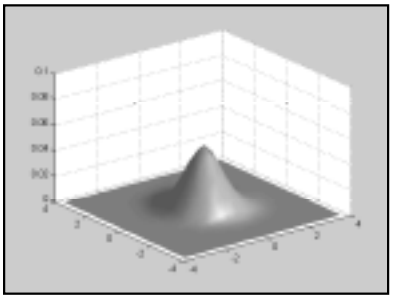

Probability density function
(Noise = Interference)

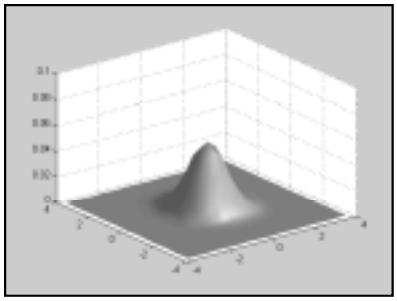

Probability density function
(Interference Only)

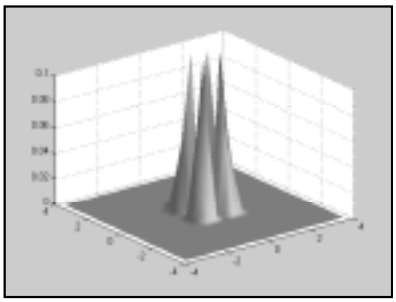

Cross-section of probability density functions

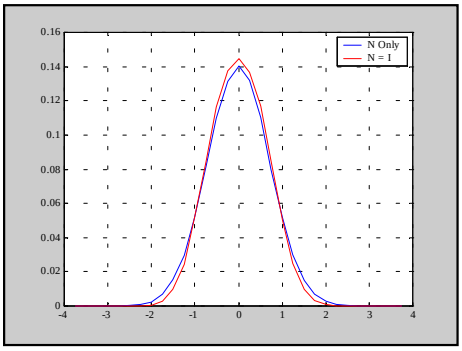

It is extremely subtle but when interference is mixed with noise, the interference has the impact of condensing the probability density function. Hence, the probability of a high enough value to cause an error decreases.

Figure 3-10. Probability Density Functions of Noise and Interference

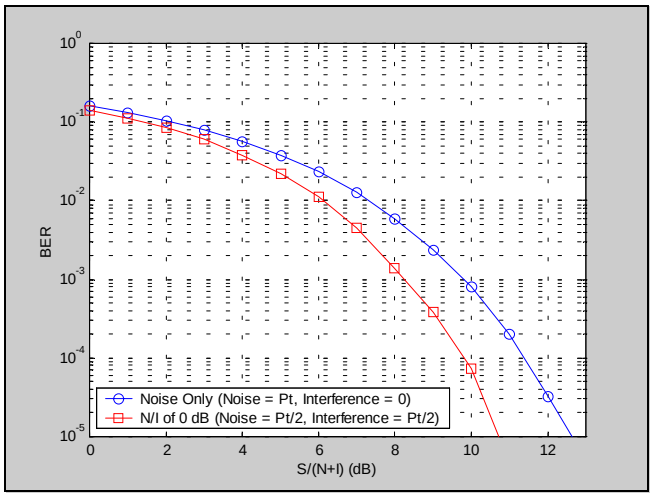

Figure 3-11. QPSK BER as Computed from Numerical Integration of Probability Density Functions

3.2 Testing of DBS Set-Top Boxes in the Presence of Northpoint MVDDS Interference

This subsection provides an overview of the laboratory tests performed to support the unavailability analysis. Detailed configurations and techniques are given in Appendix A.

3.2.1 Overview of Test Configuration for Receiver Degradation Measures

A simplified view of the test configuration used to study the impact of MVDDS interference on DBS systems is shown in Figure 3-12. In general, a closed DBS link is perturbed via the insertion of additional interference signals.

Signal quality is monitored through observation of the picture and sound quality as observed through a television connected to a DBS set-top box. Signal quality, C/(N+I) or carrier to noise plus interference ratio is calculated from data measured with an Agilent 8564E spectrum analyzer. A SAT9250 DBS installer's tool was also used to measure C/N during interference experimentation.

In order to have independent control of both the carrier-to-noise-plus-interference, and the interference-to-noise power ratios, addition of both Gaussian noise and Northpoint interference was necessary.

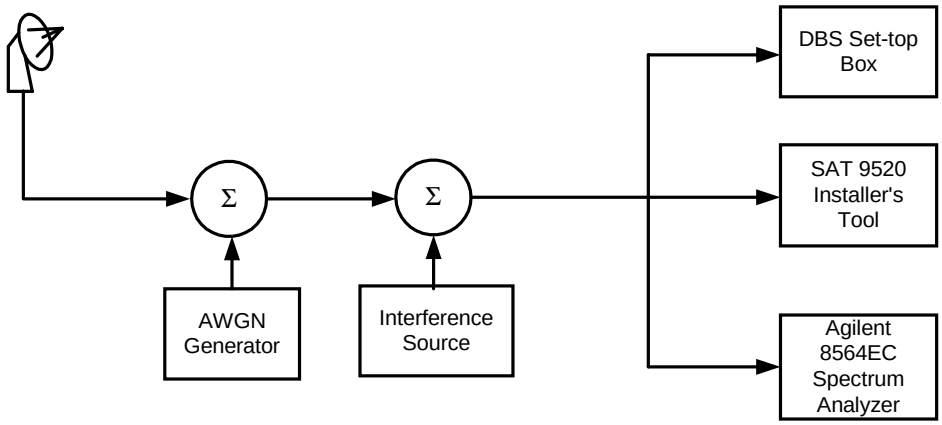

Figure 3-12. Functional Overview of DBS Video Test Configuration

3.2.2 Standard for Signal Quality Measurement

Due to the nature of the encoded DBS signal, video and audio degradation occurs over a very narrow region of carrier-to-noise plus interference, $C/(N+I)$, prior to complete loss of signal lock. Degradation in signal quality originating from a digital broadcast is unlike that from an analog broadcast, where picture quality is very subjective. Instead, degradation is quite noticeable, and occurs in burst fashion when uncorrected bit errors are presented to the Motion Picture Experts Group (MPEG) decoder. For low bit error rates, errors are corrected

by the error correction coding inherent in the system. Video and audio impairments occur when the number of bit errors exceeds what is correctable by the concatenated code. Video impairments manifest as sudden pixelization in the image. Audio errors manifest as a sudden pop or chirp sound. In general, the rate of audio and video error occurrences increases as the $C/(N+I)$ ratio degrades. A video/audio quality criteria was established for the purpose of assigning a quality measure. See Table 3-3.

Table 3-4. DBS Signal Quality Criteria

Assigned Quality Level (9=Error Free)	Video/audio characteristics (average)
9	Perfect video/audio
8	1 video/audio error per 30 minutes
7	< 1 error per minute, but > than 1 per 30 minutes
6	< 1 error per 15 seconds, but > 1 error per minute
5	> 1 error per 15 seconds
4	Freeze framing and pixelization occurring; audio chirping and momentary blanking
3	Mostly pixelized, mostly frozen, mostly audio blanked
2	Occasional video acquisition, no audio
1	Loss of lock, no signal acquisition

3.2.3 DBS Signal Quality 6 in the Presence of Northpoint MVDDS Interference Using 12 GHz RF Output with Simulated Adjacent Channels

The data used to support the analytic runs for assessment of increase in DBS unavailability were taken using the single channel MVDDS transmitter supplied by Northpoint. The center frequency of output of this transmitter is selectable to any frequency within the 12.2-12.7 GHz band. Simulated adjacent channels were generated via arbitrary waveform synthesizers and mixed with the down-converted L-Band signal at an appropriate frequency spacing.

Data is recorded at various noise-to-interference levels, +infinity (noise only) +10 dB, +3 dB, 0 dB, -3 dB, and –10 dB, and –infinity (interference only). Results for +infinity and –infinity are plotted on the +30 and –30 dB points, respectively. While holding N/I constant, the total power of the noise and interference combination was raised until the quality of the signal was reduced to Signal Quality 6, one video or audio error occurring with an average arrival rate between 15 seconds and 1 minute.

The results are shown for DIRECTV and Dish TV in Figure 3-13 and Figure 3-14, respectively.

A common trend that was observed throughout the testing of the Northpoint MVDDS transmitter's impact to the DBS receiver is the relative resilience to the constant envelope QPSK MVDDS signal as compared to Gaussian noise.

Note as well the close agreement between the SAT9250 measurement in the noise-only case and spectrum analyzer measurements. Insufficient information is available about the SAT9250 to provide an accurate scaling factor that would account for differences in measurement bandwidth between the spectrum analyzer and the SAT9250.

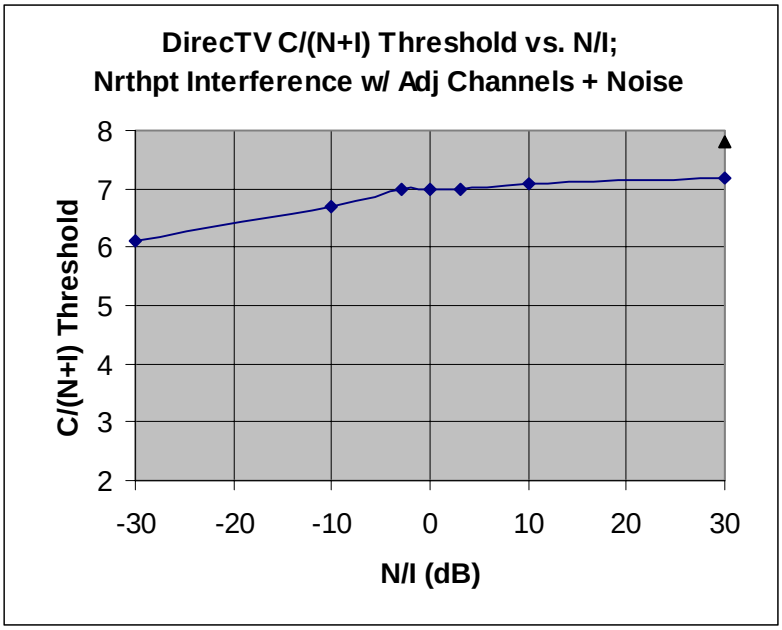

Figure 3-13. Carrier-to-Noise-Plus-Interference Required to Degrade DIRECTV to Signal Quality 6 Vs. Interference-to-Noise Power Ratio; 12 GHz RF Output

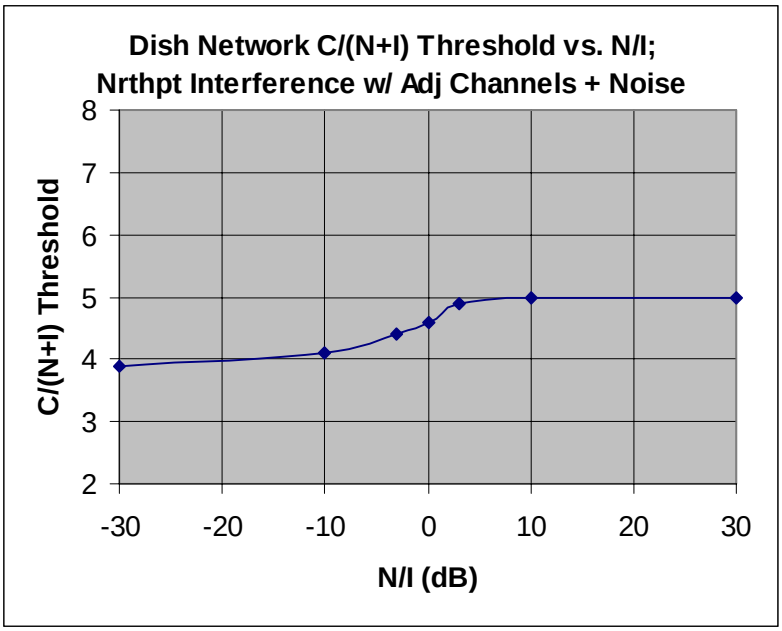

Figure 3-14. Carrier-to-Noise-Plus-Interference Required to Degrade Dish TV to Signal Quality 6 Vs. Interference-to-Noise Power Ratio; 12 GHz RF Output

3.3 Selection of Threshold Values from Theoretical and Measured Results

There are many things that need to be taken into account when making comparisons among the simulation, measured, and published threshold performance values. These include:

- Different measures of performance
- Different definitions of measurement bandwidth
- Different data rates to consider for any given system in a given mode

The following Sections provide rationale for threshold values chosen for model runs, including, where appropriate, references to support the numbers quoted. In Section 3.3.1 we discuss the values for noise dominated cases whereas in Section 3.3.2 we discuss our approach for cases dominated by MVDDS interference.

3.3.1 Threshold for Noise Dominated Cases

3.3.1.1 DishTV (EchoStar) Rate 3/4

Data for the threshold value comes from several sources including laboratory measurements, simulation-based analysis, and published documentation. Published data in

this case comes from the answers to the first set of questions posed by MITRE to the DBS proponents (Barker, 31 January 2001). This submission includes a copy of ITU-R document 6/35-E, dated 21 September 2000, which comes from source document ITU-R 6S/TEMP/1. The ITU document gives example rates in Table 1 (Barker, 31 January 2001). From these we can deduce that there is a 0.928 framing efficiency. The remaining 7.2% of the transmission is used for synchronization and other overhead needed for the satellite transmission to be successfully received. Notes to Table 2 in the ITU document (Barker, 31 January 2001) say that a bandwidth (BW) to symbol rate (Rs) ratio of 1.28 has been adopted. Ratios of data rates, but not exact data rates, can be deduced from Table 1 of the ITU document (Barker, 31 January 2001).

Page 3 of the answers to the first set of questions (Barker, 31 January 2001) shows that the effective data rate is 27.65 Mb/s. This is also called the information rate. From this and the rate ratios deduced from Table 1 of the ITU document, we get:

- Rs = 21.55 Mb/s = 27.65/(2*0.75*(188/204)*0.928)
- Rb = 27.65 Mb/s
- Total signal BW = 25.86 MHz = 1.2*Rs
- ITU measurement BW for C/N = 27.59 MHz = 1.28*Rs

In order to make comparisons to simulation results, we should not penalize the system for the framing inefficiency. So, for purposes of comparison with simulation and theoretical results, we should retain the Rb above, but multiply all other rates and bandwidths by 0.928. Doing so, and then evaluating the ratio of Rb to the new measurement bandwidth, we get a factor of 0.33 dB. ITU C/N values should be reduced by this amount to get a "comparison ready" E_b/N_0 value (see Table 3-2).

The ITU document lists a C/N of 6.8 dB (Barker, 31 January 2001). However, pages 3 and 5 of the answers to the first set of questions say 6.1 dB (Barker, 31 January 2001). These values imply an E_b/N_0 of between 5.8 and 6.5 dB. A value of 6.4 dB was chosen for the system analysis model. This is within the range of values stated, but is slightly conservative. To summarize, the E_b/N_0 values for QEF performance are provided in Table 3-5 below. The DIRECTV system will be discussed in Section 3.4.1.2.

To obtain a C/N value for the system analysis, we must convert from the E_b/N_0 values to a C/N measured in the appropriate bandwidth. Here we use 20 MHz as the noise bandwidth. For a system operating at the information rate of 27.65 Mb/s, with no framing inefficiencies, and an E_b/N_0 performance of 6.4 dB, its C/N value measured in a 20 MHz bandwidth would be 7.8 dB. Correcting for the framing inefficiencies, we get 8.1 dB C/N in a 20 MHz bandwidth for the real system with QEF performance.

Table 3-5. Summary of Eb/No for QEF Performance (dB)

	EchoStar 3/4	DIRECTV 6/7
ETS Standard (ETS, 1994)	6.5	
ITU document (Barker, 31 January 2001)	5.8	6.6
DBS Answers (Barker, 31 January 2001)	6.5	6.6
Simulation Results	6.2	7.2
Value Used in System Analysis	6.4	6.6

Now we turn from published and simulated results to laboratory results. Laboratory measurements were based on a 20 MHz bandwidth for noise power measurements. The signal was measured in the same 20 MHz bandwidth, but scaled by 0.2 dB to account for the tails of the spectrum. Graphical depiction of the test results will be presented in Section 3.3.2. Averaging the lab test results for the intermediate frequency (IF) measurement case (but leaving out the Northpoint dominated case) we get an average *C*/*N* of 5.7 dB for video quality of 6. The 12 GHz tests produce a *C*/*N* value of about 5.0 dB in noise for video quality of 6 or 7. Compromising between theses two values, we pick a value closer to the results of the IF tests because it represents more data points. In summary we use the following *C*/*N* threshold values for the EchoStar system:

- Quasi Error Free: *C*/*N* = 8.1 dB
- Video Quality 6: *C*/*N* = 5.5 dB

Note that the above values are based on noise measured in a 20 MHz bandwidth, not 24 MHz. Both cases above will be run in the system analysis model.

3.3.1.2 DIRECTV Rate 6/7

Using a similar approach to the one for EchoStar, we find that the framing efficiency is 0.9931. Rates and bandwidths are:

- *Rs* = 20 Mb/s
- *Rb* = 30.32 Mb/s
- Total signal BW = 24 MHz
- ITU measurement BW for *C*/*N* = 24 MHz

The ITU document and the answers to the first set of questions indicate a C/N of 7.6 dB (Barker, 31 January 2001). This converts to a "comparison read" E_b/N_0 value of 6.6 dB. Scaling to obtain a C/N in a 20 MHz bandwidth, we get 8.4 dB. Turning to the laboratory measurements, we get an average of 7.5 dB for the IF data set. The 12 GHz measurements yield about 7.1 dB in noise. So, to summarize, we use the following values for the DIRECTV system:

- Quasi Error Free: C/N = 8.4 dB
- Video Quality 6: C/N = 7.3 dB

Again, these C/N values are based on noise measured in a 20 MHz bandwidth. A similar analysis produced a set of values for video quality 1. These C/N values are shown below in Table 3-6, along with the C/N values discussed above.

Table 3-6. Summary of *C/N* Values (dB)

	EchoStar 3/4	**DIRECTV 6/7**
QEF	8.1	8.4
Video Quality 6	5.5	7.3
Video Quality 1	5.1	6.1

3.3.2 Threshold Values for MVDDS Interference Dominated Cases

One interesting result of the laboratory tests, is that the DBS systems seem to be less susceptible to this type of interference than to noise of the same power. This is important, since it implies that the MVDDS signal can be stronger than might otherwise be expected, for the same interference impact. From the data, it appears that the required $C/(N+I)$ ratio is a weak function of the I/N ratio. Differences of about 1 dB exist over the range of I/N values. Figure 3-15 provides an example of this. As seen in the figure, cases where the interference dominates require a lower $C/(N+I)$ ratio for video quality 6. In this figure, the two curves represent two different measurement sets, one with a Northpoint signal coupled at IF, and one with the Northpoint signal coupled through the low noise block converter (LNB).

This apparent improvement in required $C/(N+I)$ is due to the fact that the interfering signal does not have the same amplitude distribution as the Gaussian noise. See Section 3.1.11 for a detailed explanation of this phenomenon.

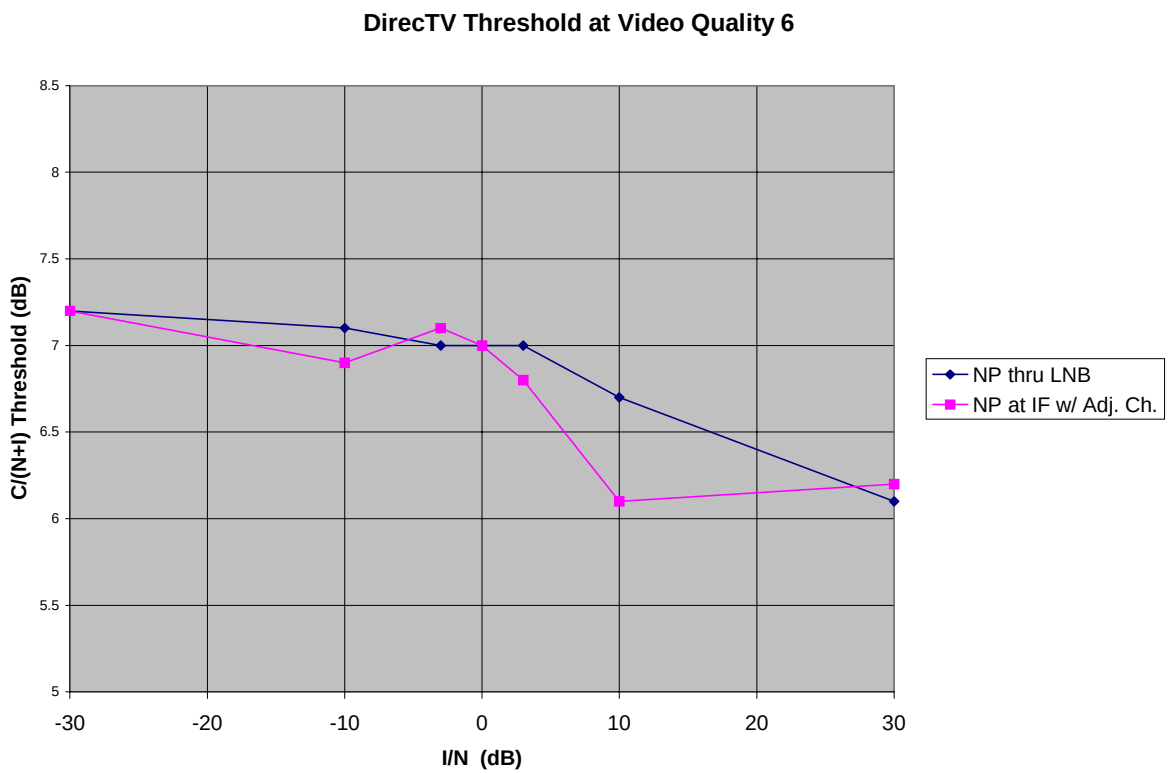

Figure 3-15. Threshold Improvement

To account for the apparent improvement in threshold value, a model for the threshold was developed. This model is as follows:

$$\gamma(x) = \gamma_0 \frac{1+(x/\mu)}{1+x} \tag{1}$$

Where:

$\gamma(x)$= the threshold $C/(N+I)$ value as a function of x, for a particular video quality

x = the I/N ratio

γ_0 = the nominal C/N value for noise dominated cases

μ = a factor that accounts for reduced susceptibility of the DBS system to interference

This model provides a way to embody the results of the tests and a means to interpolate among values of I/N. The model is plotted below along with data from numerous laboratory tests. Figure 3-16 shows the results for DIRECTV and Figure 3-17 shows the results for Dish TV (EchoStar). In both cases, the model uses a μ value that corresponds to a 1.0 dB

reduction in required $C/(N+I)$ for interference dominated cases. In Figure 3-17, note that the data from the arbitrary waveform synthesizer (AWS) seems less reliable at large values of I/N. Hence, we ignored these results in selecting μ.

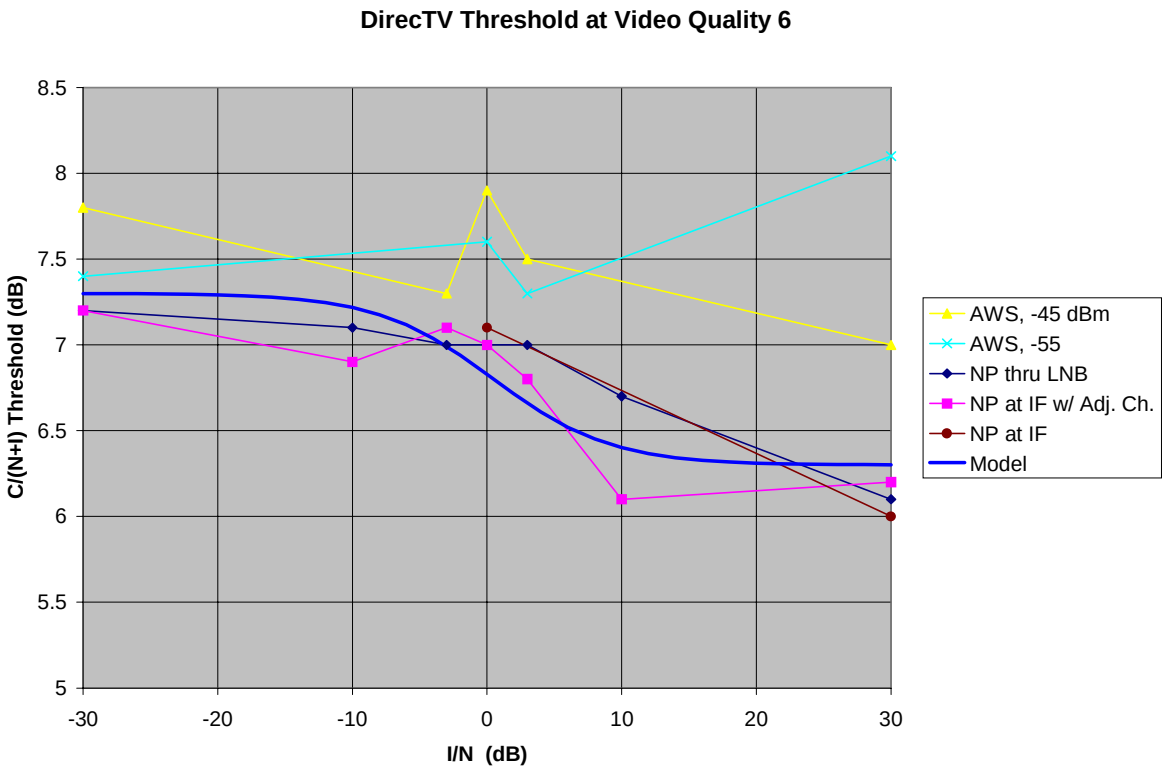

Figure 3-16. Laboratory Data and Threshold Model for DIRECTV

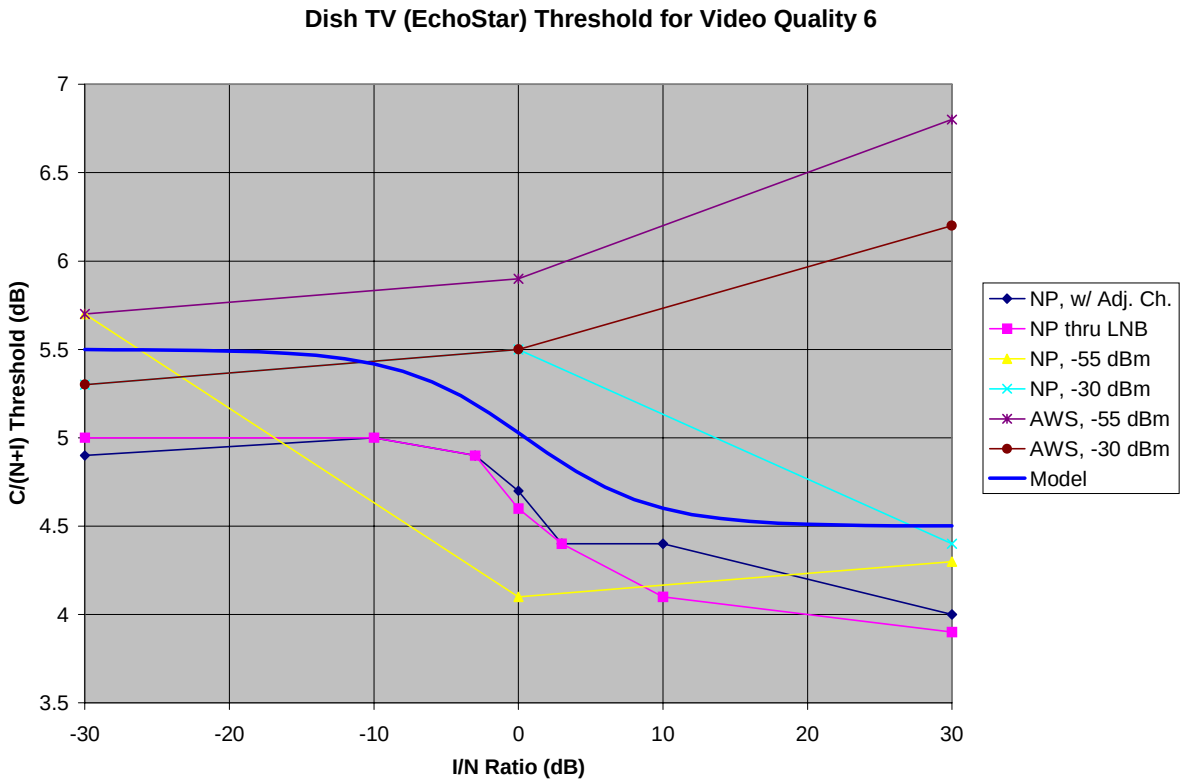

Figure 3-17. Laboratory Data and Threshold Model for Dish TV

The above model is applied to the analysis of allowable interference levels in the following way. In order for the link to operate at video quality, the following inequality must be satisfied:

$$\gamma(x) \leq \frac{C(A)}{I + N(A)} \tag{2}$$

Where:

$\gamma(x)$= the threshold value, as in equation 1 above

$C(A)$ = the received carrier power, as a function of the rain attenuation, A

A = the rain attenuation

I = the interference power

$N(A)$ = the noise power, as a function of the rain attenuation, A

For a given interference power, equation 2 could be solved for the rain attenuation, A. This rain attenuation corresponds to a particular unavailability for the DBS system. Combining equations 1 and 2 and using x = *I*/*N*, after some algebra, we get:

$$\gamma_0 \leq \frac{C(A)}{(I/\mu)+N(A)} \tag{3}$$

This expression can also be solved for the rain loss, A. Hence the analysis model scales the interference power by the quantity μ in evaluating the link unavailability.

In addition to the laboratory tests conducted with the interference centered on the DBS signal, tests were also run with an offset of 7 MHz. This results in an additional reduction in required *C*(*N*+*I*) threshold values. Test results are shown in Figure 3-18 along with a model for the threshold value.

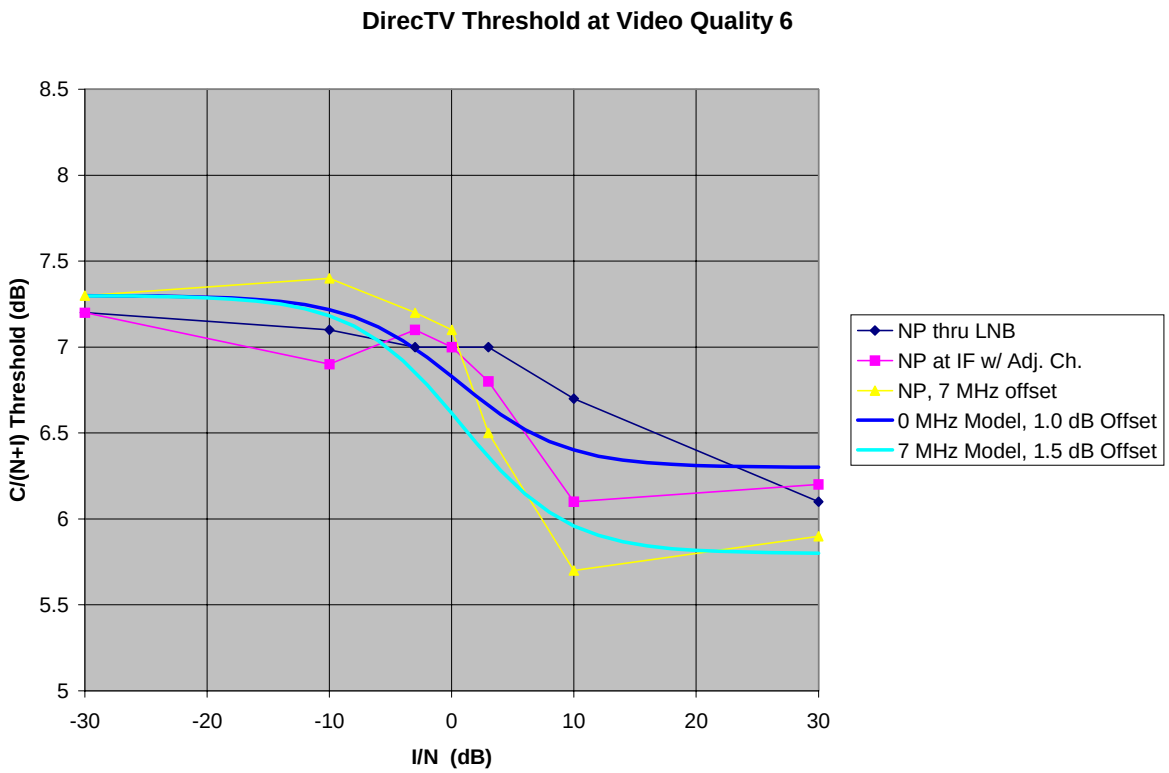

Figure 3-18. Data and Threshold Model for 7 MHz Offset

As shown in the figure, the threshold for the 7 MHz offset case is 1.5 dB below the threshold for noise alone. Also, there is an additional 1.2 dB delta, since the interference values used in the figure are based on power measurements centered on the DBS signal. The difference between the total interference power and the power measured in a 20 MHz band

centered on the DBS signal is 1.2 dB. So, for the 7 MHz offset case, a total correction of 2.7 dB is needed. In the system analysis model, the factor of 2.7 dB is implemented in two parts. First, a 1.0-dB factor is used for all cases. An additional 1.7 dB is used for cases with the 7-MHz offset. Inputs to the system analysis model are summarized in Table 3-7 below.

Table 3-7. System Model Threshold Improvement Factors

Frequency Offset (MHz)	Interference Factor (dB)	Frequency Offset Factor (dB)	Total Factor (dB)
0	1.0	0.0	1.0
7	1.0	1.7	2.7

These factors are used in the basic analysis model that evaluates the impact of MVDDS interference.

Section 4

Antenna Patterns

4.1 MVDDS Antenna Patterns

The gain and radiation patterns were measured in the D720 anechoic chamber using a spherical near-field scanner. The scanner was procured from Nearfield Systems Incorporated (NSI). It is commonly used indoors where it would be impractical to make far-field measurements. Indoor measurements offer the advantage of performing measurements during bad weather. The absorber-lined anechoic chamber minimizes reflections from the walls and ceiling. The near-field technique has been studied extensively, and it is an accepted method for measuring antenna gain and radiation patterns (Evans, 1990; Slater, 1991).

Although the scanner is capable of planar and cylindrical scans, a spherical scan was chosen because of our interest in covering as much of the sphere of observation as possible. Referring to Figure 4-1 the antenna is mounted on a spherical near-field scanner consisting of two axes of rotation. An absorber-covered beam supports one positioner that rotates the antenna under test (AUT) in azimuth with respect to the AUTs coordinates. The second positioner rotates the AUT and supporting beam in elevation with respect to the AUTs coordinates.

The probe on the left is stationary for spherical scans. The probe samples electromagnetic fields over a spherical surface surrounding the AUT. A Hewlett-Packard 8530 network analyzer measures the sampled fields. For all AUT measurements shown here the probe is a WR-75 open-end waveguide. The polarization of the probe is horizontal, initially, then it is rotated 90 degrees to obtain the vertical polarization response of the AUT. The NSI software processes these measurements to obtain far-field AUT response.

Antenna gain is obtained by the gain substitution method. In this method the AUT is measured, then a second antenna is measured whose gain is known beforehand. By comparing the relative response of the two antennas, the gain of the AUT can be determined. The gain standard antenna used here is an EMCO model 3160-08 smooth-wall pyramidal horn.

To obtain radiation patterns over the entire sphere of observation, it is necessary to measure the patterns in two pieces. The scanner is capable of moving the AUT over the full sphere; however, the absorber-covered beam blocks the pattern behind the antenna. To get around this problem the antenna is pointed away from the probe, and a second scan is performed. The antenna is elevated over the absorber-covered beam such that the main beam of the AUT clears the absorber. This is done to minimize the disturbance of the field behind

the antenna due to high-intensity fields impinging on the absorber. Figure 4-14 shows an example of a mount designed for measuring fields behind an AUT.

Once these two roughly hemispherical scans are obtained, they must be processed so that the observation angles and polarization vectors are consistent between the two measurements. In order to do this the coordinate system of the behind the antenna scan is rotated using a rotation matrix based on Euler angles, and the polarization vectors are transformed by calculating dot products based on the same rotation matrix.

The polar plots that follow depict radiation patterns in the two principal planes of the antenna, that is, azimuth and elevation through the main beam of the antenna. The azimuth patterns are based on a top down view of the antenna with the main beam pointing up. The elevation patterns are based on a side view of the antenna with the main beam pointing to the right. Although patterns were measured at 12.2, 12.45, and 12.7 GHz, only patterns measured at 12.45 GHz are included here.

4.1.1 Small Sectoral Horns

The small Northpoint H-plane sectoral horn is shown in Figure 4-1 as it was measured in the anechoic chamber. The sectoral horns are used with the flare vertical so that a broad azimuthal pattern with horizontal polarization is generated. Figure 4-2 shows an azimuth cut with a similar measurement provided by Pegasus for its own small horn. Figure 4-3 shows a Northpoint elevation cut measured by MITRE only. One can see that the azimuth pattern is very broad, and the elevation pattern is comparatively narrow.

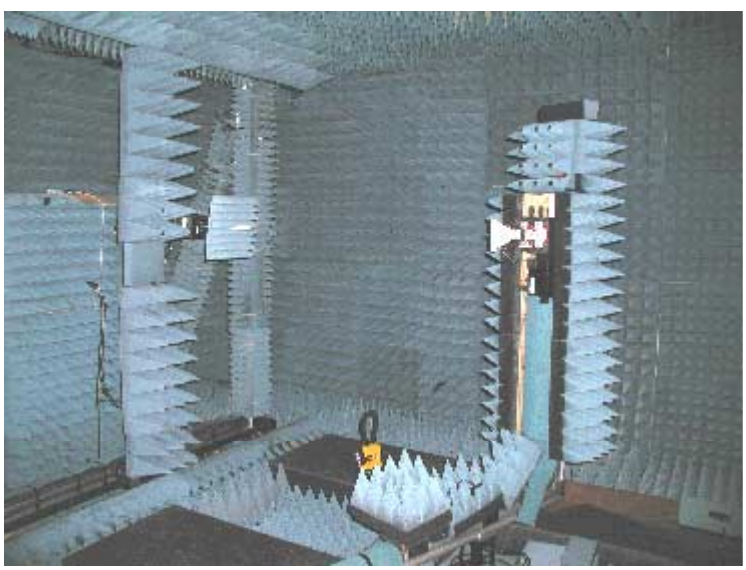

Figure 4-1. Small Sectoral Horn on Spherical Scanner

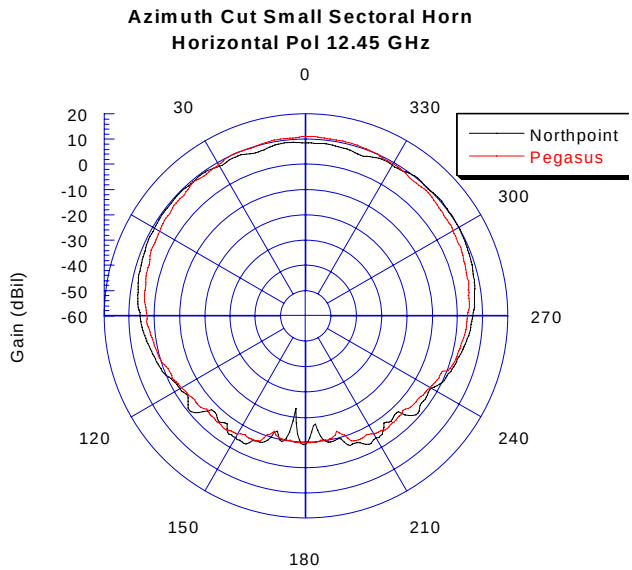

Figure 4-2. Azimuthal Radiation Patterns of Small Sectoral Horns

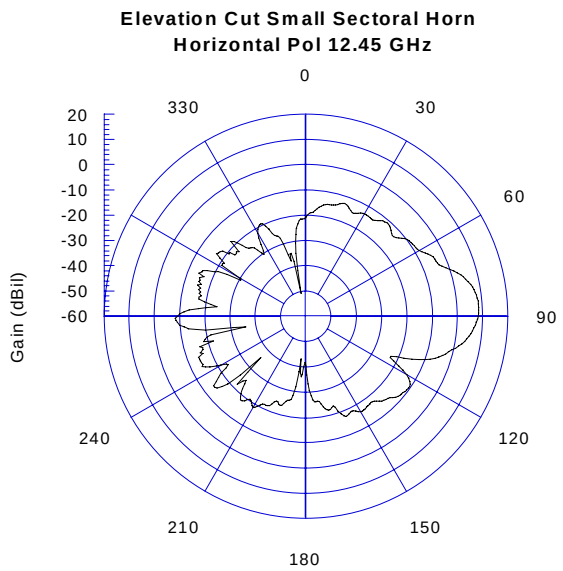

Figure 4-3. Elevation Radiation Pattern of Northpoint Small Sectoral Horn

4.1.2 Large Sectoral Horns

The large Northpoint H-plane sectoral horn is shown in Figure 4-4 in the anechoic chamber. Figure 4-5 shows an azimuthal cut with a similar measurement provided by Pegasus for its own large horn, and Figure 4-6 shows the corresponding Northpoint elevation cut. It is evident that in this case the Northpoint and Pegasus antennas have very similar main-beam patterns in the azimuthal plane. The elevation beamwidth is narrower than that for the small-sectoral horn.

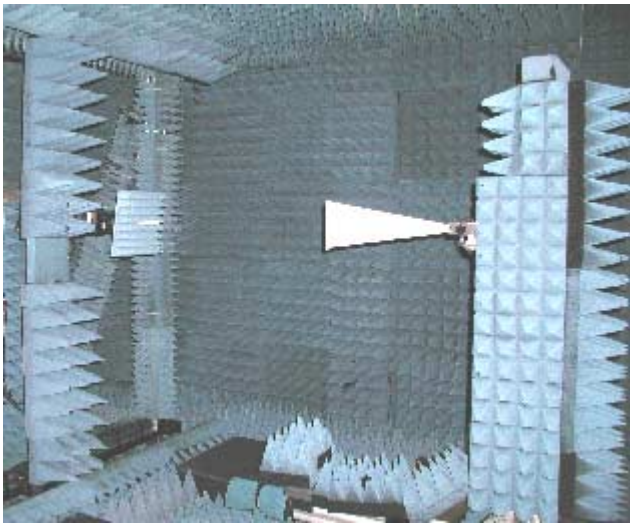

Figure 4-4. Large Sectoral Horn on Spherical Scanner

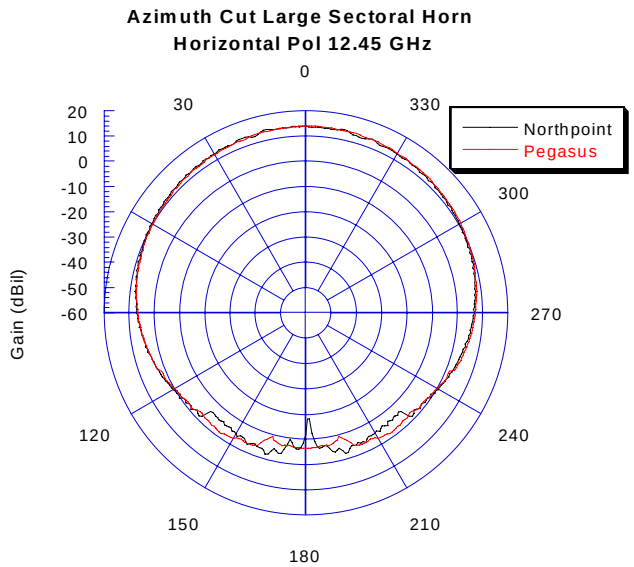

Figure 4-5. Azimuthal Radiation Patterns of Large Sectoral Horns

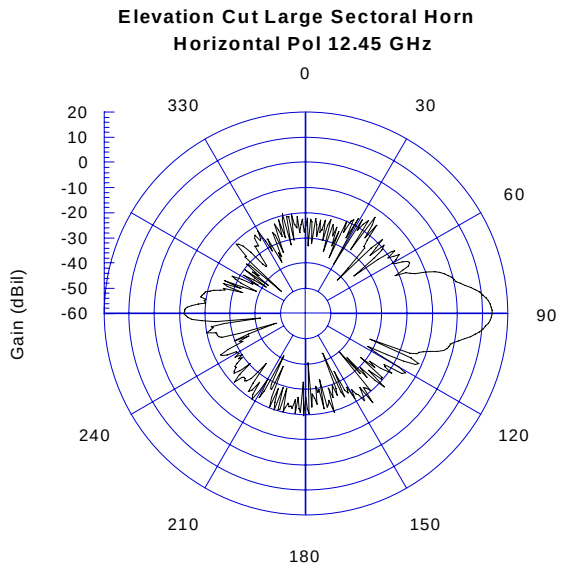

Figure 4-6. Elevation Radiation Pattern of Large Northpoint Sectoral Horn

4.2 DBS Antenna Patterns

The feed horn used on the DIRECTV antennas is integral to the LNB. In order to perform coherent measurements on these antennas, it was necessary to remove the LNB circuit board and replace it with an adapter that would allow us access to the Ku-band signal. The MITRE machine shop fabricated a fixture that connected to the back of the feed horn and allows a connection to a WR-75 waveguide to sub-miniature A (SMA) coax adapter. Care was exercised in aligning the adapter probe to the ridge polarizer in the throat of the feed. The fixture was oriented such that the horn generates right-hand circular polarization (RHCP).

4.2.1 DIRECTV 18-inch Reflector

Figure 4-7 shows the DIRECTV 18-inch reflector in the anechoic chamber. Figure 4-8 shows an azimuth cut. Note that the dominant polarization is left-hand circular polarization (LHCP). This occurs when the RHCP wave flips to LHCP upon reflection from the reflector. Figure 4-9 shows the elevation cut. The large RHCP component near 0 degrees is due to energy from the feed that bypasses the reflector; this is referred to as spillover. Figure 4-10 shows a contour plot of RHCP in which the main beam is located at the center. Theta is a polar angle, related to elevation, measured from zenith, and phi is azimuth measured from the main beam. The horizon is located at theta = 90, zenith at theta = 0, and nadir at theta = 180 degrees. Observe the comparatively high signal level at zenith and at lower elevations corresponding to spillover directions. The strut supporting the feed blocks the spillover near theta = 90 and phi = ± 180 degrees.

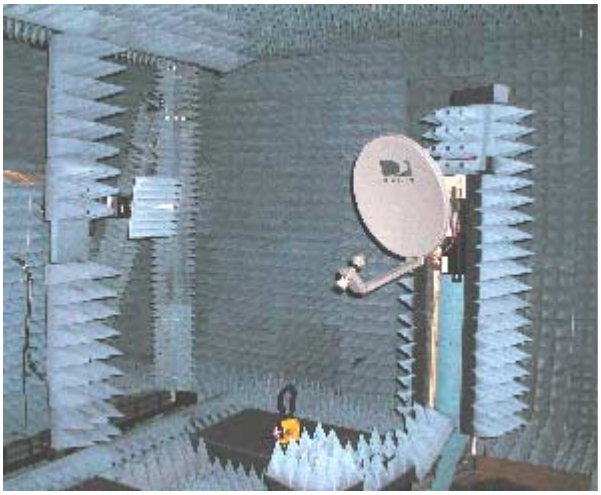

Figure 4-7. DIRECTV 18-inch Reflector on Spherical Scanner

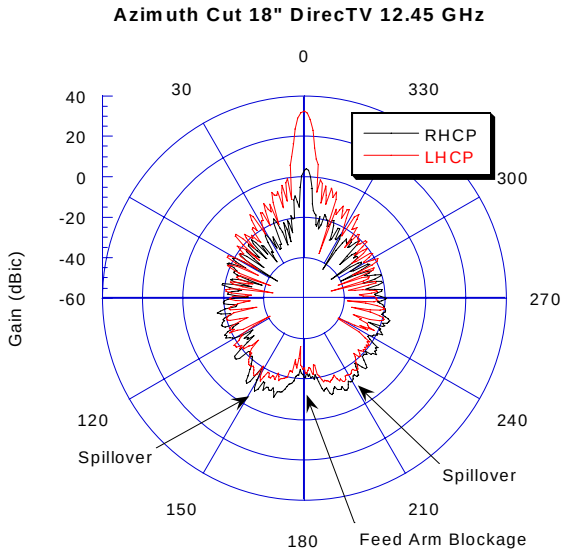

Figure 4-8. Azimuthal Radiation Pattern of DIRECTV 18-inch Reflector

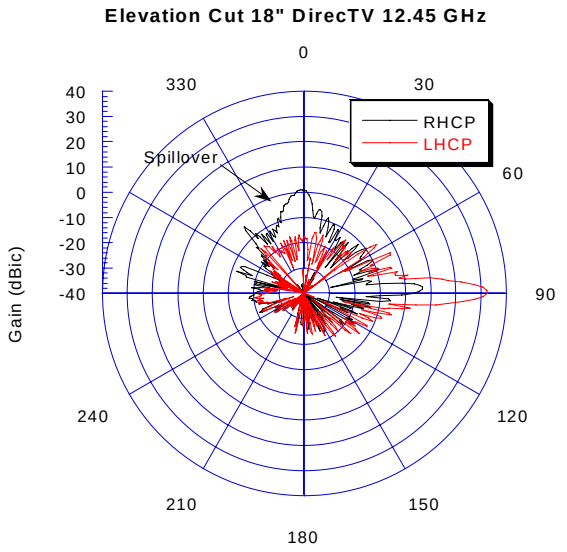

Figure 4-9. Elevation Radiation Pattern of DIRECTV 18-inch Reflector

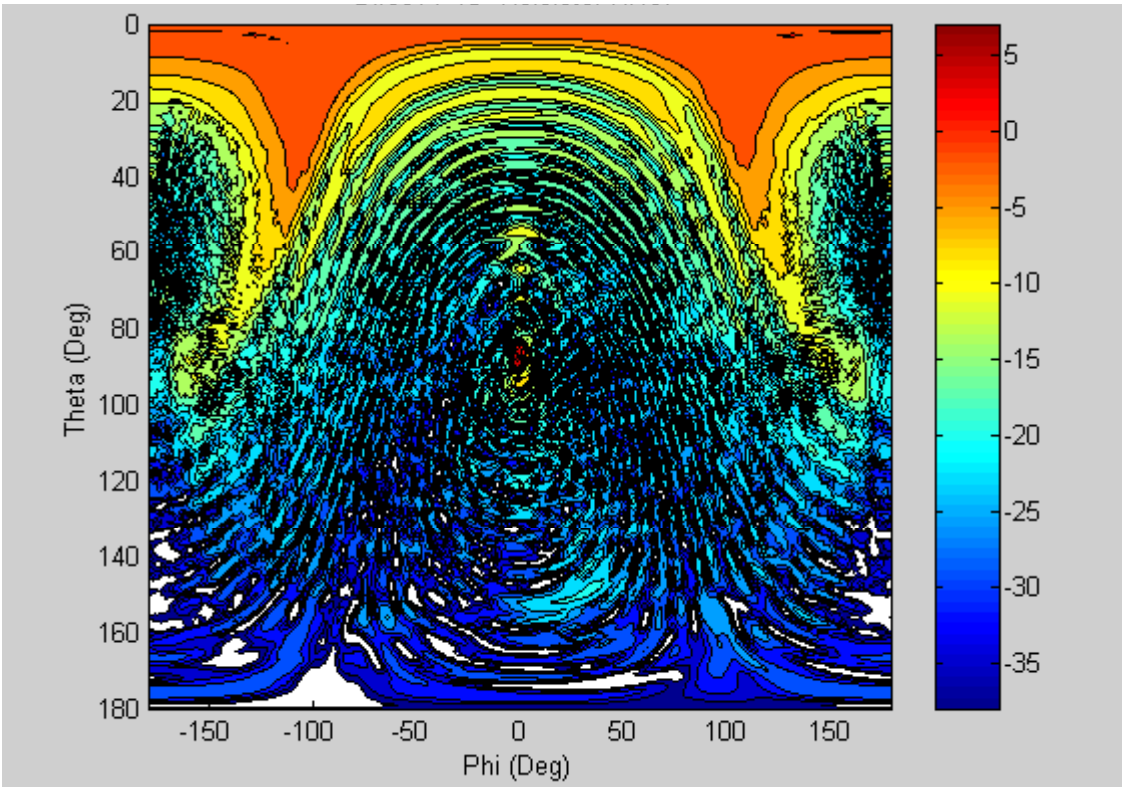

Figure 4-10. RHCP Radiation Pattern of DIRECTV 18-inch Reflector

4.2.2 DIRECTV 24" x 18" Reflector with Single Feed

A multiple feed reflector was measured that is capable of receiving signals from two satellites in different locations in the geostationary orbit. The radiation pattern is squinted by moving the feed away from the focus of the parabolic reflector. The DIRECTV 24 by 18-inch reflector can accept feeds at three locations for use with satellites at 101, 110, and 119 degrees West longitude. The single feed reflector referred to here has the feed located at the center. Figure 4-11 shows the azimuth cut. This antenna has greater spillover than the 18-inch version as shown by the larger RHCP response about 180 degrees. Spillover is also evident in the elevation cut shown in Figure 4-12. The contour plot in Figure 4-13 shows a slightly different spillover pattern due to the elliptical contour of the reflector.

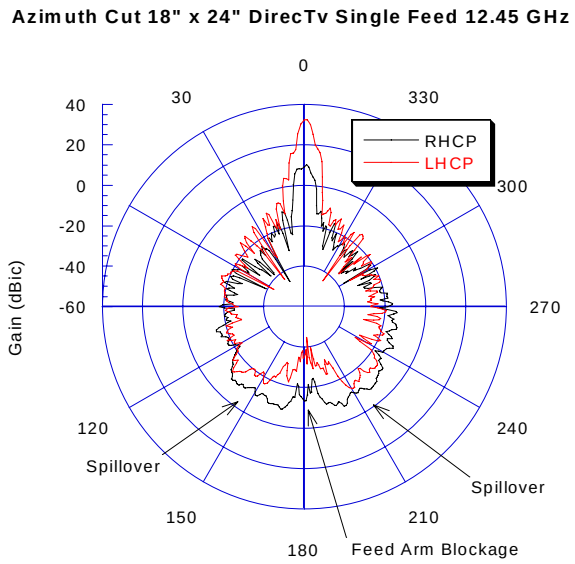

Figure 4-11. Azimuthal Radiation Pattern of DIRECTV 24-by-18-inch Reflector with Single Feed

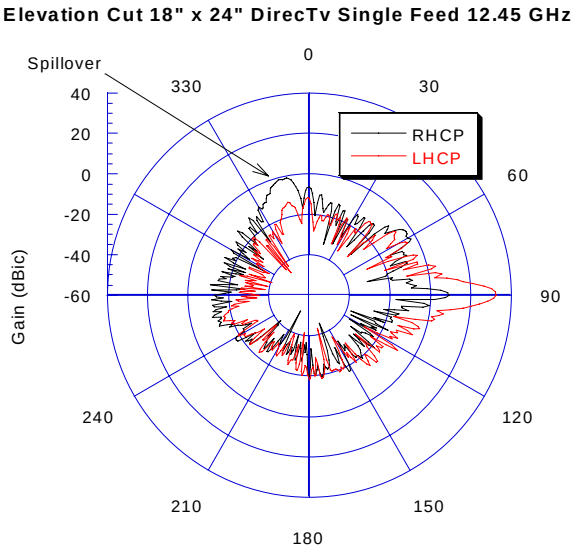

Figure 4-12. Elevation Radiation Pattern of DIRECTV 24-by-18-inch Reflector with Single Feed

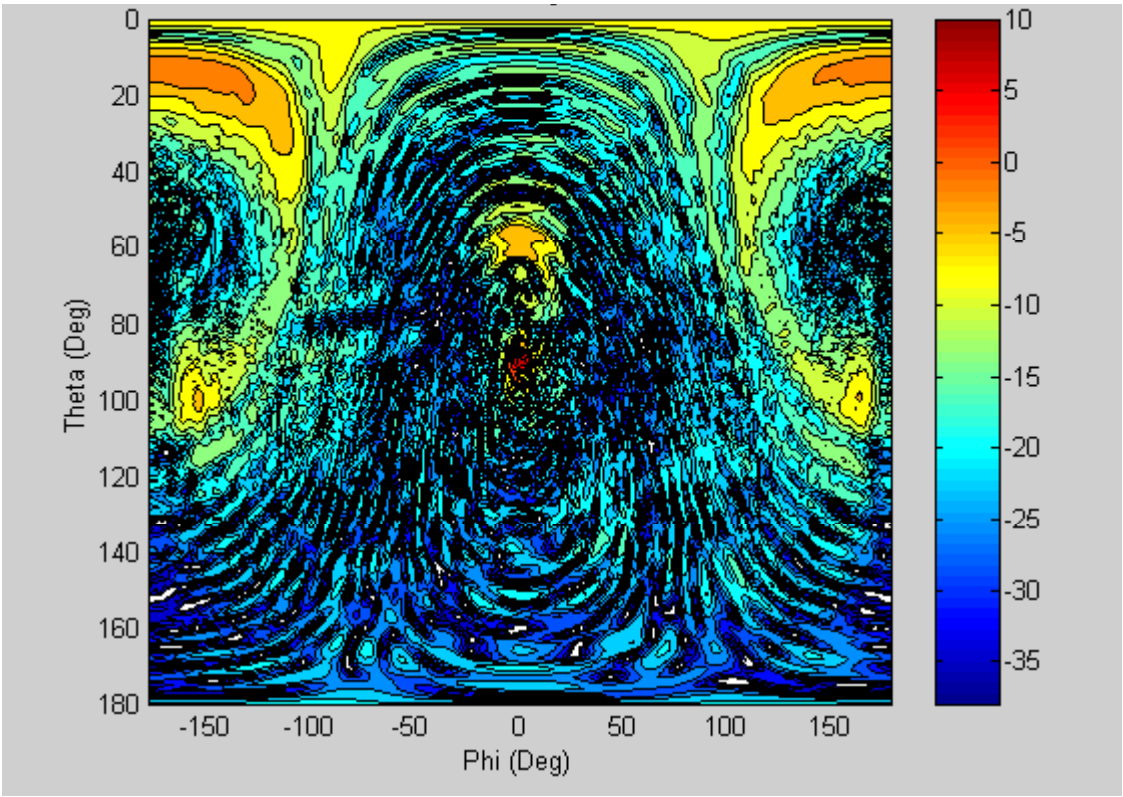

Figure 4-13. RHCP Radiation Pattern of DIRECTV 24 by 18-inch Reflector with Single Feed

4.2.3 DIRECTV 24 by 18-inch Reflector with Dual Feed

In a second measurement of the 24 by 18-inch DIRECTV reflector, two feeds at the outer positions are measured. In this case the active feed is on the right when facing the front of the reflector as shown in Figure 4-14. Figure 4-15 shows an azimuth cut in which the spillover is worse on the same side of the reflector as the feed is displaced from the focus. Spillover appears in the elevation pattern shown in Figure 4-16 around theta = 270 and 345 degrees corresponding to the top and bottom edges of the reflector. Figure 4-17 shows the asymmetrical nature of the spillover. Once again, the spillover is worse on the side where the feed is located. Since the feeds in all three positions are parallel, it is intuitively reasonable that the spillover would be worse in the direction of lateral feed displacement.

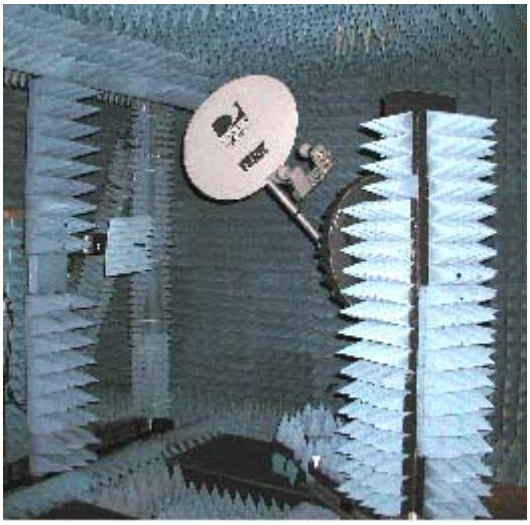

Figure 4-14. DIRECTV 24-by-18-inch Reflector with Dual Feed on Spherical Scanner

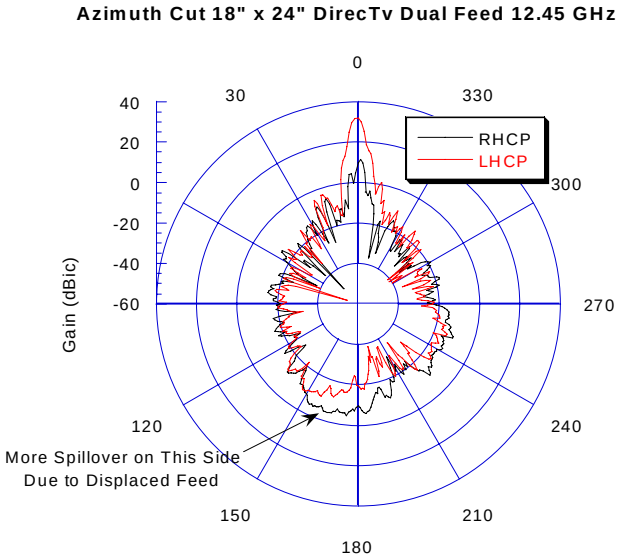

Figure 4-15. Azimuth Radiation Pattern of DIRECTV 24-by-18-inch Reflector with Dual Feed

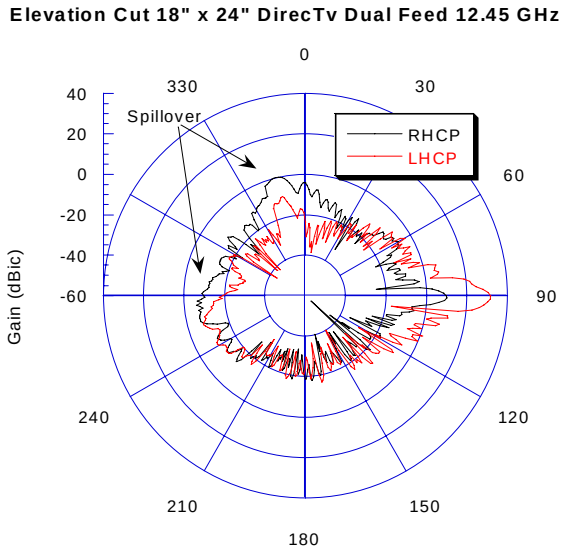

Figure 4-16. Elevation Radiation Pattern of DIRECTV 24-by-18-inch Reflector with Dual Feed

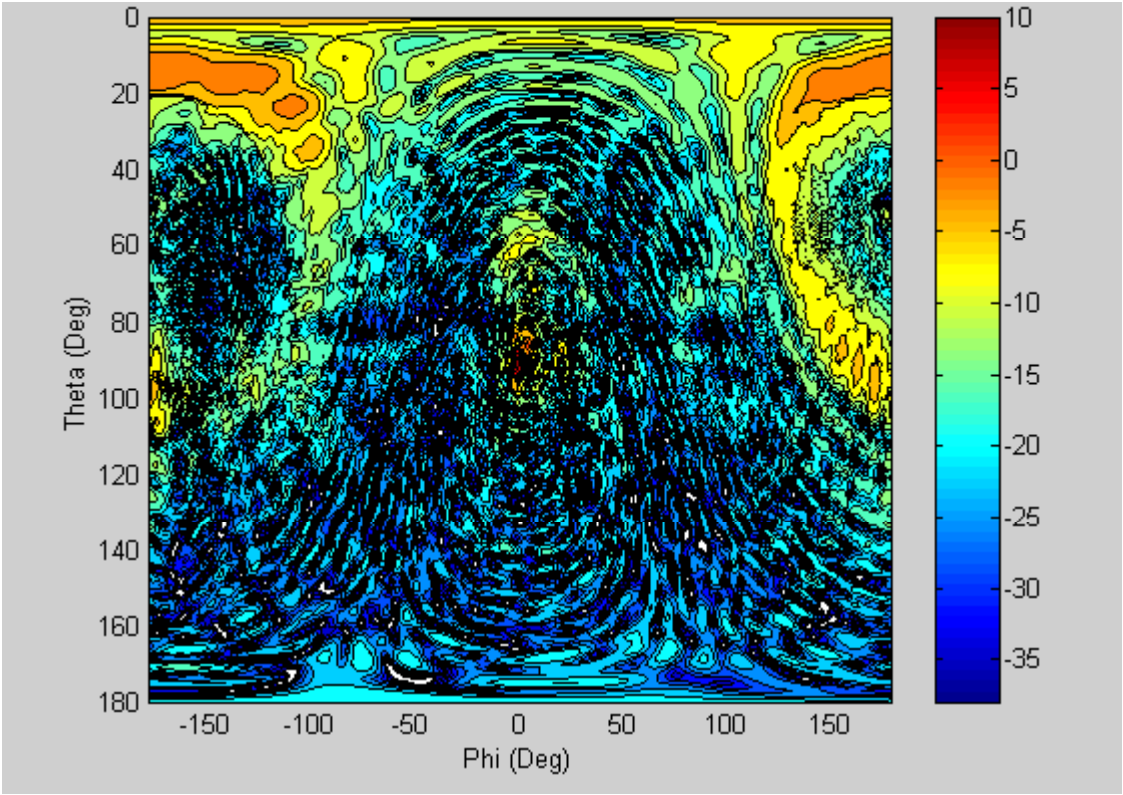

Figure 4-17. RHCP Radiation Pattern of DIRECTV 24-by-18-inch Reflector with Dual Feed

4.2.4 Fortel

A flat panel antenna produced by Fortel was also measured. The entire pattern was not measured, so part of the pattern behind the antenna is missing in the figures below. Opaque covers block examination of the radiating elements and combining network, so the exact nature of this antenna is not known. Although the LNB can be removed from the back of the antenna, a fixture is required to connect a coaxial cable for measurements. Once again care was exercised in orienting the waveguide adapter probe in a similar fashion to those in the LNB. The azimuth pattern in Figure 4-18 shows grating lobes approximately 65 degrees off boresight. The amplitude of these grating lobes is slightly higher than the spillover lobes of the reflectors. The cross polarization amplitude is comparatively high. The elevation cut in Figure 4-19 also exhibits grating lobes. Grating lobes usually occur when elements in an array are separated by more than one wavelength. The contour plot in Figure 4-20 shows the spatial distribution of the grating lobes.

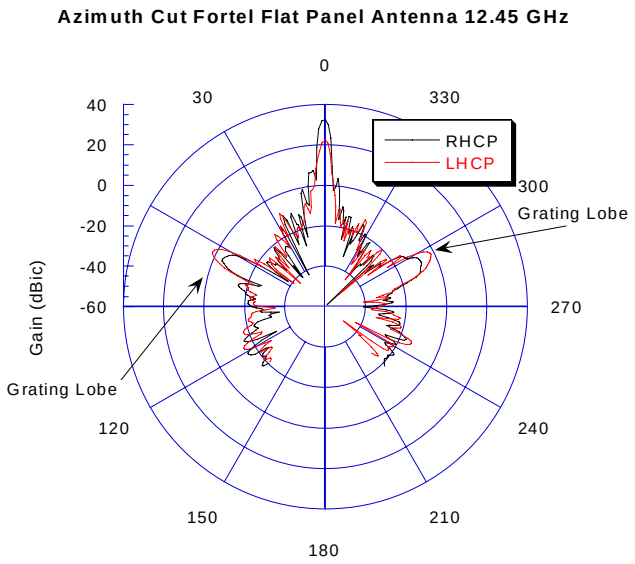

Figure 4-18. Azimuth Radiation Pattern of Fortel Flat Panel Antenna

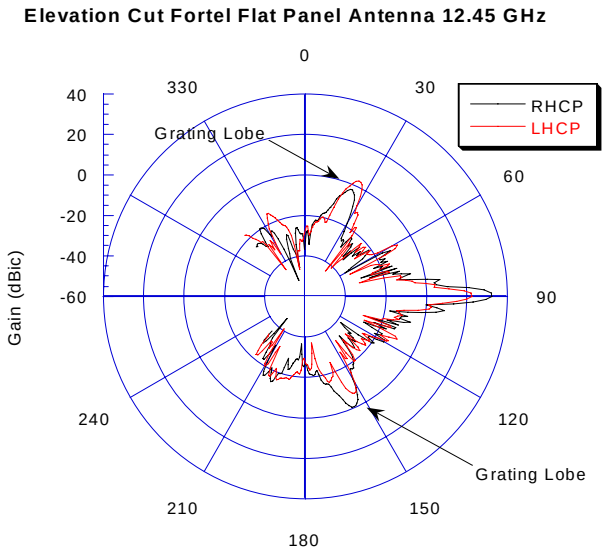

Figure 4-19. Elevation Radiation Pattern of Fortel Flat Panel Antenna

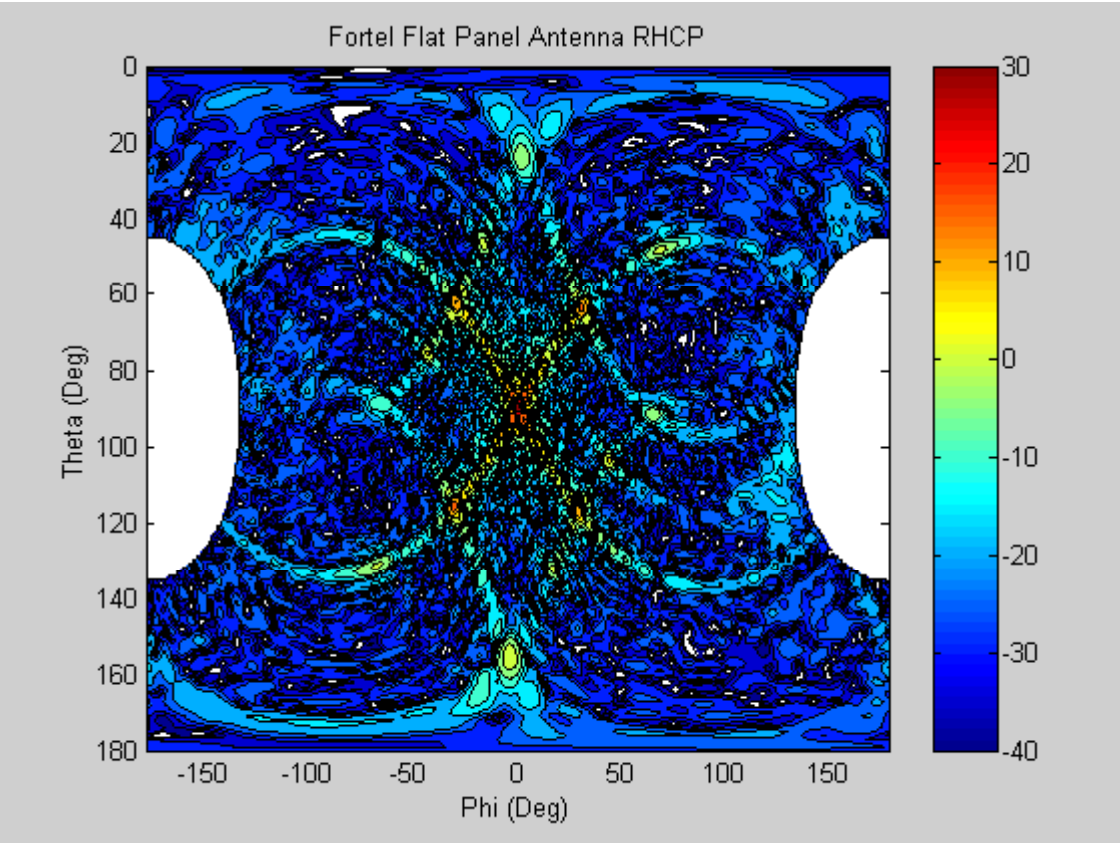

Figure 4-20. RHCP Radiation Pattern of Fortel Flat Panel Antenna

4.2.5 Boresight Gain Summary

Table 4-1 summarizes the boresight gain for the antennas at 12.2, 12.45, and 12.7 GHz. It should be clearly stated that the maximum small sectoral horn gain occurs off boresight. This can be seen in Figure 4-2 where the Northpoint gain is highest about 50 degrees off boresight. Interestingly, the DIRECTV 24-by-18-inch single feed has very similar gain to that of the DIRECTV 18-inch reflector. The gain of the DIRECTV 24-by-18-inch dual feed reflector is slightly lower that the single feed version due to the feed being located away from the focal point of the reflector. The measured gain values are approximately 1.0 to 1.5 dB lower than expected based on information provided by the vendors. For example, the efficiency of the 18-inch reflector based on the gain shown below ranges from 49 to 55% while the claimed efficiency is about 70%.

Table 4-1. Boresight Gain Summary

Antenna	12.2 GHz	12.45 GHz	12.7 GHz
Small sectoral	6.7 dBil	8.4 dBil	8.8 dBil
Large sectoral	14.3 dBil	13.9 dBil	14.8 dBil
DIRECTV 18-inch Reflector	32.2 dBic	32.4 dBic	33.0 dBic
DIRECTV 24 x 18-inch Reflector Single Feed	32.4 dBic	32.5 dBic	33.1 dBic
DIRECTV 24 by 18-inch Reflector Dual Feed	31.8 dBic	31.8 dBic	32.6 dBic
Fortel	31.9 dBic	32.4 dBic	32.9 dBic

NOTES:

dBi = dB referenced to the gain of an isotropic antenna
dBil = dB referenced to the gain of a linearly polarized isotropic antenna
dBic = dB referenced to the gain of a circularly polarized isotropic antenna

4.3 Polarization

The effects of the polarization of the MVDDS transmitted wave and the polarization of the DBS receive antenna must be considered. The following sections address polarization and its impact on received interference power.

4.3.1 The Transmitted Wave

Assume a plane wave in space is propagating along the z-axis. Let the wave have two components, one in the x (horizontal) direction and one in the y (vertical) direction. The E field of the wave can be described as:

$$E_x\vec{U}_x + E_y\vec{U}_y e^{j\alpha} \tag{4}$$

Where:

Ex = the electric field in the x (horizontal) direction

$\vec{U}_x$ = a dimensionless unit vector in the x direction

Ey = the electric field in the y (vertical) direction

$\vec{U}_y$ = a dimensionless unit vector in the y direction

α = an electrical phase angle indicating how much the vertical component leads the horizontal component

Notes:

(1) If $Ex = Ey$ and α is 90 degrees, then the wave is left-hand circular polarized (LHCP).

(2) Ex has units of Volts/meter.

(3) The power flux density (PFD) for the horizontal component is:

$$PFD_H = \frac{E_x E_x^*}{\eta_0} \tag{5}$$

Where:

Ex^* = the complex conjugate of Ex

η_0 = the impedance of free space = 120π

4.3.2 Receive Antenna Response

In order to evaluate the impact of polarization, we need to consider how the receive antenna responds to the wave described above. Let R_x be the response of the antenna to the x (horizontal) component of the E field of the incoming plane wave. Also the response to the y (vertical) component of the E field is:

$$R_y e^{j\beta} \tag{6}$$

In this formulation, β is an electrical phase angle describing how much the response to the vertical component leads the response to the horizontal component. R_x and R_y have units of meters.

4.3.3 Combined TX and RX

The output of the receive antenna as it responds to the wave above would be:

$$S = E_x R_x + E_y R_y e^{j(\beta - \alpha)} \tag{7}$$

This signal has units of Volts. Clearly, both the wave in space and the receiving antenna must be based on the same coordinate systems. The power received is as follows:

$$P_R = \frac{SS^*}{\eta_0} \tag{8}$$

Relating these quantities to well known path loss equations, we find that:

$$E_x = \sqrt{\frac{P_T G_{TH} \eta_0}{4\pi d^2}} \tag{9}$$

$$E_y = \sqrt{\frac{P_T G_{TV} \eta_0}{4\pi d^2}} \tag{10}$$

$$R_x = \sqrt{\frac{\lambda^2 G_{RH}}{4\pi}} \tag{11}$$

$$R_y = \sqrt{\frac{\lambda^2 G_{RV}}{4\pi}} \tag{12}$$

Where:

P_T = the transmitted power (Watts)

G_{TH} = the horizontal component of the gain of the transmit antenna, relative to isotropic

G_{TV} = the vertical component of the gain of the transmit antenna, relative to isotropic

G_{RH} = the horizontal component of the gain of the receive antenna, relative to isotropic

G_{RV} = the vertical component of the gain of the receive antenna, relative to isotropic

d = the distance between antennas

λ = the wavelength

Let us define two new constants:

$$C_1 = \sqrt{\frac{P_T \eta_0}{4\pi d^2}} \tag{13}$$

$$C_2 = \sqrt{\frac{\lambda^2}{4\pi}} \tag{14}$$

So that:

$$E_x = C_1 \sqrt{G_{TH}} \tag{15}$$

$$E_y = C_1 \sqrt{G_{TV}} \tag{16}$$

$$R_x = C_2\sqrt{G_{RH}} \tag{17}$$

$$R_y = C_2\sqrt{G_{RV}} \tag{18}$$

Substituting and rearranging, the received power can be rewritten as:

$$P_R = P_T C_3\left(G_{TH}G_{RH} + G_{TV}G_{RV} + 2\cos(\beta-\alpha)\sqrt{G_{TH}G_{TV}G_{RH}G_{RV}}\right) \tag{19}$$

where:

$$C_3 = \left(\frac{\lambda}{4\pi d}\right)^2 \tag{20}$$

We note that C_3 is the well-known free space path loss factor.

4.3.4 Polarization Model

The analysis model used to evaluate the effects of interference on DBS receivers must take into account polarization. The polarization approach used in this model is based on equation 16 but for simplicity, it ignores the relative phase angles. The equation used in the analysis model is:

$$P_R = P_T C_3\left(G_{TH}G_{RH} + G_{TV}G_{RV}\right) \tag{21}$$

From the above relationships, we define a new quantity, the effective gain product of the two antennas. The true effective gain product is:

$$GP_{true} = \left(G_{TH}G_{RH} + G_{TV}G_{RV} + 2\cos(\beta-\alpha)\sqrt{G_{TH}G_{TV}G_{RH}G_{RV}}\right) \tag{22}$$

Also, the effective gain product for the system analysis model is:

$$GP_{model} = \left(G_{TH}G_{RH} + G_{TV}G_{RV}\right) \tag{23}$$

Where:

GP_{true} = the true effective gain product of the two antennas, taking polarization into account

GP_{model} = the model for the effective gain product of the two antennas used in the system analysis tool

Example results are shown below. Figure 4-21 shows the true gain product for an area 6 km x 6 km, south of a Northpoint transmitter. The transmitter is at 100 meters height above level terrain. The DBS receive antenna is at terrain height. The DBS antenna is the 18-inch dish, which is aimed at a satellite at 119 W Longitude from the Washington, DC area. The Northpoint transmit antenna is the large sectoral horn. It is aimed directly south

with no up-tilt. The contour plot shows the decibel version of the true gain product, *taking polarization into account*. Contours are in 5-dB steps. As shown in Section 4.5.3, the actual received interference power would be the decibel sum of the gain product shown in the figure plus the decibel version of the transmit power less the free space loss. Note that the area of large gain product matches the area of most interference impact for the Washington DC case presented in Section 5.1.

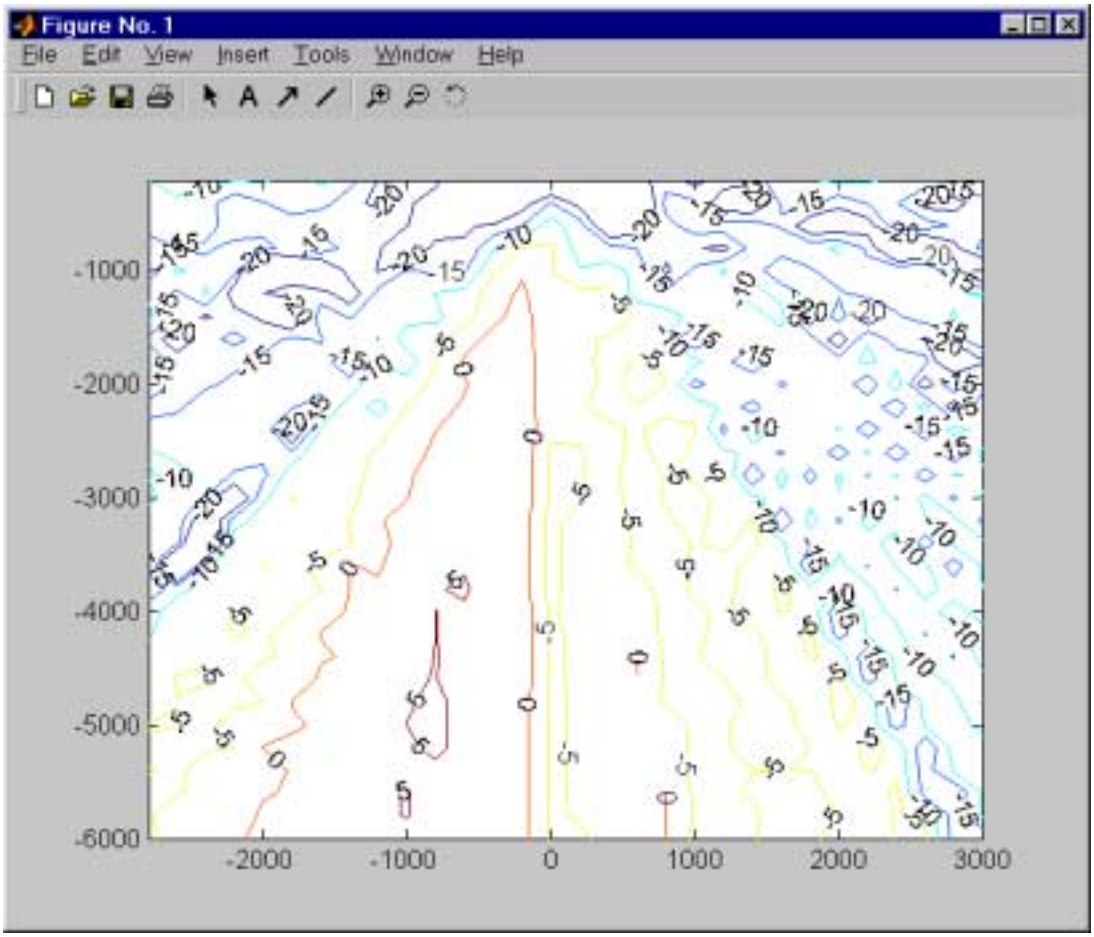

Figure 4-21. True Gain Product

The above gain product plot should be compared to the gain product model used in the system analysis tool. The latter is shown in Figure 4-22 for the same scenario described above. As seen from the figures, the model matches true performance closely, especially in regions where the gain product is largest. The model used in the system analysis tool is conservative, but only slightly conservative.

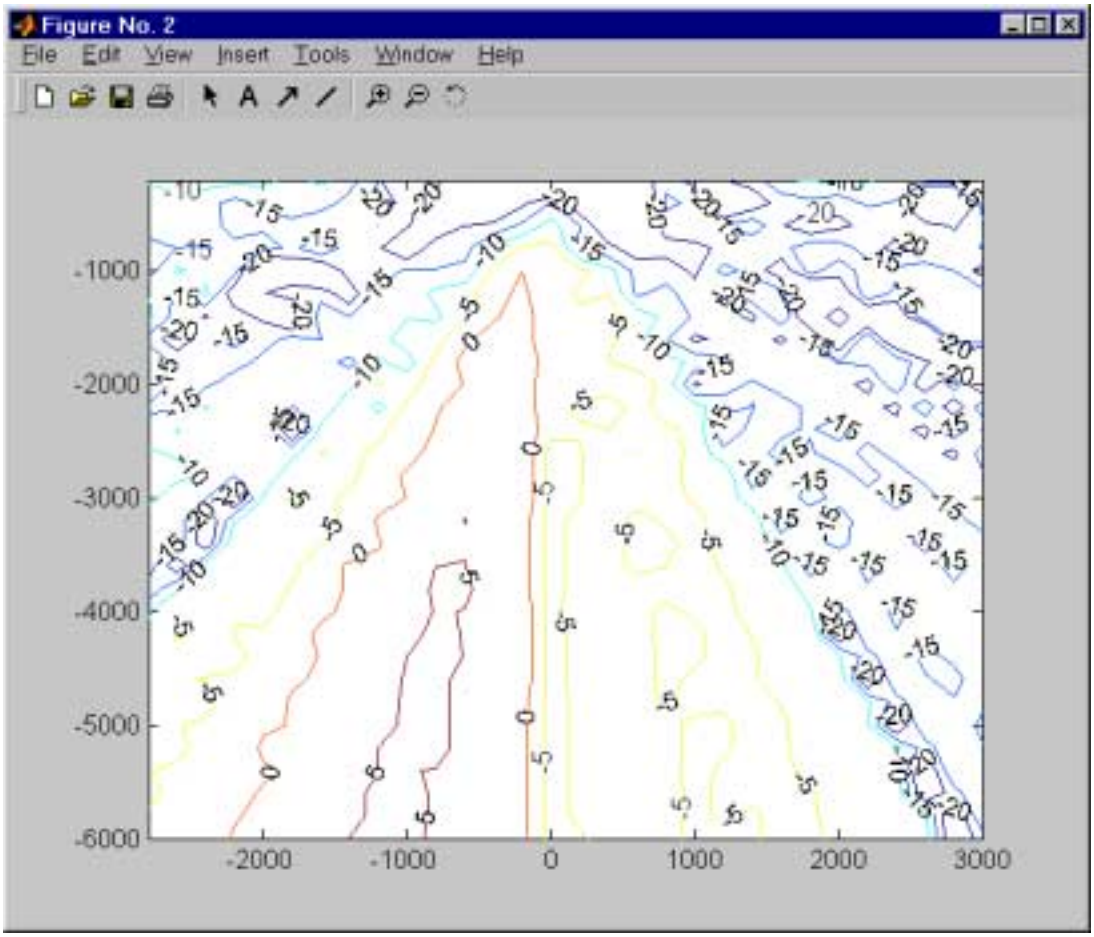

Figure 4-22. MITRE Model for Gain Product

Other analyses have apparently used different models for the effects of polarization. In some of these cases, polarization is dealt with in terms of an isolation factor. Various values for the polarization isolation from 0 to 3 dB have been used in different analyses. It is assumed that in the approaches that use this technique, the dominant-mode gain is the starting point for determining the gain product. So, such models can be described as follows:

$$GP_{dom} = \frac{G_{T\,max} G_{R\,max}}{\sigma} \tag{24}$$

Where:

GP_{dom} = the dominant-mode model for effective gain product of the two antennas

G_{Tmax} = the maximum gain of the transmit antenna at given azimuth and elevation angles, considering vertical, horizontal, right hand circular, and left hand circular polarizations

G_{Rmax} = the maximum gain of the receive antenna at given azimuth and elevation angles, considering vertical, horizontal, right hand circular, and left hand circular polarizations

σ = the polarization isolation factor used in the dominant-mode model

Results for the dominant-mode model are shown in Figure 4-23 for a polarization isolation factor of unity (zero dB). These results are based on the same scenario described in the examples above. Here we see that the dominant-mode model using a zero-decibel polarization isolation factor is also conservative. *However, the dominant-mode model is more conservative than the model used in the system analysis tool*.

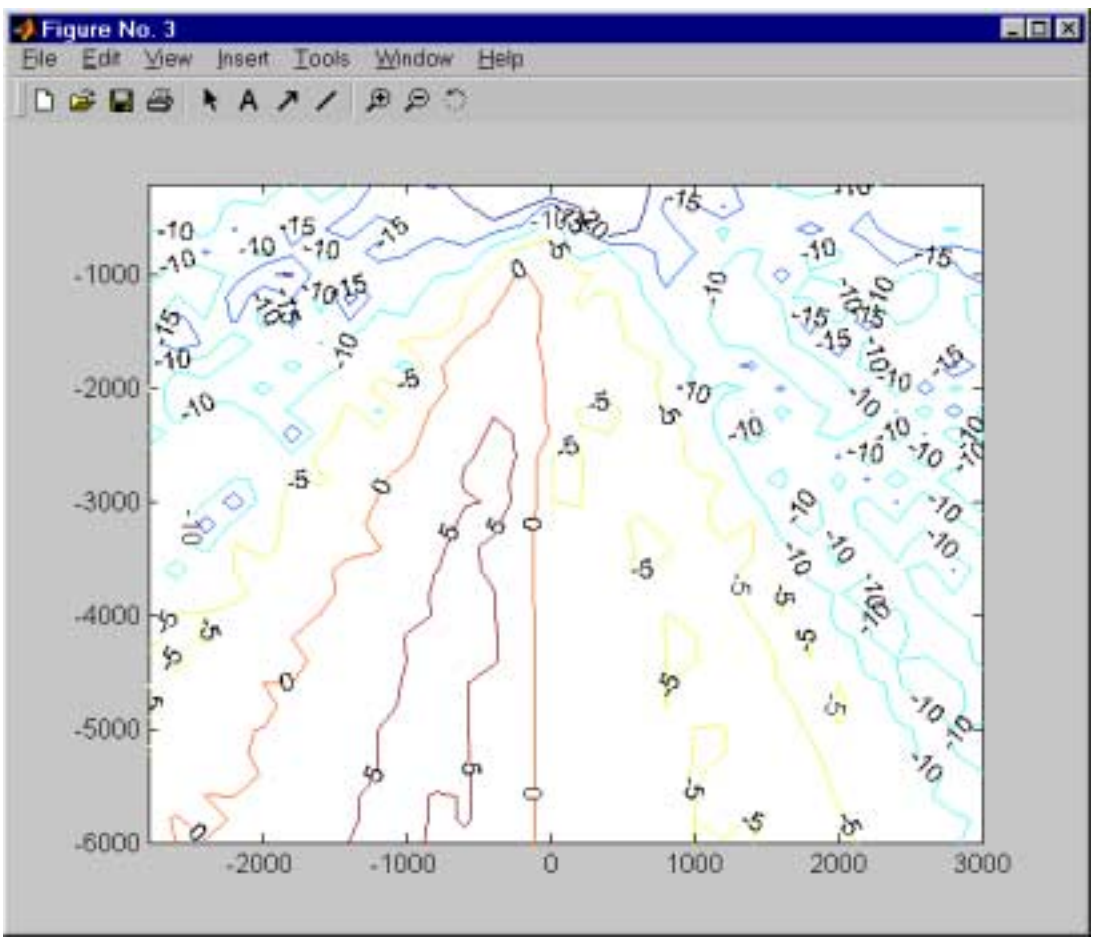

Figure 4-23. Dominant Mode Model for Gain Product

Section 5

Interference Assessment

5.1 Interference Predictions

The impact of interference from an MVDDS transmitter upon DBS receivers in its vicinity is a function of several parameters:

- The interference-impact criterion (e.g., absolute or relative increase in DBS downlink unavailability).
- The DBS-receiver performance criterion: the receiver performance level (e.g., VQ6) that must be met or exceeded for the DBS downlink to be considered "available."
- The geographical locale under consideration (e.g., Washington, DC). This determines the local rainfall statistics that very strongly affect downlink availability.
- The output power of the MVDDS transmitter.
- The modulation/channelization scheme employed by the MVDDS transmitter.
- The radiation pattern of the MVDDS transmitting antenna.
- The boresight azimuth angle of the MVDDS transmitting antenna.
- The boresight elevation (tilt) angle of the MVDDS transmitting antenna.
- The radiation patterns of the DBS receiving antennas.
- The boresight azimuth and elevation angles of the DBS receiving antennas. These are determined by satellite longitude, and by the latitude and longitude of the locale.
- The MVDDS transmitting antenna's height above average terrain.
- The assumed frequency of the DBS downlink signal.
- The offset between MVDDS and DBS carrier frequencies.
- The EIRP that each satellite directs toward the locale of interest.

In order to investigate the potential impact of MVDDS interference upon DBS, MITRE has developed a MATLAB™ application embodying the computational technique of Section 2.1. This model has been used to analyze a variety of cases involving various combinations of the parameters discussed above. Appendix B presents the resulting set of 56 contour plots, which are discussed in detail later in this section. The plots provide a

quantitative basis for gauging the severity of the potential interference problem and for evaluating the effectiveness of possible mitigation techniques.

One of those plots, generated for the Washington, DC "benchmark" case that serves as a basis for comparison with most of the other plots, is reproduced in Figure 5-1. The model has computed the absolute increase ΔU caused by MVDDS in the rain-induced unavailability U, where U and ΔU are both measured in hours per year (hr/yr), of the downlink from each of three satellites to postulated DBS receivers at each of 32,761 gridpoints on the plot. Contours have been drawn to connect points at which the *maximum* unavailability (the worst of the three single-satellite values computed for each gridpoint) is equal to certain selected values such as 0.3 hr/yr. The plots are discussed further in 5.1.2 below.

5.1.1 Ranges of Parametric Values Used in the Simulations

Four different *interference-impact criteria* were applied in the simulations:

- The maximum *absolute* unavailability increase, obtained by taking the largest value of ΔU experienced by any of the three satellite downlinks at the gridpoint under consideration, as explained above. This criterion was used in the benchmark simulation and in all but three of the other simulations done for this study. In each such simulation, contours were plotted for each of five values of ΔU: 0.3, 1, 3, 10, and 30 hours per year.
- The maximum *relative* unavailability increase ($\Delta U/U_0$), where U_0 is the "baseline" value of U that exists for a given satellite in the locale under consideration even when MVDDS is *not* present. This criterion was employed in one variation of the benchmark simulation, with contour values set at 2.86%, 10%, 30%, 100%, and 300%.
- The maximum *total* unavailability ($U_0 + \Delta U$) due to rain and MVDDS combined. This criterion was used only in one benchmark variation, with contour values set at 25, 30, 35, 40, and 45 hr/yr.
- The minimum clear-air value of (C/I_M), where C is the weakest DBS downlink power level and I_M is the MVDDS-interference power level, at the output of a DBS receiving antenna placed at the gridpoint in question. In the single simulation in which this criterion was used, the model was set to generate contours for 5, 10, 15, 20, and 25 dB.

Three different *DBS-receiver performance criteria* were employed: VQ6 (which was used in the vast majority of the simulations), QEF, and VQ1.

Ten different *locales* were considered at least once in the simulations: Washington, DC; Miami, FL; Phoenix, AZ; Boston, MA; Chicago, IL; Houston, TX; Los Angeles, CA; Denver, CO; Seattle, WA; and Fargo, ND.

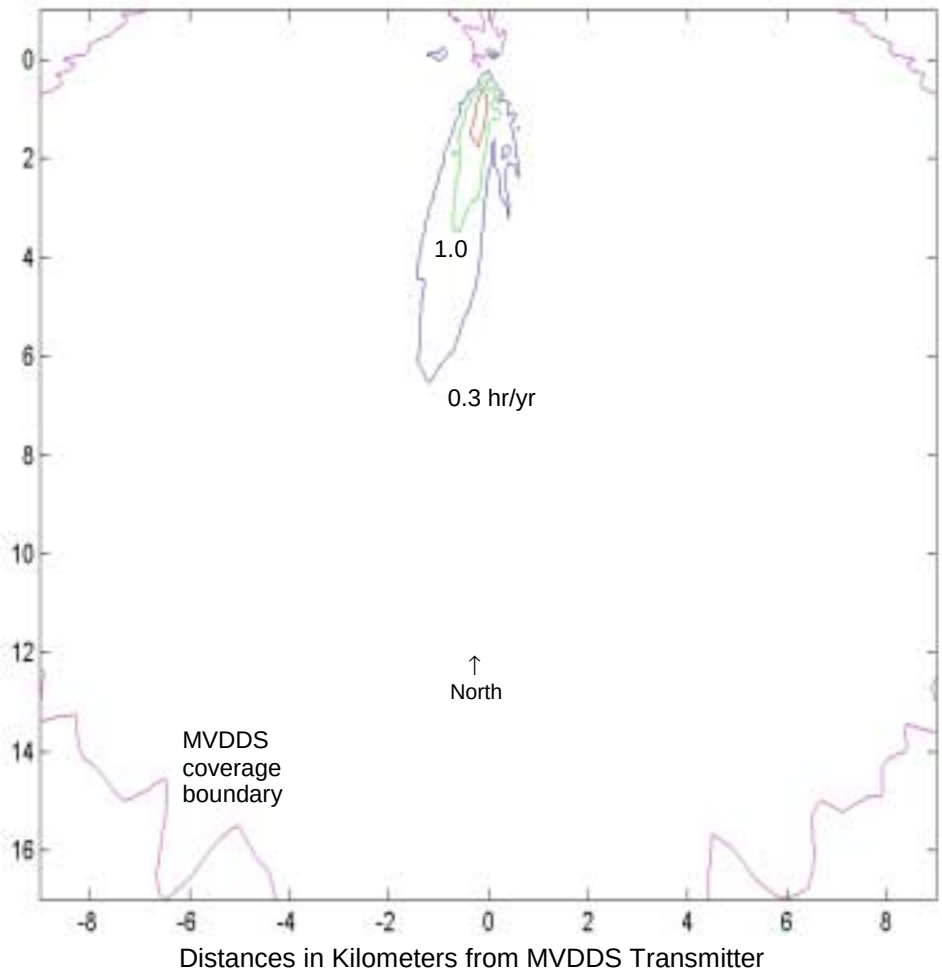

Washington, DC (12.45 GHz)
Maximum absolute increase caused by MVDDS in rain-induced DBS unavailability
Raw MVDDS transmitter power (*not* EIRP): 0 dBm
MVDDS transmitting antenna: Northpoint large sectoral horn
MVDDS transmitting-antenna boresight: 180° azimuth (S); 0° elevation tilt
MVDDS transmitting antenna 100 meters above horizontal plane
Assumed MVDDS interference scaling factor: 1 dB
Frequency offset between MVDDS and DBS carriers: none
DBS performance measure: VQ6
DBS receiving antenna: 18" single-feed dish
Minimum ratio of DBS EIRP to receiver threshold assumed for each satellite longitude
Baseline rain-induced unavailabilities (*without* MVDDS interference):

101° W:	2.17 hr/yr
110° W:	3.88 hr/yr
119° W:	24.56 hr/yr

Figure 5-1. Interference Impact Predictions for Benchmark Case

These values of *MVDDS transmitter output power* were used in the simulations: -10, –4, –1.5, 0, 10, 20, and 30 dBm, with 0 dBm the value most often used. (These are raw transmitter output power values, *not* EIRPs. The MVDDS EIRPs are 10 or 14 dB higher than the raw powers, depending on the type of transmitting antenna employed.)

All the simulations assumed an *MVDDS modulation/channelization scheme* identical to that of DBS. Alternative schemes could conceivably be implemented, but insufficient information exists on such schemes to provide an adequate basis for predicting their interference impacts.

The measured radiation patterns of four different kinds of *MVDDS transmitting antennas* were used in the simulations: the large and small sectoral horns of Northpoint and Pegasus, respectively.

Several *MVDDS boresight azimuth angles* were considered in the simulations. The most commonly used was 180° (due south). Also modeled were 135° (southeast), 225° (southwest), 090° (east), 270° (west), and 000° (north).

Two *MVDDS elevation tilt angles* were considered: 0° (used in all but one of the simulations) and 5°.

The radiation patterns of three different types of *DBS receiving antennas* were used: the 18” dish, the 24” x 18” single-feed reflector, and the 24” x 18” dual-feed reflector.

Thirty different combinations of *DBS-receiver boresight azimuth and elevation angles* were used—one for each of the three DBS satellite longitudes at each of the ten locales studied.

The following values of *MVDDS antenna height* (above the horizontal plane containing all the gridpoints) were considered: –50, 0, 50, 100 (the most commonly used value), 200, 300, and 400 meters.

Simulations were performed for three different assumed values of *DBS downlink frequency*: 12.20 GHz (the low end of the band), 12.45 GHz (the center frequency and the one most commonly assumed in the simulations), and 12.70 GHz.

Two values of *MVDDS-DBS carrier offset* were considered: 0 MHz (the value most often used) and 7 MHz.

Satellite EIRP depends on the satellite longitude of interest (101° W, 110° W, or 119° W) and the specific satellite and transponder under consideration. It also depends on the locale under consideration, because the shaped beams of the satellite transmitting antennas direct substantially different EIRPs toward different parts of the United States, as explained in (Barker, 14 March 2001). In most of our simulations we have assumed, for each of the three satellite longitudes, the satellite and transponder that produce the *minimum* ratio of satellite EIRP to receiver interference threshold that is possible for the locale of interest. The receiver

interference threshold is the minimum value of $C/(N+I)$ that allows the DBS receiver to meet the specified performance criterion, usually VQ6. The threshold is a function not only of the criterion but also of the code rate, which in turn depends on the DBS vendor—DIRECTV or EchoStar—to which the satellite belongs.

Minimizing the EIRP-to-threshold ratio allows the analysis to focus on the satellites with the tightest link budgets, and thus presumably the greatest susceptibility to MVDDS interference, in each locale studied. However, the minimum ratios were *not* used in the Phoenix or Los Angeles simulations for the 119° W satellite longitude, since those result in unacceptably weak downlinks with rain-induced unavailabilities of 323.46 and 177.67 hr/yr, respectively, even with MVDDS absent. Also, in one simulation, for comparison purposes we assumed *maximum* values for this ratio, to see how the *strongest* downlinks would fare in the presence of MVDDS interference. Table 5-1 shows the EIRP-to-threshold values and the associated "baseline" unavailabilities (without MVDDS) used in our VQ6 simulations. (Other values were assumed in our QEF and VQ1 simulations.)

Table 5-1. EIRP-to-Threshold Ratios (dBW) and Unavailabilities for VQ6

	Satellite Longitude								
	101°W			110°W			119°W		
Locale	**Vendor[a]**	**Ratio (dBW)**	**U_0 (hr/yr)**	**Vendor[a]**	**Ratio (dBW)**	**U_0 (hr/yr)**	**Vendor[a]**	**Ratio (dBW)**	**U_0 (hr/yr)**
Washington, DC (min. ratio)	D	47.7	2.17	E	46.5	3.88	D	43.3	24.56
Washington, DC (*max.* ratio)	D	48.0	1.95	D	47.7	2.62	E	49.6	1.73
Miami, FL (min. ratio)	D	48.1	8.10	E	46.0	17.46	D	43.6	57.91
Phoenix, AZ (min. ratio)	D	45.7	2.66	E	42.3	16.37	E[b]	42.1[b]	19.02[b]
Boston, MA (min. ratio)	D	46.2	2.92	E	45.5	4.77	D	42.4	44.63
Chicago, IL (min. ratio)	D	46.0	2.89	E	46.0	3.07	D	42.3	31.33
Houston, TX (min. ratio)	D	48.2	4.48	E	45.5	11.65	D	43.3	36.55
Los Angeles, CA (min. ratio)	D	45.5	1.42	E	41.9	11.69	E[b]	42.1[b]	9.29[b]
Denver, CO (min. ratio)	D	44.7	0.79	E	43.0	2.22	D	40.8	33.25
Seattle, WA (min. ratio)	D	44.0	6.84	E	41.8	28.79	D	41.3	55.87
Fargo, ND (min. ratio)	D	44.2	4.78	E	42.5	14.26	D	41.3	63.24

NOTES:

a. D = DIRECTV; E = EchoStar.

b. The *second*-smallest ratios (and their associated vendors and baseline unavailabilities) are shown for the 119° W satellite longitude for Phoenix, AZ and Los Angeles, CA.

c. Actual EIRP values fluctuate between 0 and 0.8 dB off peak, so we consistently subtracted 0.4 dB from the peak values of EIRP provided in (Barker, 14 March 2001).

d. The VQ6 receiver threshold values used in creating this table are 5.5 dB for EchoStar and 7.3 dB for DIRECTV, as explained in Section 3 of the report. To determine the satellite EIRP in dBW used for each case, add the appropriate value to the ratio shown in the table.

5.1.2 Discussion of Results

Appendix B contains 56 plots showing contours of constant predicted interference impact upon populations of postulated DBS receivers dispersed across horizontal planes in the vicinity of an MVDDS transmitter located at the origin. Free-space path losses are assumed for the MVDDS signal out to the 4/3-earth radio horizon, beyond which infinite signal attenuation is assumed. The radio horizon is located $4.126\sqrt{\Delta H_{MD}}$ km from the MVDDS transmitter, where ΔH_{MD} is the amount in meters by which that transmitter is assumed to lie above the horizontal plane being studied in a given simulation. (However, the radio horizon is ignored in the few simulations where ΔH_{MD} is zero or negative—i.e., where the MVDDS transmitter is assumed to lie in or below the horizontal plane of interest.) Color codes for the plots are discussed on pages B-1 and B-2.

The contour plot on page B-3 duplicates Figure 5-1. It addresses the "benchmark" case, in which the locale is Washington, DC, and the frequency of interest is 12.45 GHz. The MVDDS transmitter has no frequency offset, and emits a 0-dBm signal. Its antenna is a south-pointing Northpoint large sectoral horn, with no elevation tilt, 100 meters above the horizontal plane. The DBS receivers lying within that plane use 18" dish antennas and have a VQ6 performance criterion. The minimum possible EIRP-to-threshold ratio is assumed for each of the three satellite longitudes. The impact criterion is the maximum *absolute* unavailability increase. The contour associated with the smallest unavailability increase considered (0.3 hr/yr) extends about 6.5 km south of the transmitter, while the 1.0- and 3.0-hr/yr contours enclose considerably smaller areas.

The assumption of free-space path loss out to the radio horizon in this and the other plots means that "natural shielding" by terrain, foliage, and buildings is not being taken into account. This omission, necessitated by the lack of adequate data for predicting such shielding, undoubtedly exaggerates the sizes of the interference contours shown on the plots. If natural shielding were considered, those contours would certainly enclose smaller areas. However, the same is probably even more true of the MVDDS service boundaries. Natural shielding has the greatest effect when signals arrive at low elevation angles, as the desired MVDDS signals will nearly always be doing at the outskirts of their nominal service areas.

It is important to keep in mind that the real-world advantages and disadvantages of natural shielding are partially offset by reflection, scattering, and diffraction effects that also are not modeled here. These tend to illuminate the "shadows" cast by obstacles and reduce the degree of shielding in many cases.

Another simplifying assumption used in our analysis has been to disregard rain attenuation of the MVDDS signal. Had it been feasible to consider this factor, the interference contours would probably have shrunk further—but, again, so would the MVDDS coverage boundaries (during rain).

Our implicit assumption that only one MVDDS transmitter is involved represents yet another analytical simplification. Although multiple transmitters are likely to coexist in a given locale, in all but very limited regions a single transmitter will be the predominant source of interference to any single DBS receiver pointed toward a particular satellite. The reason is the strong dependence of received MVDDS signal strength on path distance and on the gain function of the DBS receiving antenna in the direction of the arriving signal. These effects will typically cause differences well in excess of 10 dB between the strongest MVDDS signal and the runner-up. Cases where the cumulative effect of additional MVDDS transmitters would exceed that of the predominant transmitter are expected to be relatively unusual and are not modeled here.

All the remaining plots represent "excursions" from the benchmark case, in which one, two, three, or four parameters are varied from their benchmark values to determine the sensitivity of the results to such variations. The legend beneath each such plot highlights in bold type the parametric changes that distinguish the scenario in question from the benchmark scenario.

Pages B-4, B-5, and B-6 revisit the benchmark case, except that they show separate unavailability results for each of the three satellite longitudes: 101° W, 110° W, and 119° W. Even though, as usual, the "weakest" downlink (the one with the smallest possible EIRP-to-threshold ratio) is being considered for each longitude, it is evident that for the 101° W satellite the unavailability increase is less than 0.3 hr/yr everywhere in the region studied. For 110° W the increase exceeds 0.3 hr/yr only within a region much smaller than a square kilometer. For 119° W the results are almost identical to those for the multisatellite result of page B-3, because the downlink from that satellite longitude is much weaker (in relation to the DBS receiver's interference threshold) than those arriving from the other longitudes. Consequently, its unavailability exceeds that of the other downlinks virtually everywhere in the region studied, completely overshadowing the "contributions" of the two other downlinks to the worst-case unavailability values depicted in the composite multisatellite benchmark plot of page B-3.

All plots after page B-6 show composite multisatellite results, in the manner of the initial benchmark plot of page B-3. The plot on page B-7 depicts in detail the one-square-kilometer region *behind* (north of) the south-pointing MVDDS transmitting antenna. Here the MVDDS coverage boundary is very complex, and the interference-impact regions are quite small but very intense, rising steeply to values above 30 hr/yr in the three "hot spots" that exist in the parts of the horizontal plane where DBS receivers pointing at the three satellites will also have to point very close to the source of MVDDS interference.

The plots of pages B-8 through B-10 evaluate the benchmark scenario in the light of alternative interference-impact criteria. On page B-8, the criterion is the maximum *relative* unavailability increase, expressed as a percentage of baseline unavailability; on page B-9, it is the maximum *total* unavailability increase; and on page B-10 it is the minimum clear-air

(C/I_M) value. Note that the relative-increase and total-unavailability numbers are based on the simplifying assumption that rain and MVDDS are the only causes of unavailability. If solar unavailability and other items in the unavailability budget were considered, the baseline unavailability would be larger and the relative increase due to MVDDS would shrink accordingly.

Pages B-11 and B-12 display the effects of increasing the MVDDS antenna height. When this rises to 200 meters (B-11), the maximum-absolute-unavailability-increase contours shrink noticeably—a shrinkage that becomes dramatic when the height increases to 400 meters (B-12). The shrinkage results from the relatively high vertical directivity of the MVDDS sectoral horn antenna. (The same vertical directivity also produces a much smaller but still noticeable shrinkage in the MVDDS coverage boundary as the antenna height increases.)

On the other hand, pages B-13 through B-15 show that *reducing* the antenna height below 100 meters has relatively little effect on the interference impact. The interference contours for heights of 50 meters (B-13), 0 meters (B-14), and –50 meters (B-15) all look quite similar to those obtained for 100 meters in the benchmark case. Of course, natural shielding would undoubtedly reduce the interference regions (as well as the MVDDS coverage area) if such obstructions were considered in our model. The results at low heights, especially when ΔH_{MD} is zero or negative, are useful mainly for quantifying the possible effects of MVDDS interference on DBS receivers that might happen to be located on hillsides rising above the level of an MVDDS transmitter.

Page B-16 shows the effect of a 5° upward *elevation tilt* in the MVDDS antenna. The tilt directs the antenna's main beam away from the horizontal plane and obviously reduces the size of the interference contours, although a substantial reduction in MVDDS coverage area also occurs.

In the simulation of page B-17, a 7-MHz *frequency offset* is postulated between the MVDDS and DBS carriers. The resultant 1.7 dB of interference protection, documented in Section 3, substantially shrinks the interference contours while leaving the MVDDS coverage boundary unchanged.

Page B-18 shows the effect of using the Northpoint *small* sectoral horn instead of the large one. The effects are reminiscent of those produced earlier when large horn was tilted 5° upward: shrinkage of the interference region, but with a concomitant reduction in MVDDS coverage to the south. The slightly "squashed" radiation pattern of the small horn antenna actually provides slightly better coverage to the sides than directly in front of the antenna.

Pages B-19 through B-25 depict the effects of changes in the *azimuth angle* of the MVDDS transmitting antenna in the Washington, DC area. When a Northpoint large sectoral horn antenna is pointed to the southeast (B-19), the interference contours are smaller

than for the south-pointing benchmark case, but a southwestern orientation (B-20) makes the situation worse. An eastern orientation (B-21) helps substantially, but not a western one (B-22). Contrary to widespread expectation, pointing the antenna *north* (B-23) seems to work quite well, undoubtedly by ensuring that the "butterfly backlobes" of the DBS receiving antenna will not be illuminated by the Northpoint main beam. The plots of pages B-24 and B-25 explore this scenario further. On page B-24 is a detail of the region in front (i.e., north) of the north-pointing MVDDS transmitter, with hot spots that are larger—and undoubtedly also more intense—than the ones in the detail of page B-7 for the south-pointing case. Page B-25, reverting to the usual scale, shows the region behind (south of) the north-pointing transmitter.

Page B-26 shows what happens when the *maximum EIRP-to-threshold ratio* (rather than the minimum) is assumed for each satellite longitude. In this case the interference contours virtually disappear from the map, because here the simulation is addressing the strongest downlinks, which are best able to resist MVDDS interference.

The plot of page B-27 depicts the effect of ignoring the 1-dB *interference-scaling factor* used in nearly all the other simulations. It is assumed here that MVDDS interference has exactly the same disruptive effect as Gaussian noise. This changed assumption produces a significant but not particularly dramatic enlargement of the interference contours.

Pages B-28 and B-29 show interference contours for two alternative *DBS-receiver performance criteria*: QEF (B-28), which greatly enlarges the regions of apparent interference impact; and VQ1 (B-29), which dramatically shrinks them.

Pages B-30 and B-31 depict the effects of alternative *DBS receiving antennas*. The 24"x18" single-feed antenna (B-30) greatly reduces the interference regions, presumably by eliminating the butterfly backlobes. The 24"x18" dual-feed antenna (B-31) seems somewhat less effective in controlling interference.

Two plots consider the frequencies at the low and high ends of the band: 12.20 GHz (B-32) and 12.70 GHz (B-33). The interference regions seem smaller in the latter plot.

Variations in the *MVDDS output power* are explored in the plots of pages B-34 through B-41. Unsurprisingly, as the power increases the interference contours expand (and so does the MVDDS coverage boundary, although the radio horizon limits this effect unless the MVDDS antenna height is increased along with the power.)

In the next fourteen plots, nine alternative *locales* are considered. DBS receivers in those locales all seem more susceptible to MVDDS interference than they are in Washington, DC, at least in the scenarios considered. In Miami, FL (B-42), the area encompassed by the 0.3-hr/yr contour seems to be well over twice as large as in the benchmark Washington, DC scenario. Much the same is true of Phoenix, AZ (B-43). (Page B-44 shows another Phoenix plot where the interference-scaling factor has been ignored, as it was on page B-27, with

similar results.) The interference contours are also relatively large in Boston, MA (B-45), Chicago, IL (B-46), and Houston, TX (B-47). (The prominent "spike" in the Houston plot appears to result from a similar spike that exists in the backlobe region of the DBS 18" receiving antenna.) Los Angeles (B-48) seems to have the smallest interference contours of any locale studied except for Washington, DC.

Potential MVDDS-to-DBS interference problems seem relatively severe in Denver, CO, Seattle, WA, and Fargo, ND. However, mitigation techniques are available and were simulated for Denver and Seattle. The serious problems indicated in the first Denver plot (B-49) were greatly mitigated when the MVDDS antenna was turned northward and a 7-MHz frequency offset was used (B-50). Even greater improvements were obtained for Denver when these expedients were supplemented by raising the MVDDS antenna 300 meters above the plane of interest. The same measures yielded similar improvements in the Seattle simulations of pages B-52 through B-54, although the improvements there were not as dramatic as for Denver. This is partly because the problem in Seattle was smaller to begin with, but a more important reason may be that satellite elevation angles are lower in Seattle than in Denver. This decreases the angular separation between the DBS receiving antennas' main beams and the horizontal plane containing the MVDDS main beam, thereby tending to increase the gain product and thus the amount of MVDDS interference coupled into the DBS receiver. The results for Fargo appear on page B-55; mitigation techniques were not tried for that locale.

All the simulations discussed above assumed the use of Northpoint antennas. The final three simulations employed *Pegasus* antenna patterns instead. Pegasus did not provide its actual antennas to MITRE for testing, so MITRE had to rely on a limited set of previously measured data supplied by Pegasus in modeling the radiation patterns of the Pegasus antennas. Of the patterns supplied by Pegasus, the only ones usable in these simulations were azimuthal-plane cuts, so our Pegasus simulations had to be confined to cases where the MVDDS antenna lies within the horizontal plane of interest (*not* above or below it) and the elevation tilt angle is zero. Page B-56 displays the results obtained under these conditions for the Pegasus large sectoral horn; the interference contours appear similar to those obtained under the same conditions for the Northpoint antenna and depicted on page B-14. Page B-57 shows results for the Pegasus *small* sectoral horn; the interference contours are larger than for its Northpoint counterpart (B-18) and the associated MVDDS coverage boundary has a rounder shape.

A Pegasus consultant has claimed (Telecommunications Systems, 2001) that Pegasus can increase the G/T of its own receivers 4 dB, to 15.2 dB/K, through the use of measures including the use of 67-cm receiving antennas. If Pegasus does this and then reduces its transmitter power by the same 4 dB (to –4 dBm), thus keeping its coverage boundary constant while reducing its interference contours, the results will look as shown on page B-58 if the Pegasus large sectoral horn is used. It must be noted that Northpoint or any other

MVDDS vendor could obtain equivalent results by using the same measures (including larger receiving antennas) to increase G/T.

5.2 Criteria for Sharing

The analysis provided in previous sections provides insight into the potential extent of possible interference from MVDDS transmitters. The analysis and results shown above describe how bad interference might be. However, it is important to recognize that the results given are representative only. In any given MVDDS deployment many factors are available to the system designer and these factors may be used to reduce the real impact of potential interference. In light of this, the FCC may decide to impose certain criteria for the deployment of an MVDDS system. The goal of this section is to suggest some possible criteria that might be used by the FCC for this purpose.

Section 5.2.1 provides a list of some possible types of criteria. From these, two are selected for discussion in more detail. Section 5.2.2 presents criteria in terms of *C*/*I* ratios. Quantitative results are provided for a wide range of impacts on DBS unavailability. If the FCC chooses to impose criteria, these results will be an aid to determine a specific quantitative set of values for these criteria. Section 5.2.3 presents similar results in terms of interference levels at the DBS receiver. Again quantitative results are given as an aid to the FCC for selection of specific criteria.

5.2.1 Possible Sharing Criteria

Many different criteria are possible for the protection of DBS receivers in the presence of MVDDS transmitters. In general these limit either the computed unavailability or the interference power. Some possible criteria are as follows:

1. Maximum total unavailability
2. Maximum increase in unavailability
3. Maximum relative increase in unavailability (in percent)
4. Minimum *C*/*I*
5. Maximum interference power at the DBS LNB
6. Maximum power flux density (PFD)
7. Maximum power or EIRP

The exact wording of a given criterion would depend on a number of policy issues. Some of these issues are discussed in Section 6.1. However, an example criterion might limit one of the quantities above for any possible DBS receiver location in areas zoned residential or industrial. Criteria would also need to take into account the envelope of possible DBS antenna patterns and the various DBS satellites that are in view. Clearly many

things affect each parameter above and the FCC would need to decide which to hold constant and which might be allowed to vary. For example, a limit on total unavailability might vary by city, but a particular DBS antenna envelope might be used in all cases.

The following Sections discuss two of the above criteria in detail.

5.2.2 Minimum *C/I* Criteria

Recall that the long-term (i.e., in an average year) DBS basic service outage caused by rain depends on the rainfall rate at the geographic location under consideration. As the MVDDS is introduced into the operating environment, the effective noise floor of the DBS system is increased. The compatibility of the MVDDS with the DBS system can be described in terms of three critical parameters as mentioned in Section 2.1, namely:

- V—the percentage increase of the unavailability of the DBS service from its basic service outage rate p_{Rm}.
- ΔU—the increase in time of the DBS service unavailability from its basic service outage time U_0.
- P_{total}—the total percentage of time in an average year that the DBS service is unavailable (due to rain plus MVDDS).

The geographic dependence of these parameters at selected U.S. cities has been investigated and discussed in Section 5.1. Note that each of these parameters can be expressed, either explicitly or implicitly, as a function of the received rainy-sky carrier-to-MVDDS interference power ratio $[CI_{MV}]_{rainy\text{-}sky}$ which is related to the clear-sky C/I, $[CI_{MV}]_0$, through the effective rain margin A_{eRm} as discussed in Section 2.1, i.e.,

$$[CI_{MV}]_0 = [CI_{MV}]_{rainy\text{-}sky} + A_{eRm}$$

where all quantities are measured in dB.

Based on the results presented in Section 5.1 for the "worst case" satellite (longitude 119° W) scenario, Figure 5-2 illustrates the relationship between V and $[CI_{MV}]_0$ at ten selected U.S. cities.

(a): Boston, MA

(b): Chicago, IL

(c): Denver, CO

(d): Fargo, ND

(e): Houston, TX

(f): Los Angeles, CA

(g): Miami, FL

(h): Phoenix, AZ

(i): Seattle, WA

(j): Washington, DC

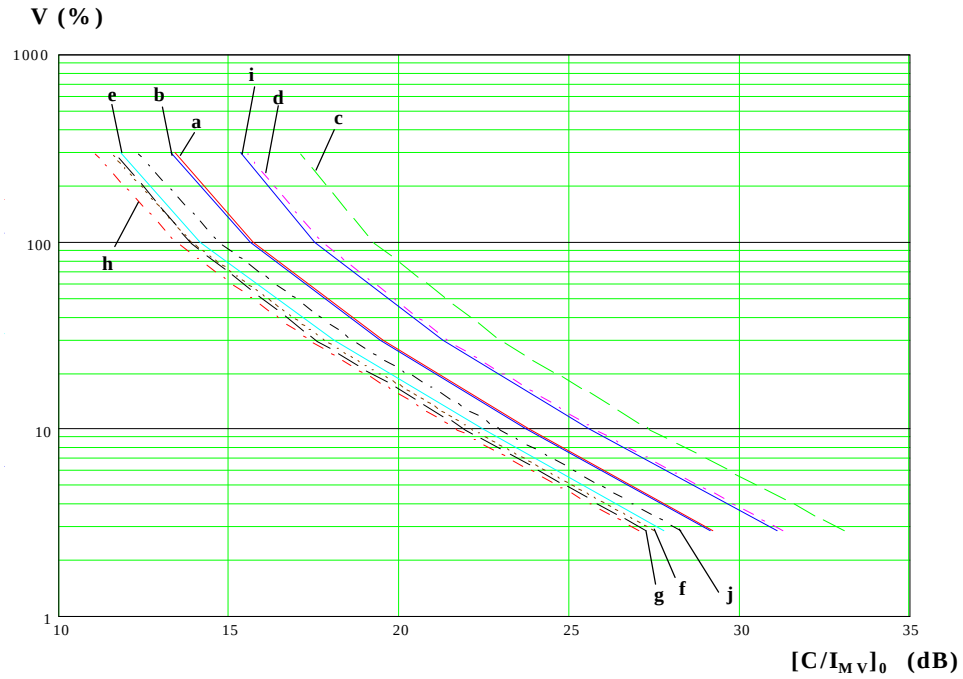

Figure 5-2. Percentage of Increase of Unavailability for DBS System

Figure 5-3 shows ΔU, in hours per year, at these sites as a function of $[CI_{MV}]_0$.

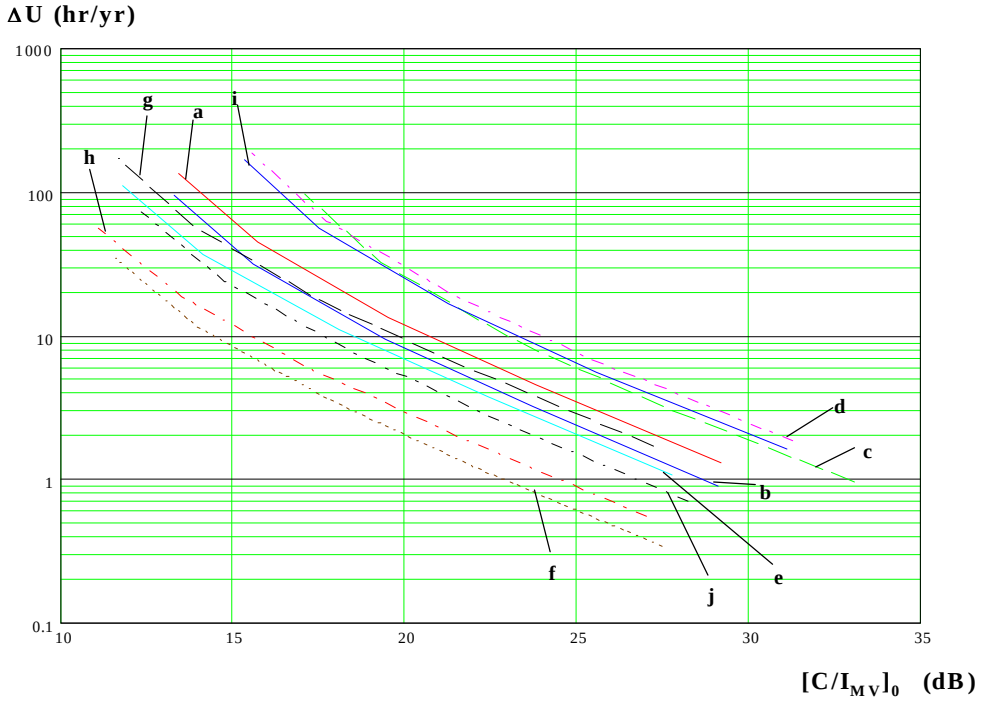

Figure 5-3. Increase in Time of Unavailability for DBS System

The resulting total unavailability probability of the DBS system (due to the effects of rain and MVDDS) is depicted in Figure 5-4.

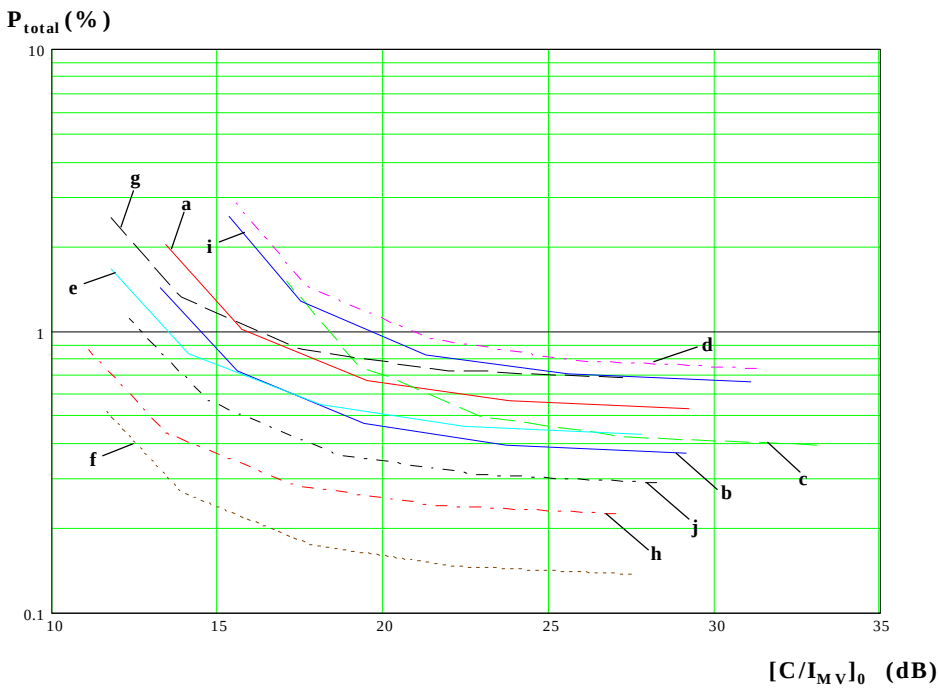

Figure 5-4. Total Percentage of Time of Unavailability in an Average Year for DBS System

The figures are developed to facilitate the FCC policy decision makers to formulate the overall criteria, and /or specific requirements at an individual locale, in terms of these parameters. Once the maximum acceptable value of a given parameter is decided, the required minimum value of $[CI_{MV}]_0$ can be established to meet the specification. For example, the minimum $[CI_{MV}]_0$ associated with the requirement that the MVDDS should cause no more than 10 % increase in the DBS system unavailability time can be determined from Figure 5-2 for different locales and the results are listed in Table 5-2.

Table 5-2. Example of Minimum $[CI_{MV}]_0$ to Satisfy the Requirement $V \leq 10$ (%)

Location	Minimum $[CI_{MV}]_0$ (dB)
Boston, MA	23.8
Chicago, IL	23.7
Denver, CO	27.3
Fargo, ND	25.7
Houston TX	22.4
Los Angeles, CA	22.1
Miami, FL	21.9
Phoenix, AZ	21.6
Seattle, WA	25.5
Washington, D.C.	22.9

Similarly, Figures 5-3 and 5-4 can be used to establish the minimum $[CI_{MV}]_0$ when dealing with the respective requirement categories.

5.2.3 Maximum Interference Level Criteria

Another possible set of criteria could be based on limiting the interference power level at the input to the LNB of the DBS receive antenna. Criteria would be of the form

$$I_{actual} \leq I_{max} \tag{25}$$

The actual interference power, $\boldsymbol{I}_{actual}$, would need to be computed for each MVDDS transmitter and for each possible location of a DBS receiver. Clearly the left side of the expression will vary dramatically as a function of the location near the MVDSS transmitter. In fact, plots of these values will depend on the DBS receive antenna pattern and will bear a resemblance to the figures discussed in Section 5.1. The right side of the expression above forms the limiting value that must be met. If the FCC chooses criteria of this type, the value for $\boldsymbol{I}_{\max}$ would be specified. This value might vary by city because of differences in rain statistics and available DBS satellite EIRP.

It would be helpful to establish a relationship between the interference power level and various measures of unavailability. This can be done as follows. We recall the following equation from Section 3.4:

$$\gamma_0 \leq \frac{C(A)}{(I/\mu)+N(A)} \tag{26}$$

Where:

γ_0= the threshold C/N value for noise

$C(A)$ = the received carrier power, as a function of the rain attenuation ratio, A

A = the rain attenuation ratio

I = the interference power

$N(A)$ = the noise power, as a function of the rain attenuation, A

μ = a factor that accounts for reduced susceptibility to MVDDS

All quantities are power levels or dimensionless power ratios. Now, the received carrier power is equal to the clear sky signal level divided by the rain attenuation ratio. Also, the "noise" is actually made up of thermal noise and other interference terms. These other terms account for adjacent satellite interference, uplink noise, and cross-polarization interference. Any downlink rain attenuates all these other types of interference. Further, the thermal noise is also affected by downlink rain. So, the $N(A)$ term above can be expanded as follows:

$$N(A) = N_1 - \frac{N_2}{A} + \frac{S}{\rho A} \tag{27}$$

Where:

N_1 = the noise power of the system when rain attenuation is very large

N_1 - N_2 = the noise power of the system with no rain attenuation

N_2 = the difference between the noise power with large rain attenuation and the noise power with no rain attenuation

S = the clear sky signal level

ρ = the C/N value for other types of interference

Substituting into equation 1 and remembering that the carrier is attenuated by noise, we get:

$$\gamma_0 \leq \frac{(S/A)}{(I/\mu)+N_1-(N_2/A)+(S/\rho A)} \tag{28}$$

This can be rearranged to solve for the rain attenuation ratio, A, as follows:

$$A \le \frac{N_2 + S[(1/\gamma_0) - (1/\rho)]}{N_1 + (I/\mu)} \tag{29}$$

So, for a given interference level, I, the rain attenuation must be less than the value given above for the link to work. From the rain attenuation, A, the link unavailability can be computed. (In the figures below, unavailabilities greater then 5% have been interpolated between the 5% point and 100% at the 0 dB rain loss point.) This unavailability can be compared to the value that results from setting $I = 0$ in the equation above.

To illustrate this approach, we provide several examples. These are shown for several cities with 8 different satellites. Figure 5-5 shows the total unavailability, in percent, as a function of interference power level for Washington DC. Results are shown for eight different satellites with a range of EIRP and threshold values. Otherwise, the scenario is approximately the same as for the baseline case in Section 5.1. Results shown are for a threshold based on video quality 6.

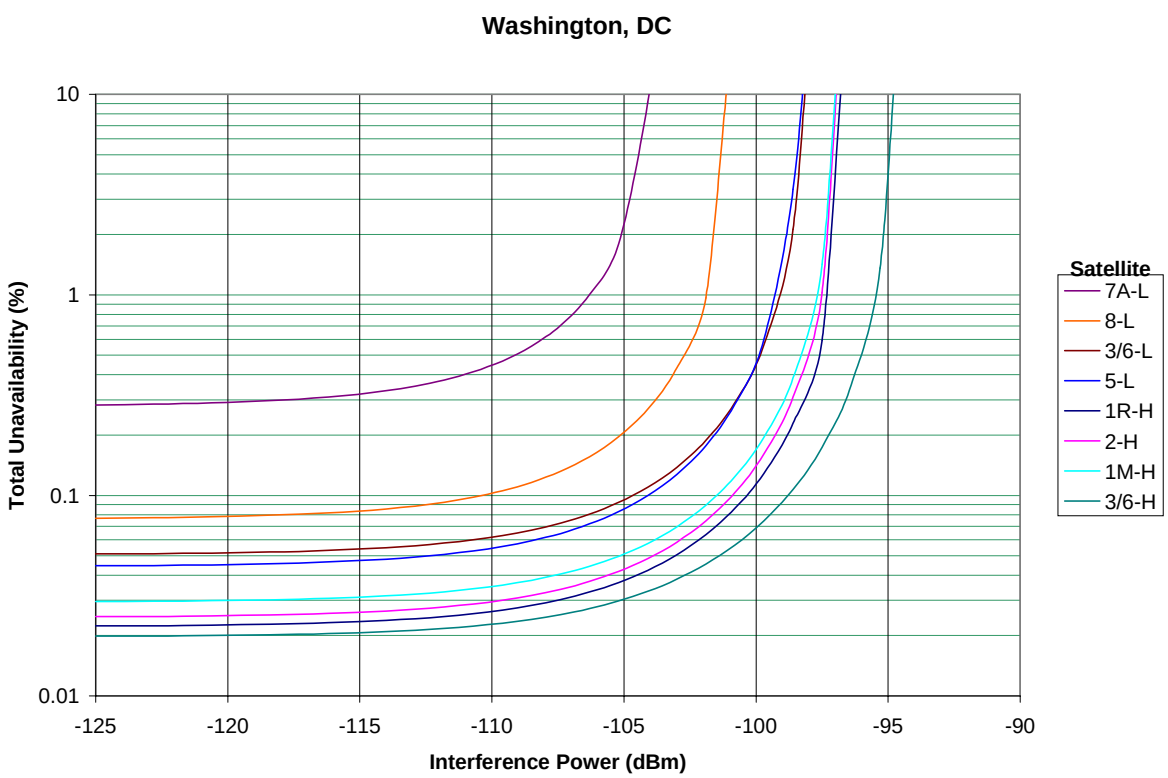

Figure 5-5. Total Unavailability for Washington, DC

In the figure, the prefix indicates the satellite and the suffix for each case indicates whether the satellite uses a high EIRP value or a low EIRP. The location of satellites is summarized in Table 5-3.

Table 5-3. Satellite Summary

Satellite	Location	System
USABSS-7A	119 W	DIRECTV
USABSS-8	61.5 W	EchoStar
USABSS-3, USABSS-6	119 W	EchoStar
USABSS-5	110 W	EchoStar
USABSS-1R	101 W	DIRECTV
USABSS-2	101 W	DIRECTV
USABSS-1M	110 W	DIRECTV

The results shown above can also be presented in terms of the hours of outage per year. These results are shown in Figure 5-6.

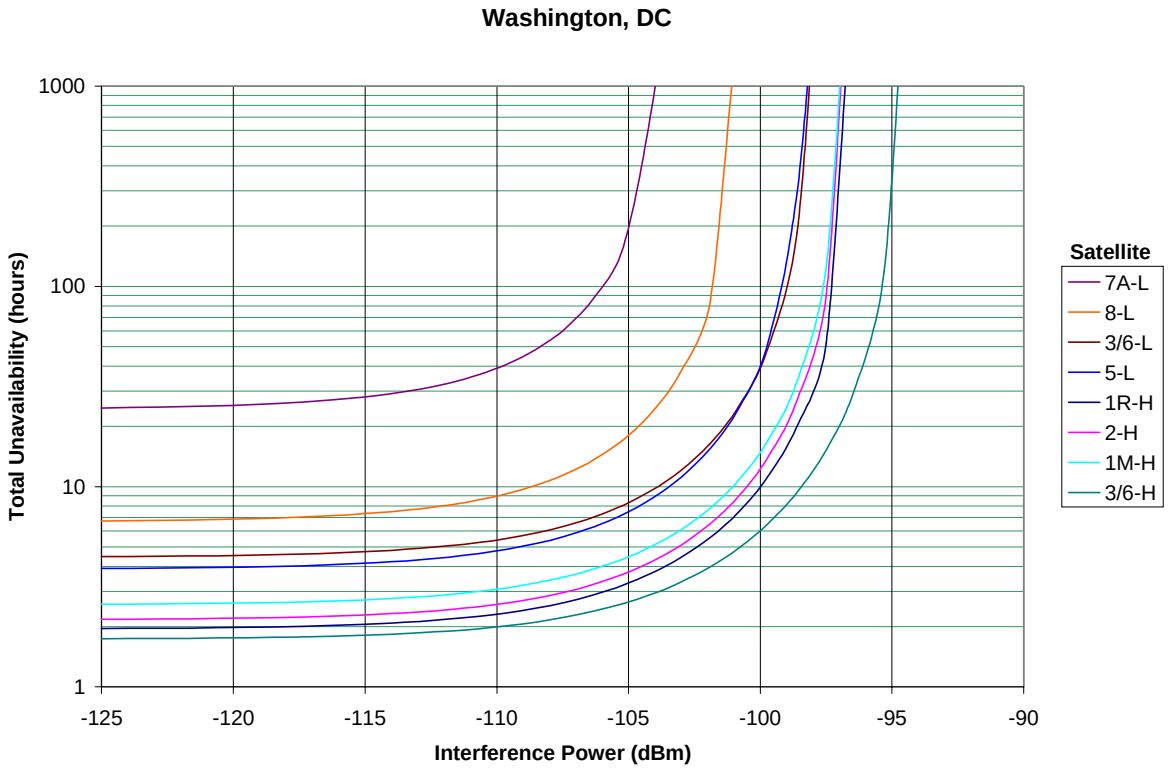

Figure 5-6. Total Unavailability in Hours for Washington, DC

From the results above, the increase in unavailability can also be computed. This is shown in Figure 5-7 in terms of the increase in the number of hours of outage.

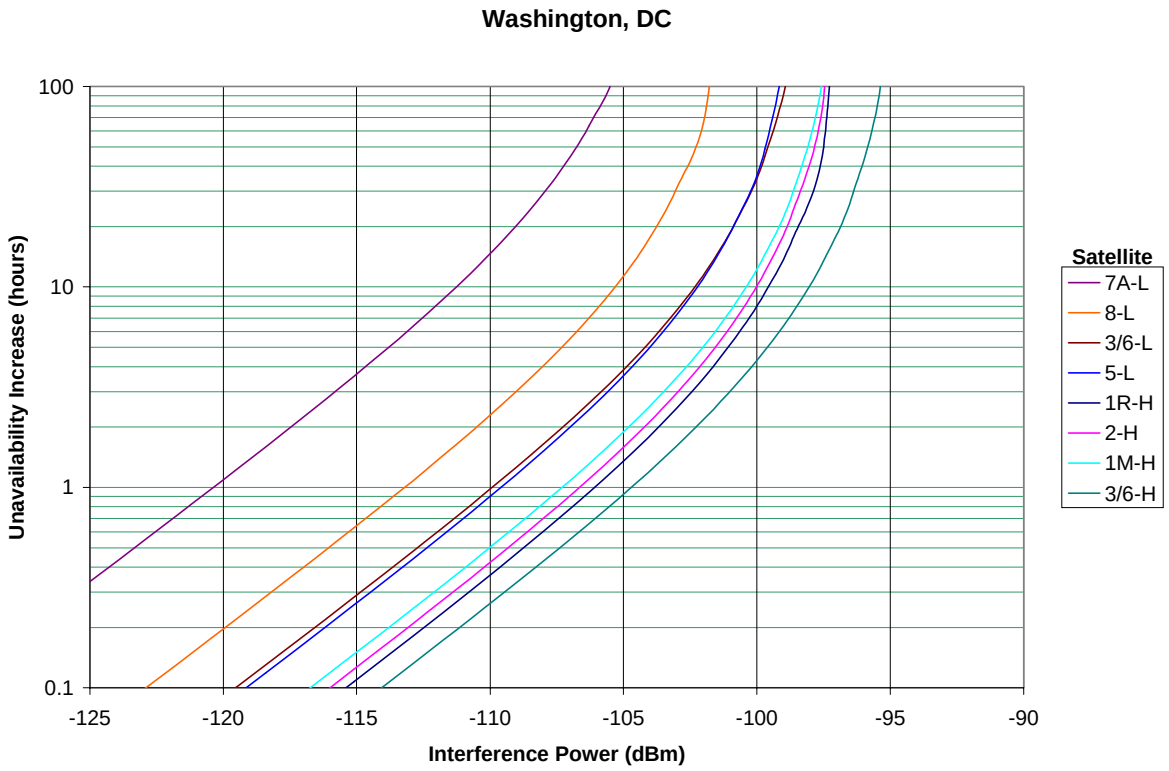

Figure 5-7. Increase in Unavailability

The relative increase in unavailability can also be computed. This is shown as a percentage of the baseline unavailability in Figure 5-8.

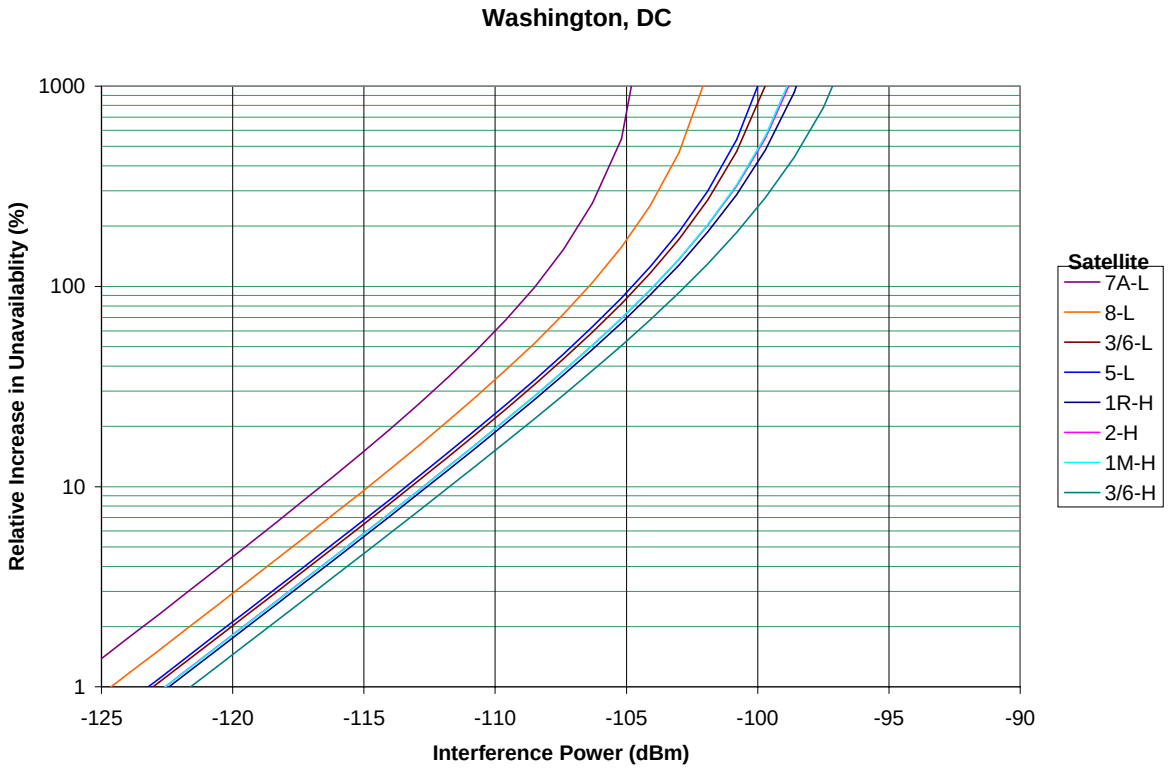

Figure 5-8. Relative Increase in Unavailability

As another example Figure 5-9, Figure 5-10, Figure 5-11, and Figure 5-12 show the impact of various levels of interference for Fargo, ND. For this scenario, the USABSS-8 satellite at 61.5 West longitude does not provide enough power to support the link, even with no interference.

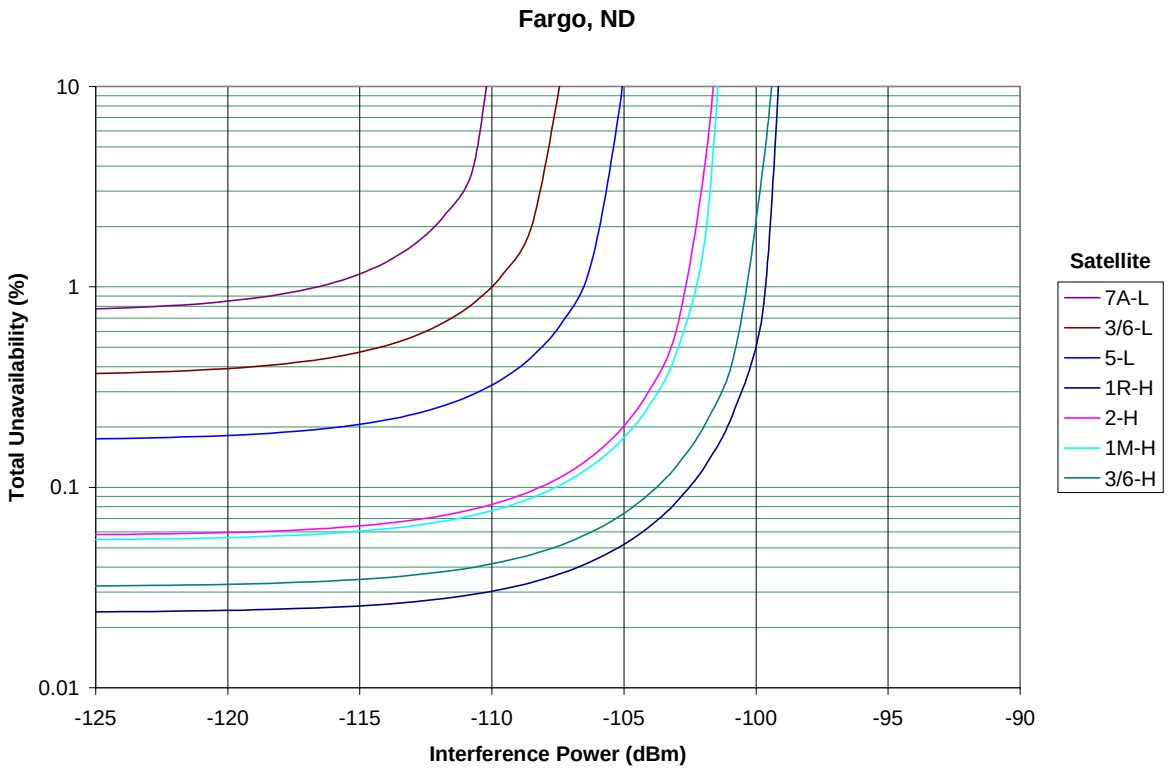

Figure 5-9. Total Unavailability, Fargo

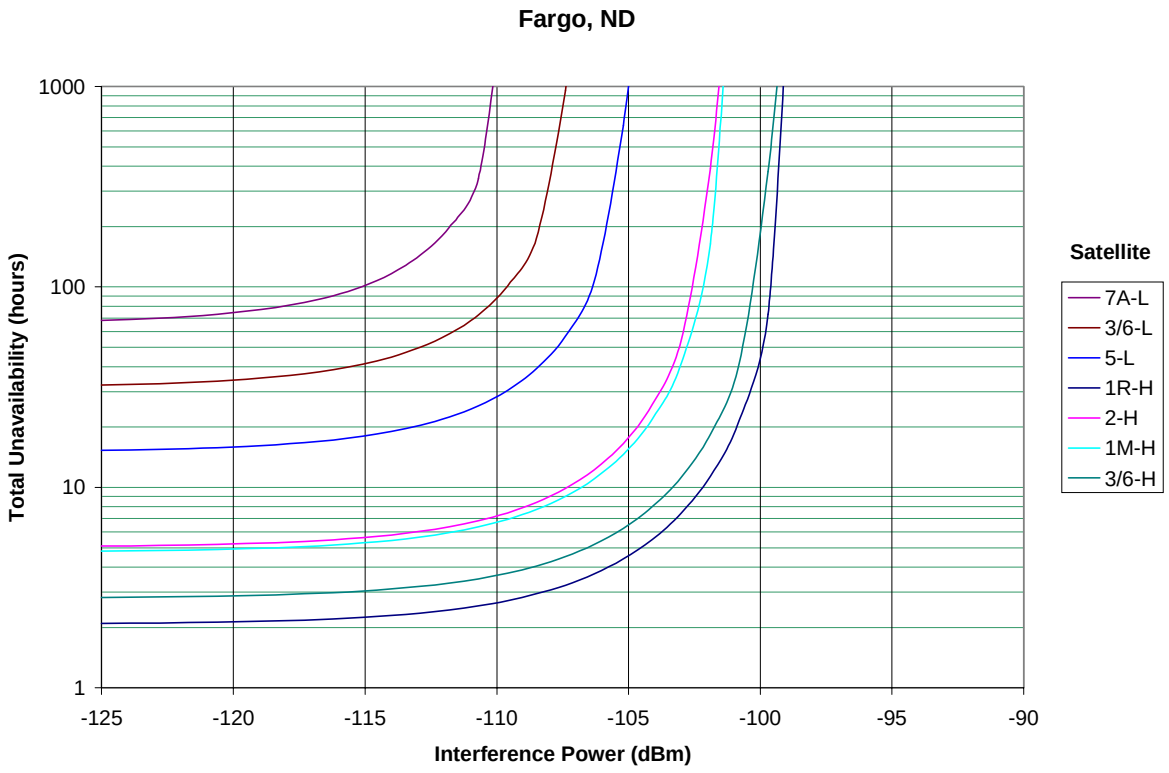

Figure 5-10. Unavailability in Hours, Fargo

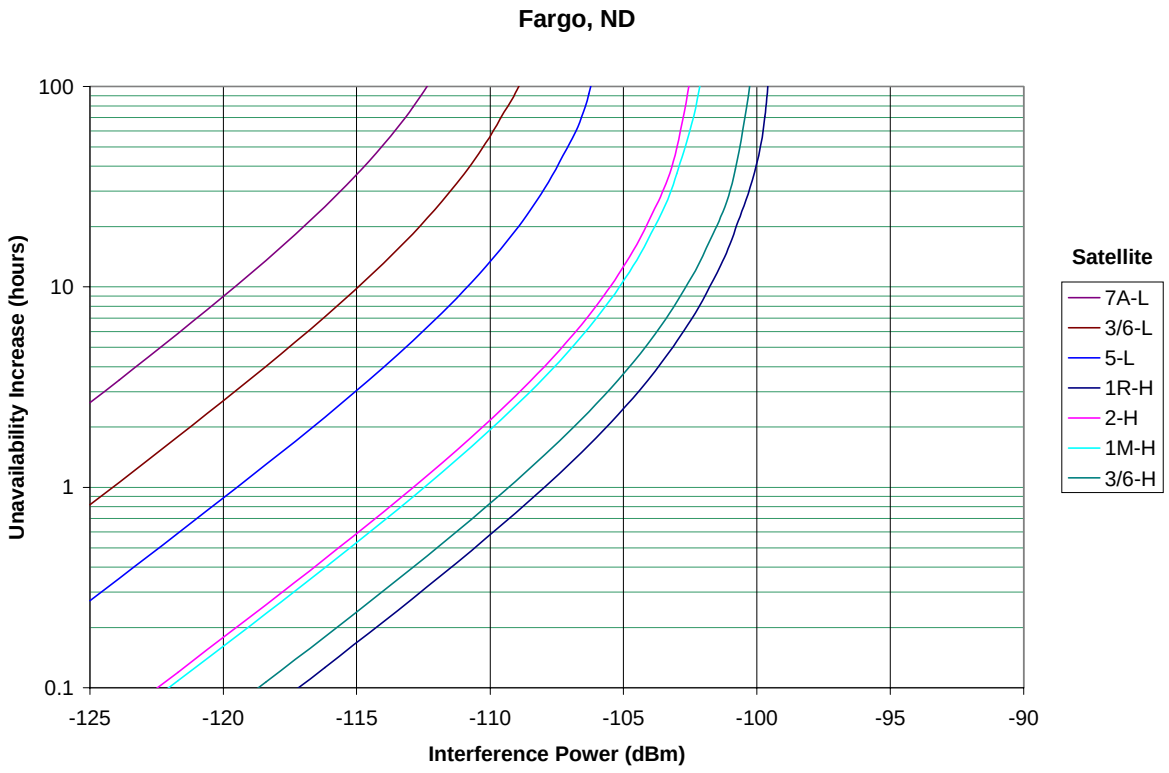

Figure 5-11. Unavailability Increase, Fargo

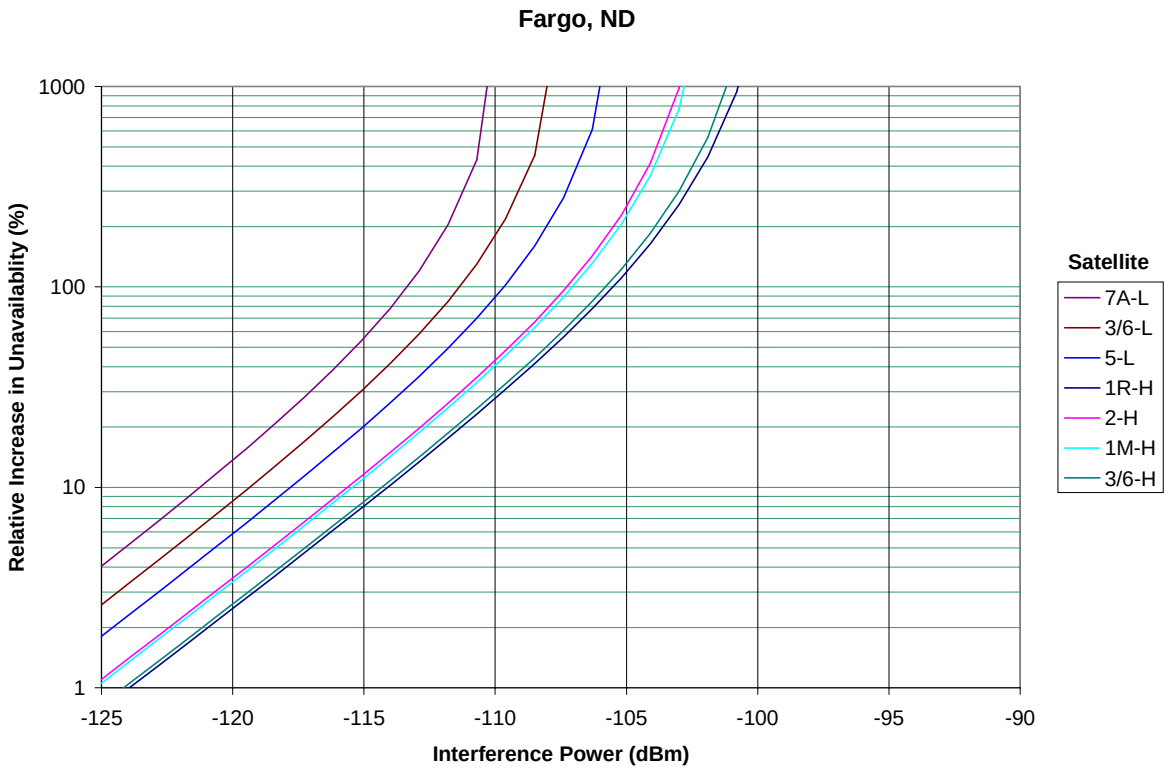

Figure 5-12. Relative Increase in Unavailability, Fargo

The following figures show the impact of interference for the city of Miami. Again the various measures of unavailability degradation are plotted as a function of the interference power level, in dBm.

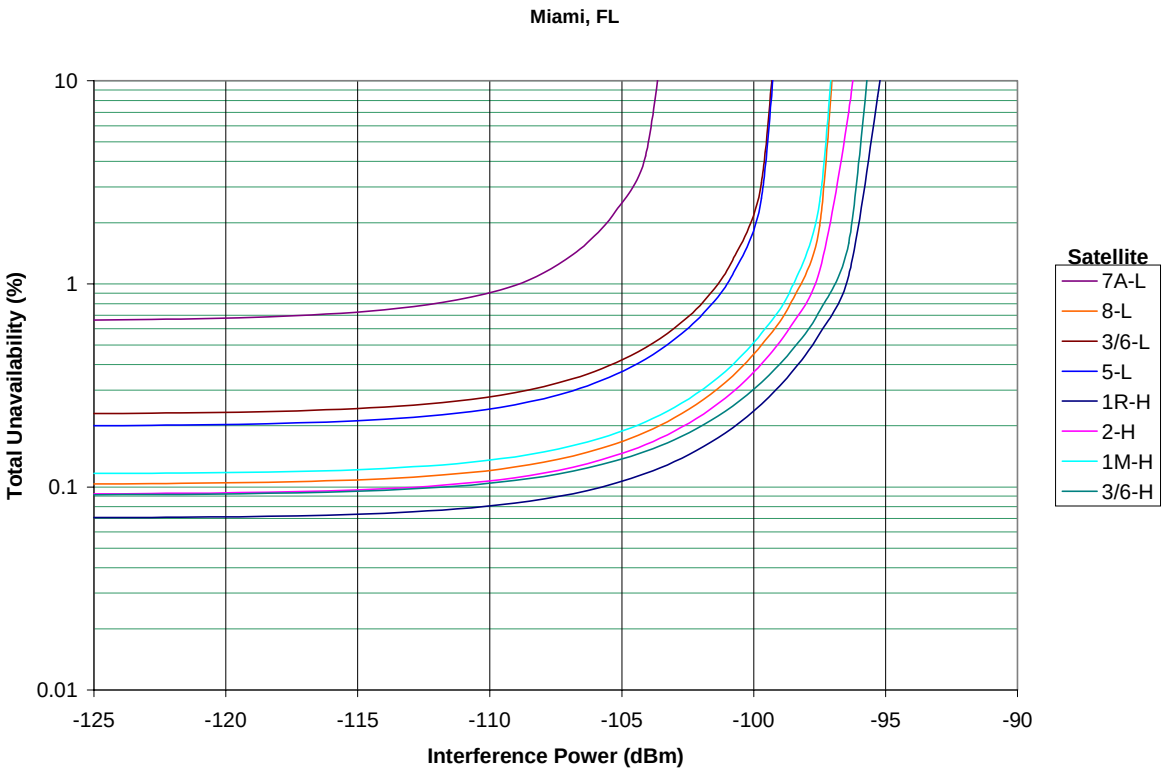

Figure 5-13. Unavailability (%) for Miami, FL

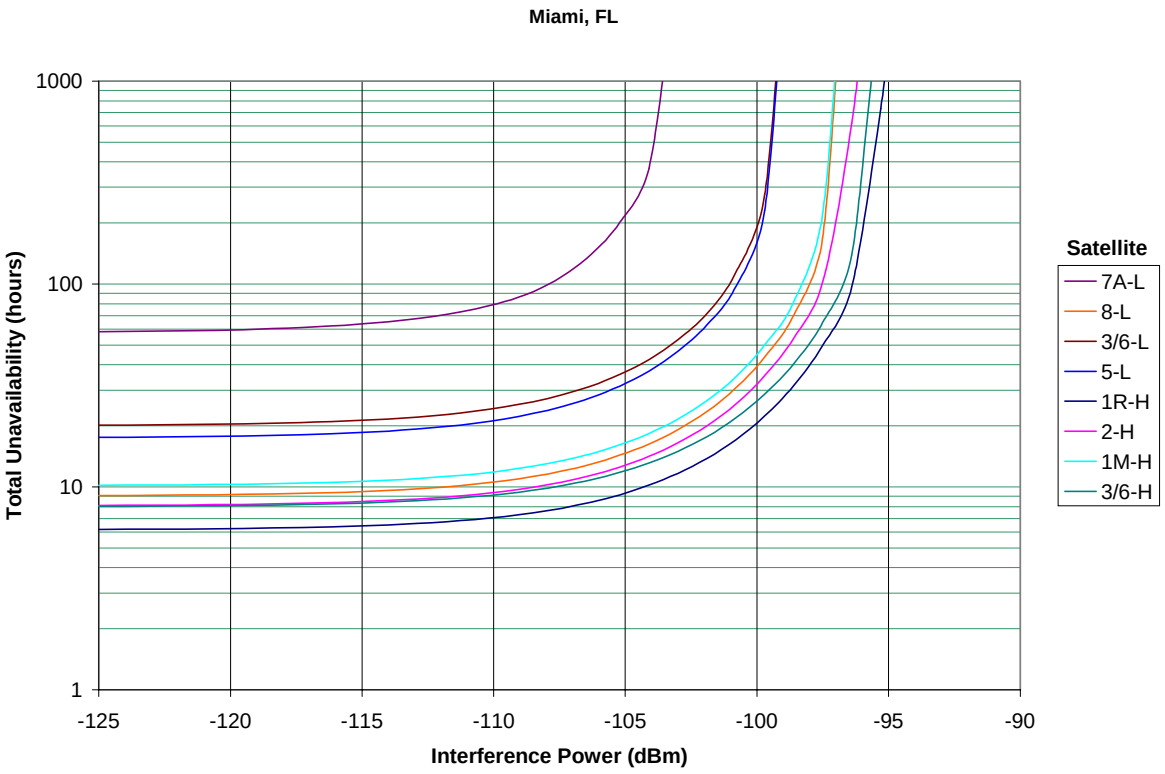

Figure 5-14. Unavailability (Hours) for Miami, FL

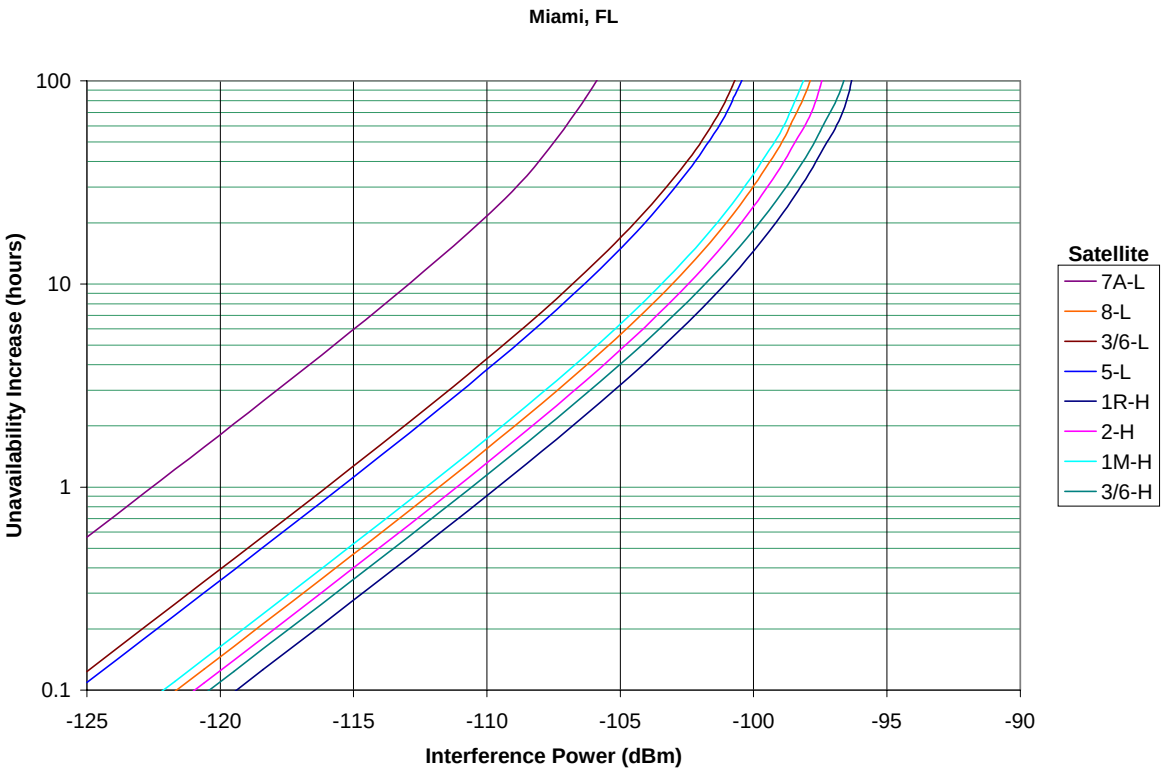

Figure 5-15. Increase in Unavailability (Hours) for Miami, FL

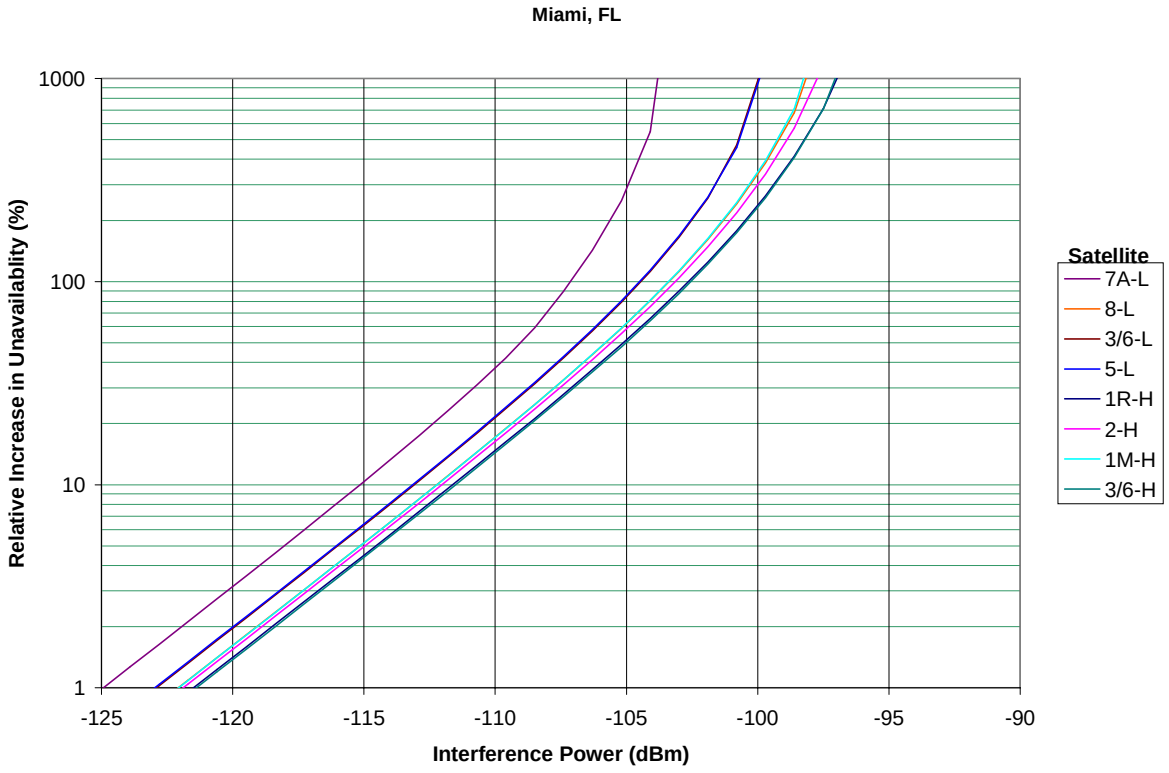

Figure 5-16. Relative Increase in Unavailability (%) for Miami, FL

The following figures present the impact of interference based on QEF video performance. These results are shown for the city of Washington, DC.

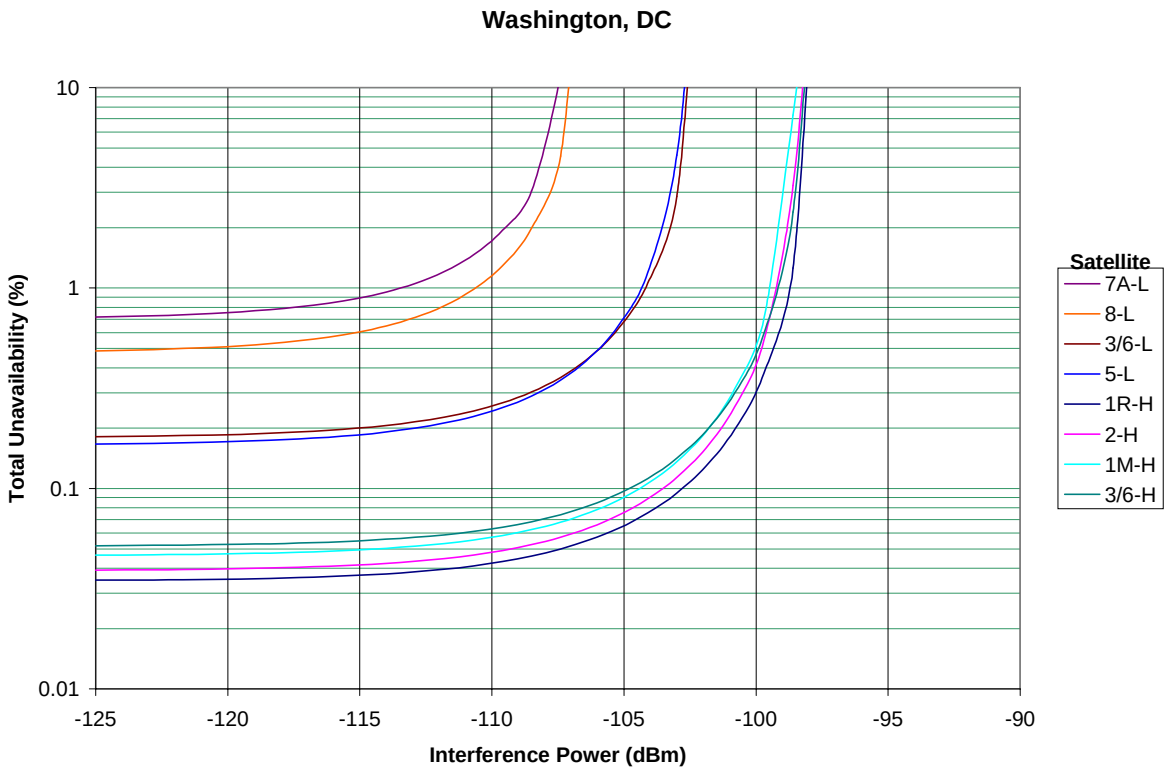

Figure 5-17. Total Unavailability (%) for QEF in Washington, DC

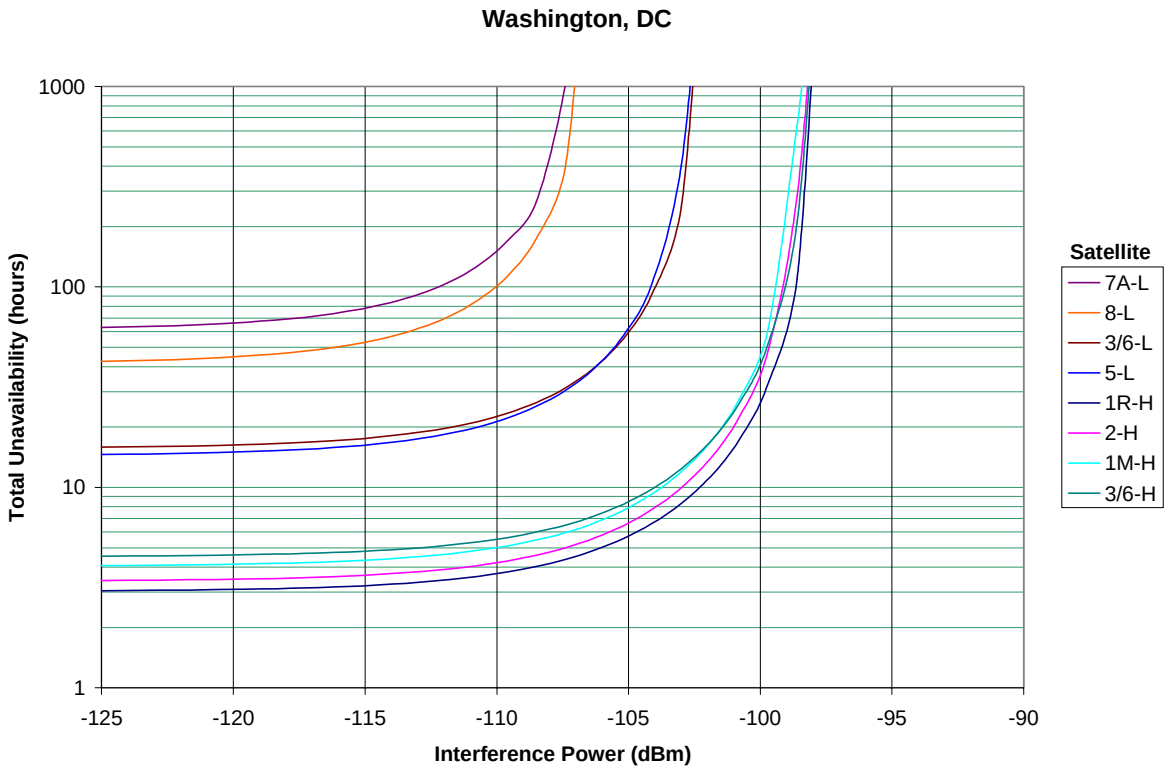

Figure 5-18. Total Unavailability (Hours) for QEF in Washington, DC

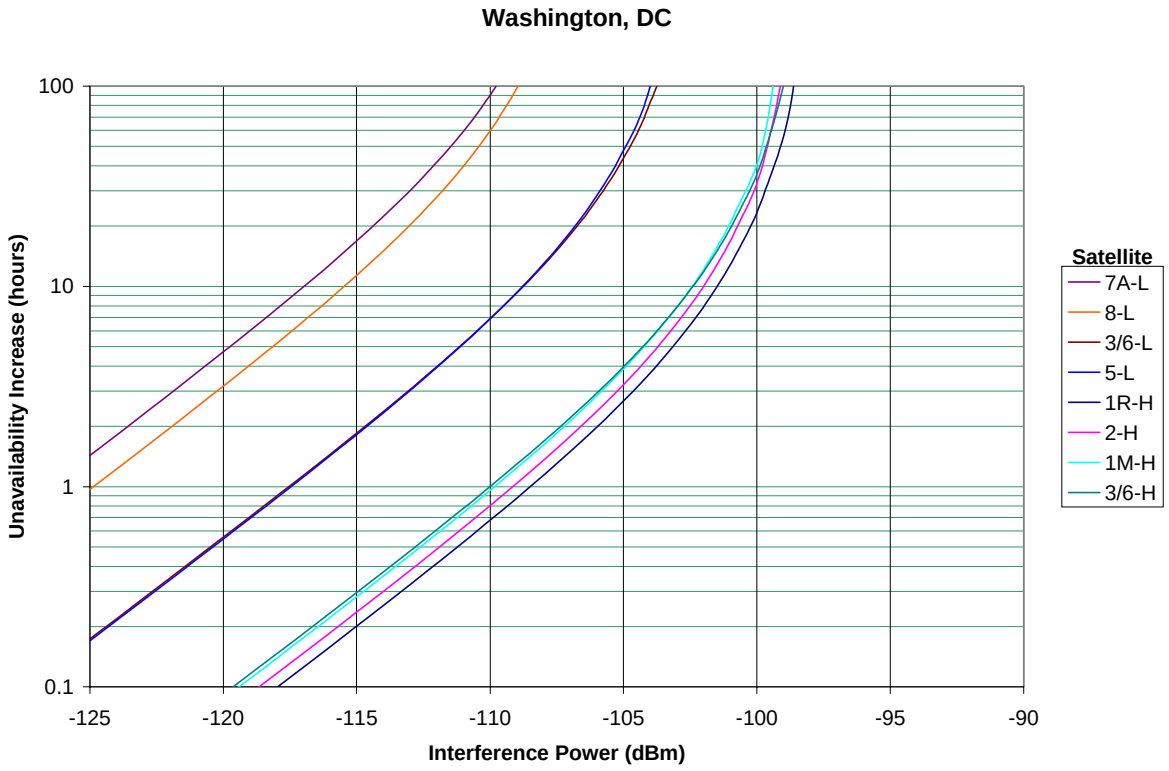

Figure 5-19. Unavailability Increase (Hours) for QEF in Washington, DC

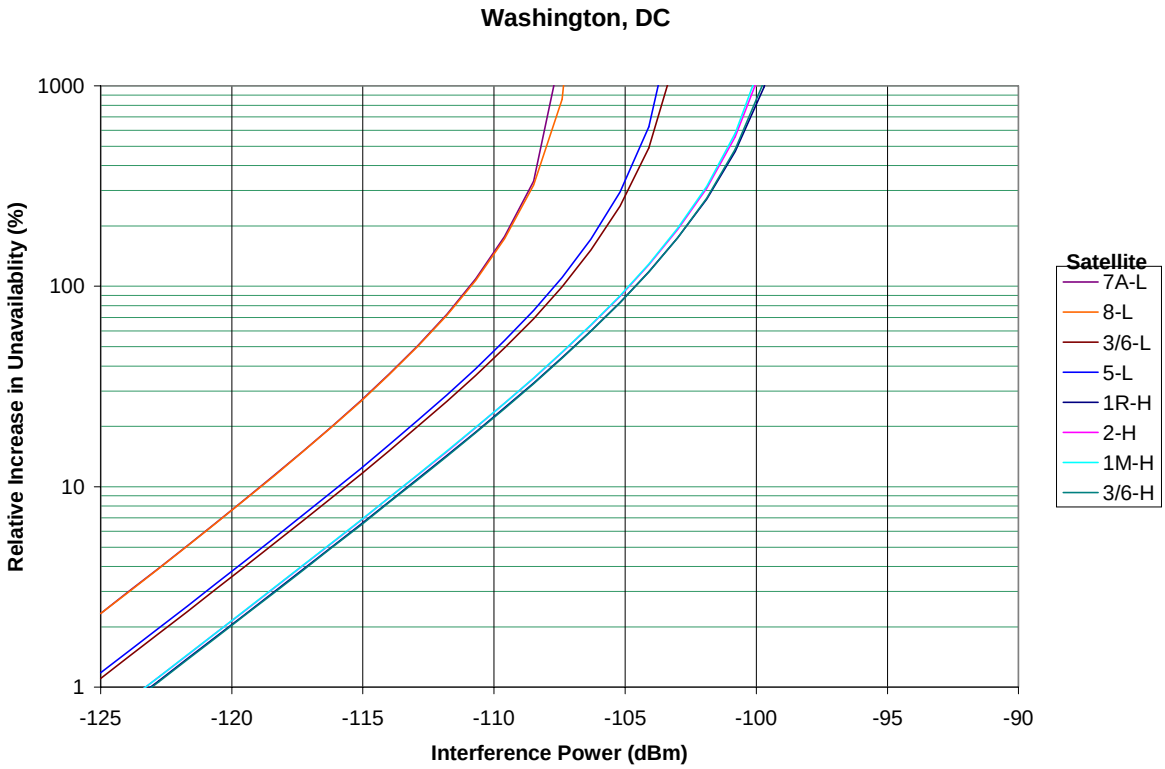

Figure 5-20. Relative Increase in Unavailability (%) for QEF in Washington, DC

Several observations can be made about the plots shown above. First, it is clear that the baseline unavailability varies dramatically depending on which satellite is used. These baseline unavailabilities without MVDDS interference can be seen by looking at the left end of, for example, Figure 5-9. For some satellites, the baseline unavailability is significantly worse than the desired value of 0.3%. Of course, we would expect changes in these baseline unavailabilities for different rain statistics, variations in DBS antenna gain, the video quality assumed, and a number of other parameters.

Also, we note that considering the relative increase in unavailability (measured in %) reduces some of the variability that exist for other measures of interference outage time. See, for example, Figure 5-6 as compared to Figure 5-9. This reduction in variability makes the relative increase in unavailability more attractive as a measure of degradation.

The interference levels shown above could also be converted to a power flux density (PFD) using the following equation:

$$PFD = I \frac{4\pi}{\lambda^2 G_R} \tag{30}$$

Where:

G_R = the gain of the DBS receive antenna

PFD = the power flux density limit

λ = the wavelength of the RF signal

Clearly, the PFD will vary with position of the DBS receiver as a result of the variations in the gain pattern of the DBS antenna. The equation above is suitable if the DBS receive antenna gain is based on the dominant mode polarization. See Section 4.5 for a discussion of polarization. If the polarization characteristics of the MVDDS and DBS antenna are such that a more sophisticated polarization analysis is required, then criteria would be better specified in terms of allowable interference levels, as shown here in this section. Either way, the characteristics of the DBS antenna must be known in order to determine whether a given criterion is met.

Section 6

Conclusions and Recommendations

In the preceding sections, typical results for various scenarios have been provided. In addition, suggested sharing criteria have been provided. In this final section, we draw conclusions from those results and suggest a way forward for the FCC. Section 6.1 discusses the general feasibility of MVDDS/DBS bandsharing. Section 6.2 provides a discussion of some interference-mitigation techniques that might be used. Finally, Section 6.3 highlights major policy issues and makes recommendations for resolving them.

6.1 Feasibility of MVDDS/DBS Bandsharing

The analysis and testing performed by MITRE and described elsewhere in this report have demonstrated that:

- MVDDS sharing of the 12.2–12.7 GHz band currently reserved for DBS poses a significant interference threat to DBS operation in many realistic operational situations.
- However, a wide variety of mitigation techniques exists that, if properly applied under appropriate circumstances, can greatly reduce the geographical extent of the regions of potential MVDDS interference impact upon DBS.
- MVDDS/DBS bandsharing appears feasible if and only if suitable mitigation measures are applied. Different combinations of measures are likely to prove “best” for different locales and situations.

The question remains: Do the potential costs of applying the necessary mitigatory measures, together with the impact of the residual MVDDS-to-DBS interference that might remain after applying such measures, outweigh the benefits that would accrue from allowing MVDDS to coexist with DBS in this band? Deciding that question is beyond the scope of MITRE’s charter for the present study. The FCC must make the decision after considering the analytical and test results presented in this report, and after resolving the policy issues discussed in Section 6.3.

6.2 Potential Interference-Mitigation Techniques

Techniques for preventing or reducing MVDDS interference in DBS receivers fall into three general categories:

- Selection of MVDDS operational parameters
- Possible MVDDS system-design changes

- Corrective measures at DBS receiver locations

In the following subsections we identify potentially useful interference-mitigation techniques in each category, and discuss the probable effectiveness of each in reducing the potential impact and geographical extent of MVDDS interference upon DBS operations. The techniques can be used separately or in combination, although a few are mutually exclusive, for reasons discussed below.

6.2.1 Selection of MVDDS Operational Parameters

The most important operational parameters that can be adjusted to control interference in existing MVDDS system designs are transmitter power, frequency offset, tower height, elevation tilt, and azimuthal orientation. Properly selecting these parameters can reduce the regions of potential interference impact, or direct much of that impact to areas containing few DBS subscribers.

- Keeping the MVDDS transmitter power as low as possible without sacrificing coverage requirements is often a prerequisite for minimizing interference to DBS.
- The use of a *7-MHz frequency offset* between the MVDDS and DBS carriers has been shown through MITRE's testing to reduce effective interference levels by 1.7 dB. The simulation whose results are shown on page B-17 demonstrates that this reduction noticeably shrinks the areas in which DBS receivers are potentially affected by MVDDS interference.
- *Increasing the MVDDS transmitting antenna height* reduces the sizes of the areas susceptible to a given level of interference. However, the simulations of pages B-11 through B-15 indicate that substantial benefits may not accrue unless the tower height is at least 100, or perhaps even 200, meters above the level of the DBS receiving antennas in the surrounding area. Fully utilizing this particular degree of freedom might be controversial in many locales.
- *Adjusting the elevation tilt* of the MVDDS transmitting antenna is not controversial, but our simulation results on page B-16 indicate that it may not be particularly effective either. Tilting the antenna up 5° reduces the interference-impact area but shrinks the MVDDS coverage area in roughly the same proportion. This presumably means that more MVDDS towers (creating additional interference-impact areas) would be needed to cover a given geographical region than if the antennas had not been tilted. The effect of a downward tilt has not been simulated, but there seems to be little reason to think it would be any more successful.
- *Pointing the MVDDS transmitting antennas* ***away from*** *the satellites*, rather than toward them as generally envisioned, could have beneficial effects in many situations. These are indicated by the simulation results of pages B-21 and B-23, and by the outputs of several other simulations in which easterly and northerly MVDDS

transmitter boresight azimuths were used. When the satellites are generally to the south and their elevation angle is reasonably high, as in Denver, dramatic improvements in interference protection appear possible when the MVDDS transmitting antenna points north. A major advantage of a north-pointing transmitter is that it does not illuminate the relatively high-gain "butterfly backlobes" of typical 18" DBS dishes. When satellite elevation angles are somewhat lower (as in Seattle) the geometry is somewhat less favorable, but north-pointing seems to yield significant benefits in all locales where it has been simulated. Further field testing to validate this concept is recommended. **Caveats:** The "hot spots" appearing on the opposite side of the MVDDS transmitting antenna from the satellites (see pages B-7 and B-24) are somewhat larger—although actually still quite small—and undoubtedly more intense for a north-pointing than for a south-pointing MVDDS transmitter. If this technique is tested or used, care must be taken not to place the north-pointing MVDDS antenna so close to the line of sight between a satellite and a DBS receiver, and so close to the receiver itself, that physical damage to the receiver could result. Another possible pitfall of this technique might be a reduction in opportunities for "natural shielding" of the kind mentioned in 6.2.3 below.

6.2.2 Possible MVDDS System-Design Changes

Potential MVDDS design changes that might reduce the interference impact on DBS downlinks include real-time power control, multiple narrow transmitting-antenna beams, the use of circular polarization, and increasing the sizes of MVDDS receiving antennas.

- *Real-time power control*, which would reduce MVDDS transmitter power as necessary to protect DBS downlinks from degradation during rain, has sometimes been proposed as a technique for controlling MVDDS-to-DBS interference. However, this might require an elaborate monitoring system. Worse, it would inevitably degrade MVDDS operation at the very times when it might be needed most (i.e., when DBS downlinks were shut down by heavy rain).

- The use of *multiple MVDDS transmitting-antenna beams*, each having a much narrower azimuthal beamwidth than the existing sectoral horns, might provide much better flexibility than the present antenna design in directing the interference-impact regions away from areas containing DBS subscribers.

- *Circularly polarized MVDDS transmitting antennas*, if they used the same system of alternate senses for adjacent channels that is employed by DBS, might pose a considerably smaller interference threat than the currently planned exclusive use of horizontal polarization. When a DBS signal on a particular channel is using RHC polarization, the butterfly backlobes of the DBS receiving antenna are highly susceptible to signals of the opposite (LHC) polarization sense for reasons discussed earlier in the report; about 3 dB less susceptible to the horizontally polarized

MVDDS signals to which they would be exposed under present MVDDS designs; and *much* less susceptible to MVDDS signals having the same (RHC) polarization as the desired DBS signal. The adjacent channels would be similarly protected, except that the senses of the circularly polarized desired and undesired signals would all be reversed, yielding the same net effect. (However, this suggested mitigation technique is *not* compatible with the existing 7-MHz frequency-offset method, and probably would also negate the benefits of the previously suggested technique of pointing MVDDS transmitting antennas away from the DBS satellites. The frequency offset would disrupt the necessary alignment of MVDDS and DBS channels, while north-pointing might largely eliminate the benefits of butterfly-backlobe polarization reversal, on which this technique depends.)

- *Larger MVDDS receiving antennas*, recently suggested by Pegasus, would increase their achievable gains and hence the G/T ratios of MVDDS receivers. This in turn would allow an MVDDS system to cover an identical service area with a smaller output power and hence with smaller resultant interference contours, as shown in the simulation of page B-58.

6.2.3 Possible Corrective Measures at DBS Receiver Locations

Corrective measures that can be applied at DBS receiver installations include relocation and retrofitting of existing DBS antennas, the use of alternative antenna designs, and the replacement of older DBS set-top boxes.

- *Relocation of DBS receiving* antennas to put nearby buildings between them and nearby MVDDS interferers, while still leaving desired satellites in view, is a well-known corrective measure (sometimes called “natural shielding”) that would undoubtedly be effective in many situations.

- The use of absorptive or reflective *clip-on shielding for existing DBS antennas*, to block any direct lines of sight that might exist between their LNBs (antenna feeds) and potentially interfering MVDDS transmitting antennas, is a technique that worked quite well during MITRE’s open-air testing.

- *DBS receiving-antenna replacement* is a relatively expensive but potentially effective mitigatory technique. The simulation of page B-30 has shown the potential benefits of using single-feed 24”x18” antennas instead of the more commonly used 18” dishes. Dual-feed 24”x18” antennas would probably also work well with careful selection of feed azimuths, to avoid aiming a butterfly backlobe toward an MVDDS transmitter. The use of Fortel planar arrays has also been proposed, although the prominent grating lobes evident on the measured radiation patterns shown in section 4 could pose a problem. Finally, research could be done to develop an improved DBS receiving dish antenna having a better-shaped feed pattern and a lower ratio of

focal length to reflector diameter, with the intent of reducing sidelobe levels without adversely affecting antenna gain.

- *Replacement of older DBS set-top boxes* may prove to be a useful mitigation technique if more recent models are more resistant to in-band interference.

6.3 Policy Issues and Recommendations

If licensing of new MVDDS services is to be successful, while preventing significant interference to DBS services, a number of policy issues need to be considered and resolved. These resolutions naturally lead to a licensing and deployment process for new MVDDS services. On the basis of the results shown in other sections of the report, MITRE recommends the following outline for this process:

1. The MVDDS service provider would compute a *C/I* ratio consistent with 10% relative increase in unavailability. This would be done for the locale of interest and for the U.S. DBS satellites at each longitude in view of that locale. The calculations would use the satellite at each longitude with the worst baseline unavailability but that still meets the baseline unavailability described below. The *C/I* ratio would be computed on the basis of a DBS receiver *G/T* of 11.2 dB and with a DBS receiver threshold consistent with performance criterion #6 (also called video quality 6) plus 0.1 dB.

2. An MVDDS configuration would be chosen in a way that minimizes interference and places interference-mitigation regions outside of populated areas to the maximum extent possible. Interference-mitigation regions are defined as those regions with *C/I* ratios of less than the value computed in Step 1, plus 1.0 dB. The MVDDS configuration includes transmit power, antenna selection, antenna azimuth, antenna tilt angle, antenna height, and any other parameters that impact DBS unavailability.

3. A construction permit would be obtained and the MVDDS site would be built.

4. The MVDDS service provider would implement interference-mitigation techniques at the DBS receivers anywhere in the interference-mitigation region defined above. These techniques would be implemented prior to obtaining a license to begin transmitting. Mitigation techniques include, but are not limited to, replacement of the DBS antenna, moving the DBS antenna to take advantage of natural shielding, and the placement of shields on, or near, the DBS antenna.

5. The MVDDS service provider would apply for a license to operate. If the license application requests an EIRP value greater than 14 dBm, a study of the impact of rain scatter would be required. Once the license is granted, the MVDDS transmitter would be allowed to begin transmitting for test purposes.

6. The MVDDS service provider would measure *C/I* values at the output of the LNB for all DBS receivers in the interference-mitigation region. The MVDDS service provider would implement any further mitigation techniques necessary to keep the measured *C/I* lower than the *C/I* value computed in Step 1 above.
7. A final license to begin operation would be granted.

Some further discussion of this process outline may be helpful. A number of measures of interference have been suggested in Section 5.2, including:

- Maximum total unavailability
- Maximum increase in unavailability
- Maximum relative increase in unavailability
- Minimum *C/I*
- Maximum interference power at the DBS LNB
- Maximum PFD
- Maximum EIRP

Of these MITRE believes that relative increase in unavailability is particularly advantageous, since it prevents large increases in absolute unavailability where initial unavailability is small. This approach recognizes that the increase in unavailability that is noticeable to the consumer depends on what the consumer is used to. An increase of 2.86% seems very small and there is precedent for 10% increase as a criterion. We note that *C/I* ratios are measurable at the LNB output. Also, the *C/I* ratio can be associated with relative increase in unavailability by straightforward calculations.

Video quality 6 (VQ6) is easily measurable, and many results based on VQ6 are provided here in this report. Based on results shown in Figure A-7, the performance curves are very steep at the VQ6 point. The threshold for VQ6 plus 0.1 dB is approximately the same as the threshold for VQ7.

The interference-mitigation region is defined as the region where the *C/I* value is 1.0 dB above the *C/I* computed in step one above. This is done to ensure that vulnerable DBS receivers are not missed due to measurement inaccuracies or inaccuracies in the modeling.

The process described above could form the basis for a licensing policy for MVDDS services. However, a number of additional policy issues should be considered. These issues and questions are discussed below, along with MITRE's recommendation to the FCC.

- Should future DBS customers be protected and for how long?
  Recommendation: Yes, future DBS customers should be protected for as long as the MVDDS transmitter operates. The MVDDS service provider would need to measure

C/I values and provide mitigation solutions to these new customers in the interference-mitigation region.

- Test results and analyses have been based on known MVDDS waveforms. Should new waveforms be allowed?
  Recommendation: New waveforms create an unknown vulnerability. MITRE recommends that these not be licensed without further study.

- Should the evaluation of sharing consider any DBS satellite in the geostationary arc, or should only existing U.S. satellites be considered? What about new U.S. satellites?
  Recommendation: DBS receivers operating with new and different satellites could be at risk in unforeseen ways. MITRE recommends that any satellites not addressed in the current report be studied further.

- If changes and improvements are made to any DBS system waveform, how should this impact policy?
  Recommendation: Results in this report are based on specific systems with known parameters. MITRE recommends that any new DBS waveforms be subject to further study.

- Should DBS satellites with weak coverage be protected? If so, how weak can these be and at what level should they be protected? (See examples in Section 5.2.3 and elsewhere.) What is the maximum baseline and degraded unavailability that should be allowed?
  Recommendation: MITRE recommends that only DBS satellites with baseline unavailabilities of 100 hours/year or less when operating without MVDDS interference into a DBS antenna with *G/T* of 11.2 dB/K be protected. DBS receivers operating with satellites that do not meet this criterion should not be protected from MVDDS interference when operating with such satellites.

- How should the advent of new DBS antennas affect the policy for MVDDS licensing?
  Recommendation: DBS antennas with *G/T* performance below 11.2 dB/K could seriously degrade DBS availability in rain. In all cases the *C/I* criterion must be met. If the MVDDS service provider opts to mitigate MVDDS interference with the use of a different antenna, the replacement antenna should have a *G/T* at least as great as that of the original antenna.

- Should other causes of unavailability be included in the total budget?
  Recommendation: Other sources of outage should be considered, if they are significant and if their effect is known and documented. Sun-transit outages are an example.

- MVDDS antenna backlobes can interfere with a DBS antenna main beam. This would typically occur close to the MVDDS transmitter, generally north of the antenna. These regions are typically very small. Should very small regions of interference be exempted because of their small size?
  Recommendation: These small regions should not be exempted because of their size. All regions of the interference-mitigation region should be considered, regardless of size.

- Should MVDDS mitigation be based solely on customer complaints?
  Recommendation: MITRE believes that DBS customers may not know what is causing a particular outage, or the reason for its duration. Consequently, mitigation should not await DBS customer complaints. MITRE believes that mitigation should be done proactively, regardless of the presence or absence of such complaints.

- How much time should the MVDDS service provider be allowed in order to implement mitigation to the DBS receivers?
  Recommendation: To the maximum extent possible, mitigation should be accomplished prior to a license being granted for MVDDS operation.

MITRE believes that with implementation of the licensing process and other policy recommendations outlined above, spectrum sharing between DBS and MVDDS services in the 12.2–12.7 GHz band is feasible. However, MITRE recognizes that it is the FCC that must ultimately resolve the various policy issues and the approach to licensing new MVDDS services.

List of References

Barker, J. H., and P. Michalopoulos, 31 January 2001, *Answers from the DBS Operators to Questions Posed by the MITRE Corporation*, DIRECTV and EchoStar.

Barker, J. H., and P. Michalopoulos, 14 March 2001, *Additional Answers from the DBS Operators to Third Set of Questions Posed by The MITRE Corporation*, DIRECTV and EchoStar.

Combs, B., 9 February 2001, Answers to the Second Set of Questions for the MVDDS Industry from The MITRE Corporation, email document, Broadwave USA.

DIRECTV, 31 March 2000, Ex Parte submission to FCC regarding ET Docket No. 98-206.

European Telecommunication Standard, December 1994, *Digital broadcasting systems for television sound and data services; Framing structure, channel coding and modulation for 11/12 GHz satellite services*, ETS 300 421.

Evans, G. E., 1990, *Antenna Measurement Techniques*, Artech House, Boston, MA.

Federal Communications Commission (FCC) DA 01-441, 16 February 2001, *Fourth Erratum, First Report and Order and Further Notice of Proposed Rule Making (FCC 00-418)*, Washington, DC.

International Telecommunications Union (ITU), 1997, *Propagation Data and Prediction Methods Required for the Design of Earth-Space Telecommunication Systems*, ITU-R P.681-5.

ITU, 1999a, *Propagation Data and Prediction Methods Required for the Design of Earth-Space Telecommunication Systems*, ITU-R P.618-6.

ITU, 1999b, *Characteristics of Precipitation for Propagation Modeling*, ITU-R P.837-2.

ITU, 21 September 2000, *Digital Multiprogramme Television Systems for Use by Satellites Operating in the 11/12 GHz Frequency Range*, Document 6/35-E.

Slater, D., 1991, *Near-Field Antenna Measurements*, Artech House, Boston, MA.

Telecommunications Systems, 6 April 2001, Letter to The MITRE Corporation, Washington, DC.

Appendix A

Testing of DBS Set-Top Boxes in the Presence of Northpoint MVDDS Interference

A.1 Overview of Test Configuration for Receiver Degradation Measures

A simplified view of the test configuration used to study the impact of MVDDS interference on DBS systems is shown in Figure A-1. In general, a closed DBS link is perturbed via the insertion of additional interference signals.

Signal quality is monitored through observation of the picture and sound quality as observed through a television connected to a DBS set-top box. Signal quality, $C/(N+I)$ or carrier to noise plus interference ratio is calculated from data measured with an Agilent 8564E spectrum analyzer. An SAT9520 DBS installer's tool was also used to measure C/N during interference experimentation.

In order to have independent control of both the carrier-to-noise-plus-interference, and the noise-to-interference power ratios, addition of both Gaussian noise and Northpoint interference was necessary.

Specific details of the test set-up and procedures are discussed in the following sections.

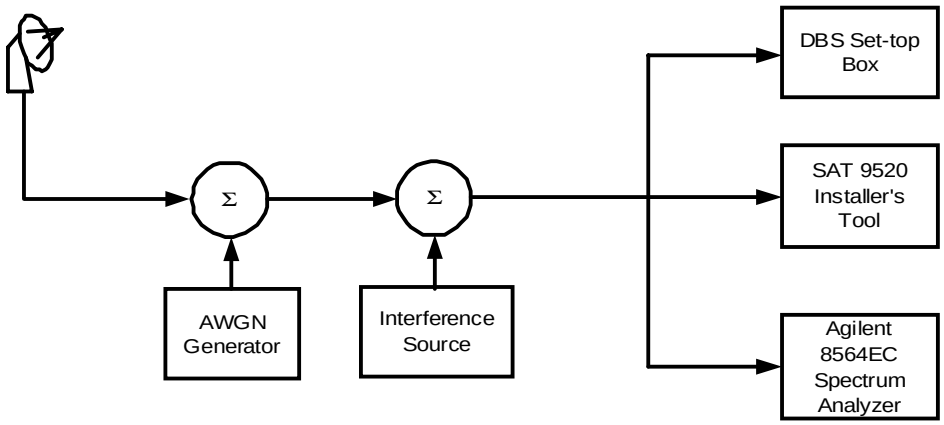

Figure A-1. Functional Overview of DBS Video Test Configuration

A.2 Details of the Test Configuration

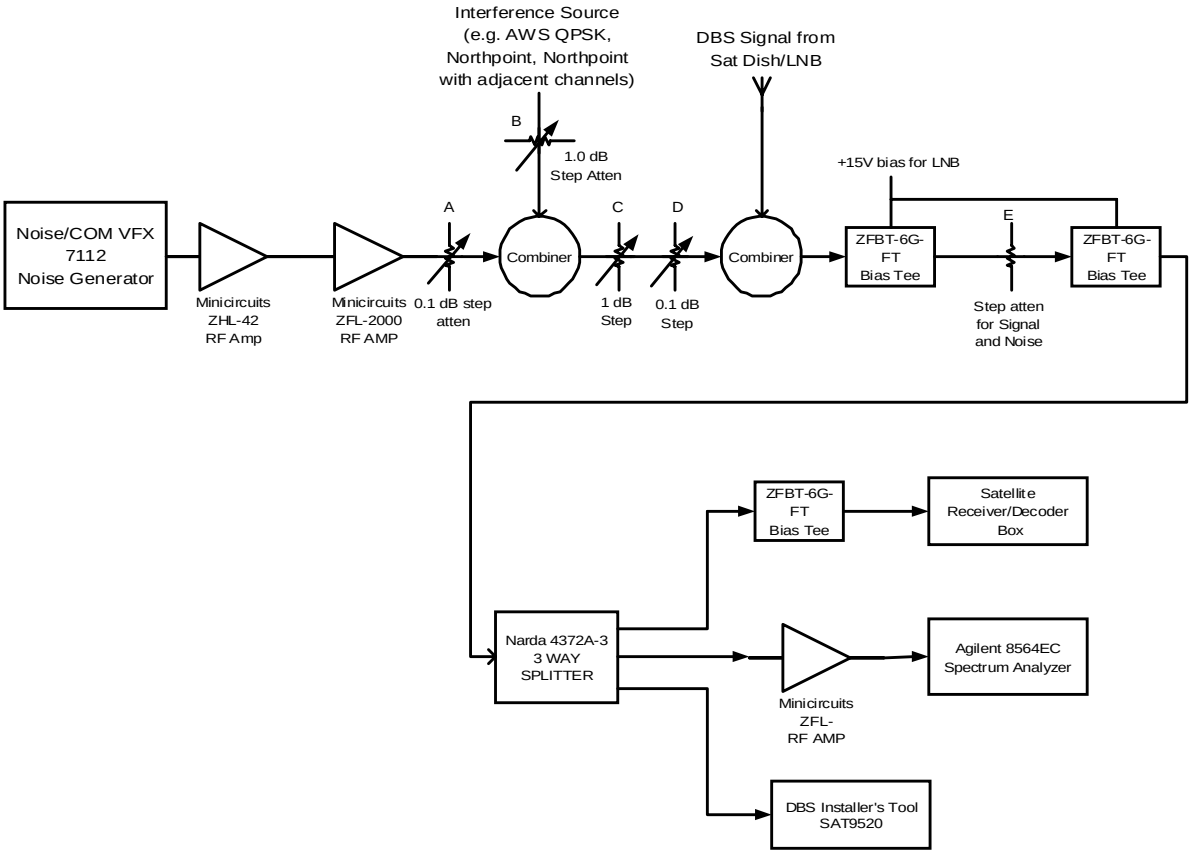

Figure A-2. Details of the Test Configuration for DBS Video Testing

Figure A-2 shows, in detail, the test configuration used to measure the impact of interference from MVDDS on DBS systems. A Noise/Com Model 7112 noise generator is amplified using two cascaded RF amplifiers, namely a Mini-circuits ZHL-42 and a Mini-circuits ZFL-2000, respectively. The amplified noise source level is controlled by both the 1 dB steps available on the noise generator, and the 0.1 dB step attenuator labeled "A" in Figure A-2. MVDDS interference is added to the noise using an Anzac H-8-4 combiner. Interference levels are controlled through step attenuator B. The power of the combined noise and interference is controlled using attenuators C and D and is then added to the DBS LNB video signal using another Anzac H-8-4 combiner. Attenuators C and D control the level of the composite noise and interference, $N+I$, relative to that of the DBS signal, C. A level of 15 volts bias is made available to the DBS receive satellite dish LNB by way of a ZFBT-6G-FT bias tee through the combiner. Attenuator "E" is used to control the composite DBS signal, interference, and noise level into the satellite decoder box. The composite

signal is split three ways using a Narda 4372A-3 signal splitter. One output is fed to the satellite decoder box, a second is fed to an Agilent 8564EC spectrum analyzer, and a third to the SAT 9520 DBS Installer's Tool. The installer's tool monitors DBS signal quality, displaying signal strength, bit error rate, etc. A Mini-circuits ZFL-2000 RF amplifier is used to improve the noise performance of the spectrum analyzer.

A.2.1 Audiovisual (A/V) Signal Quality Determination

Due to the nature of the encoded DBS signal, video and/or audio degradation occurs over a very narrow region of carrier-to-noise plus interference, $C/(N+I)$, prior to complete loss of signal lock. Degradation in A/V quality originating from a digital broadcast is unlike that from an analog broadcast, where picture quality is very subjective. Instead, degradation is quite noticeable, and occurs in burst fashion when uncorrectable bit errors are presented to the Motion Picture Experts Group (MPEG) decoder. For low bit error rates, errors are corrected by the error correction coding inherent in the system. Video and audio impairments occur when the number of bit errors exceeds what is correctable by the concatenated code. Video impairments manifest as sudden pixelization in the image. Audio errors manifest as a sudden pop or chirp sound. In general, the rate of audio and video error occurrences increases as the $C/(N+I)$ ratio degrades. A video/audio quality criteria set was established for the purpose of assigning a quality measure. See Table A-1.

Table A-1. DBS A/V Quality Criteria

Assigned Quality Level (9=perfect)	Video/audio characteristics (average)
9	Perfect video/audio
8	1 video/audio error per 30 minutes
7	< 1 error per minute, but > than 1 per 30 minutes
6	< 1 error per 15 seconds, but > 1 error per minute
5	> 1 error per 15 seconds
4	Freeze framing and pixelization occurring; audio chirping and momentary blanking
3	Mostly pixelized, mostly frozen, mostly audio blanked
2	Occasional video acquisition, no audio
1	Loss of lock, no signal acquisition

A.3 Power Measurement for DBS, MVDDS, and Noise Signals

Evaluating the DBS system performance in the presence of MVDDS interference required that a consistent, repeatable measurement technique be used throughout the duration of the testing. The following sections describe the settings used for the measurement equipment as well as the rationale for choosing the measurement bandwidth.

A.3.1 Signal/Noise Power Measurements Using the Agilent 8564EC Spectrum Analyzer

Signal and noise power measurements are performed with an Agilent 8564EC spectrum analyzer. The analyzer settings used throughout the testing are given in Table A-2.

Table A-2. Spectrum Analyzer Settings

Resolution bandwidth	300 kHz
Video bandwidth	3 kHz
RF Attenuation	0 dB
Center frequency	Center of DBS video IF frequency
Span	30 MHz
Reference level	-20 dBm

A.3.1.1 Signal Power Measurements

Using the Agilent 8564EC spectrum analyzer, the power occupied bandwidth for the DBS video signal was performed at various percentages of the total power. While performing these measurements, the noise input is disabled. The results are presented Table A-3.

Table A-3. Power Occupied Bandwidth of DBS Signal

Percentage of Total DBS Signal Power	Occupied Bandwidth
50%	10 MHz
75%	15 MHz
90%	18.4 MHz
95%	20.0 MHz
96%	20.46 MHz
97%	21.04 MHz
98%	21.7 MHz
99%	22.7 MHz

In order to perform total signal, noise and interference power measurements, a common measurement bandwidth must be chosen. Recall that an important goal of the test configuration of Figure A-2 was to allow for independent control of the received carrier power, *C*, the total noise power, *N*, and the interference power, *I*. Special consideration was given to measurement of the total carrier power, *C*.

Because the carrier power was a measurement of a live satellite signal, it is not possible to measure without consideration of the atmospheric noise. To overcome the inaccuracy introduced by the noise, a receive dish much larger than typically used by the consumer (90 cm) was used to collect the signal. Use of this large dish resulted in received carrier-to-noise ratios much greater than 10dB. Because of this, the intermediate frequency (IF) power measured at the output across the bandwidth of a single transponder could be attributed entirely to the radiated space vehicle (SV) power. To further substantiate, the 90cm dish was pointed at "clear sky". Although the resulting measure of sky noise power was still above the noise floor of the spectrum analyzer, its power level did not modify the least significant digit of the former carrier power measurement when subtracted. That is to say that the total carrier power plus noise measured when the large dish was appropriately pointed at the DBS satellite, minus the sky noise power measured when pointed at "clear sky" was for all practical purposes, equal to the total power measured in the first measurement.

Although a bandwidth of 24 MHz would account for the entire power contained in the DBS signal, the signal to noise ratio of the received satellite signal degrades in the roll off region of the transponder. Thus it was more accurate to make the signal power measurements in as small a bandwidth as was reasonable. As an alternative to 24 MHz, power and noise measurements can be made over the effective bandwidth of the DBS signal.

The effective bandwidth of the DBS signal is found by computing the bandwidth of a uniformly rectangular spectrally shaped signal with spectral density equal to that of the center of the DBS signal, which would contain the same total power as the DBS signal. See figure A-3. Measurements of the effective signal bandwidth were measured to be 20 MHz. This can be visualized by observing that the 50% and 75% power occupied bandwidths (over which the spectral density is flat) are 10 MHz and 15 MHz, respectively. Note however that when using a 20 MHz bandwidth to measure the DBS signal power, a 0.2 dB underreporting occurs. This is because only 95% of the DBS signal power (10*log(0.95) = -0.2 dB) is contained in that bandwidth. A correction factor of +0.2 dB was added to all DBS signal power measurements to account for the missing power in the tails.

Signal power measurements are obtained using the Measure/User softkey available on the spectrum analyzer.

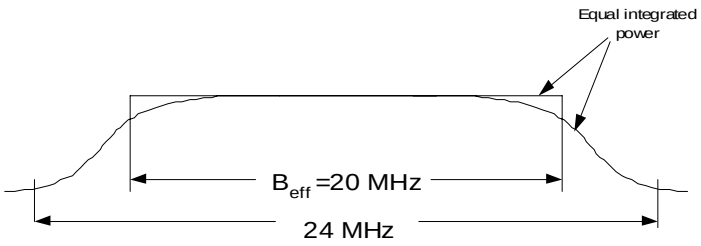

Figure A-3. Notional Depiction of DBS Effective Bandwidth

A.3.1.2 Noise Power Measurements

Noise power measurements are performed using the Measure/User softkey available on the analyzer. A measurement bandwidth of 20 MHz is specified as a parameter to the analyzer using the appropriate entry keys. While performing noise measurements, the DBS video signal is disconnected. The analyzer computes integrated noise power over the specified bandwidth.

A.4 Notes on Interference Testing

This section contains notes applicable to the equipment and methods of the testing that is articulated in the subsequent sections.

A.4.1 Test Objectives

The goal of the receiver testing was to characterize how the DBS systems performed in the presence of MVDDS interference at various levels of $C/(N+I)$ and N/I. Throughout the testing, N/I was varied to achieve the following levels: +infinity (noise only), +10dB, +3dB, 0 dB, -3dB, -10dB, and –infinity (MVDDS interference only). Once N/I was established, the aggregate combination of $N+I$ was raised in power to degrade the signal quality to a pre-determined level.

A.4.2 DBS Equipment

In order to maintain the independence of the tests, DBS set-top boxes were procured that were not traceable back to MITRE. This was done thanks to a close family member of one of the members of the testing staff, (with a different surname), independently procuring DBS set-top boxes for both Dish TV and DIRECTV at retail locations that were not in the immediate vicinity of the Bedford facility.

The set top equipment procured was Philips Magnavox Dish model DSK2812S and RCA DIRECTV plus! model DRD420RE. These set-top boxes are shown in Figure A-4.

Figure A-4. Set-Top Boxes Used in Receiver Testing

Although a great deal of set-top equipment was made available by the DBS manufacturers, it was not deemed acceptable for use in an independent test, and the constraints of time and budget did not permit any detailed testing of that equipment.

A.4.3 MVDDS Equipment

The only MVDDS equipment received for testing was a single channel transmitter made by L3 Communications. The unit consists of an AAA NTSC to MPEG converter, a BBB quadrature phase shift keying (QPSK) modulator, and a CCC amplifier. The unit is shown in Figure A-5.

Figure A-5. Northpoint MVDDS Single Channel Transmitter

A.4.4 Signal Quality Level 6

Initial experimentation injecting representative MVDDS interference signals into closed DBS links revealed it was simple and reliable to control the relative rate of occurrences of disturbances to the DBS signal using the test configurations identified in Appendix A. However reliably measuring a small number of disturbances that occurred over the course of an hour (or even hours for that matter) is extremely time consuming and potentially fraught with inaccuracy due to too small a sample space, and the likelihood of changing atmospheric conditions over long periods of time.

An A/V quality level of 6, (see Table A-1), an audio or visual degradation occurring on the average of 1 to 4 times per minute was chosen as the measurement standard. This A/V quality level was chosen primarily for its repeatability and the reduction of time in test execution that it offered. Additionally, an A/V quality level of 6 occurs roughly mid-range in the narrow span over which signal degradation can actually be observed, between no degradation and total loss of signal lock.

Selection of video quality 6 is not intended to be an advocation of that level as either acceptable or unacceptable to the consumer. Rather it is a convenient point to identify in a short range between perfect quality and loss of lock in the vicinity of the mean of that range.

A.4.4.1 Dynamic Allocation of DBS Transponder Bandwidth to Stations

Another factor important to mention is that the bandwidth for any given channel is dynamically allocated from a transponder that carries the burden of several channels. This adjustment is made automatically based upon the need for bandwidth post compression. Typically, television scenes with more action result in lower compression ratios and require more bandwidth for quality transmission.

Typically, a fixed $C/(N+I)$ would result in a fixed bit error rate, but the number of errors per second would be the largest on those channels consuming the most instantaneous bandwidth on that transponder. Thus every attempt was made to measure video quality during programming sequences that had high levels of action.

The impact to the laboratory measurements of this artifact of the DBS systems is that a fixed A/V quality may trace back to bit error performances between transponders. Additionally, since the uncorrected bit errors will be distributed ratiometrically according to the channel utilization relative to the total transponder bandwidth, the measured $C/(N+I)$ required to drive one particular channel to A/V quality 6 may be different than another channel. However, since the range of perceptible A/V degradation (between A/V quality 9 and loss of lock) is relatively narrow, then comparative results between channels on different transponders should compare reasonably.

A.4.5 Elimination of Drive Power as Testing Variable

In order to reduce the dimensionality of the testing, it was necessary to determine whether the drive power of the signal to the DBS set-top box had an impact on the $C/(N+I)$ that would degrade the signal quality. The DBS set-top boxes are specified for a drive input between –25 dBm to –65 dBm. A visual test was performed. With the drive power attenuated to near the –65 dBm minimum, the $C/(N+I)$ was adjusted so that the video quality was within 1 dB of noticeable degradation. Drive power was successively increased in 5 dB steps. After each step, 1 additional dB of interference was added, and a visually equivalent degradation to the quality of the video signal at the previous step was observed. The 1 dB of additional interference was then removed prior to the next step. This test was performed at several N/I ratios.

Figures A-6 and A-7 are presented (beyond the anecdotal results discussed above) to show the impact of changing the drive power. In Figure A-6 the resulting signal quality for varying $C/(N+I)$ are shown for 2 different drive powers, -45 dBm and –55 dBm (DIRECTV). In Figure A-7 the conditions are –30 dBm and –55 dBm are used for DISH Network (i.e.,

EchoStar). Note the consistency between the *C*/(*N*+*I*) values required to drive the signal quality to level 6, for both systems.

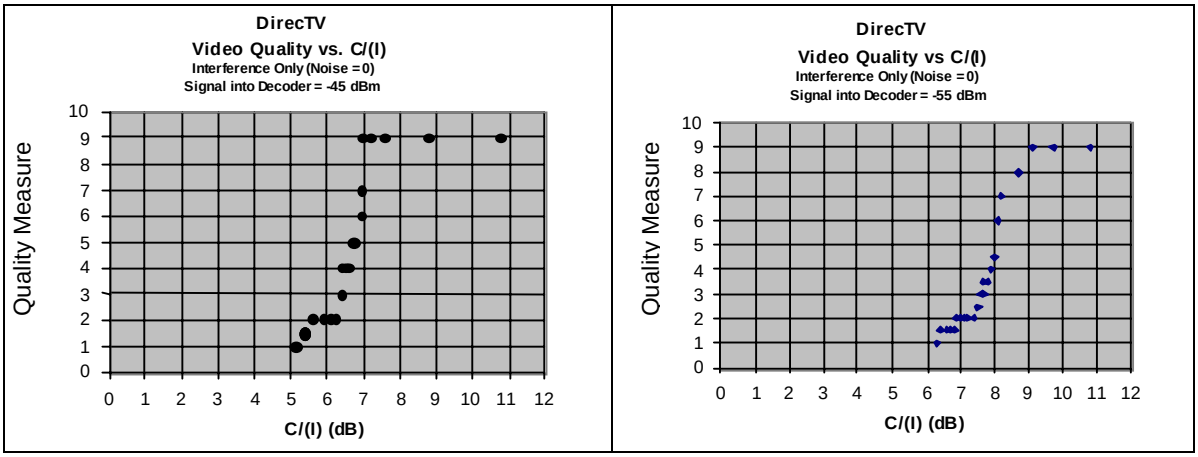

Figure A-6. Comparison of 2 Different Drive Powers for DIRECTV

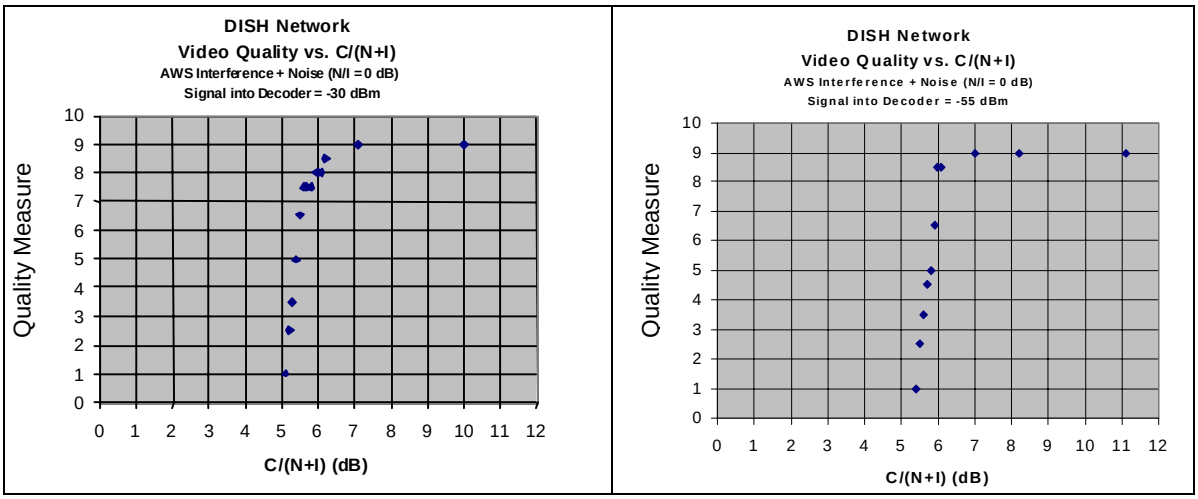

Figure A-7. Comparison of 2 Different Drive Powers for Dish TV

A.4.6 Selection of Programming

As discussed above, programming with action sequences was chosen due to the likelihood of consumption of larger instantaneous portions of the transponder bandwidth.

Because of the flexibility of the equipment, any television channel could be targeted. Prior to execution of tests, available channels were scanned for the most promising television program. Upon selection of programming, the corresponding transponder was identified. The selected television program was used for the duration of any test.

A.4.7 Determination of Transponder Transmitting a Particular Television Channel

As discussed above, every effort was made to choose programming that contained frequent action scenes, and ostensibly consumed an above average share of the transponder bandwidth. Upon determination of appropriate programming, we determined the corresponding transponder from which the programming was being broadcast by moving a high powered tone to the (I.F.) center frequency of each of the transponders. As the power of the tone was sufficient to jam any single transponder at a time, determination of the appropriate transponder was a matter of visual inspection.

A.5 DBS A/V Quality 6 in the Presence of Northpoint MVDDS Interference Using 70 MHz IF Output Translated to L Band with Simulated Adjacent Channels

Some MVDDS interference experiments were conducted upon arrival of the MVDDS transmitter suite, but prior to an appropriate LNB downconverter being available. To proceed without the LNB, it was necessary to make use of the 70 MHz IF output of the MVDDS transmitter.

A.5.1 Test Configuration

The configuration that properly mixed the IF output of the Northpoint MVDDS transmitter and combined the mixed output with the arbitrary waveform synthesizer (AWS) to provide the adjacent MVDDS channels is shown in Figure A-8.

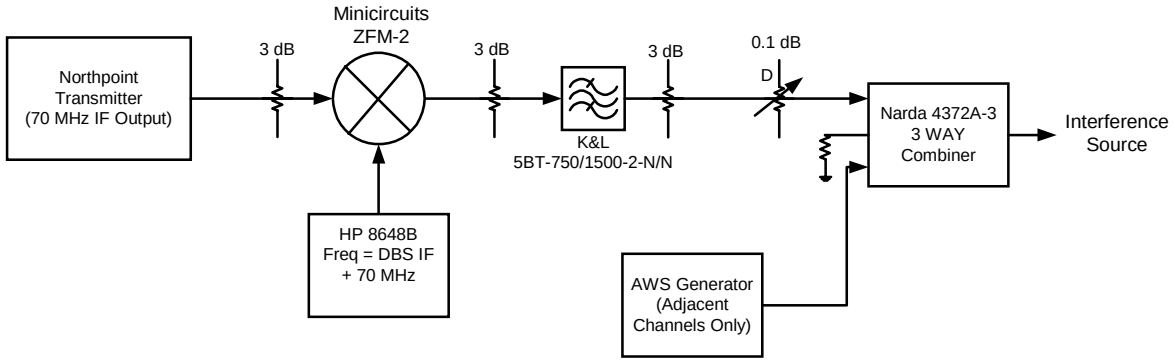

Figure A-8. Configuration for Northpoint Transmitter IF Output with Adjacent Channels

The 70 MHz output is attenuated using a 3 dB pad, upconverted using a Mini-circuits ZFM-2 mixer terminated by a 3 dB pad, and filtered with a K&L tunable bandpass filter. The signal at the output of the filter is combined (for cases with adjacent channel testing) with an arbitrary waveform synthesizer programmed to simulate MVDDS adjacent channels.

The signals are combined with a Narda 4372A-3 combiner, with the third port terminated in 50 ohms. The combined signal labeled as "interference source" is applied to the interference source input of Figure A-2. Relative power levels between the MVDDS signal and the AWS adjacent channels are adjusted using the Northpoint MVDDS Tx control keypad, the PC control interface to the AWS, and the fine adjustment attenuator D. The interference signal resulting from the combination of the Northpoint MVDDS IF output and the AWS is shown in Figure A-9.

Figure A-9. Single Channel MVDDS IF Interference Plus Adjacent Channels Generated from Arbitrary Waveform Synthesizers

A.5.2 Test Results

Results for DIRECTV and Dish TV are shown in Figure A-10 and Figure A-11 respectively. Note that values for Figures A-10 and A-11 were determined at *N*/*I* ratios of –infinity (MVDDS interference only), -10 dB, -3dB, 0 dB, 3dB, 10 dB, and +infinity (noise only). Both DIRECTV and Dish TV are more resilient to the constant envelope, Northpoint MVDDS signal, than to the Gaussian noise. Results for +infinity and –infinity are plotted on the +30 and –30dB points, respectively.

Note the proximity of the SAT9520 measurement to the spectrum analyzer measurement in the noise-only case. Insufficient information is available about the SAT9520 to provide an

accurate scaling factor that would account for the small differences in measurement bandwidth between the spectrum analyzer and the SAT9520.

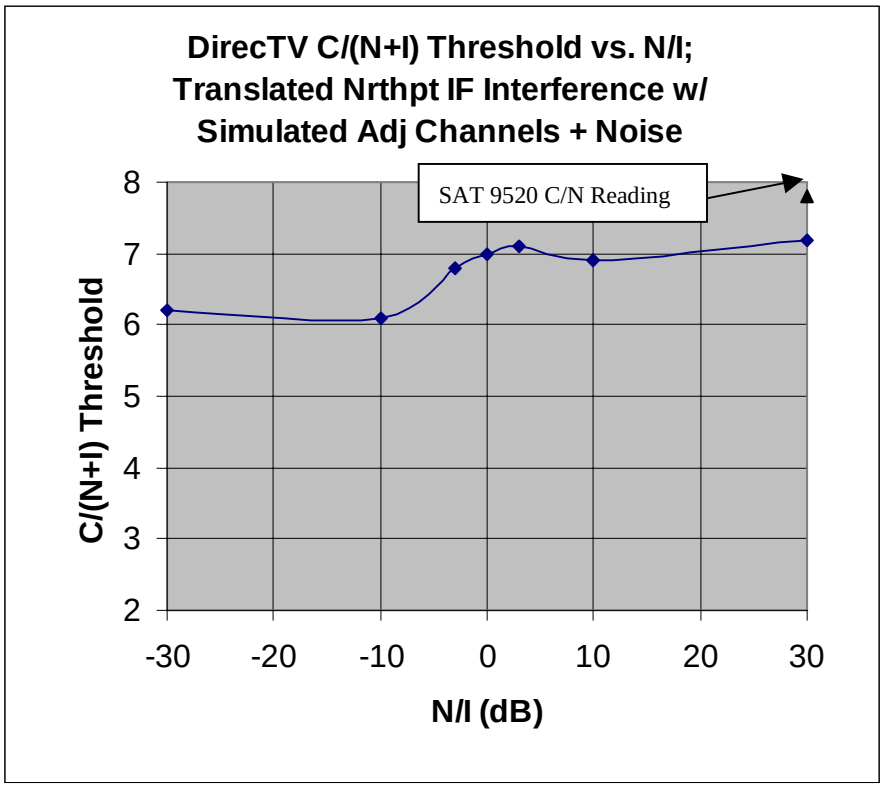

Figure A-10. Carrier-to-Noise-Plus-Interference Required to Degrade DIRECTV to A/V Quality 6 Vs. Noise-to-Interference Power Ratio; 70 MHz IF

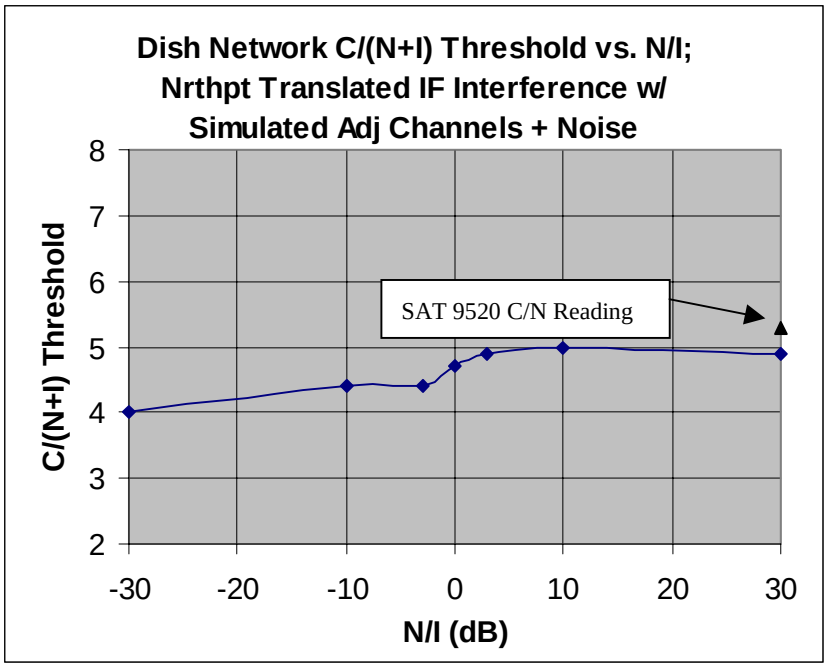

Figure A-11. Carrier-to-Noise-Plus-Interference Required to Degrade Dish TV to A/V Quality 6 Vs. Noise-to-Interference Power Ratio; 70 MHz IF

A.6 DBS A/V Quality 6 in the Presence of Northpoint MVDDS Interference Using RF Output with Simulated Adjacent Channels

The test results in Section A.5 were repeated using the 12 GHz RF output of the Northpoint MVDDS transmitter coupled into an LNB.

A.6.1 Test Configuration

The configuration for interference testing using a Northpoint MVDDS Transmitter and LNB downconverter is shown in Figures A-2 and A-12. The signal made available to the "Interference Source" in Figure A-2 is generated in Figure A-12.

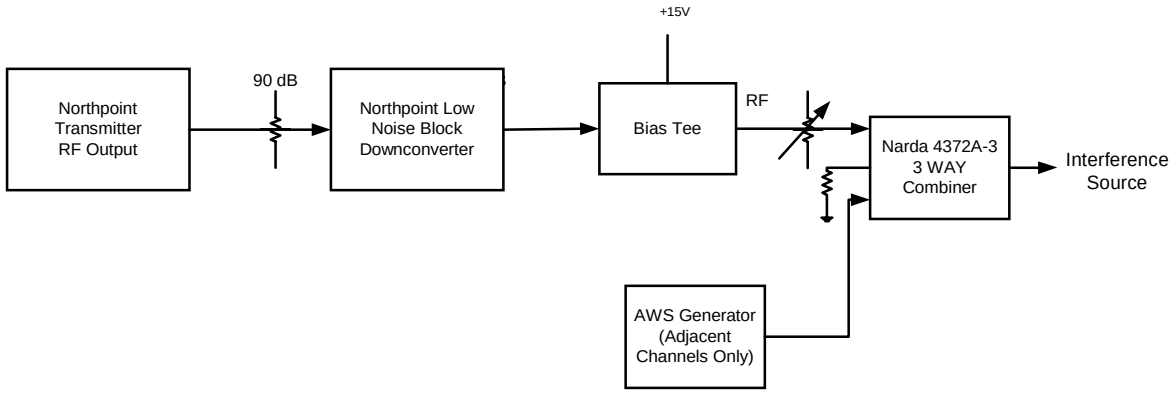

Figure A-12. Interference Test Configuration Using Northpoint Transmitter with LNB

The 12 GHz output of the Northpoint MVDDS transmitter is attenuated using a 90 dB attenuator. This signal is applied to an LNB downconverter. 15 volts is applied to the LNB using a bias tee. The RF signal is applied to the input of a Narda 4372A-3 combiner. An HP AWS programmed to generate left and right adjacent channels, is applied to the combiner. The third port of the combiner is terminated in 50 ohms. The adjacent channel power level is controlled by the PC interface to the AWS generator. This level is adjusted to equalize the adjacent channel to the Northpoint interference level.

Attenuators A and B are adjusted to fine-tune the relative levels of the noise and interference power. Attenuator C is used to control the composite noise and interference level relative to that of the DBS signal. The composite output of the Northpoint MVDDS transmitter and AWS at L-Band IF is shown in Figure A-13.

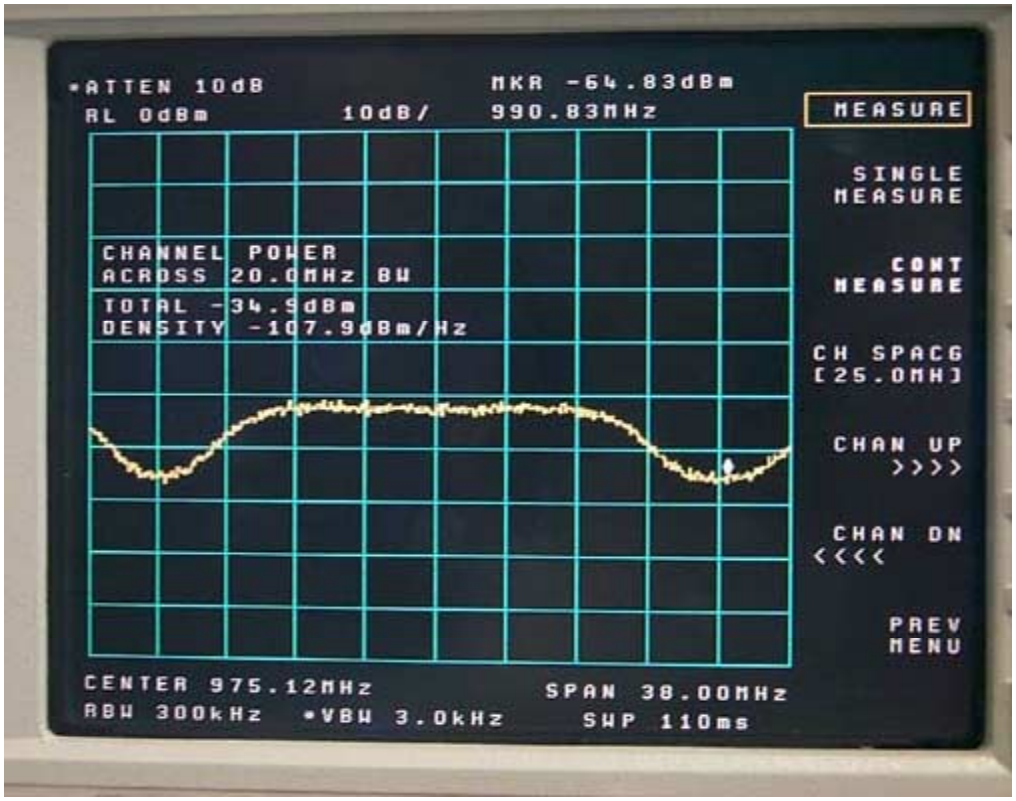

Figure A-13. Single Channel MVDDS Downcoverted RF Interference Plus Adjacent Channels Generated from Arbitrary Waveform Synthesizers

A.6.2 Test Results

Data is recorded at various noise to interference power levels, namely, +infinity, (noise only), +10 dB, +3 dB, 0 dB, -3 dB, –10 dB, and –infinity (interference only). As in the previous section, results for +infinity and –infinity are plotted on the +30 and –30dB points, respectively.

The results are shown for Direct TV and Dish TV in Figure A-14 and Figure A-15, respectively.

The same trend is observed relative to the resilience to the constant envelope QPSK MVDDS signal as compared to Gaussian noise as was observed in the previous section.

Note as well the Proximity of the SAT9520 Measurement in the noise-only case to spectrum analyzer measurements. Insufficient information is available about the SAT9520 to provide an accurate scaling factor that would account for differences in measurement bandwidth between the spectrum analyzer and the SAT9520.

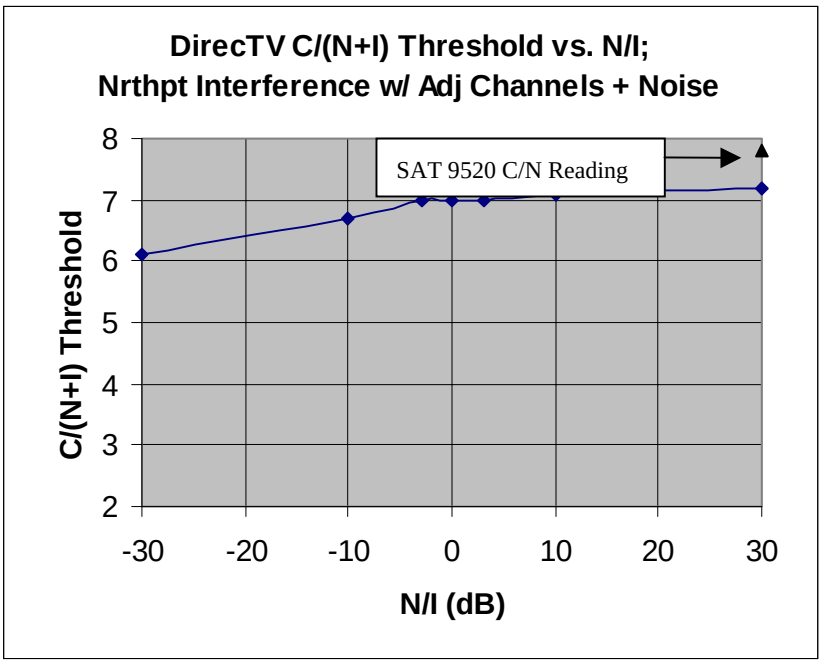

Figure A-14. Carrier-to-Noise-Plus-Interference Required to Degrade DIRECTV to A/V Quality 6 Vs. Noise-to-Interference Power Ratio; 12 GHz RF Output

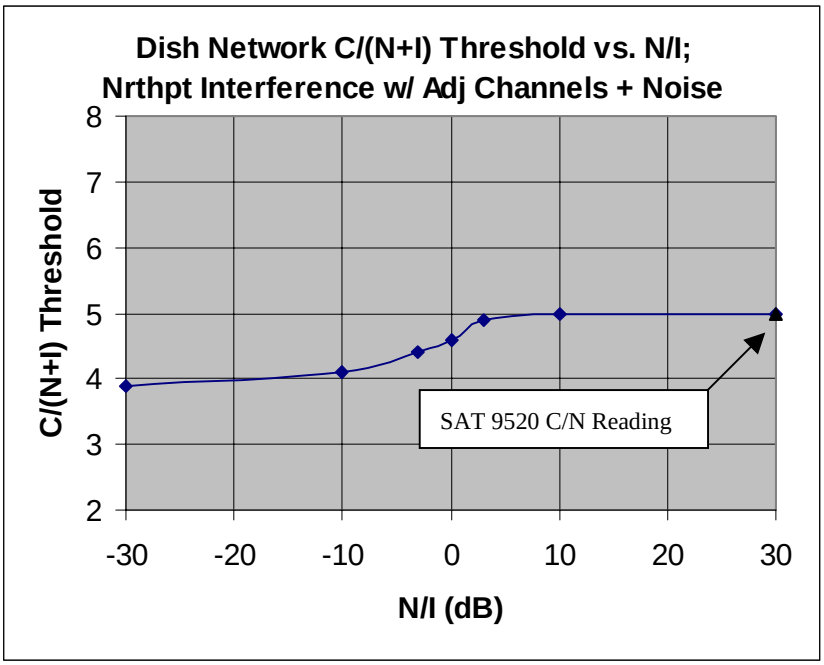

Figure A-15. Carrier-to-Noise-Plus-Interference Required to Degrade Dish TV to A/V Quality 6 Vs. Noise-to-Interference Power Ratio; 12 GHz RF Output

A.7 DBS A/V Quality 6 in the Presence of Northpoint MVDDS Interference Using RF Output with +7 MHz Offset and Simulated Adjacent Channels

Northpoint had identified a 7 MHz frequency offset between the center frequencies of the MVDDS channelization and DBS channelization as one potential means of isolation from the DBS system at their disposal. This section details the laboratory work to substantiate that claim.

A.7.1 Test Configuration

The configuration for interference testing using a Northpoint transmitter with +7 MHz offset and LNB downconverter with adjacent channels is shown in Figure A-16.

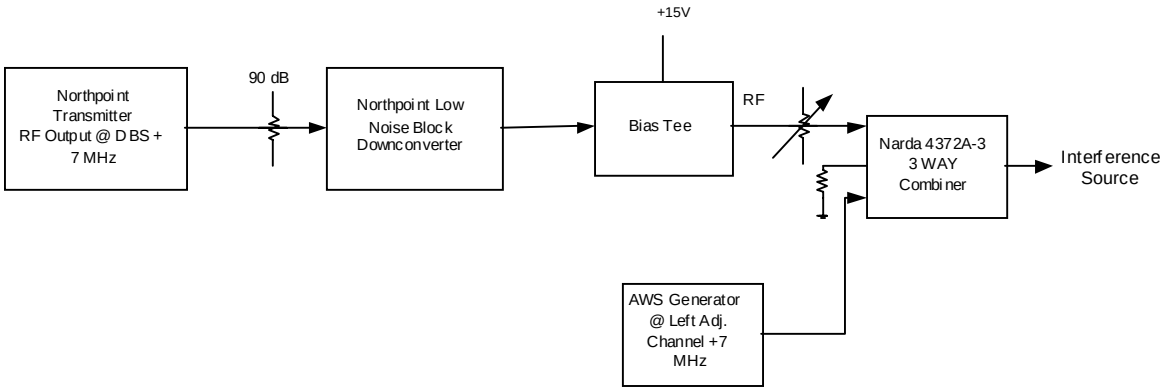

Figure A-16. Interference Test Configuration Using Northpoint Transmitter with +7 MHz Offset and LNB Downconverter

The RF output of the Northpoint MVDDS transmitter centered at the DBS frequency with a + 7 MHz offset is attenuated using a 90 dB attenuator. The 7MHz offset was achieved through programmability in the Northpoint MVDDS transmitter and verified with the Agilent spectrum analyzer. This signal is applied to an LNB downconverter. 15 volts is applied to the LNB using a bias tee. The resulting L-band IF signal is applied to the input of a Narda 4372A-3 combiner. An HP AWS programmed to generate the left adjacent channel + 7 MHz (at L band IF frequency), is applied to the combiner. The third port of the combiner is terminated in 50 ohms. The adjacent channel power level is controlled by the PC interface to the AWS generator. This level is adjusted to equalize the adjacent channel level to that of the Northpoint MVDDS interference level.

Attenuators A and B are adjusted to fine-tune the relative levels of the noise and interference power. Attenuators C and D (of Figure 2) are used to control the composite noise and interference level relative to that of the DBS signal.

A view of the total (actual plus simulated) MVDDS output translated into the L-band IF of the DBS system is shown in Figure A-17.

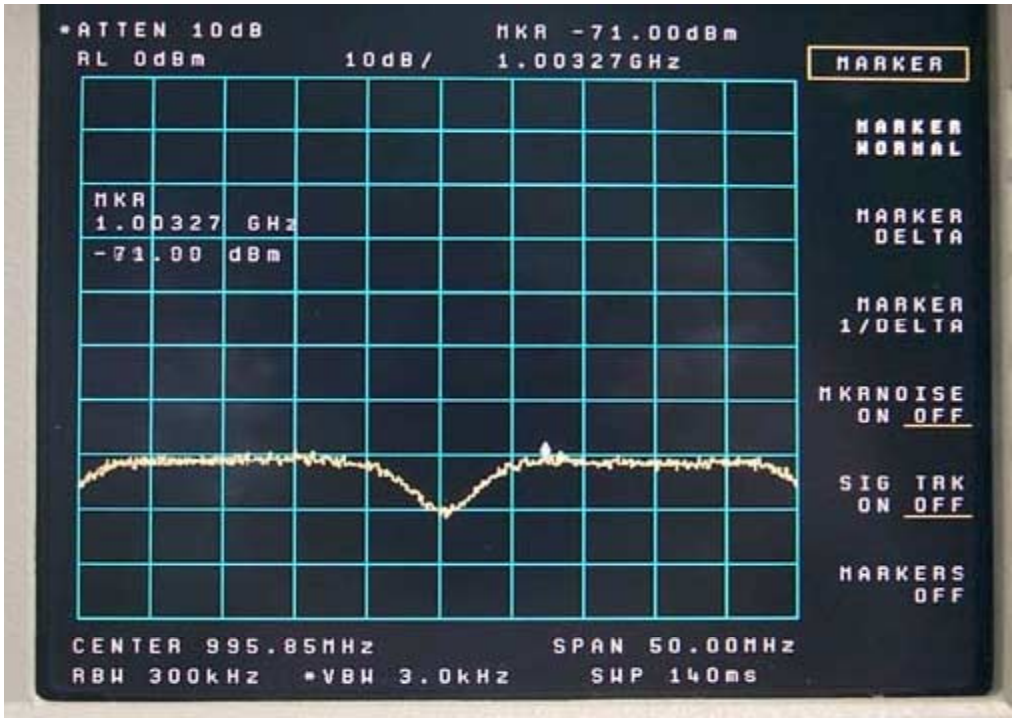

Figure A-17. Single Channel MVDDS (with 7 MHz Offset With Respect to DBS Channelization) Downcoverted RF Interference Plus One Adjacent Channel Generated from Arbitrary Waveform Synthesizer

A.7.2 Test Results

Data is recorded at various noise and interference levels, namely with noise only, interference only, and noise to interference ratios of +10 dB, +3 dB, 0 dB, -3 dB, and –10 dB. As in the previous section, results for +infinity and –infinity are plotted on the +30 and –30dB points, respectively.

The results for DIRECTV are compiled in Figure A-17. The same trend is observed relative to the resilience to the constant envelope QPSK MVDDS signal as compared to Gaussian noise.

Note as well the proximity of the SAT9520 measurement in the noise-only case to spectrum analyzer measurements. Insufficient information is available about the SAT9520 to provide an accurate scaling factor that would account for differences in measurement bandwidth between the spectrum analyzer and the SAT9520.

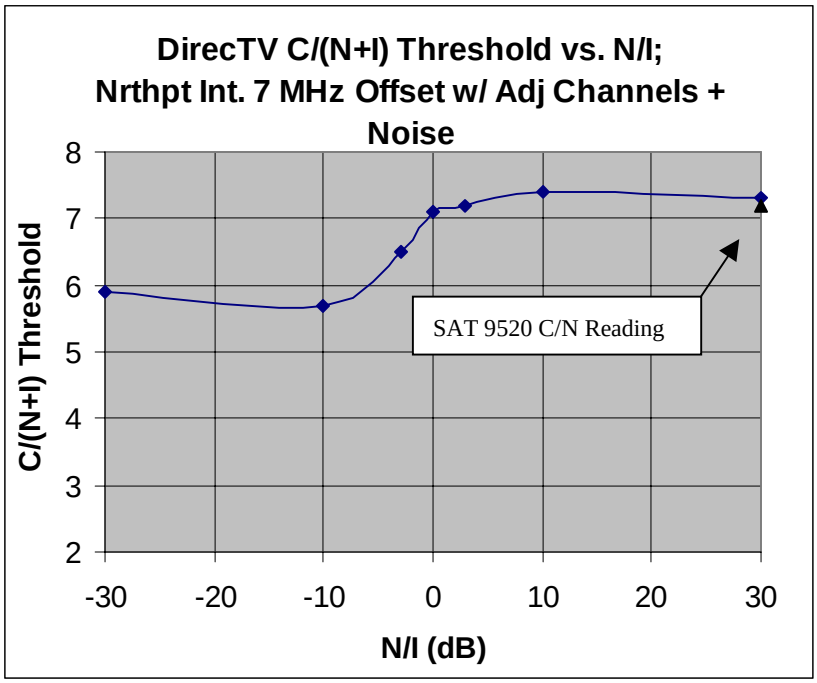

Figure A-18. Carrier-to-Noise-Plus-Interference Required to Degrade DIRECTV to A/V Quality 6 Vs. Noise-to-Interference Power Ratio; Northpoint MVDDS 12 GHz RF Output, + 7 MHz Offset from DBS Channelization

An additional test was performed with regard to the 7 MHz offset. Power over the 20 MHz bandwidth was computed for the Northpoint MVDDS transmitter plus adjacent channel, when the center frequencies of the DBS signals were aligned, and when the signals were offset by 7MHz. We noted that a power difference of 1.2 dB between the 2 signals, (the perfectly aligned signal had the greater power.) This 1.2 dB of additional isolation, that is not obvious from Figure A-18 was factored into total MVDDS power that would be required to degrade the DBS signal unavailability to a specified level.

A.8 DBS A/V Quality 6 in the Presence of Northpoint MVDDS Interference Using Open Air RF Transmission

This section describes the results of testing when a transmitted Northpoint MVDDS signal was used as interference source.

A.8.1 Test Configuration

Transmitted Northpoint MVDDS signals were coupled into a DBS receive dish mounted on a movable pedestal. The pedestal is capable of motion in both azimuth and elevation, and was oriented as to maximally couple energy from the Northpoint MVDDS transmit antenna

into the L-band IF of the receive Dish. This maximal coupling occurred when the there was a direct-ray path between the transmit antenna and the Dish LNB. This coupling appeared to be relatively insensitive to small changes in elevation, as long as the direct ray path remained.

The configuration for the test is shown in Figure A-19.

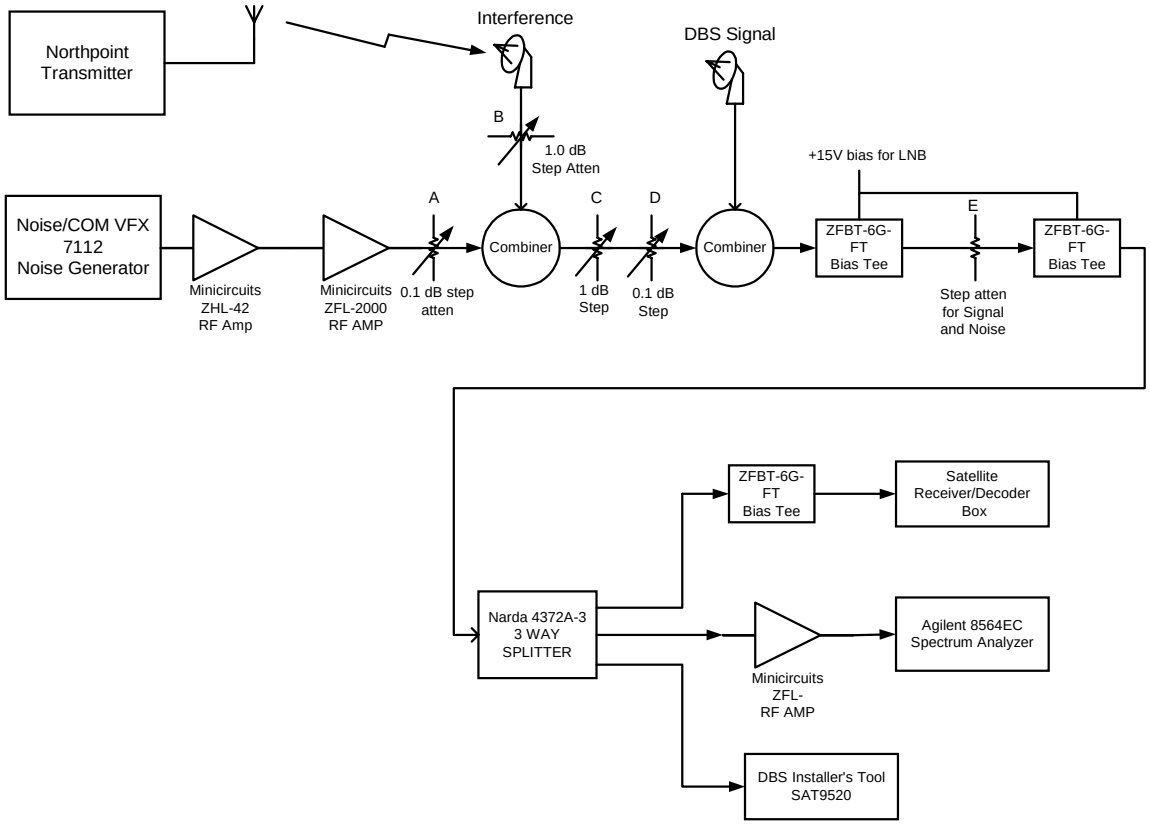

Figure A-19. Configuration for Open Range Testing of Northpoint MVDDS Interference to DBS Systems

The Northpoint transmitter/antenna broadcasts a signal which is received by a DBS dish antenna, and is converted to L band IF by the LNB contained within the dish. The L band interference signal is combined with a noise signal using an Anzac H-8-4 combiner. Noise is generated using a Noise/COM VFX 7112 generator and amplifier chain. The noise/interference signal is combined with the DBS "desired" signal using a second H-8-4 combiner. Attenuators A and B along with the variable about level capability of the Noise/COM generator serve to control the relative levels of *N* and *I*. Attenuators C and D vary the *N*+*I* total, relative to the carrier level C. Bias tees provide DC power for the LNBs of the two dishes. A Narda 3 way splitter provides outputs for the Satellite Set-top box,

Agilent spectrum analyzer, and DBS SAT 9520 Installer's Tool. Note that the pedestal mounted DBS receive antenna was pointed at clear sky, and the 90 cm dish was used to collect DIRECTV signals.

A view of the received power spectrum of the transmitted Northpoint MVDDS coupled into the spillover lobe of the receive dish is shown in Figure A-20.

Figure A-20. Single Channel MVDDS Open Range Transmission Coupled into Spillover Region of a DBS Receive Dish

A.8.2 Test Results

Data is recorded at various noise to interference power levels, namely, +infinity, (noise only), +10 dB, +3 dB, 0 dB, -3 dB, –10 dB, and –infinity (interference only). As in the previous section, results for +infinity and –infinity are plotted on the +30 and –30dB points, respectively.

Due to lack of time, results were compiled for DIRECTV only and are shown in Figure A-21.

The same trend is observed relative to the resilience to the constant envelope QPSK MVDDS signal as compared to Gaussian noise as was observed in the previous section. That is that there is approximately 1 dB resilience to the constant envelope QPSK interference versus Gaussian interference.

The performance curve given in Figure A-21 sits nearly 1 dB higher in $C/(N+I)$ than the curve of Figure A-14, the lab 12 GHz measures, and the translated IF measurements of Figure A-10. This 1 dB difference is easily accounted for through the combination of measurement error and DBS transponder bandwidth channelization differences.

Note as well the Proximity of the SAT9520 Measurement in the noise-only case to spectrum analyzer measurements. Insufficient information is available about the SAT9520 to provide an accurate scaling factor that would account for differences in measurement bandwidth between the spectrum analyzer and the SAT9520.

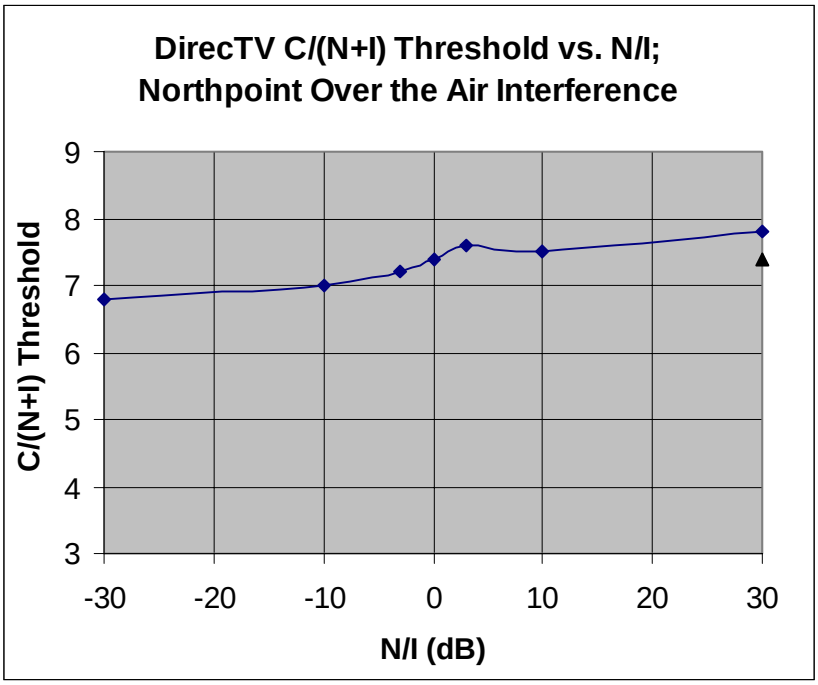

Figure A-21. Carrier-to-Noise-Plus-Interference Required to Degrade DIRECTV to A/V Quality 6 Vs. Noise-to-Interference Power Ratio; Northpoint MVDDS 12 GHz RF Output, Open Range

A.8.3 Notes on Open Air Testing

This subsection contains anecdotal notes on some ad-hoc tests that were performed during the process of antenna installation and measurement.

A.8.3.1 MVDDS Antenna Azimuth and Elevation

During installation of the MVDDS transmit antenna on the roof of the MITRE facility in preparation for open range testing, one ad-hoc test was performed for the purpose of assessing the impact of MVDDS antenna azimuth and elevation on existing DBS installations.

With the MVDDS antenna pointed due North and 0 degrees elevation, the transmit power of the antenna was raised to the point of interfering with the DBS installation used for the laboratory interference measurements discussed in the previous sections, (approximately 300 feet away). Turning the antenna due east, at 5 degrees elevation, the transmit power was raised by 13 dB prior to any degradation of the previous installation.

While not intended to be a quantitative test, it is interesting to note that Northpoint engineers were able to predict and mitigate the impact of the MVDDS transmission on a nearby installation.

A.8.3.2 Shielding of DBS Antenna as a Means of Interference Mitigation

As alluded to above, the range was configured to maximally couple the MVDDS transmit energy into any portion of the DBS antenna excluding the main beam. As suspected from the antenna gain pattern measurements, maximum coupling occurred when a direct ray from the MVDDS transmission could be drawn to the LNB of the DBS antenna.

This direct path was blocked by holding a lightweight piece of scrap aluminum between the MVDDS transmitter and the dish. We were subsequently able to couple the unattenuated input from the DBS dish (bypassing attenuator B of Figure A-19) without degrading the AV quality of the channel under test. Note that the total power across a 20 MHz bandwidth for the unattenuated signal at the output of the LNB was –34 dBm, on the same order of magnitude as the DBS signal.

A.9 Summary of Results

The lab measurements show that the constant amplitude of the MVDDS interference signal gives it a slight compatibility advantage with the DBS signal as opposed to Gaussian noise of the same power. This advantage is on the order of 1 dB when the total interference is dominated by MVDDS interference. Results vary slightly between Dish TV and DIRECTV when the interference and noise are close to the same power. Any practical advantage was very difficult to identify when the interference signal power was 3 dB or more below the noise power for either of the two DBS systems.

Several mitigation techniques were tested:

- When a 7 MHz offset is used by the MVDDS transmission with respect to the DBS channelization, and additional isolation of approximately 1.2 dB from the DBS signal

can be achieved due to the spectral mismatch between the victim signal and interferer.

- Appropriate selection of antenna azimuth and elevation angles was demonstrated to be effective in mitigating interference in areas close by. This is perhaps done at the expense of the MVDDS cell size.
- Blocking of the direct path between an MVDDS transmitter and a DBS dish LNB proved very effective in mitigating interference.

Appendix B

Interference Predictions for Selected Scenarios

This appendix contains a series of plots that present contours of constant predicted interference impact, expressed according to several different criteria, upon populations of postulated Direct Broadcast Satellite (DBS) receivers dispersed across horizontal planes in the vicinity of a Multichannel Video Distribution and Data Service (MVDDS) transmitter located at the origin. The plots are discussed and interpreted in Section 5.1.2. As explained in that section, the plot on page B-3 represents a "benchmark" scenario, and all the remaining plots represent "excursions" from the benchmark case, in which one, two, three, or four parameters are varied from their benchmark values to determine the sensitivity of the results to such variations. The legend beneath each such plot highlights in bold type the parametric changes that distinguish the scenario in question from the benchmark scenario.

The impact criterion used in most of the plots is the absolute increase ΔU caused by MVDDS in annual rain-induced DBS unavailability U, where U and ΔU are both measured in hours per year (hr/yr). In those plots the contours are color-coded as follows:

Magenta	MVDDS coverage boundary
Blue	ΔU = 0.3 hr/yr
Green	ΔU = 1 hr/yr
Red	ΔU = 3 hr/yr
Cyan	ΔU = 10 hr/yr
Black	ΔU = 30 hr/yr

In one plot where the criterion is the *relative* increase ($\Delta U/U_0$) expressed as a percentage, and U_0 is the "baseline" value of U that exists even *without* MVDDS present, this set of color codes is used:

Magenta	MVDDS coverage boundary
Blue	$\Delta U/U_0$ = 2.86%
Green	$\Delta U/U_0$ = 10%
Red	$\Delta U/U_0$ = 30%
Cyan	$\Delta U/U_0$ = 100%
Black	$\Delta U/U_0$ = 300%

In the plot where the criterion is the total unavailability ($U_0 + \Delta U$) caused by rain and MVDDS combined, this color code is employed:

Magenta	MVDDS coverage boundary
Blue	$U_0 + \Delta U$ = 25 hr/yr
Green	$U_0 + \Delta U$ = 30 hr/yr

Red	$U_0 + \Delta U = 35$ hr/yr
Cyan	$U_0 + \Delta U = 40$ hr/yr
Black	$U_0 + \Delta U = 45$ hr/yr

Finally, the following color code is used in the single plot whose criterion is $(C/I_M)_0$, the clear-air value of (C/I_M), where C is the carrier power and I_M is the MVDDS interference power at the DBS receiver:

Magenta	MVDDS coverage boundary
Blue	$(C/I_M)_0 = 25$ dB
Green	$(C/I_M)_0 = 20$ dB
Red	$(C/I_M)_0 = 15$ dB
Cyan	$(C/I_M)_0 = 10$ dB
Black	$(C/I_M)_0 = 5$ dB

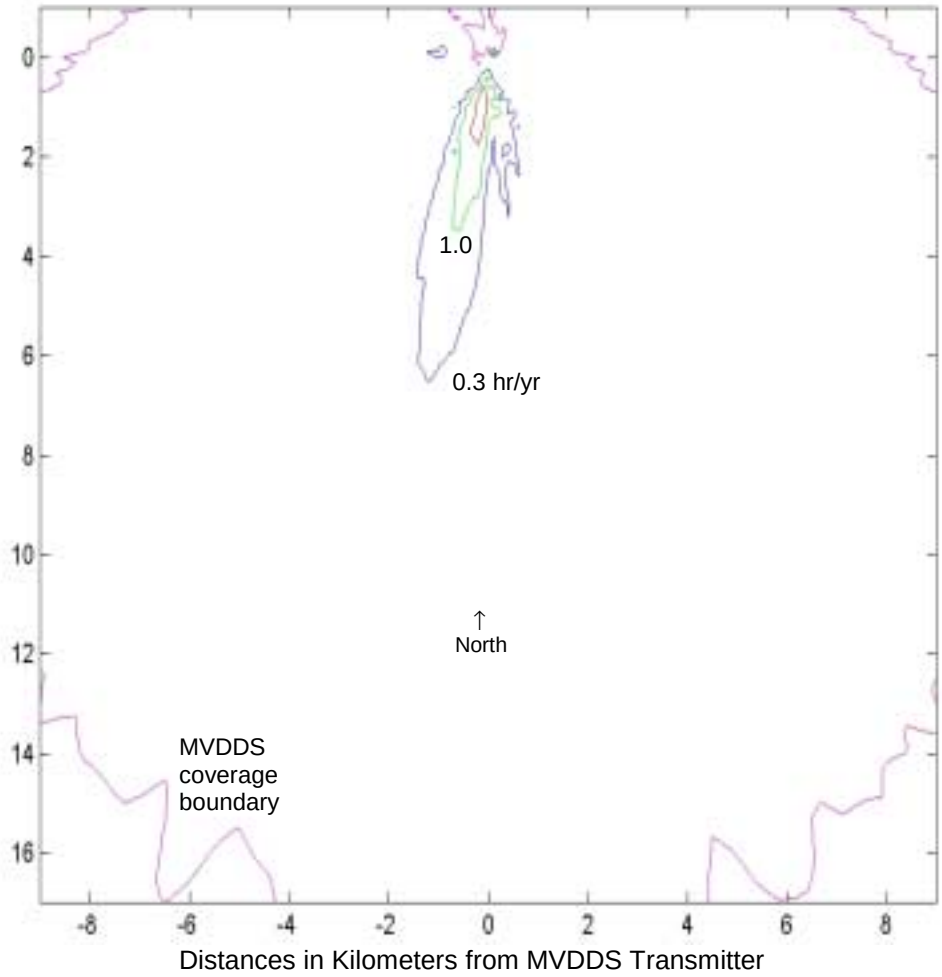

Washington, DC (12.45 GHz): **benchmark case**
Maximum absolute increase caused by MVDDS in rain-induced DBS unavailability
Raw MVDDS transmitter power (*not* EIRP): 0 dBm
MVDDS transmitting antenna: Northpoint large sectoral horn
MVDDS transmitting-antenna boresight: 180° azimuth (S); 0° elevation tilt
MVDDS transmitting antenna 100 meters above horizontal plane
Assumed MVDDS interference scaling factor: 1 dB
Frequency offset between MVDDS and DBS carriers: none
DBS performance measure: VQ6
DBS receiving antenna: 18" single-feed dish
Minimum ratio of DBS EIRP to receiver threshold assumed for each satellite longitude
Baseline rain-induced unavailabilities (*without* MVDDS interference):

101° W:	2.17 hr/yr
110° W:	3.88 hr/yr
119° W:	24.56 hr/yr

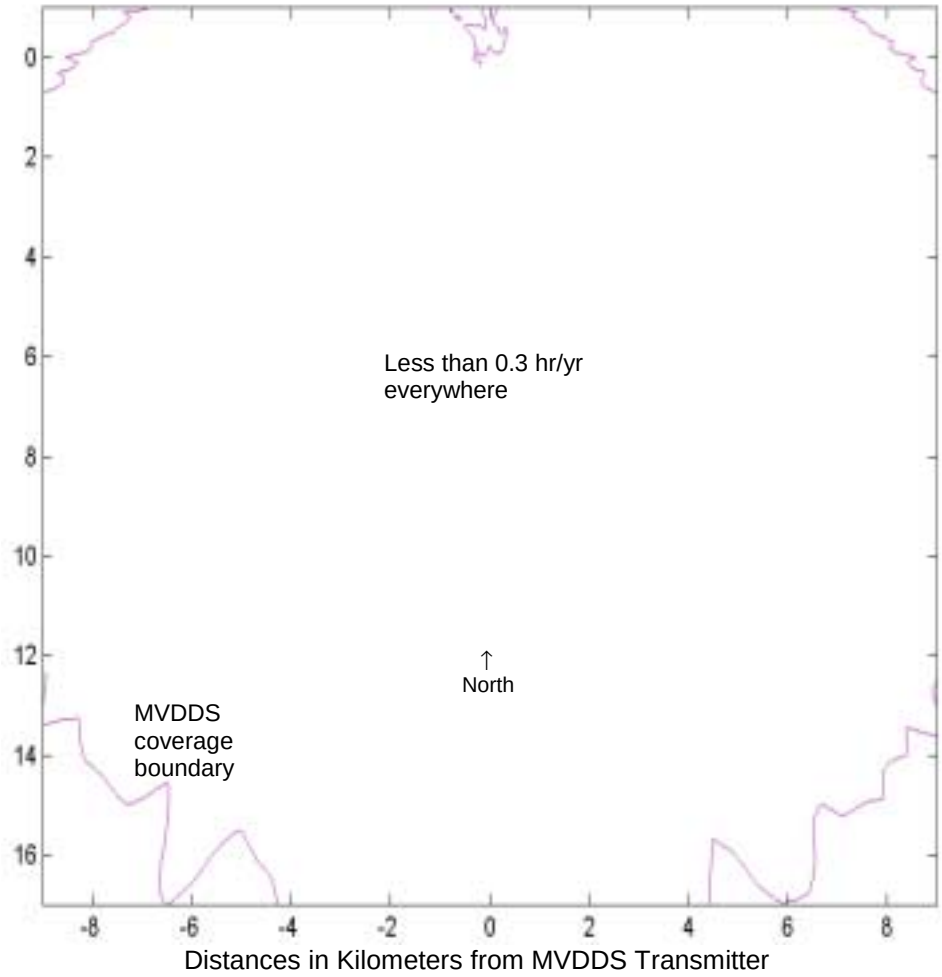

Washington, DC (12.45 GHz): **101° W satellite longitude only**
Absolute increase caused by MVDDS in rain-induced DBS unavailability
Raw MVDDS transmitter power (*not* EIRP): 0 dBm
MVDDS transmitting antenna: Northpoint large sectoral horn
MVDDS transmitting-antenna boresight: 180° azimuth (S); 0° elevation tilt
MVDDS transmitting antenna 100 meters above horizontal plane
Assumed MVDDS interference scaling factor: 1 dB
Frequency offset between MVDDS and DBS carriers: none
DBS performance measure: VQ6
DBS receiving antenna: 18” single-feed dish
Minimum ratio of DBS EIRP to receiver threshold assumed for this satellite longitude
Baseline rain-induced unavailability (*without* MVDDS interference): 2.17 hr/yr

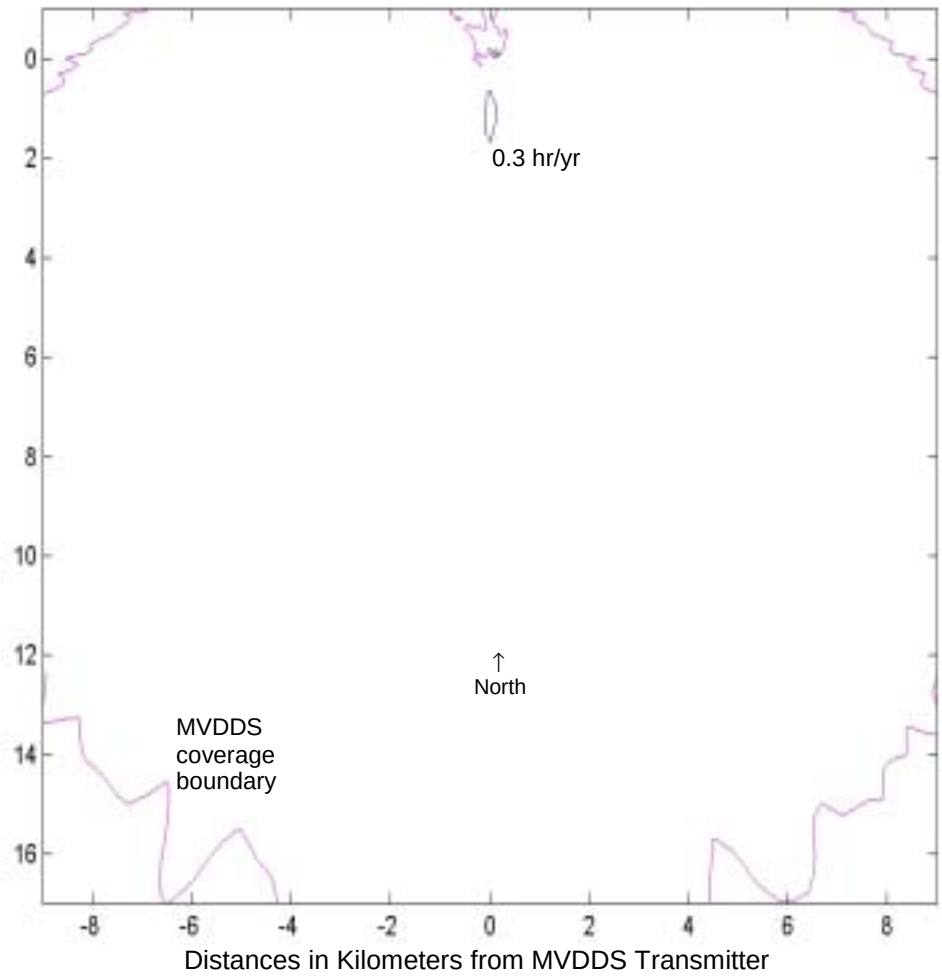

Washington, DC (12.45 GHz): **110° W satellite longitude only**
Absolute increase caused by MVDDS in rain-induced DBS unavailability
Raw MVDDS transmitter power (*not* EIRP): 0 dBm
MVDDS transmitting antenna: Northpoint large sectoral horn
MVDDS transmitting-antenna boresight: 180° azimuth (S); 0° elevation tilt
MVDDS transmitting antenna 100 meters above horizontal plane
Assumed MVDDS interference scaling factor: 1 dB
Frequency offset between MVDDS and DBS carriers: none
DBS performance measure: VQ6
DBS receiving antenna: 18” single-feed dish
Minimum ratio of DBS EIRP to receiver threshold assumed for this satellite longitude
Baseline rain-induced unavailability (*without* MVDDS interference): 3.88 hr/yr

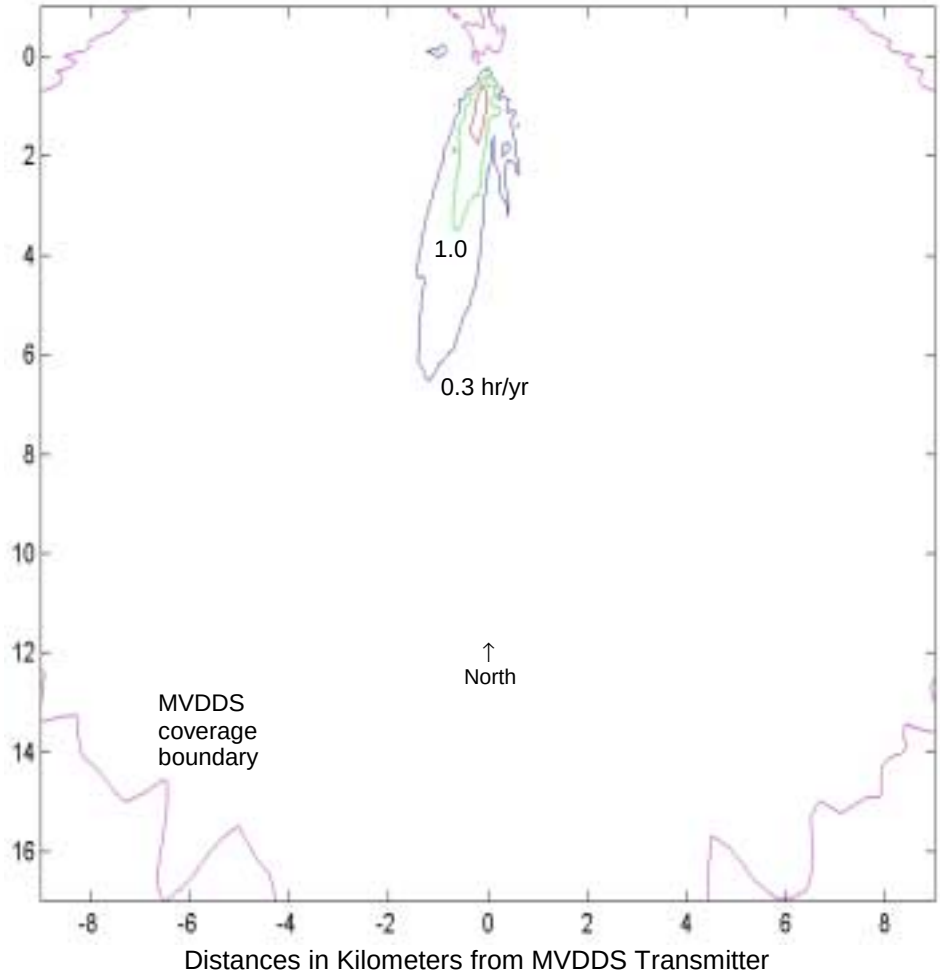

Washington, DC (12.45 GHz): **119° W satellite longitude only**
Absolute increase caused by MVDDS in rain-induced DBS unavailability
Raw MVDDS transmitter power (*not* EIRP): 0 dBm
MVDDS transmitting antenna: Northpoint large sectoral horn
MVDDS transmitting-antenna boresight: 180° azimuth (S); 0° elevation tilt
MVDDS transmitting antenna 100 meters above horizontal plane
Assumed MVDDS interference scaling factor: 1 dB
Frequency offset between MVDDS and DBS carriers: none
DBS performance measure: VQ6
DBS receiving antenna: 18" single-feed dish
Minimum ratio of DBS EIRP to receiver threshold assumed for this satellite longitude
Baseline rain-induced unavailability (*without* MVDDS interference): 24.56 hr/yr

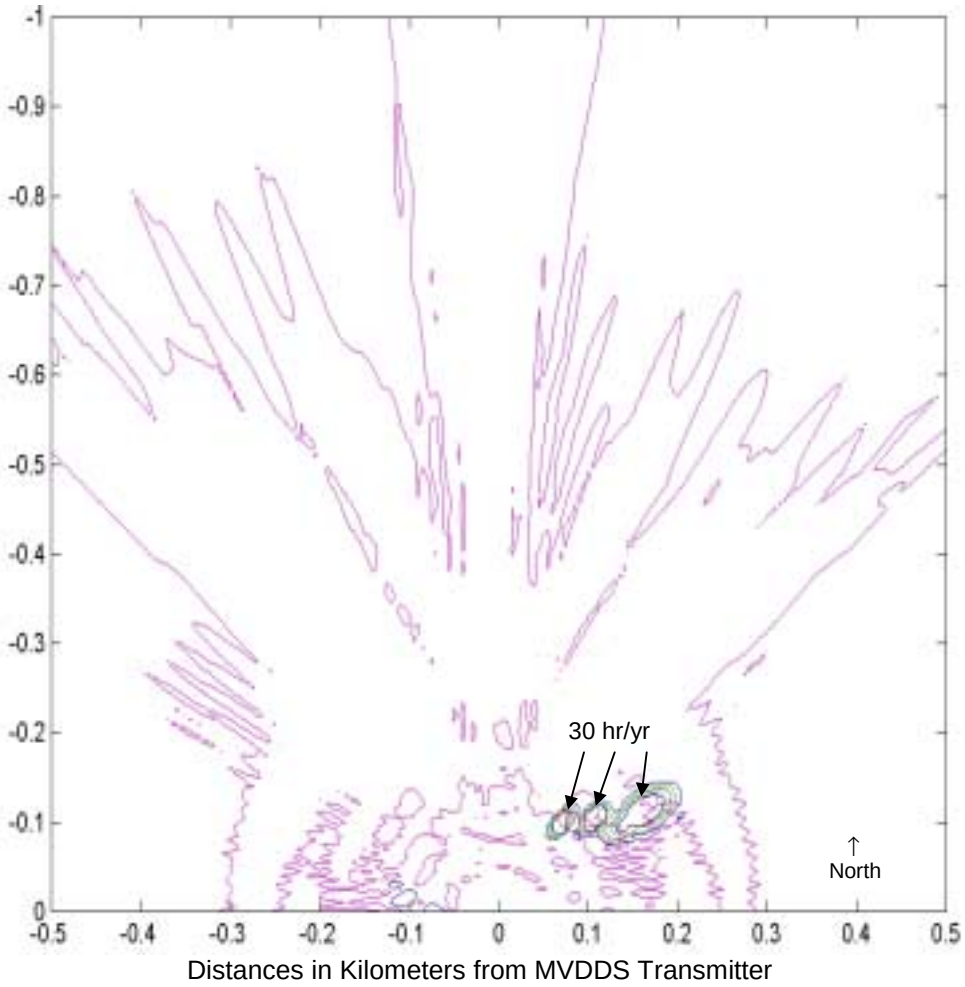

Washington, DC (12.45 GHz) benchmark case: region **behind** transmitter
Maximum absolute increase caused by MVDDS in rain-induced DBS unavailability
Raw MVDDS transmitter power (*not* EIRP): 0 dBm
MVDDS transmitting antenna: Northpoint large sectoral horn
MVDDS transmitting-antenna boresight: 180° azimuth (S); 0° elevation tilt
MVDDS transmitting antenna 100 meters above horizontal plane
Assumed MVDDS interference scaling factor: 1 dB
Frequency offset between MVDDS and DBS carriers: none
DBS performance measure: VQ6
DBS receiving antenna: 18" single-feed dish
Minimum ratio of DBS EIRP to receiver threshold assumed for each satellite longitude
Baseline rain-induced unavailabilities (*without* MVDDS interference):

101° W:	2.17 hr/yr
110° W:	3.88 hr/yr
119° W:	24.56 hr/yr

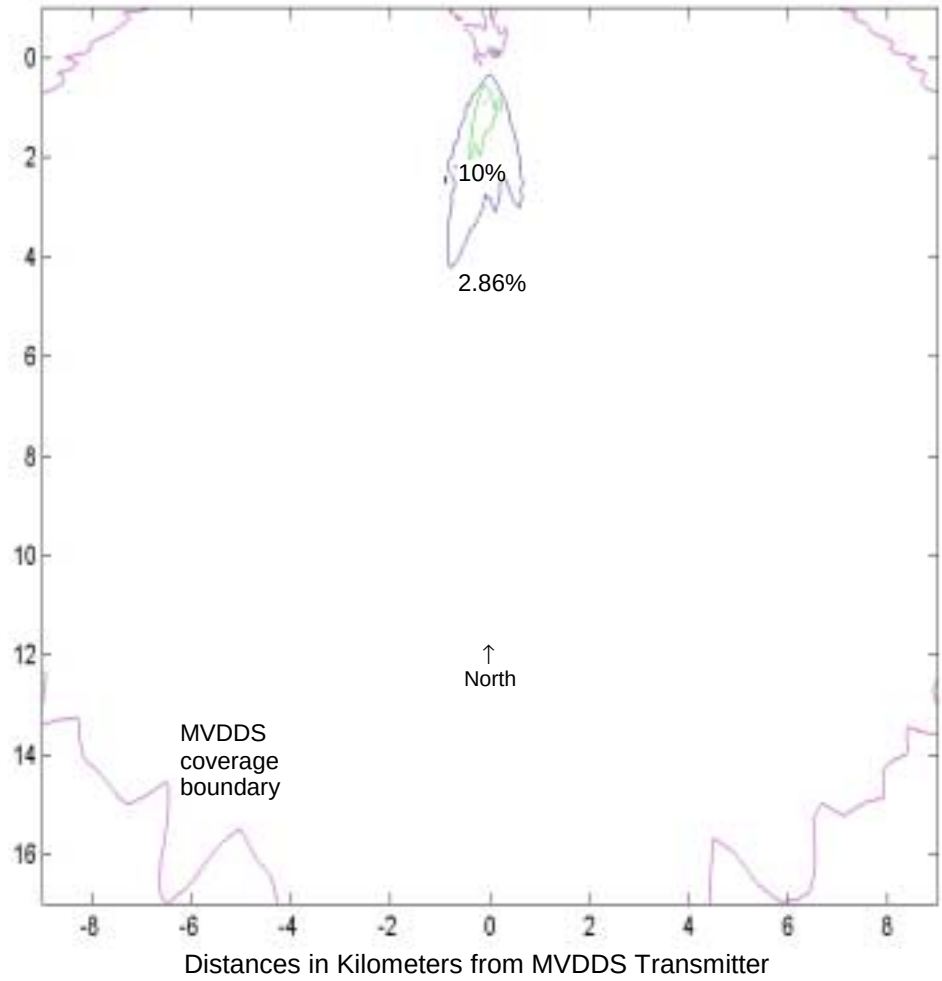

Washington, DC (12.45 GHz)
Maximum **relative** increase caused by MVDDS in rain-induced DBS unavailability
Raw MVDDS transmitter power (*not* EIRP): 0 dBm
MVDDS transmitting antenna: Northpoint large sectoral horn
MVDDS transmitting-antenna boresight: 180° azimuth (S); 0° elevation tilt
MVDDS transmitting antenna 100 meters above horizontal plane
Assumed MVDDS interference scaling factor: 1 dB
Frequency offset between MVDDS and DBS carriers: none
DBS performance measure: VQ6
DBS receiving antenna: 18" single-feed dish
Minimum ratio of DBS EIRP to receiver threshold assumed for each satellite longitude
Baseline rain-induced unavailabilities (*without* MVDDS interference):

101° W:	2.17 hr/yr
110° W:	3.88 hr/yr
119° W:	24.56 hr/yr

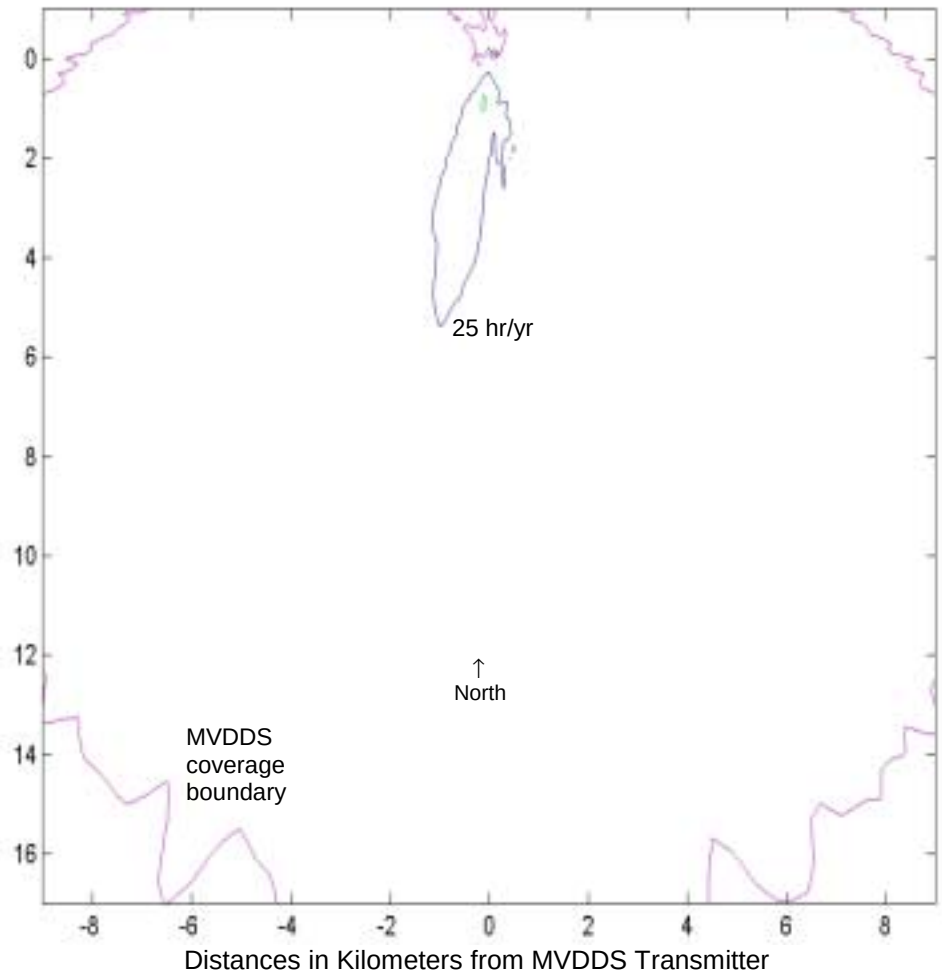

Washington, DC (12.45 GHz)
Maximum **total** DBS unavailability caused by rain and MVDDS combined
Raw MVDDS transmitter power (*not* EIRP): 0 dBm
MVDDS transmitting antenna: Northpoint large sectoral horn
MVDDS transmitting-antenna boresight: 180° azimuth (S); 0° elevation tilt
MVDDS transmitting antenna 100 meters above horizontal plane
Assumed MVDDS interference scaling factor: 1 dB
Frequency offset between MVDDS and DBS carriers: none
DBS performance measure: VQ6
DBS receiving antenna: 18" single-feed dish
Minimum ratio of DBS EIRP to receiver threshold assumed for each satellite longitude
Baseline rain-induced unavailabilities (*without* MVDDS interference):

101° W:	2.17 hr/yr
110° W:	3.88 hr/yr
119° W:	24.56 hr/yr

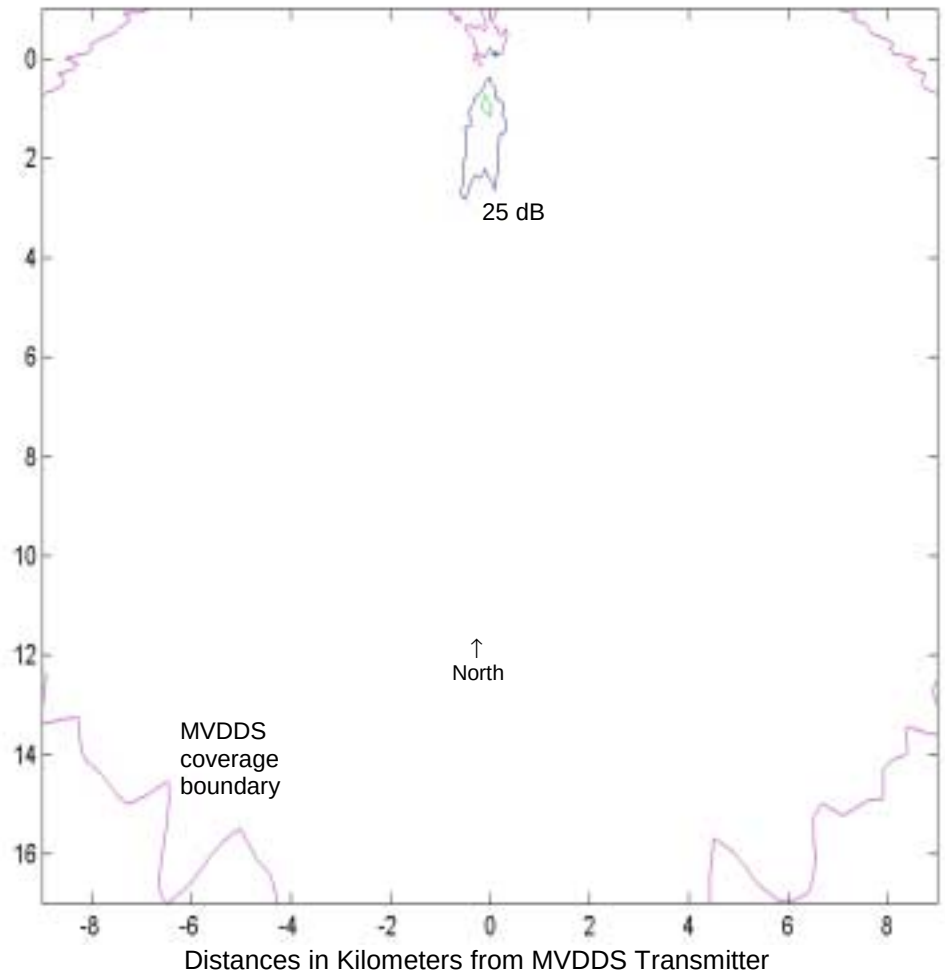

Washington, DC (12.45 GHz)
Minimum clear-air *(C/I_M)* value at DBS receiver
Raw MVDDS transmitter power (*not* EIRP): 0 dBm
MVDDS transmitting antenna: Northpoint large sectoral horn
MVDDS transmitting-antenna boresight: 180° azimuth (S); 0° elevation tilt
MVDDS transmitting antenna 100 meters above horizontal plane
Assumed MVDDS interference scaling factor: 1 dB
Frequency offset between MVDDS and DBS carriers: none
DBS performance measure: VQ6
DBS receiving antenna: 18" single-feed dish
Minimum ratio of DBS EIRP to receiver threshold assumed for each satellite longitude

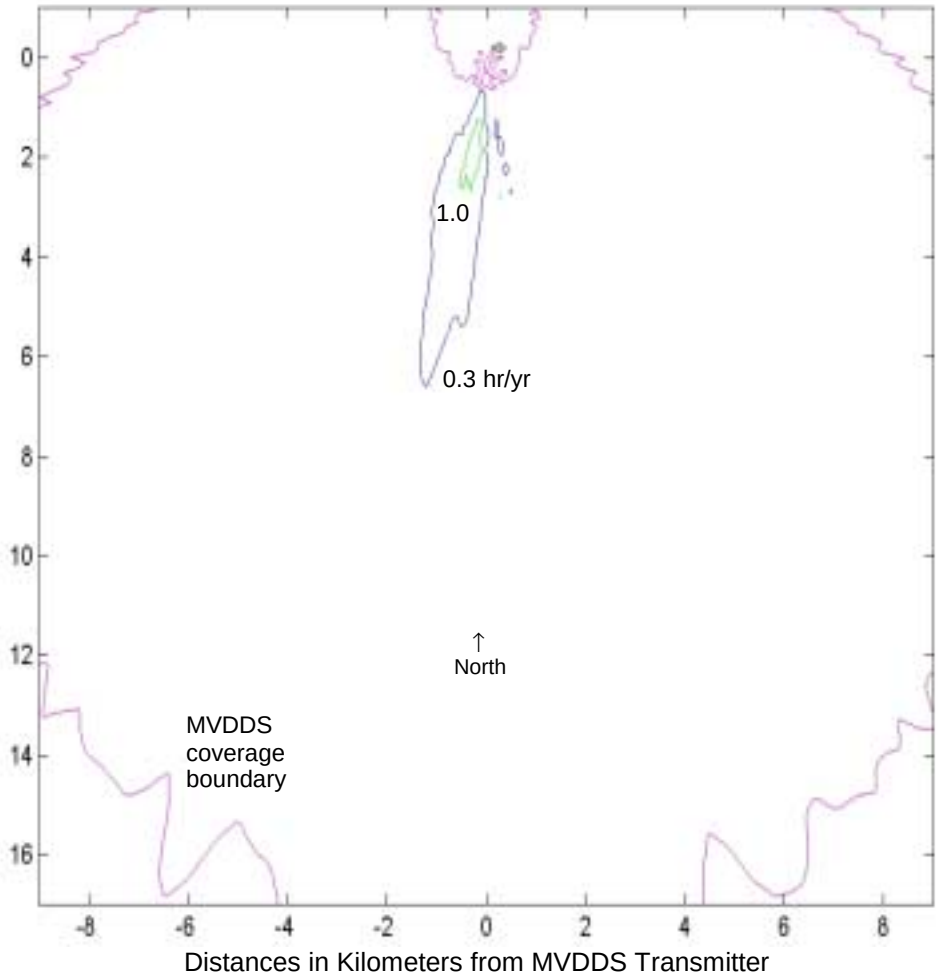

Washington, DC (12.45 GHz)
Maximum absolute increase caused by MVDDS in rain-induced DBS unavailability
Raw MVDDS transmitter power (*not* EIRP): 0 dBm
MVDDS transmitting antenna: Northpoint large sectoral horn
MVDDS transmitting-antenna boresight: 180° azimuth (S); 0° elevation tilt
MVDDS transmitting antenna **200** meters above horizontal plane
Assumed MVDDS interference scaling factor: 1 dB
Frequency offset between MVDDS and DBS carriers: none
DBS performance measure: VQ6
DBS receiving antenna: 18" single-feed dish
Minimum ratio of DBS EIRP to receiver threshold assumed for each satellite longitude
Baseline rain-induced unavailabilities (*without* MVDDS interference):

101° W:	2.17 hr/yr
110° W:	3.88 hr/yr
119° W:	24.56 hr/yr

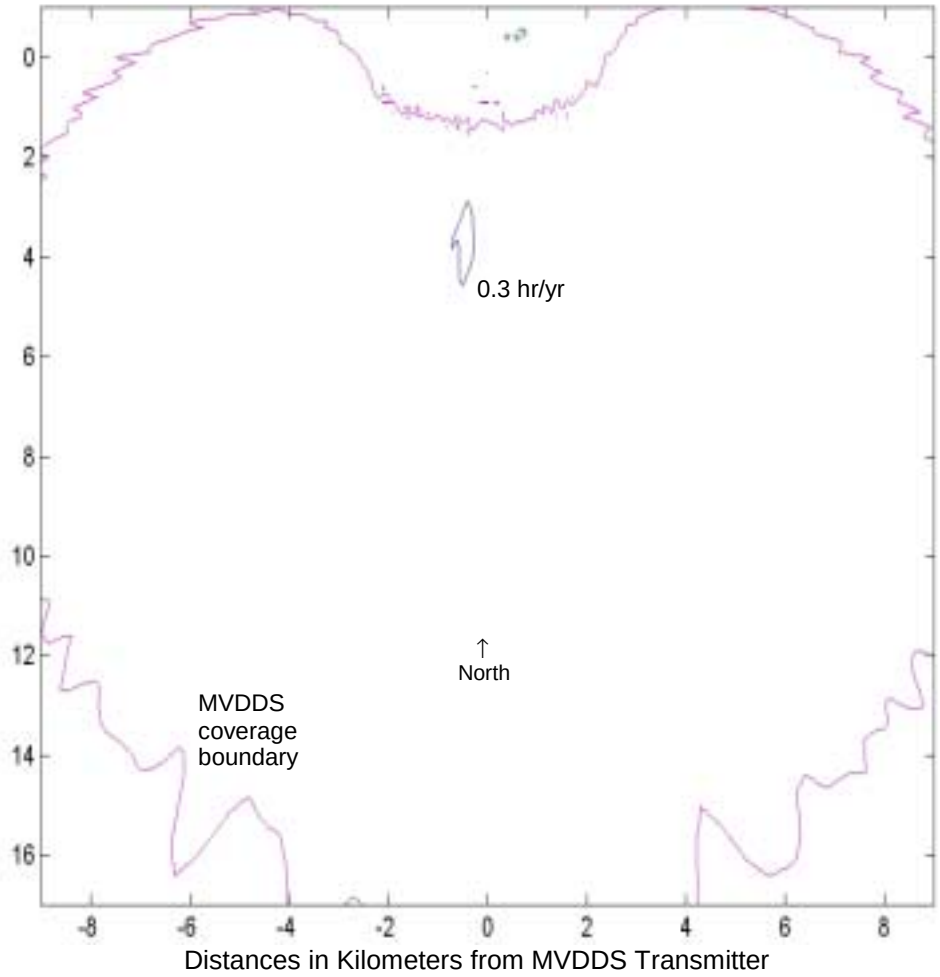

Washington, DC (12.45 GHz)
Maximum absolute increase caused by MVDDS in rain-induced DBS unavailability
Raw MVDDS transmitter power (*not* EIRP): 0 dBm
MVDDS transmitting antenna: Northpoint large sectoral horn
MVDDS transmitting-antenna boresight: 180° azimuth (S); 0° elevation tilt
MVDDS transmitting antenna **400** meters above horizontal plane
Assumed MVDDS interference scaling factor: 1 dB
Frequency offset between MVDDS and DBS carriers: none
DBS performance measure: VQ6
DBS receiving antenna: 18" single-feed dish
Minimum ratio of DBS EIRP to receiver threshold assumed for each satellite longitude
Baseline rain-induced unavailabilities (*without* MVDDS interference):

101° W:	2.17 hr/yr
110° W:	3.88 hr/yr
119° W:	24.56 hr/yr

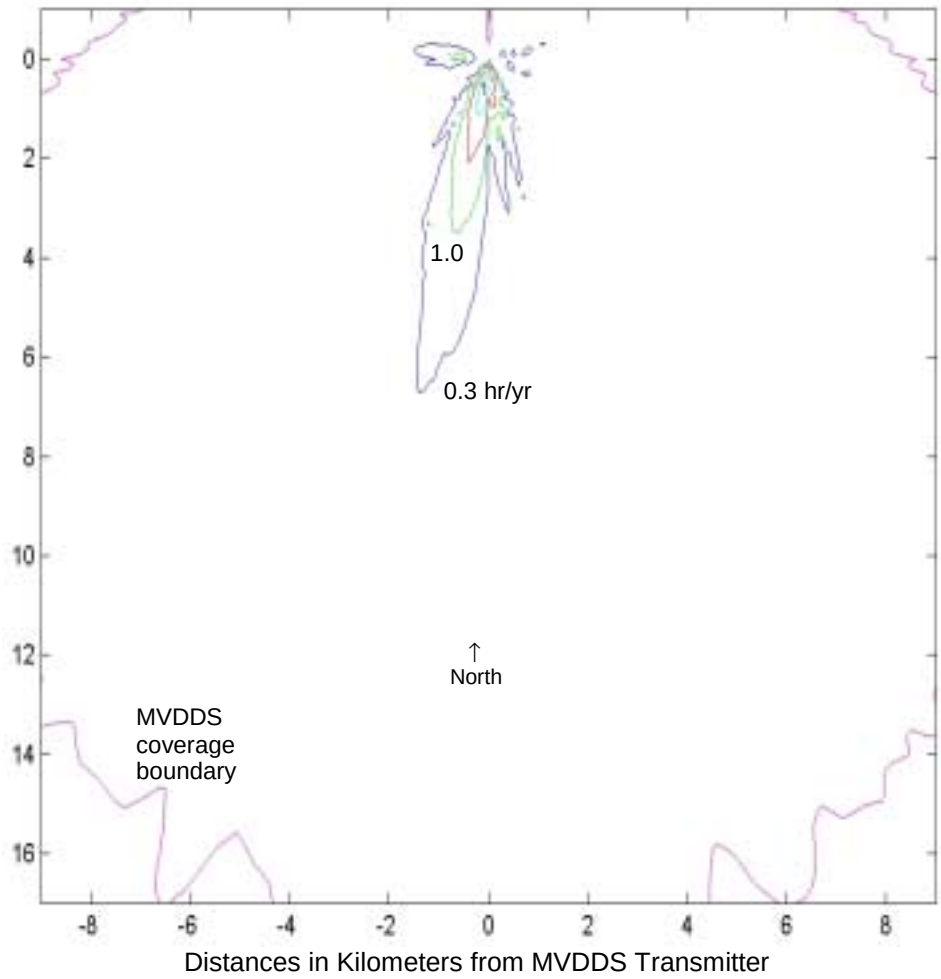

Washington, DC (12.45 GHz)
Maximum absolute increase caused by MVDDS in rain-induced DBS unavailability
Raw MVDDS transmitter power (*not* EIRP): 0 dBm
MVDDS transmitting antenna: Northpoint large sectoral horn
MVDDS transmitting-antenna boresight: 180° azimuth (S); 0° elevation tilt
MVDDS transmitting antenna **50** meters above horizontal plane
Assumed MVDDS interference scaling factor: 1 dB
Frequency offset between MVDDS and DBS carriers: none
DBS performance measure: VQ6
DBS receiving antenna: 18" single-feed dish
Minimum ratio of DBS EIRP to receiver threshold assumed for each satellite longitude
Baseline rain-induced unavailabilities (*without* MVDDS interference):

101° W:	2.17 hr/yr
110° W:	3.88 hr/yr
119° W:	24.56 hr/yr

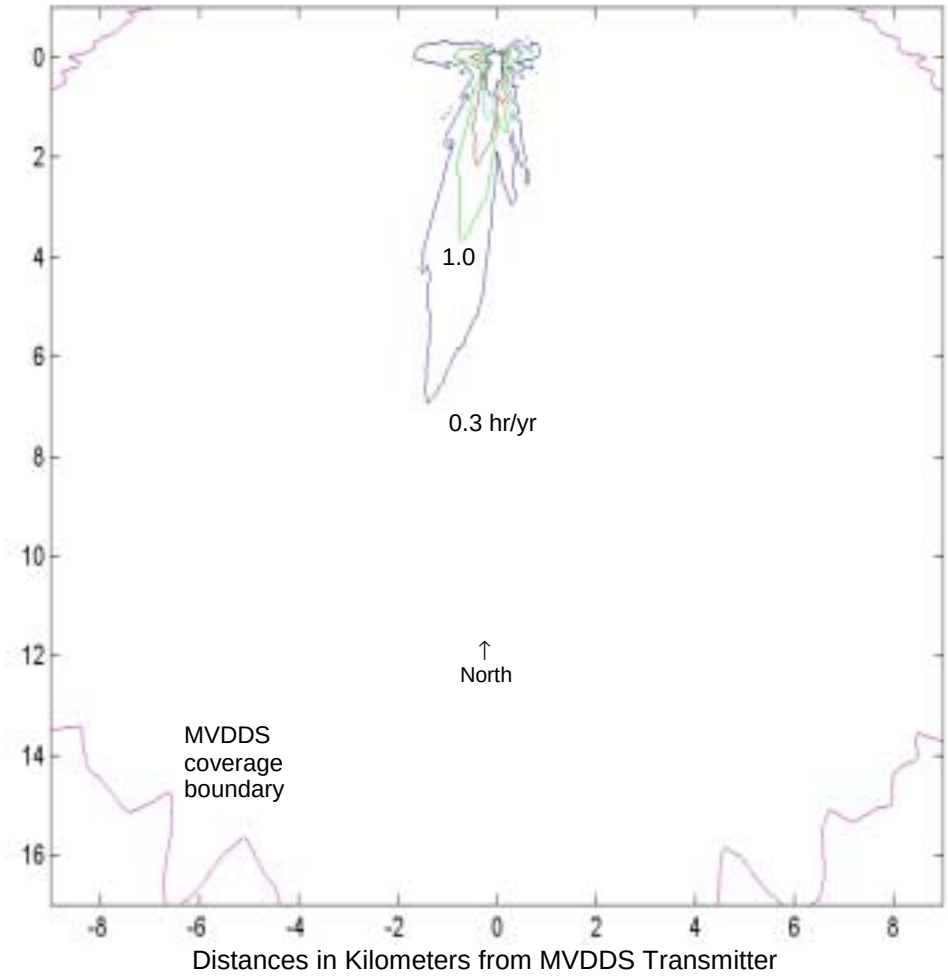

Washington, DC (12.45 GHz)
Maximum absolute increase caused by MVDDS in rain-induced DBS unavailability
Raw MVDDS transmitter power (*not* EIRP): 0 dBm
MVDDS transmitting antenna: Northpoint large sectoral horn
MVDDS transmitting-antenna boresight: 180° azimuth (S); 0° elevation tilt
MVDDS transmitting antenna **0** meters above horizontal plane
Assumed MVDDS interference scaling factor: 1 dB
Frequency offset between MVDDS and DBS carriers: none
DBS performance measure: VQ6
DBS receiving antenna: 18" single-feed dish
Minimum ratio of DBS EIRP to receiver threshold assumed for each satellite longitude
Baseline rain-induced unavailabilities (*without* MVDDS interference):

101° W:	2.17 hr/yr
110° W:	3.88 hr/yr
119° W:	24.56 hr/yr

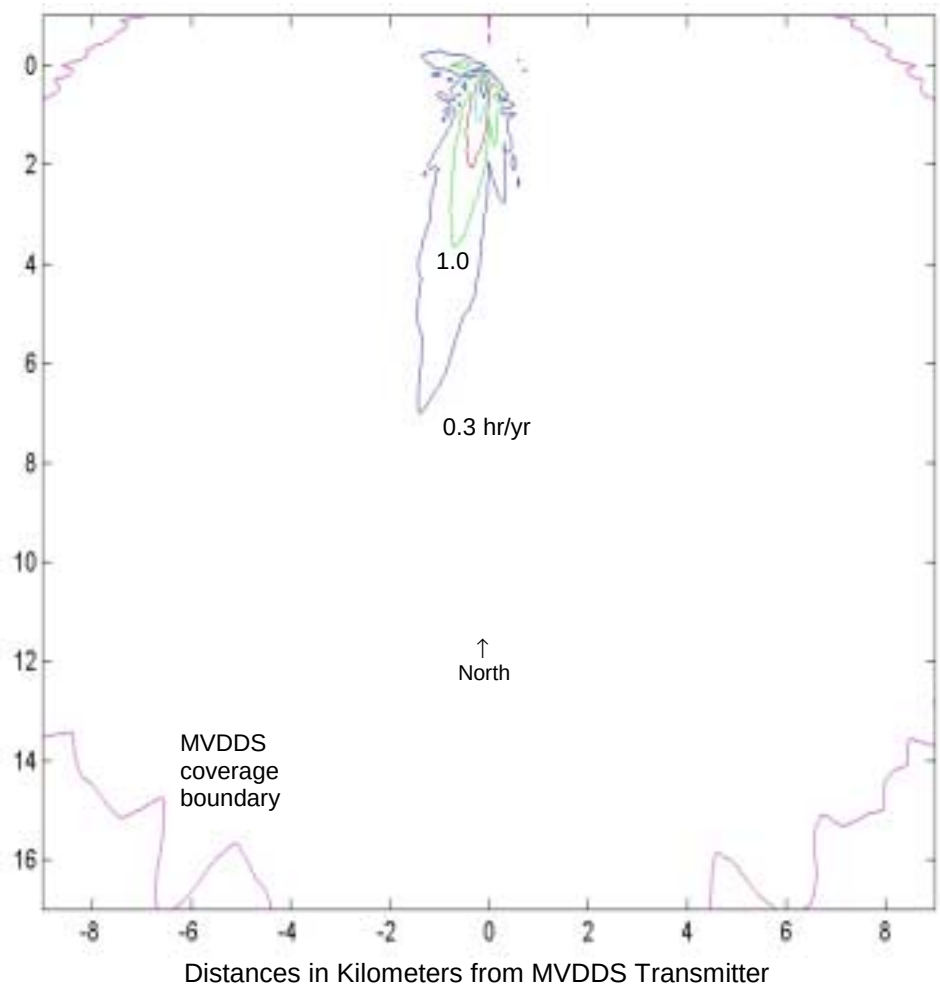

Washington, DC (12.45 GHz)
Maximum absolute increase caused by MVDDS in rain-induced DBS unavailability
Raw MVDDS transmitter power (*not* EIRP): 0 dBm
MVDDS transmitting antenna: Northpoint large sectoral horn
MVDDS transmitting-antenna boresight: 180° azimuth (S); 0° elevation tilt
MVDDS transmitting antenna **50** meters **below** horizontal plane
Assumed MVDDS interference scaling factor: 1 dB
Frequency offset between MVDDS and DBS carriers: none
DBS performance measure: VQ6
DBS receiving antenna: 18" single-feed dish
Minimum ratio of DBS EIRP to receiver threshold assumed for each satellite longitude
Baseline rain-induced unavailabilities (*without* MVDDS interference):

101° W:	2.17 hr/yr
110° W:	3.88 hr/yr
119° W:	24.56 hr/yr

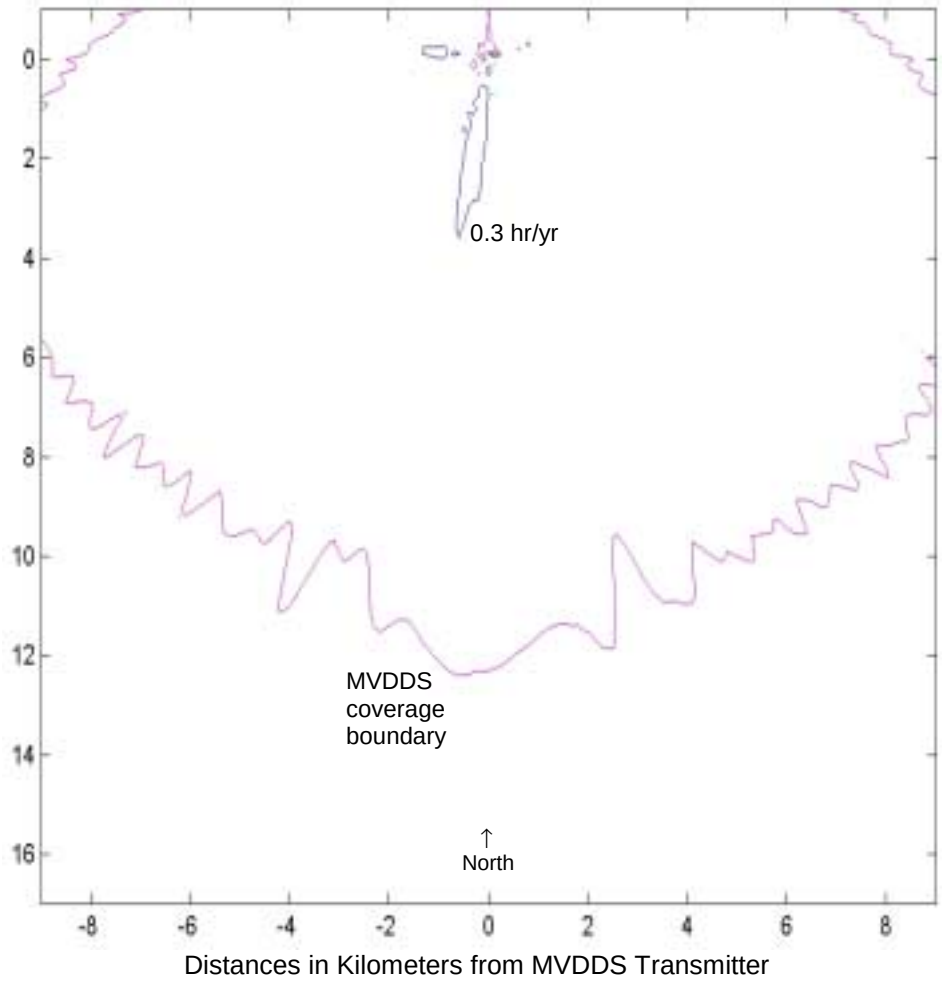

Washington, DC (12.45 GHz)
Maximum absolute increase caused by MVDDS in rain-induced DBS unavailability
Raw MVDDS transmitter power (*not* EIRP): 0 dBm
MVDDS transmitting antenna: Northpoint large sectoral horn
MVDDS transmitting-antenna boresight: 180° azimuth (S); **5° elevation tilt**
MVDDS transmitting antenna 100 meters above horizontal plane
Assumed MVDDS interference scaling factor: 1 dB
Frequency offset between MVDDS and DBS carriers: none
DBS performance measure: VQ6
DBS receiving antenna: 18" single-feed dish
Minimum ratio of DBS EIRP to receiver threshold assumed for each satellite longitude
Baseline rain-induced unavailabilities (*without* MVDDS interference):

101° W: 2.17 hr/yr
110° W: 3.88 hr/yr
119° W: 24.56 hr/yr

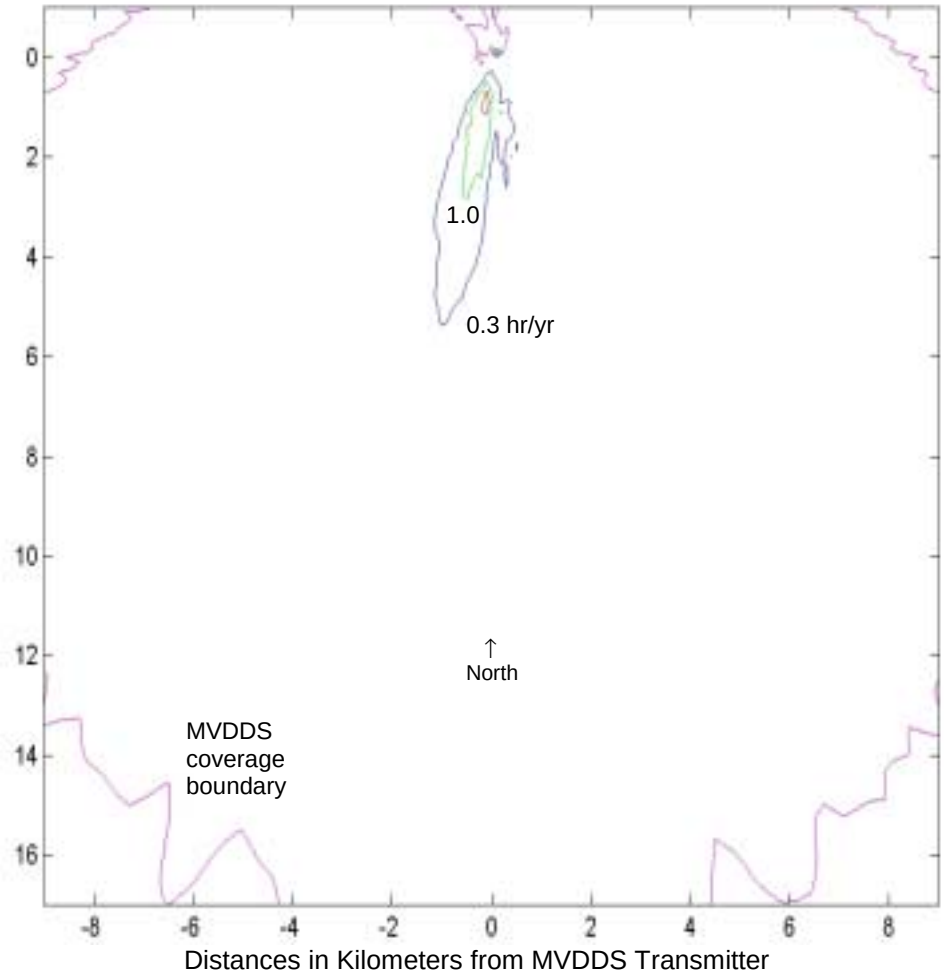

Washington, DC (12.45 GHz)
Maximum absolute increase caused by MVDDS in rain-induced DBS unavailability
Raw MVDDS transmitter power (*not* EIRP): 0 dBm
MVDDS transmitting antenna: Northpoint large sectoral horn
MVDDS transmitting-antenna boresight: 180° azimuth (S); 0° elevation tilt
MVDDS transmitting antenna 100 meters above horizontal plane
Assumed MVDDS interference scaling factor: 1 dB
Frequency offset between MVDDS and DBS carriers: **7 MHz**
DBS performance measure: VQ6
DBS receiving antenna: 18" single-feed dish
Minimum ratio of DBS EIRP to receiver threshold assumed for each satellite longitude
Baseline rain-induced unavailabilities (*without* MVDDS interference):

101° W:	2.17 hr/yr
110° W:	3.88 hr/yr
119° W:	24.56 hr/yr

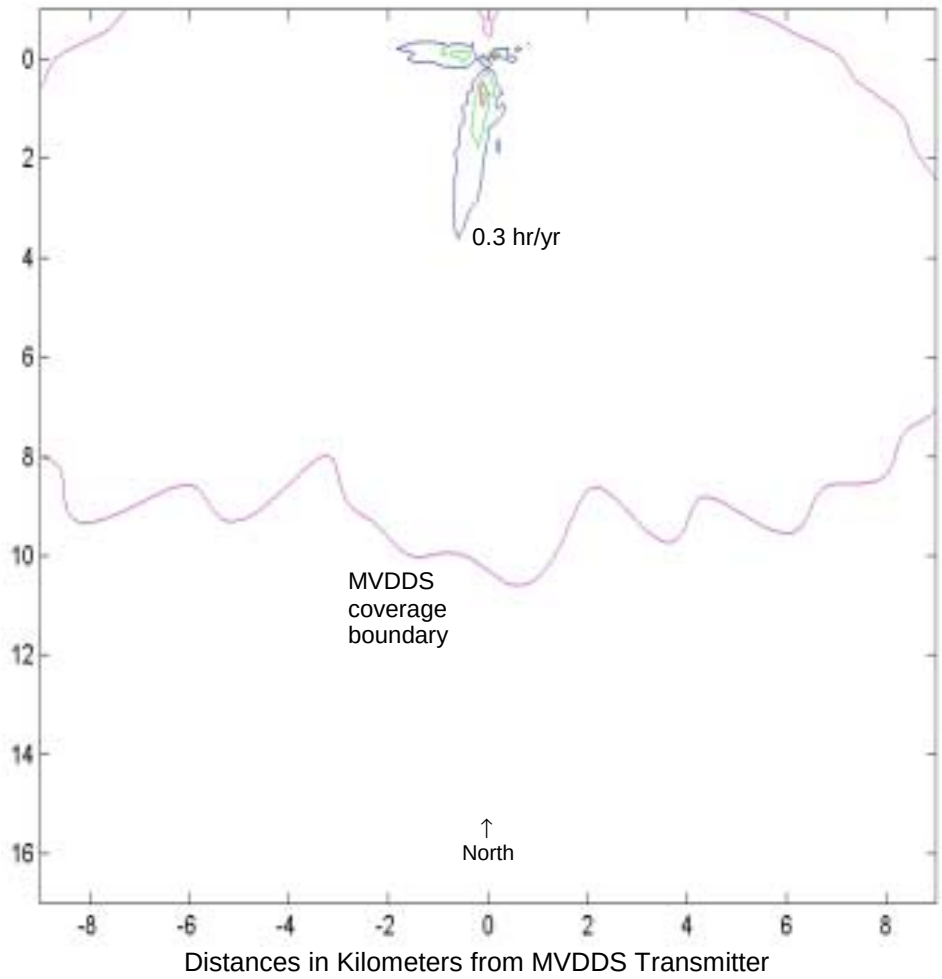

Washington, DC (12.45 GHz)
Maximum absolute increase caused by MVDDS in rain-induced DBS unavailability
Raw MVDDS transmitter power (*not* EIRP): 0 dBm
MVDDS transmitting antenna: Northpoint **small** sectoral horn
MVDDS transmitting-antenna boresight: 180° azimuth (S); 0° elevation tilt
MVDDS transmitting antenna 100 meters above horizontal plane
Assumed MVDDS interference scaling factor: 1 dB
Frequency offset between MVDDS and DBS carriers: none
DBS performance measure: VQ6
DBS receiving antenna: 18" single-feed dish
Minimum ratio of DBS EIRP to receiver threshold assumed for each satellite longitude
Baseline rain-induced unavailabilities (*without* MVDDS interference):

101° W:	2.17 hr/yr
110° W:	3.88 hr/yr
119° W:	24.56 hr/yr

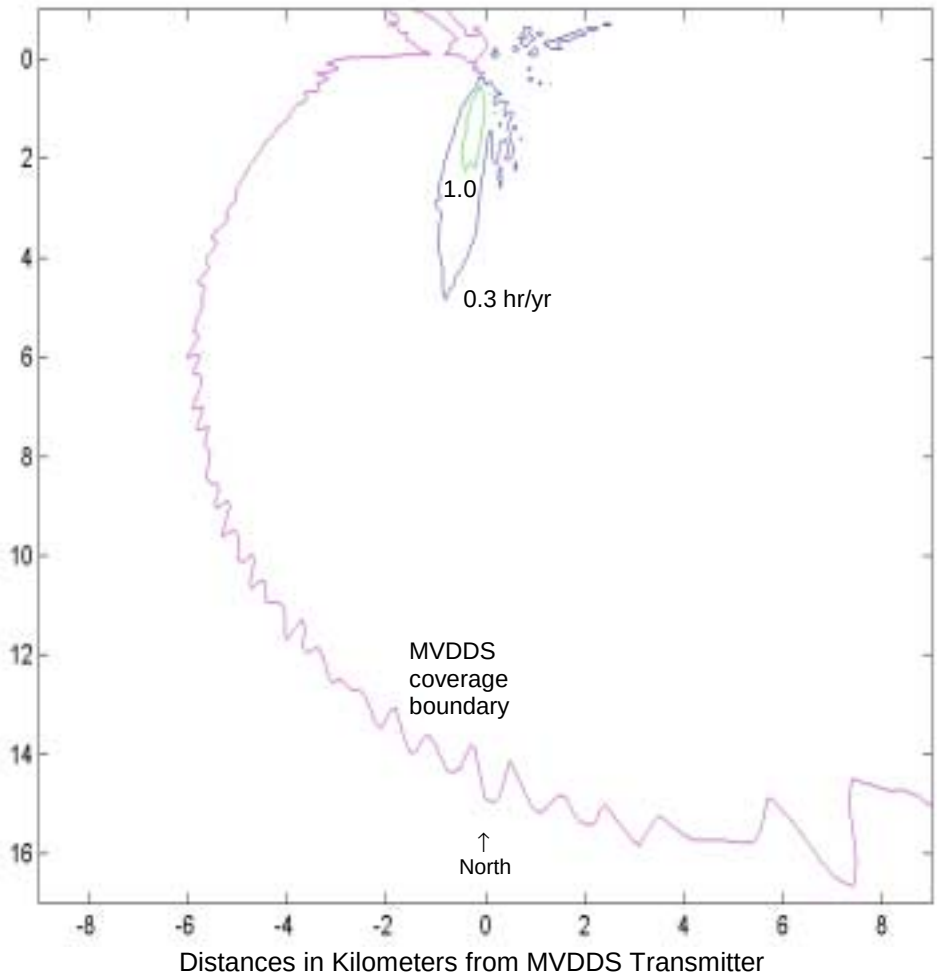

Washington, DC (12.45 GHz)
Maximum absolute increase caused by MVDDS in rain-induced DBS unavailability
Raw MVDDS transmitter power (*not* EIRP): 0 dBm
MVDDS transmitting antenna: Northpoint large sectoral horn
MVDDS transmitting-antenna boresight: **135°** azimuth **(SE)**; 0° elevation tilt
MVDDS transmitting antenna 100 meters above horizontal plane
Assumed MVDDS interference scaling factor: 1 dB
Frequency offset between MVDDS and DBS carriers: none
DBS performance measure: VQ6
DBS receiving antenna: 18" single-feed dish
Minimum ratio of DBS EIRP to receiver threshold assumed for each satellite longitude
Baseline rain-induced unavailabilities (*without* MVDDS interference):

101° W:	2.17 hr/yr
110° W:	3.88 hr/yr
119° W:	24.56 hr/yr

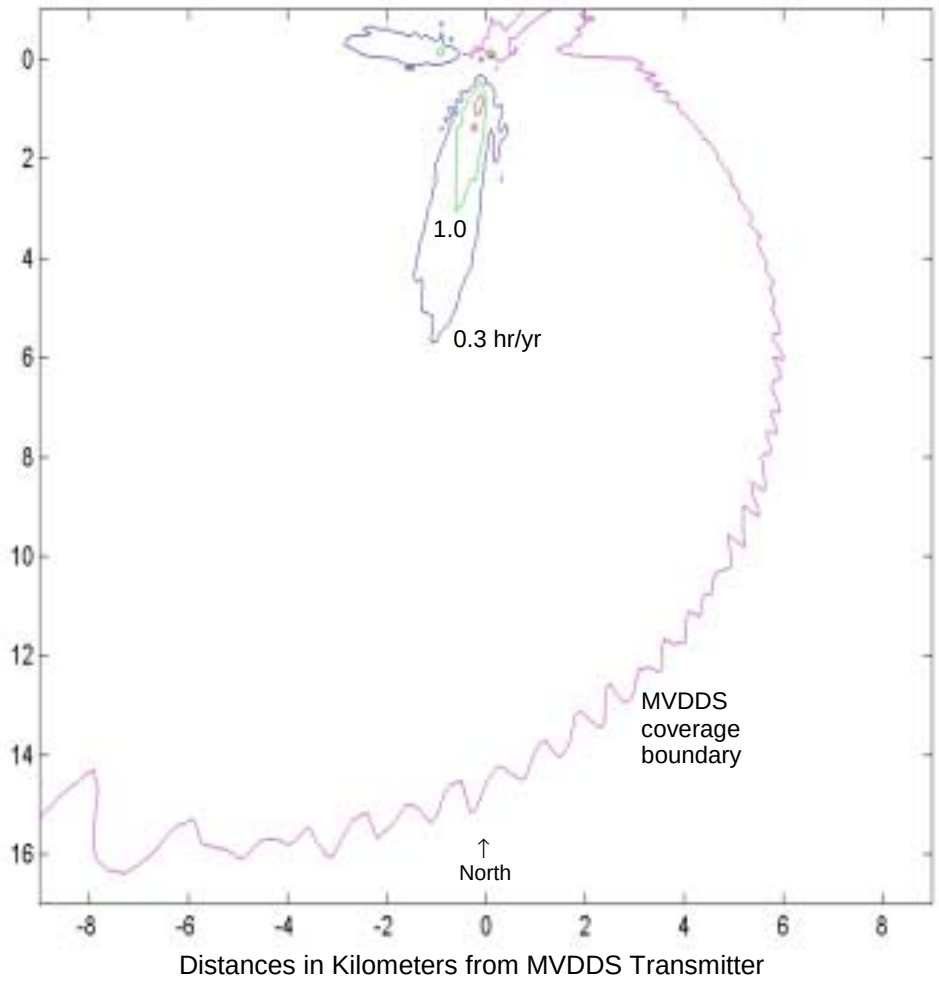

Washington, DC (12.45 GHz)
Maximum absolute increase caused by MVDDS in rain-induced DBS unavailability
Raw MVDDS transmitter power (*not* EIRP): 0 dBm
MVDDS transmitting antenna: Northpoint large sectoral horn
MVDDS transmitting-antenna boresight: **225°** azimuth **(SW)**; 0° elevation tilt
MVDDS transmitting antenna 100 meters above horizontal plane
Assumed MVDDS interference scaling factor: 1 dB
Frequency offset between MVDDS and DBS carriers: none
DBS performance measure: VQ6
DBS receiving antenna: 18" single-feed dish
Minimum ratio of DBS EIRP to receiver threshold assumed for each satellite longitude
Baseline rain-induced unavailabilities (*without* MVDDS interference):

101° W:	2.17 hr/yr
110° W:	3.88 hr/yr
119° W:	24.56 hr/yr

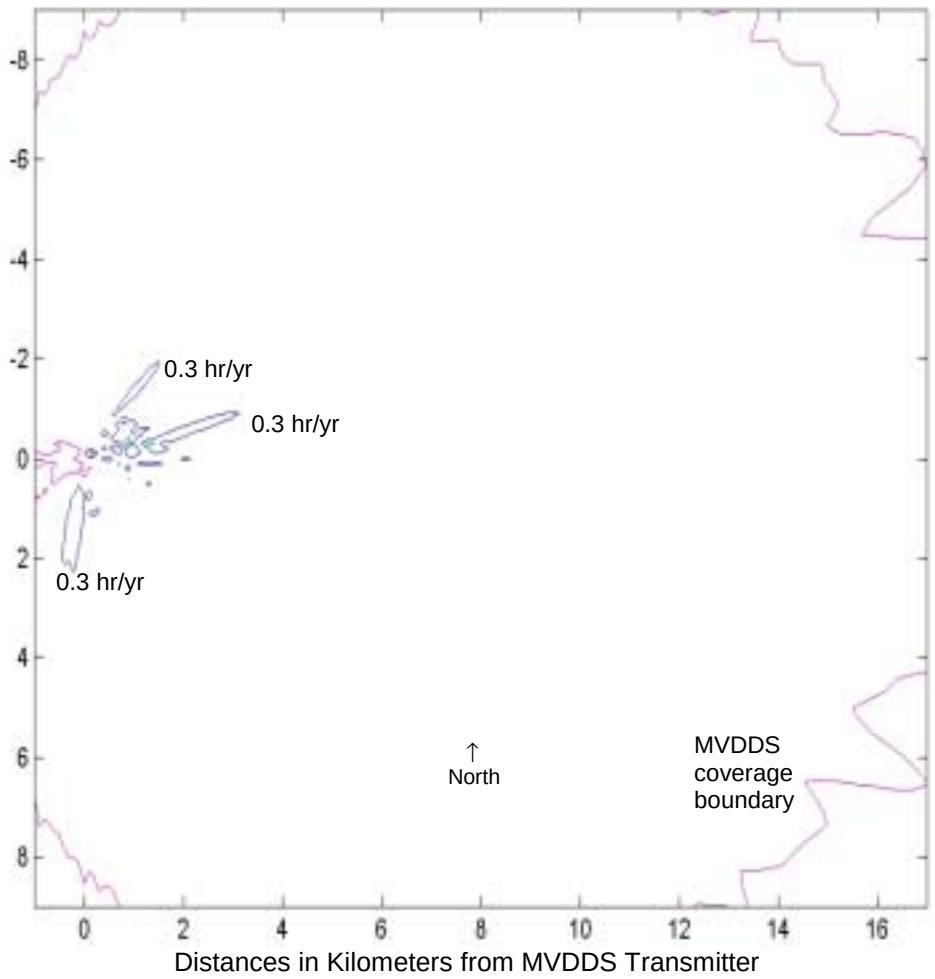

Washington, DC (12.45 GHz)
Maximum absolute increase caused by MVDDS in rain-induced DBS unavailability
Raw MVDDS transmitter power (*not* EIRP): 0 dBm
MVDDS transmitting antenna: Northpoint large sectoral horn
MVDDS transmitting-antenna boresight: **90°** azimuth **(E)**; 0° elevation tilt
MVDDS transmitting antenna 100 meters above horizontal plane
Assumed MVDDS interference scaling factor: 1 dB
Frequency offset between MVDDS and DBS carriers: none
DBS performance measure: VQ6
DBS receiving antenna: 18" single-feed dish
Minimum ratio of DBS EIRP to receiver threshold assumed for each satellite longitude
Baseline rain-induced unavailabilities (*without* MVDDS interference):

101° W: 2.17 hr/yr
110° W: 3.88 hr/yr
119° W: 24.56 hr/yr

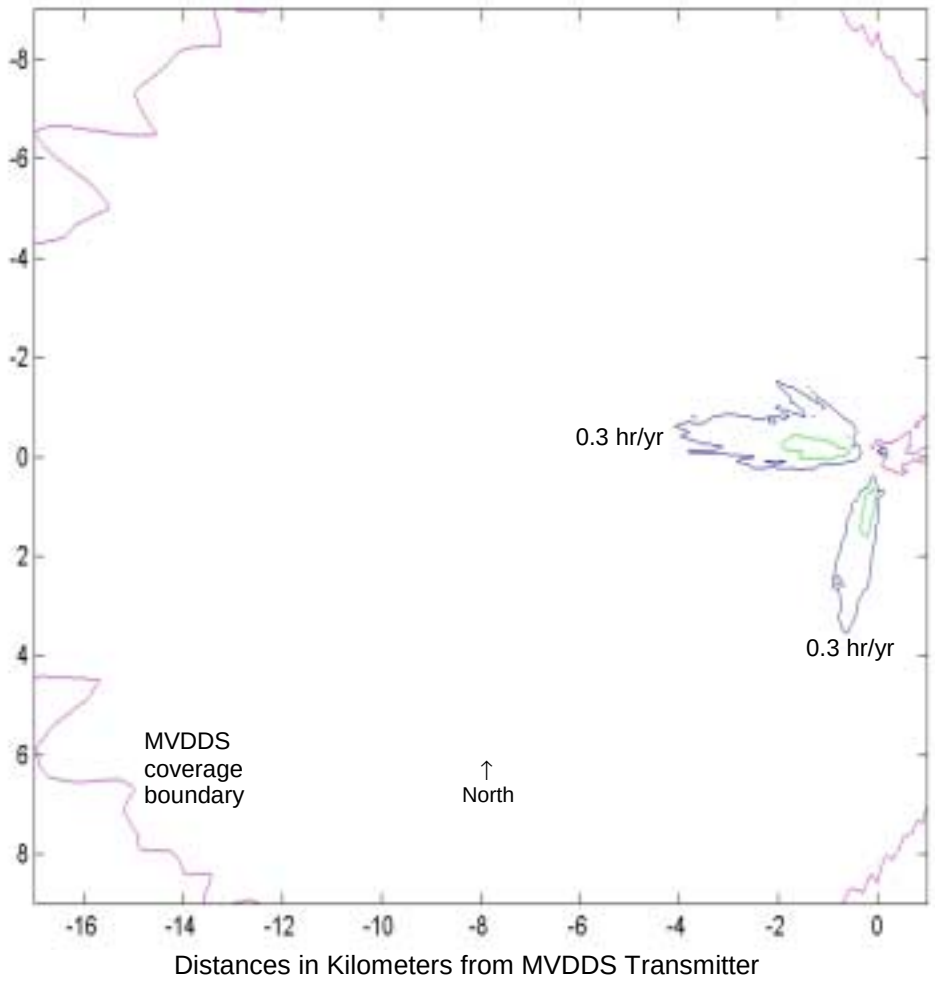

Washington, DC (12.45 GHz)
Maximum absolute increase caused by MVDDS in rain-induced DBS unavailability
Raw MVDDS transmitter power (*not* EIRP): 0 dBm
MVDDS transmitting antenna: Northpoint large sectoral horn
MVDDS transmitting-antenna boresight: **270°** azimuth **(W)**; 0° elevation tilt
MVDDS transmitting antenna 100 meters above horizontal plane
Assumed MVDDS interference scaling factor: 1 dB
Frequency offset between MVDDS and DBS carriers: none
DBS performance measure: VQ6
DBS receiving antenna: 18" single-feed dish
Minimum ratio of DBS EIRP to receiver threshold assumed for each satellite longitude
Baseline rain-induced unavailabilities (*without* MVDDS interference):

101° W:	2.17 hr/yr
110° W:	3.88 hr/yr
119° W:	24.56 hr/yr

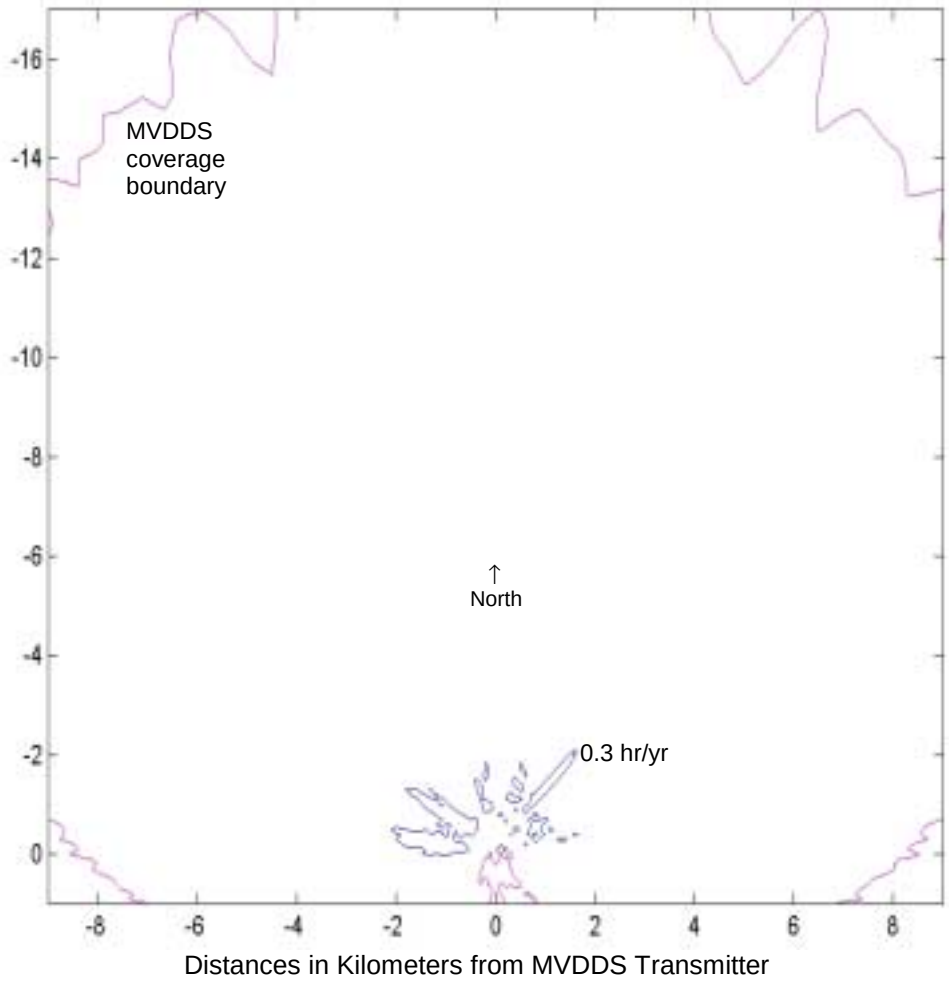

Washington, DC (12.45 GHz)
Maximum absolute increase caused by MVDDS in rain-induced DBS unavailability
Raw MVDDS transmitter power (*not* EIRP): 0 dBm
MVDDS transmitting antenna: Northpoint large sectoral horn
MVDDS transmitting-antenna boresight: **000°** azimuth **(N)**; 0° elevation tilt
MVDDS transmitting antenna 100 meters above horizontal plane
Assumed MVDDS interference scaling factor: 1 dB
Frequency offset between MVDDS and DBS carriers: none
DBS performance measure: VQ6
DBS receiving antenna: 18" single-feed dish
Minimum ratio of DBS EIRP to receiver threshold assumed for each satellite longitude
Baseline rain-induced unavailabilities (*without* MVDDS interference):

101° W:	2.17 hr/yr
110° W:	3.88 hr/yr
119° W:	24.56 hr/yr

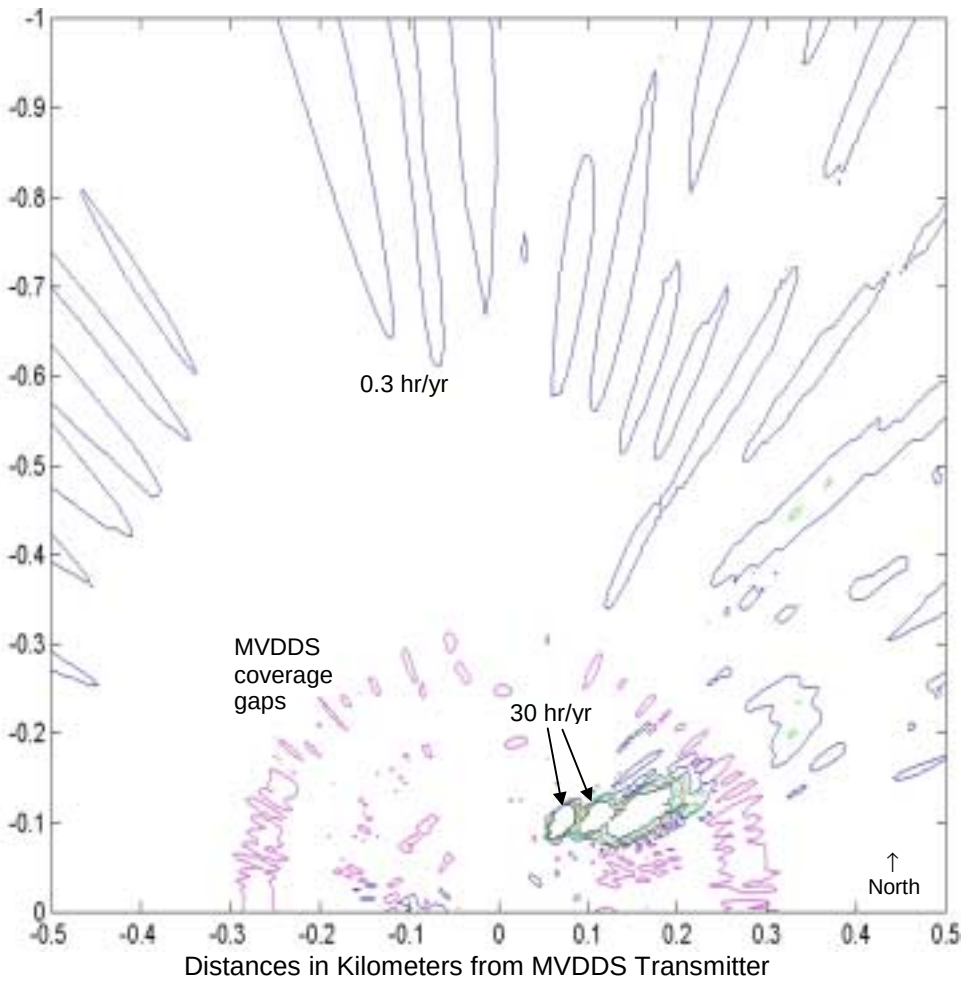

Washington, DC (12.45 GHz): Detail of region in front of transmitter
Maximum absolute increase caused by MVDDS in rain-induced DBS unavailability
Raw MVDDS transmitter power (*not* EIRP): 0 dBm
MVDDS transmitting antenna: Northpoint large sectoral horn
MVDDS transmitting-antenna boresight: **000°** azimuth **(N)**; 0° elevation tilt
MVDDS transmitting antenna 100 meters above horizontal plane
Assumed MVDDS interference scaling factor: 1 dB
Frequency offset between MVDDS and DBS carriers: none
DBS performance measure: VQ6
DBS receiving antenna: 18" single-feed dish
Minimum ratio of DBS EIRP to receiver threshold assumed for each satellite longitude
Baseline rain-induced unavailabilities (*without* MVDDS interference):

101° W: 2.17 hr/yr
110° W: 3.88 hr/yr
119° W: 24.56 hr/yr

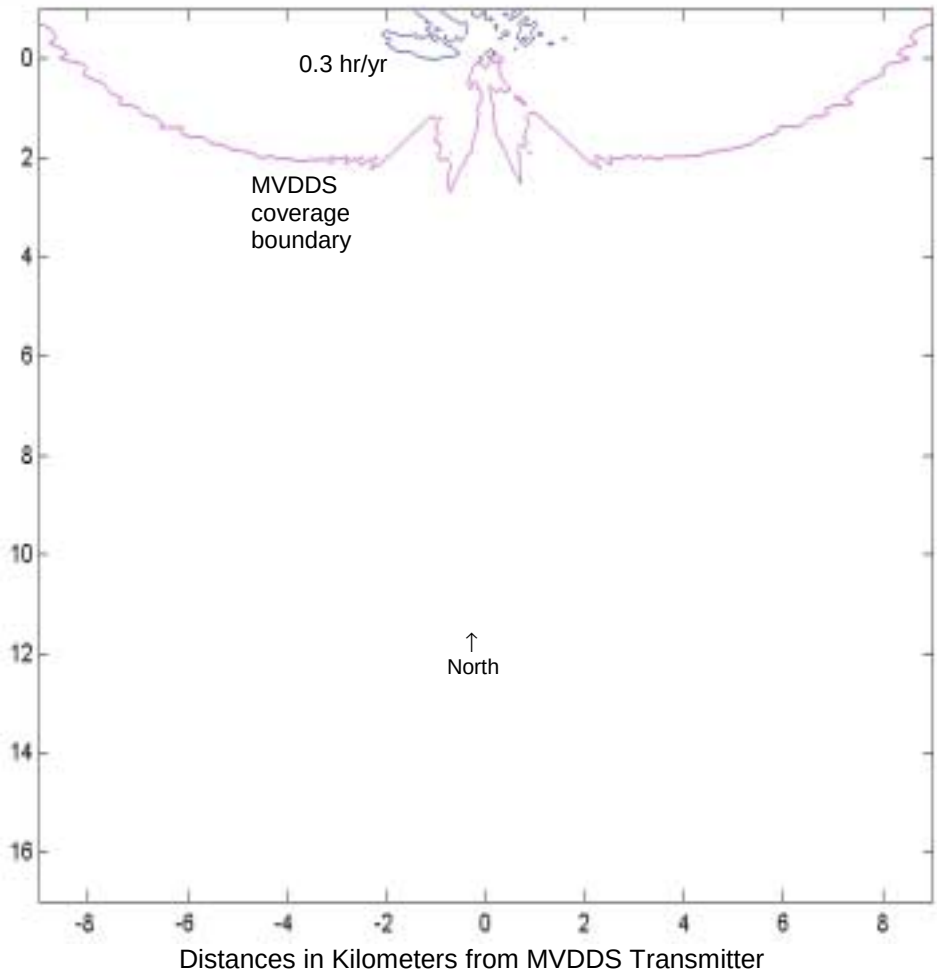

Washington, DC (12.45 GHz): Region behind transmitter
Maximum absolute increase caused by MVDDS in rain-induced DBS unavailability
Raw MVDDS transmitter power (*not* EIRP): 0 dBm
MVDDS transmitting antenna: Northpoint large sectoral horn
MVDDS transmitting-antenna boresight: **000°** azimuth **(N)**; 0° elevation tilt
MVDDS transmitting antenna 100 meters above horizontal plane
Assumed MVDDS interference scaling factor: 1 dB
Frequency offset between MVDDS and DBS carriers: none
DBS performance measure: VQ6
DBS receiving antenna: 18" single-feed dish
Minimum ratio of DBS EIRP to receiver threshold assumed for each satellite longitude
Baseline rain-induced unavailabilities (*without* MVDDS interference):

101° W:	2.17 hr/yr
110° W:	3.88 hr/yr
119° W:	24.56 hr/yr

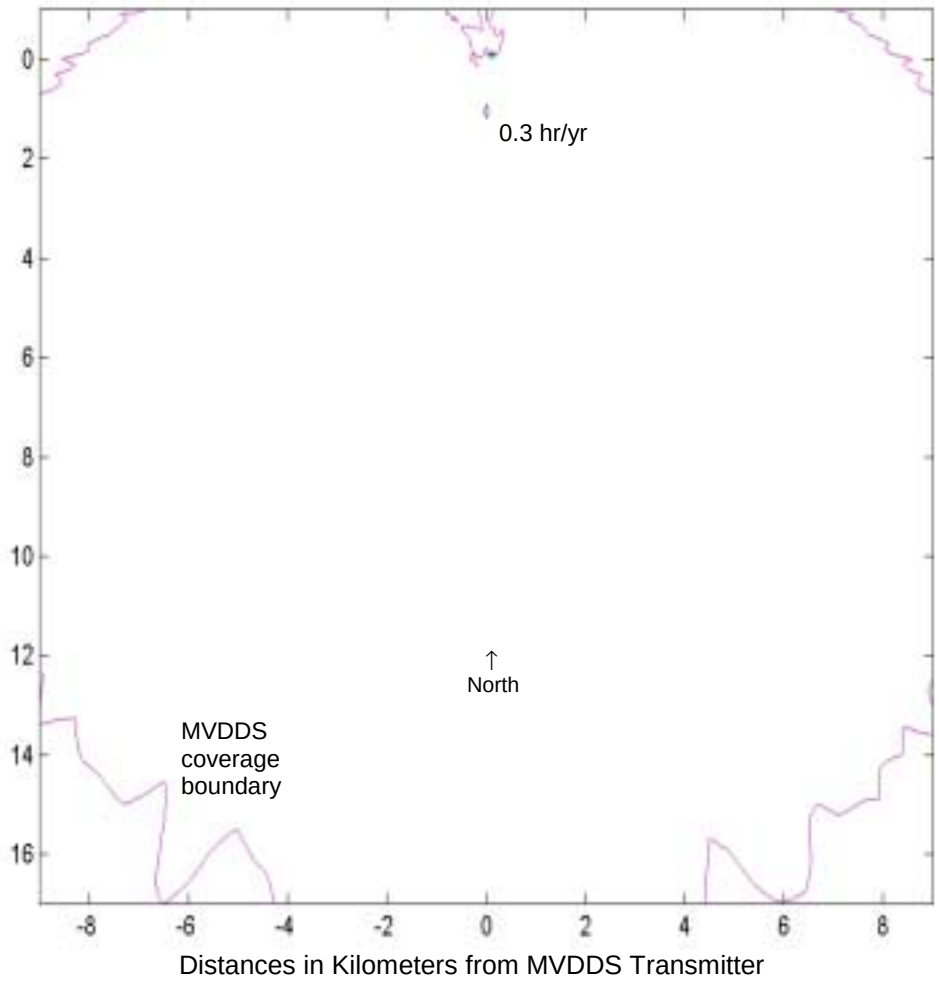

Washington, DC (12.45 GHz)
Maximum absolute increase caused by MVDDS in rain-induced DBS unavailability
Raw MVDDS transmitter power (*not* EIRP): 0 dBm
MVDDS transmitting antenna: Northpoint large sectoral horn
MVDDS transmitting-antenna boresight: 180° azimuth (S); 0° elevation tilt
MVDDS transmitting antenna 100 meters above horizontal plane
Assumed MVDDS interference scaling factor: 1 dB
Frequency offset between MVDDS and DBS carriers: none
DBS performance measure: VQ6
DBS receiving antenna: 18" single-feed dish
Maximum ratio of DBS EIRP to receiver threshold assumed for each satellite longitude
Baseline rain-induced unavailabilities (*without* MVDDS interference):

101° W:	1.95 hr/yr
110° W:	2.62 hr/yr
119° W:	1.73 hr/yr

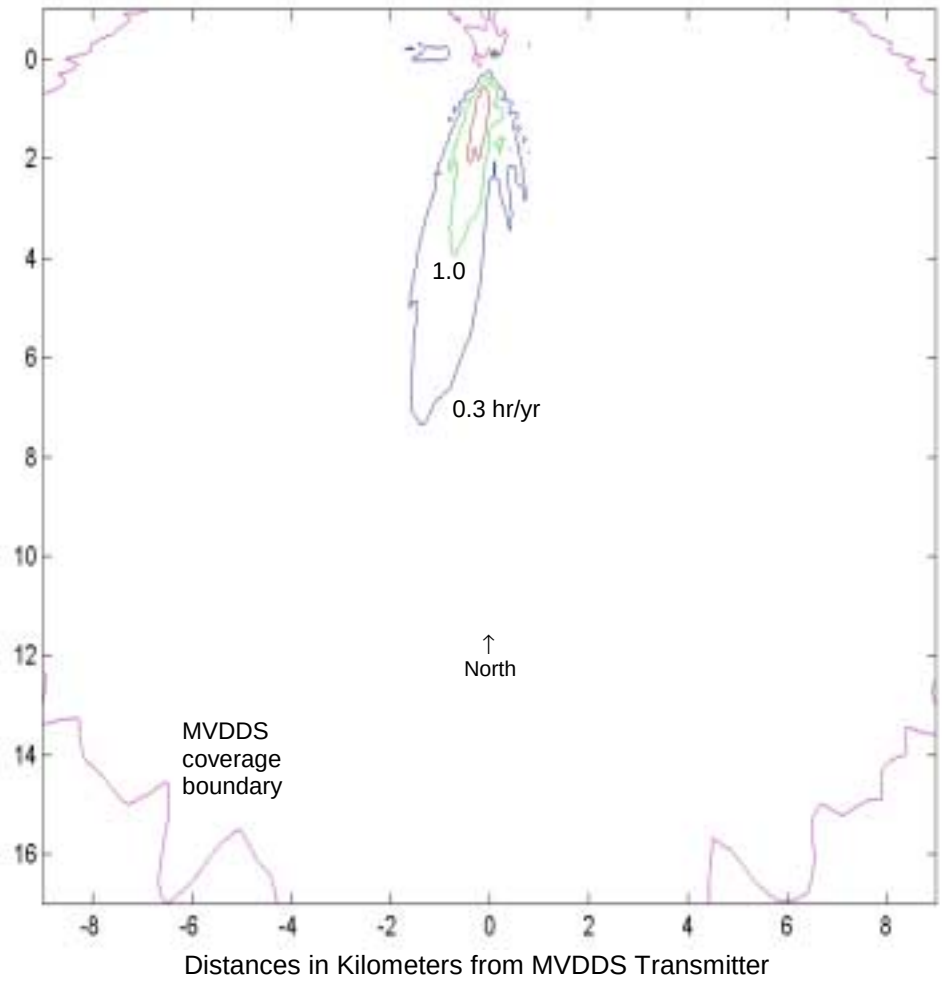

Washington, DC (12.45 GHz)
Maximum absolute increase caused by MVDDS in rain-induced DBS unavailability
Raw MVDDS transmitter power (*not* EIRP): 0 dBm
MVDDS transmitting antenna: Northpoint large sectoral horn
MVDDS transmitting-antenna boresight: 180° azimuth (S); 0° elevation tilt
MVDDS transmitting antenna 100 meters above horizontal plane
Assumed MVDDS interference scaling factor: **0 dB**
Frequency offset between MVDDS and DBS carriers: none
DBS performance measure: VQ6
DBS receiving antenna: 18" single-feed dish
Minimum ratio of DBS EIRP to receiver threshold assumed for each satellite longitude
Baseline rain-induced unavailabilities (*without* MVDDS interference):

101° W: 2.17 hr/yr
110° W: 3.88 hr/yr
119° W: 24.56 hr/yr

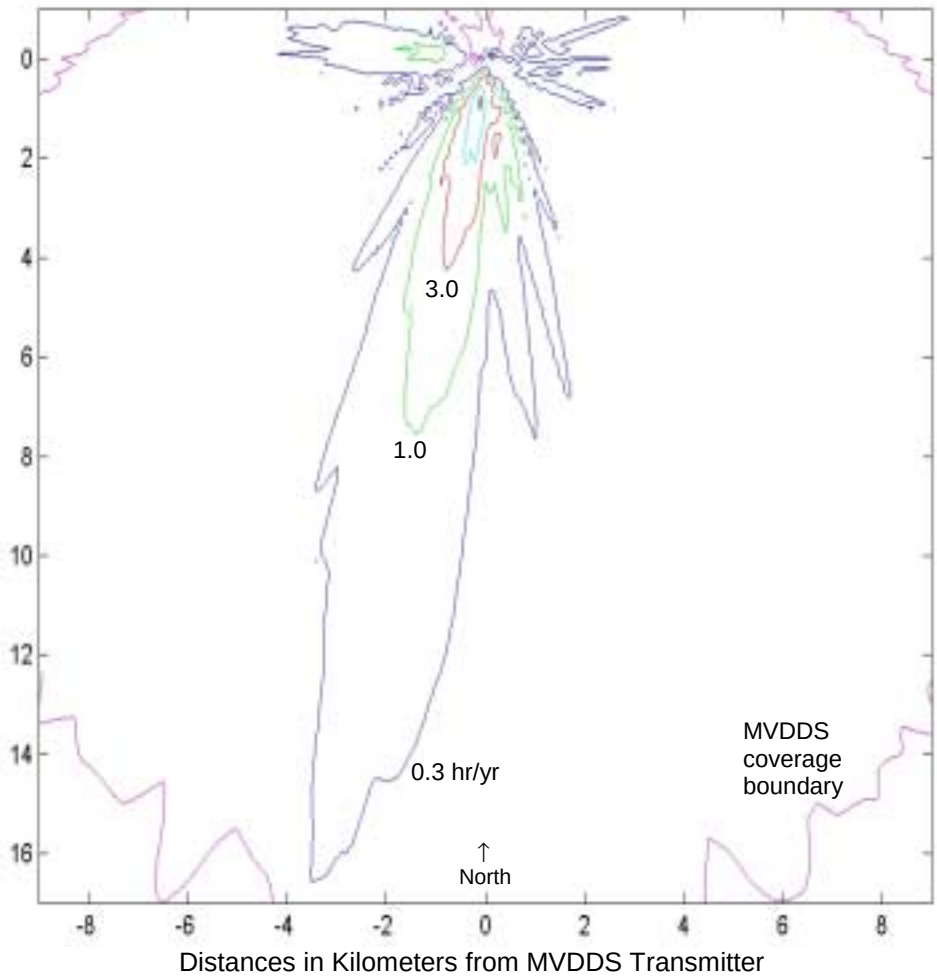

Washington, DC (12.45 GHz)
Maximum absolute increase caused by MVDDS in rain-induced DBS unavailability
Raw MVDDS transmitter power (*not* EIRP): 0 dBm
MVDDS transmitting antenna: Northpoint large sectoral horn
MVDDS transmitting-antenna boresight: 180° azimuth (S); 0° elevation tilt
MVDDS transmitting antenna 100 meters above horizontal plane
Assumed MVDDS interference scaling factor: 1 dB
Frequency offset between MVDDS and DBS carriers: none
DBS performance measure: **QEF**
DBS receiving antenna: 18" single-feed dish
Minimum ratio of DBS EIRP to receiver threshold assumed for each satellite longitude
Baseline rain-induced unavailabilities (*without* MVDDS interference):

101° W: 3.43 hr/yr
110° W: 14.37 hr/yr
119° W: 61.96 hr/yr

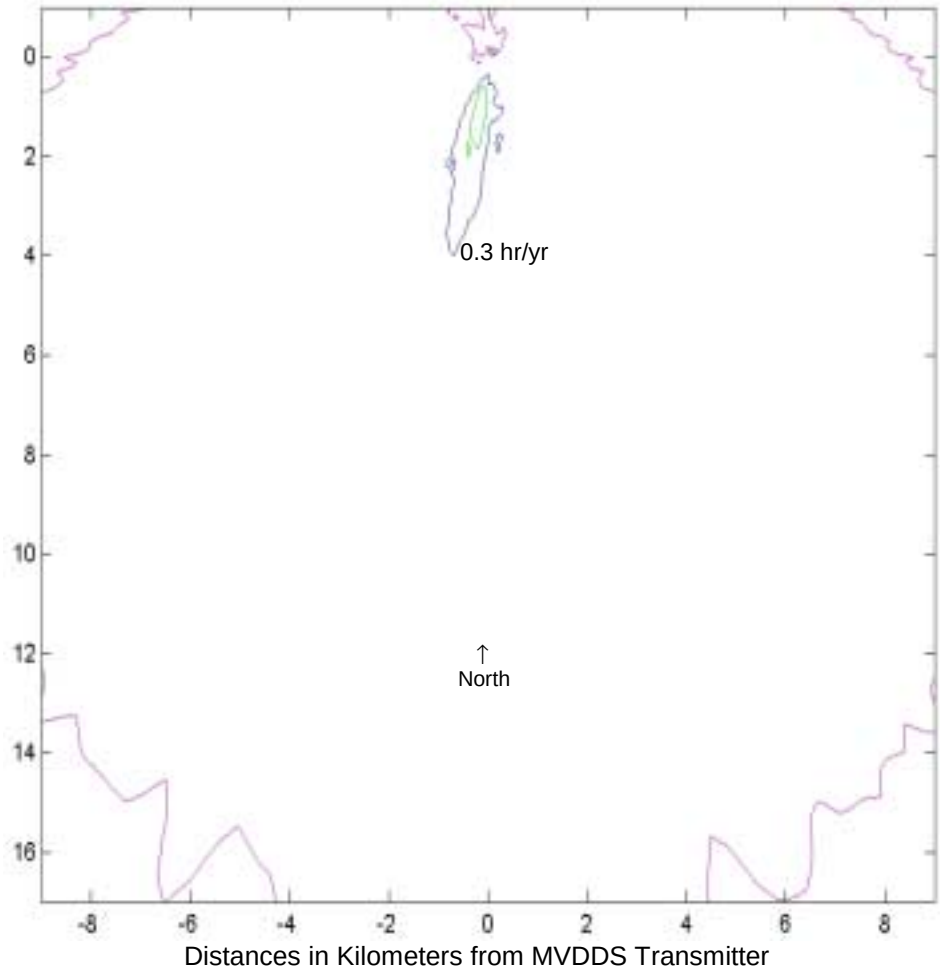

Washington, DC (12.45 GHz)
Maximum absolute increase caused by MVDDS in rain-induced DBS unavailability
Raw MVDDS transmitter power (*not* EIRP): 0 dBm
MVDDS transmitting antenna: Northpoint large sectoral horn
MVDDS transmitting-antenna boresight: 180° azimuth (S); 0° elevation tilt
MVDDS transmitting antenna 100 meters above horizontal plane
Assumed MVDDS interference scaling factor: 1 dB
Frequency offset between MVDDS and DBS carriers: none
DBS performance measure: **VQ1**
DBS receiving antenna: 18" single-feed dish
Minimum ratio of DBS EIRP to receiver threshold assumed for each satellite longitude
Baseline rain-induced unavailabilities (*without* MVDDS interference):

101° W: 1.40 hr/yr
110° W: 3.30 hr/yr
119° W: 11.96 hr/yr

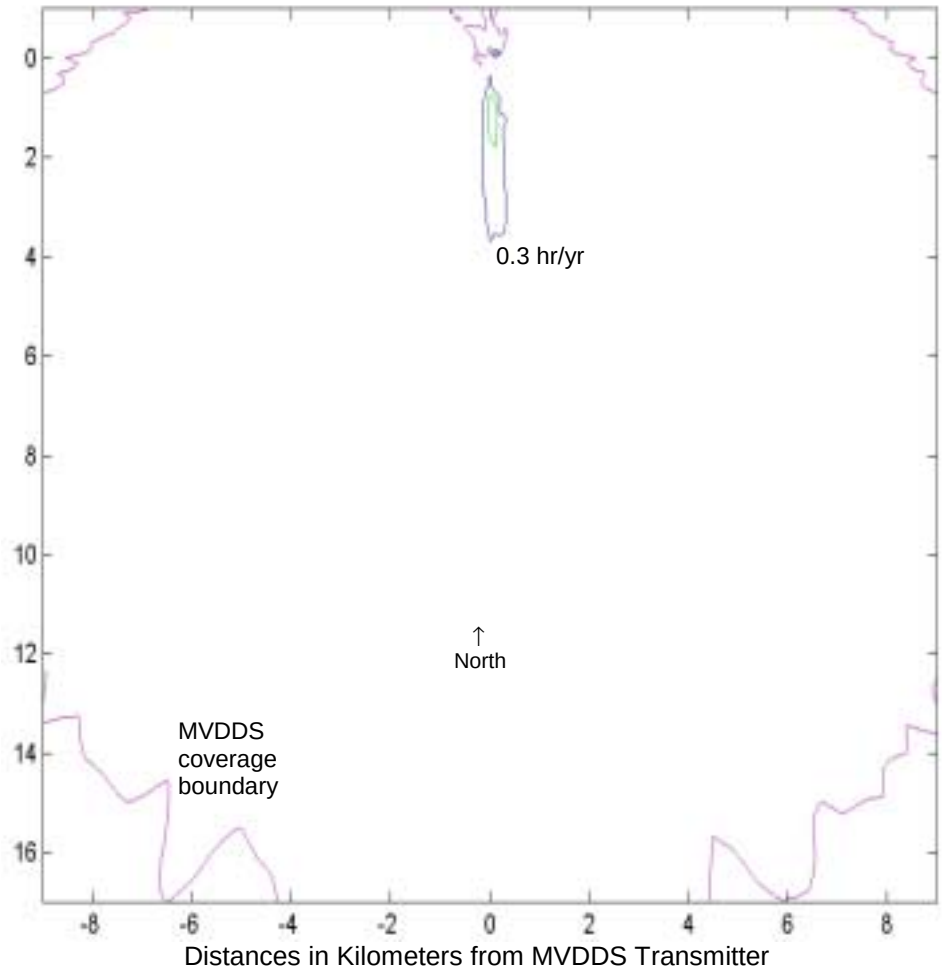

Washington, DC (12.45 GHz)
Maximum absolute increase caused by MVDDS in rain-induced DBS unavailability
Raw MVDDS transmitter power (*not* EIRP): 0 dBm
MVDDS transmitting antenna: Northpoint large sectoral horn
MVDDS transmitting-antenna boresight: 180° azimuth (S); 0° elevation tilt
MVDDS transmitting antenna 100 meters above horizontal plane
Assumed MVDDS interference scaling factor: 1 dB
Frequency offset between MVDDS and DBS carriers: none
DBS performance measure: VQ6
DBS receiving antenna: **24" x 18" single-feed**
Minimum ratio of DBS EIRP to receiver threshold assumed for each satellite longitude
Baseline rain-induced unavailabilities (*without* MVDDS interference):

101° W: 2.09 hr/yr
110° W: 3.72 hr/yr
119° W: 22.94 hr/yr

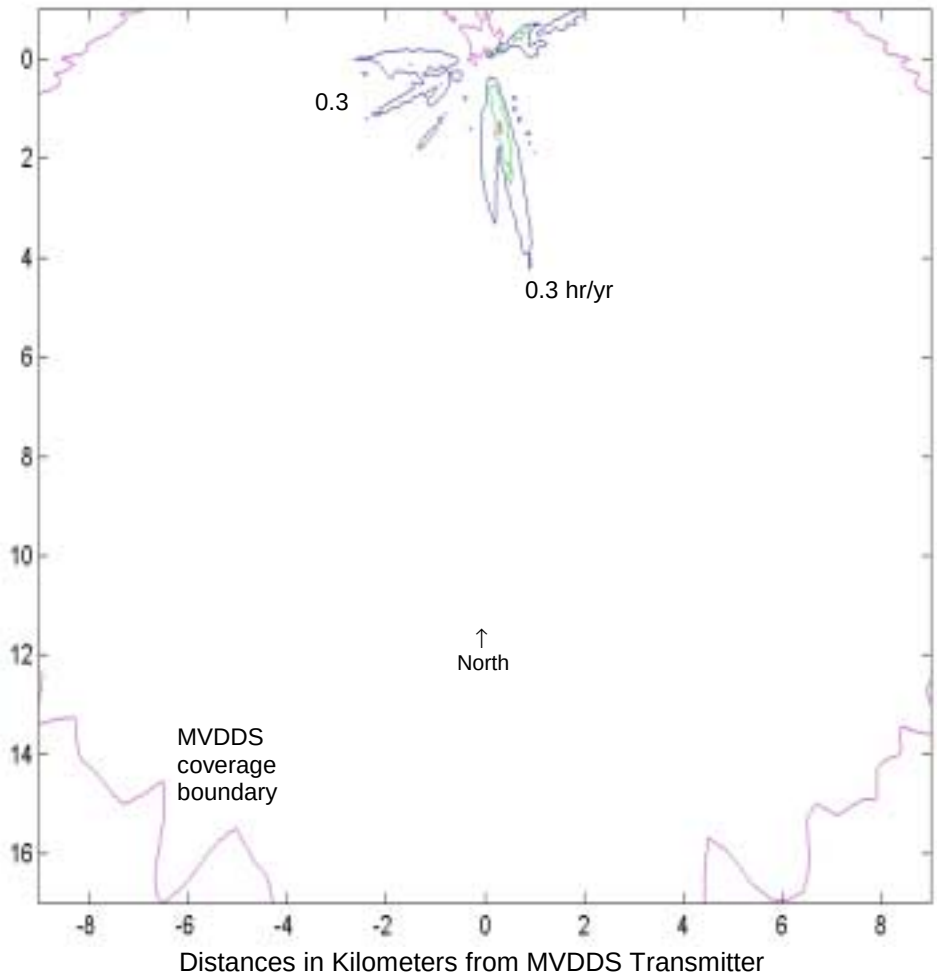

Washington, DC (12.45 GHz)
Maximum absolute increase caused by MVDDS in rain-induced DBS unavailability
Raw MVDDS transmitter power (*not* EIRP): 0 dBm
MVDDS transmitting antenna: Northpoint large sectoral horn
MVDDS transmitting-antenna boresight: 180° azimuth (S); 0° elevation tilt
MVDDS transmitting antenna 100 meters above horizontal plane
Assumed MVDDS interference scaling factor: 1 dB
Frequency offset between MVDDS and DBS carriers: none
DBS performance measure: VQ6
DBS receiving antenna: **24" x 18" dual-feed**
Minimum ratio of DBS EIRP to receiver threshold assumed for each satellite longitude
Baseline rain-induced unavailabilities (*without* MVDDS interference):

101° W: 2.69 hr/yr
110° W: 4.90 hr/yr
119° W: 36.55 hr/yr

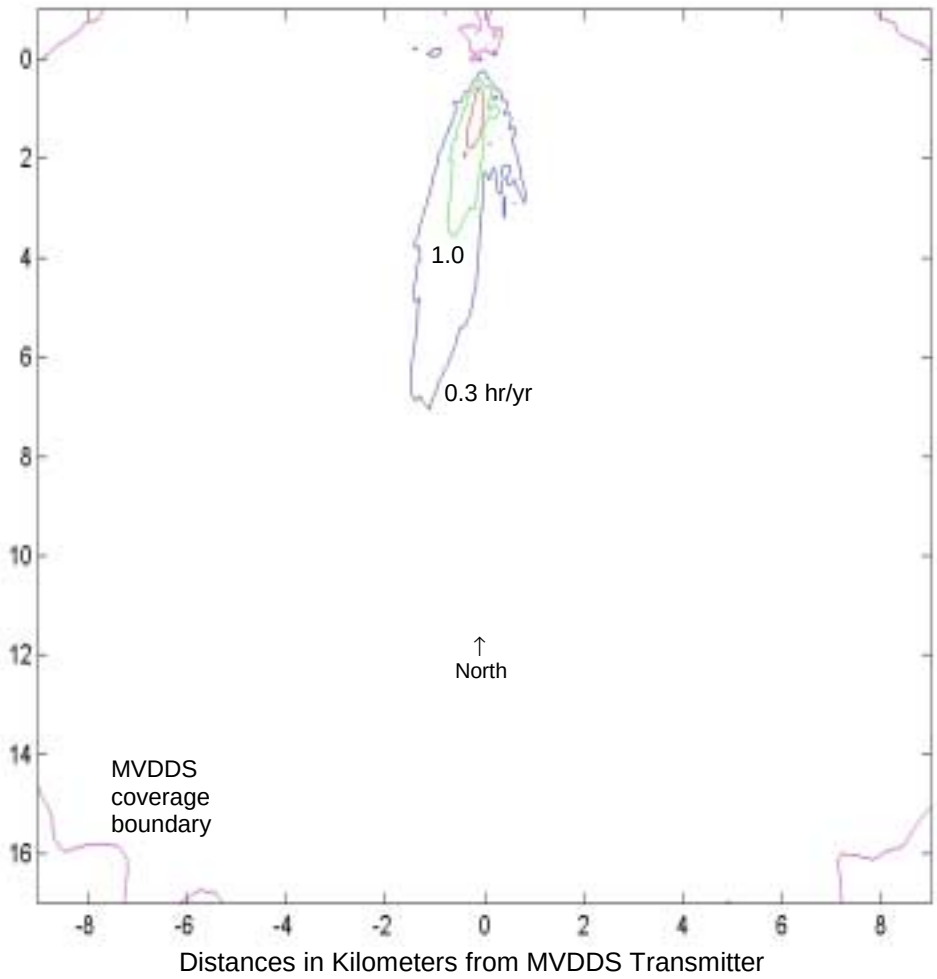

Washington, DC **(12.20 GHz)**
Maximum absolute increase caused by MVDDS in rain-induced DBS unavailability
Raw MVDDS transmitter power (*not* EIRP): 0 dBm
MVDDS transmitting antenna: Northpoint large sectoral horn
MVDDS transmitting-antenna boresight: 180° azimuth (S); 0° elevation tilt
MVDDS transmitting antenna 100 meters above horizontal plane
Assumed MVDDS interference scaling factor: 1 dB
Frequency offset between MVDDS and DBS carriers: none
DBS performance measure: VQ6
DBS receiving antenna: 18" single-feed dish
Minimum ratio of DBS EIRP to receiver threshold assumed for each satellite longitude
Baseline rain-induced unavailabilities (*without* MVDDS interference):

101° W:	1.97 hr/yr
110° W:	3.54 hr/yr
119° W:	22.65 hr/yr

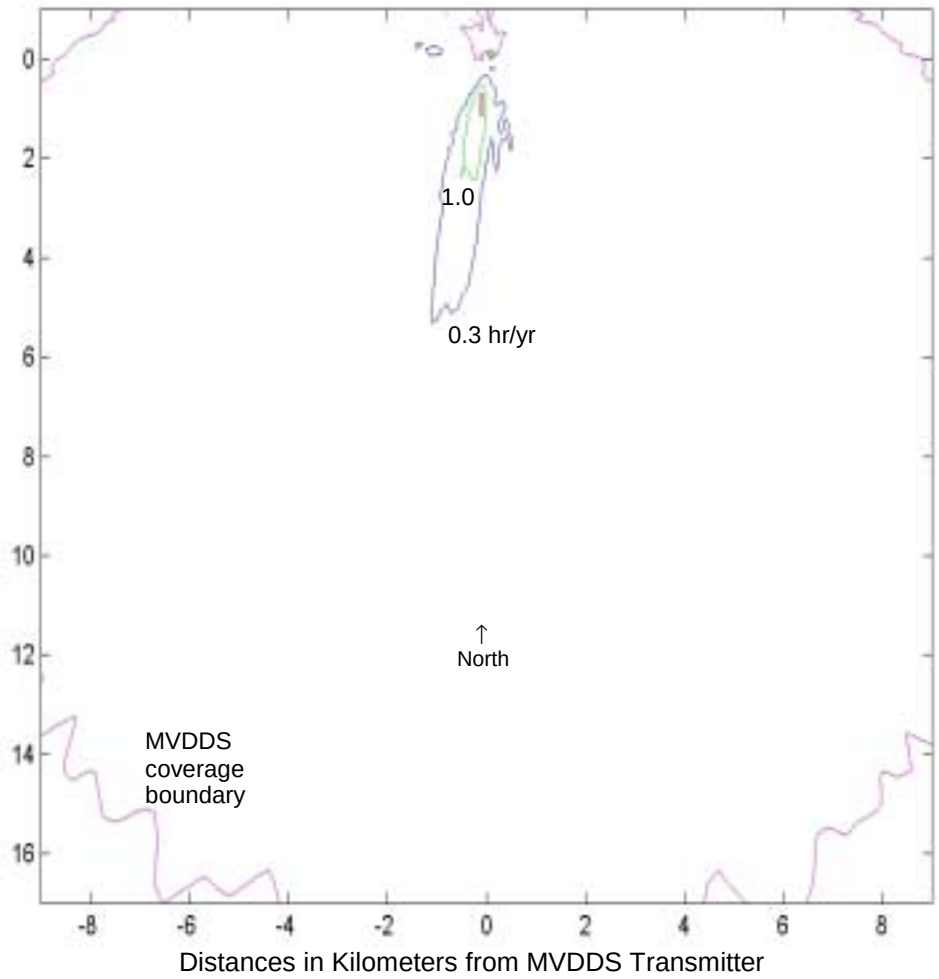

Washington, DC **(12.70 GHz)**
Maximum absolute increase caused by MVDDS in rain-induced DBS unavailability
Raw MVDDS transmitter power (*not* EIRP): 0 dBm
MVDDS transmitting antenna: Northpoint large sectoral horn
MVDDS transmitting-antenna boresight: 180° azimuth (S); 0° elevation tilt
MVDDS transmitting antenna 100 meters above horizontal plane
Assumed MVDDS interference scaling factor: 1 dB
Frequency offset between MVDDS and DBS carriers: none
DBS performance measure: VQ6
DBS receiving antenna: 18" single-feed dish
Minimum ratio of DBS EIRP to receiver threshold assumed for each satellite longitude
Baseline rain-induced unavailabilities (*without* MVDDS interference):

101° W:	2.04 hr/yr
110° W:	3.57 hr/yr
119° W:	20.27 hr/yr

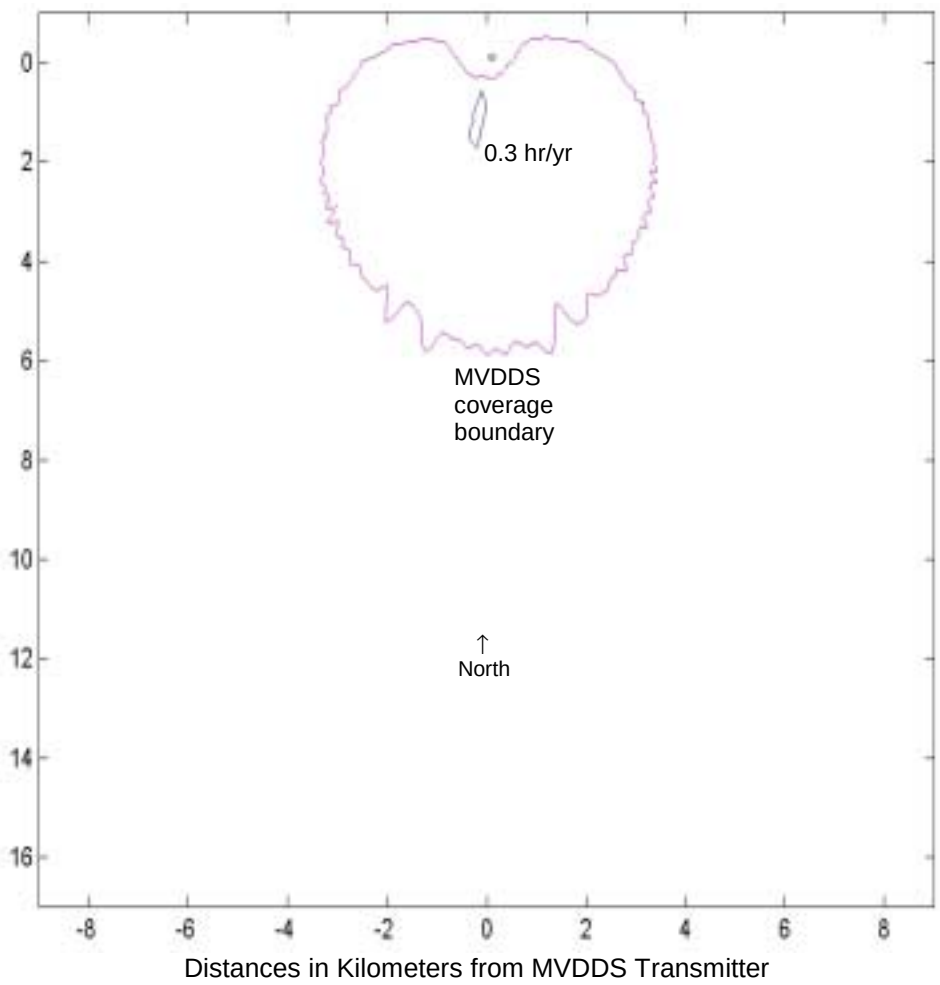

Washington, DC (12.45 GHz)
Maximum absolute increase caused by MVDDS in rain-induced DBS unavailability
Raw MVDDS transmitter power (*not* EIRP): **-10 dBm**
MVDDS transmitting antenna: Northpoint large sectoral horn
MVDDS transmitting-antenna boresight: 180° azimuth (S); 0° elevation tilt
MVDDS transmitting antenna 100 meters above horizontal plane
Assumed MVDDS interference scaling factor: 1 dB
Frequency offset between MVDDS and DBS carriers: none
DBS performance measure: VQ6
DBS receiving antenna: 18" single-feed dish
Minimum ratio of DBS EIRP to receiver threshold assumed for each satellite longitude
Baseline rain-induced unavailabilities (*without* MVDDS interference):

101° W:	2.17 hr/yr
110° W:	3.88 hr/yr
119° W:	24.56 hr/yr

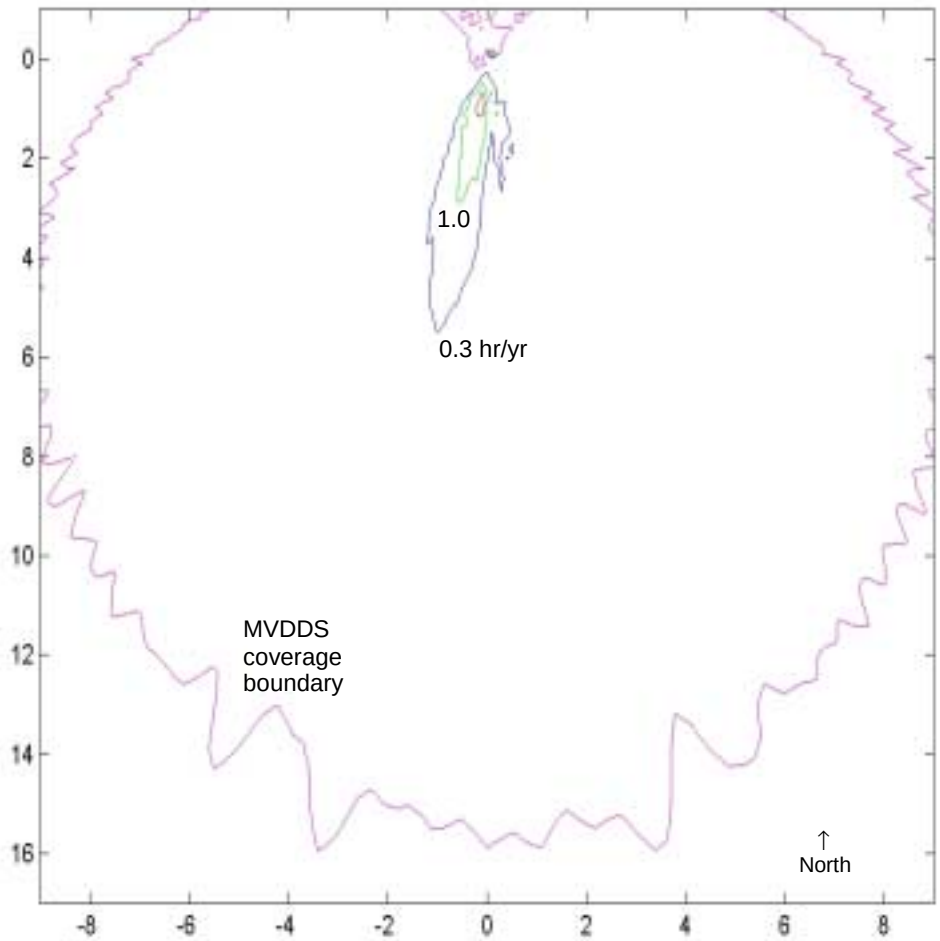

Distances in Kilometers from MVDDS Transmitter

Washington, DC (12.45 GHz)
Maximum absolute increase caused by MVDDS in rain-induced DBS unavailability
Raw MVDDS transmitter power (*not* EIRP): **-1.5 dBm**
MVDDS transmitting antenna: Northpoint large sectoral horn
MVDDS transmitting-antenna boresight: 180° azimuth (S); 0° elevation tilt
MVDDS transmitting antenna 100 meters above horizontal plane
Assumed MVDDS interference scaling factor: 1 dB
Frequency offset between MVDDS and DBS carriers: none
DBS performance measure: VQ6
DBS receiving antenna: 18" single-feed dish
Minimum ratio of DBS EIRP to receiver threshold assumed for each satellite longitude
Baseline rain-induced unavailabilities (*without* MVDDS interference):

101° W:	2.17 hr/yr
110° W:	3.88 hr/yr
119° W:	24.56 hr/yr

Note: Maximum MVDDS EIRP for this case is 12.5 dBm.

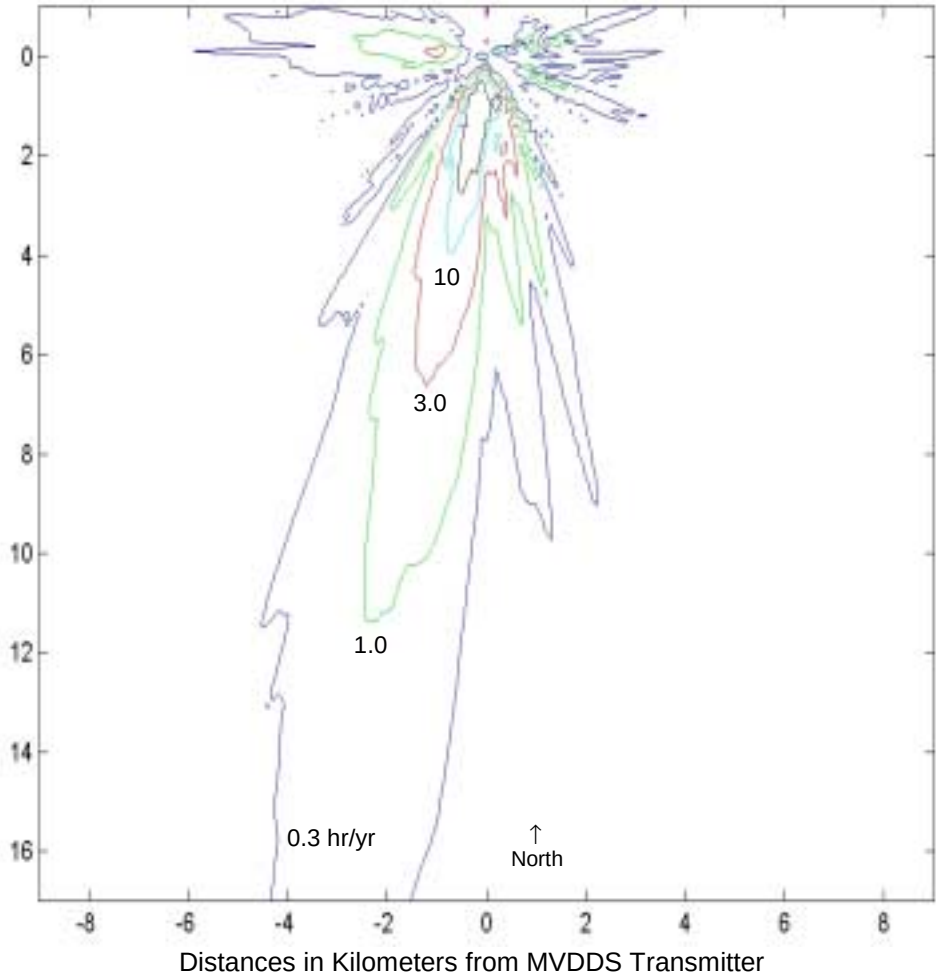

Washington, DC (12.45 GHz)
Maximum absolute increase caused by MVDDS in rain-induced DBS unavailability
Raw MVDDS transmitter power (*not* EIRP): **10 dBm**
MVDDS transmitting antenna: Northpoint large sectoral horn
MVDDS transmitting-antenna boresight: 180° azimuth (S); 0° elevation tilt
MVDDS transmitting antenna 100 meters above horizontal plane
Assumed MVDDS interference scaling factor: 1 dB
Frequency offset between MVDDS and DBS carriers: none
DBS performance measure: VQ6
DBS receiving antenna: 18" single-feed dish
Minimum ratio of DBS EIRP to receiver threshold assumed for each satellite longitude
Baseline rain-induced unavailabilities (*without* MVDDS interference):

101° W:	2.17 hr/yr
110° W:	3.88 hr/yr
119° W:	24.56 hr/yr

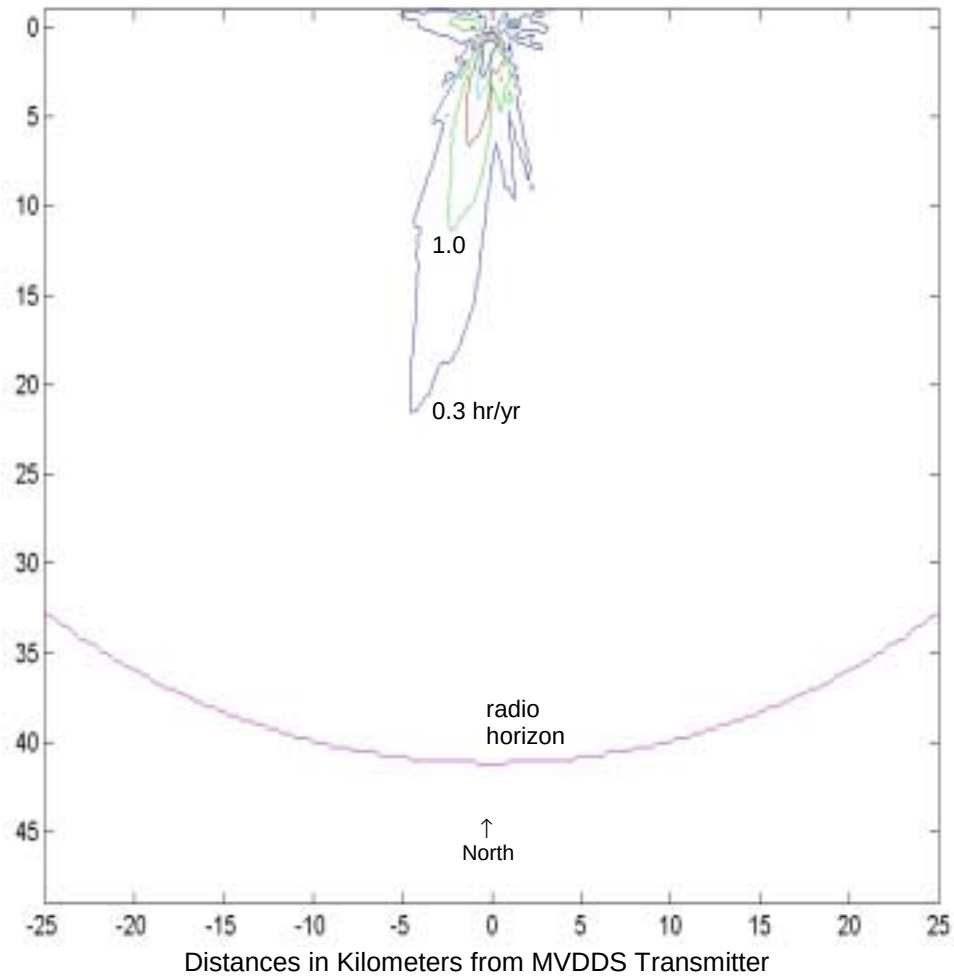

Washington, DC (12.45 GHz)
Maximum absolute increase caused by MVDDS in rain-induced DBS unavailability
Raw MVDDS transmitter power (*not* EIRP): **10 dBm**
MVDDS transmitting antenna: Northpoint large sectoral horn
MVDDS transmitting-antenna boresight: 180° azimuth (S); 0° elevation tilt
MVDDS transmitting antenna 100 meters above horizontal plane
Assumed MVDDS interference scaling factor: 1 dB
Frequency offset between MVDDS and DBS carriers: none
DBS performance measure: VQ6
DBS receiving antenna: 18" single-feed dish
Minimum ratio of DBS EIRP to receiver threshold assumed for each satellite longitude
Baseline rain-induced unavailabilities (*without* MVDDS interference):

101° W:	2.17 hr/yr
110° W:	3.88 hr/yr
119° W:	24.56 hr/yr

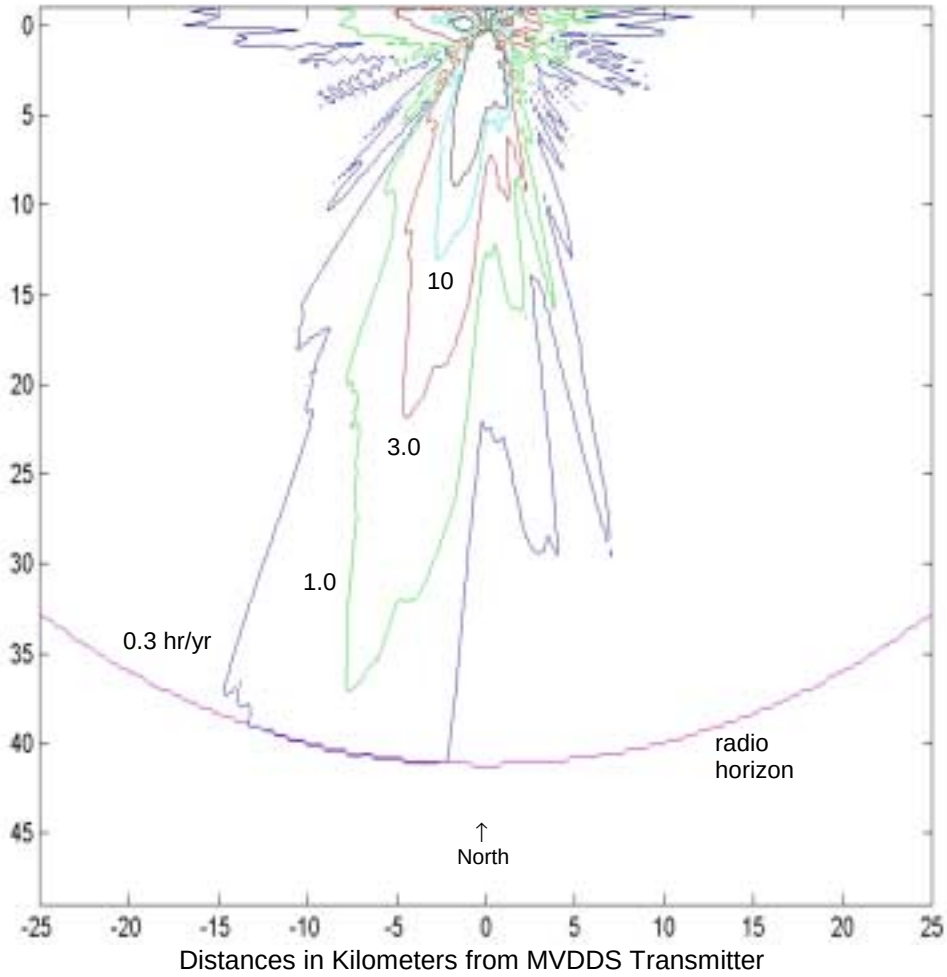

Washington, DC (12.45 GHz)
Maximum absolute increase caused by MVDDS in rain-induced DBS unavailability
Raw MVDDS transmitter power (*not* EIRP): **20 dBm**
MVDDS transmitting antenna: Northpoint large sectoral horn
MVDDS transmitting-antenna boresight: 180° azimuth (S); 0° elevation tilt
MVDDS transmitting antenna 100 meters above horizontal plane
Assumed MVDDS interference scaling factor: 1 dB
Frequency offset between MVDDS and DBS carriers: none
DBS performance measure: VQ6
DBS receiving antenna: 18" single-feed dish
Minimum ratio of DBS EIRP to receiver threshold assumed for each satellite longitude
Baseline rain-induced unavailabilities (*without* MVDDS interference):

101° W:	2.17 hr/yr
110° W:	3.88 hr/yr
119° W:	24.56 hr/yr

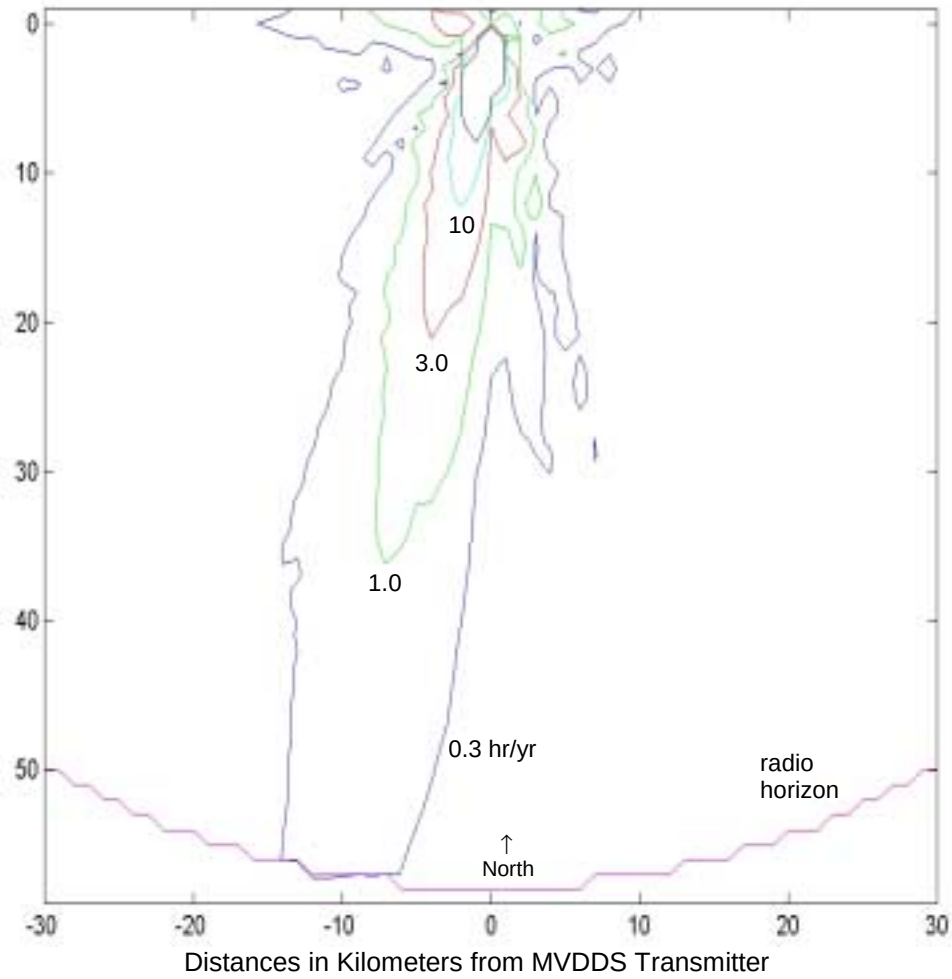

Washington, DC (12.45 GHz)
Maximum absolute increase caused by MVDDS in rain-induced DBS unavailability
Raw MVDDS transmitter power (*not* EIRP): **20 dBm**
MVDDS transmitting antenna: Northpoint large sectoral horn
MVDDS transmitting-antenna boresight: 180° azimuth (S); 0° elevation tilt
MVDDS transmitting antenna **200 meters** above horizontal plane
Assumed MVDDS interference scaling factor: 1 dB
Frequency offset between MVDDS and DBS carriers: none
DBS performance measure: VQ6
DBS receiving antenna: 18" single-feed dish
Minimum ratio of DBS EIRP to receiver threshold assumed for each satellite longitude
Baseline rain-induced unavailabilities (*without* MVDDS interference):

101° W:	2.17 hr/yr
110° W:	3.88 hr/yr
119° W:	24.56 hr/yr

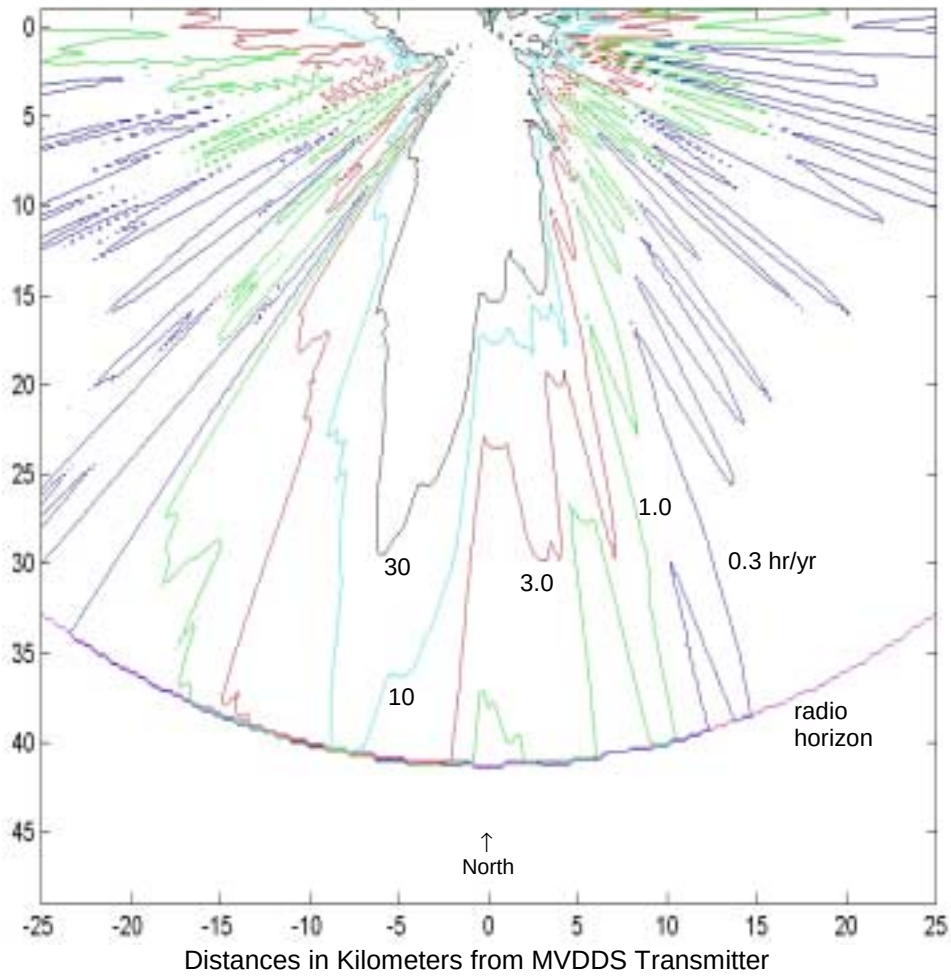

Washington, DC (12.45 GHz)
Maximum absolute increase caused by MVDDS in rain-induced DBS unavailability
Raw MVDDS transmitter power (*not* EIRP): **30 dBm**
MVDDS transmitting antenna: Northpoint large sectoral horn
MVDDS transmitting-antenna boresight: 180° azimuth (S); 0° elevation tilt
MVDDS transmitting antenna 100 meters above horizontal plane
Assumed MVDDS interference scaling factor: 1 dB
Frequency offset between MVDDS and DBS carriers: none
DBS performance measure: VQ6
DBS receiving antenna: 18" single-feed dish
Minimum ratio of DBS EIRP to receiver threshold assumed for each satellite longitude
Baseline rain-induced unavailabilities (*without* MVDDS interference):

101° W:	2.17 hr/yr
110° W:	3.88 hr/yr
119° W:	24.56 hr/yr

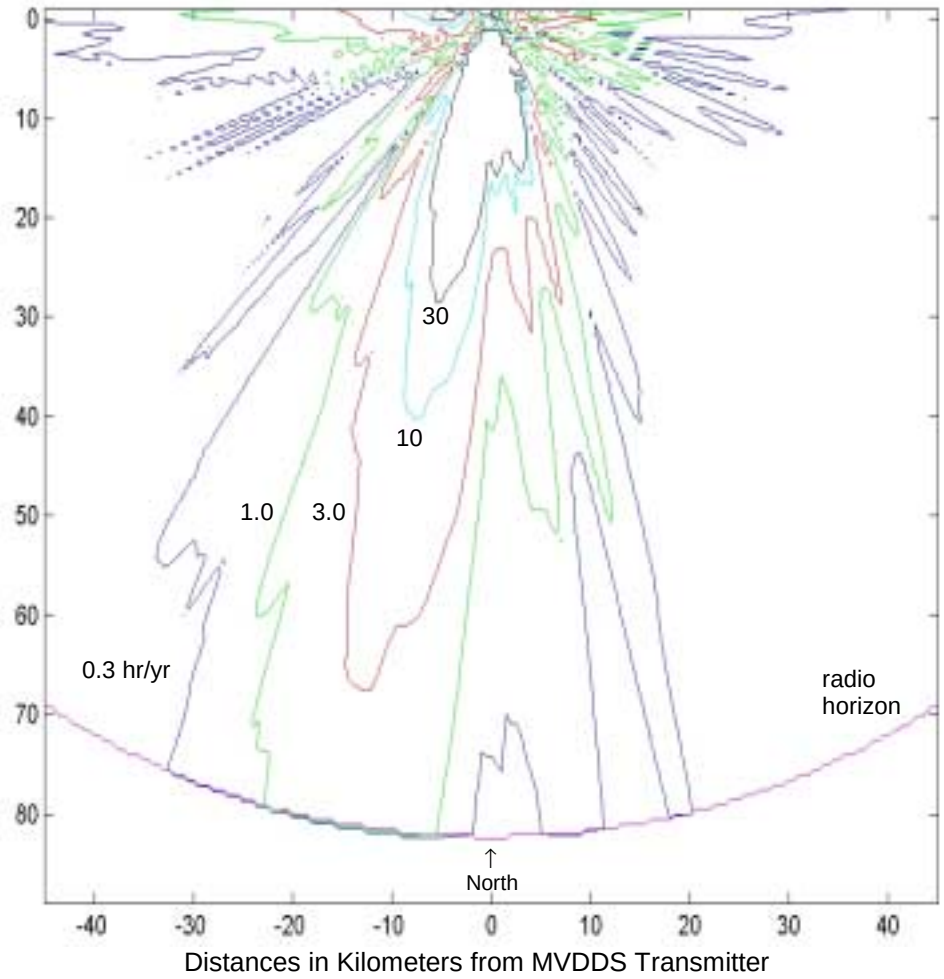

Washington, DC (12.45 GHz)
Maximum absolute increase caused by MVDDS in rain-induced DBS unavailability
Raw MVDDS transmitter power (*not* EIRP): **30 dBm**
MVDDS transmitting antenna: Northpoint large sectoral horn
MVDDS transmitting-antenna boresight: 180° azimuth (S); 0° elevation tilt
MVDDS transmitting antenna **400 meters** above horizontal plane
Assumed MVDDS interference scaling factor: 1 dB
Frequency offset between MVDDS and DBS carriers: none
DBS performance measure: VQ6
DBS receiving antenna: 18" single-feed dish
Minimum ratio of DBS EIRP to receiver threshold assumed for each satellite longitude
Baseline rain-induced unavailabilities (*without* MVDDS interference):

101° W:	2.17 hr/yr
110° W:	3.88 hr/yr
119° W:	24.56 hr/yr

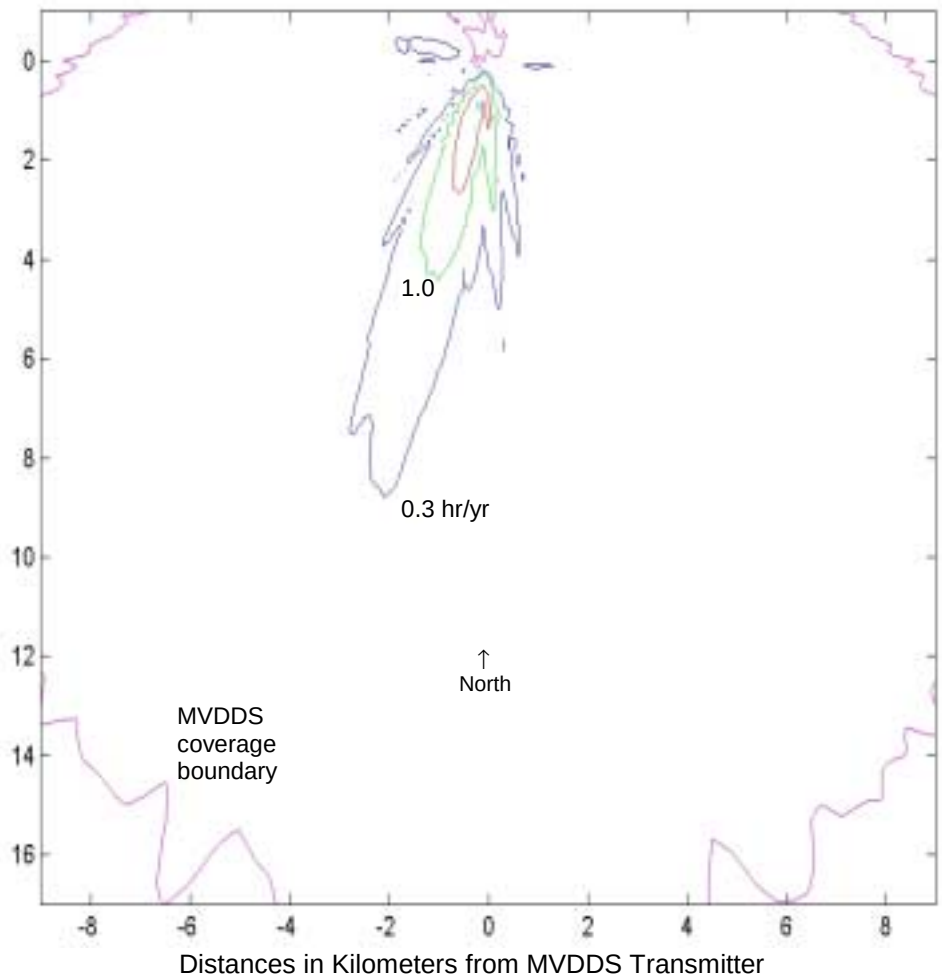

Miami, FL (12.45 GHz)
Maximum absolute increase caused by MVDDS in rain-induced DBS unavailability
Raw MVDDS transmitter power (*not* EIRP): 0 dBm
MVDDS transmitting antenna: Northpoint large sectoral horn
MVDDS transmitting-antenna boresight: 180° azimuth (S); 0° elevation tilt
MVDDS transmitting antenna 100 meters above horizontal plane
Assumed MVDDS interference scaling factor: 1 dB
Frequency offset between MVDDS and DBS carriers: none
DBS performance measure: VQ6
DBS receiving antenna: 18" single-feed dish
Minimum ratio of DBS EIRP to receiver threshold assumed for each satellite longitude
Baseline rain-induced unavailabilities (*without* MVDDS interference):

101° W:	8.10 hr/yr
110° W:	17.46 hr/yr
119° W:	57.91 hr/yr

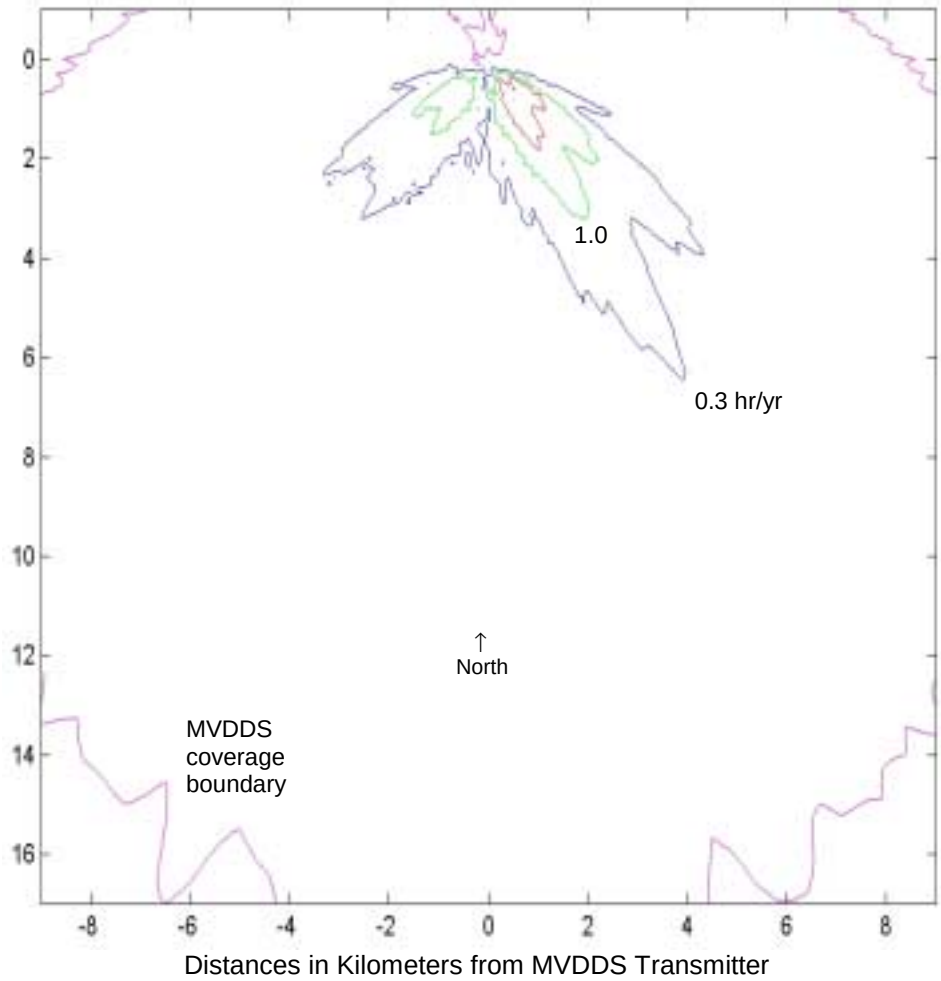

Phoenix, AZ (12.45 GHz)
Maximum absolute increase caused by MVDDS in rain-induced DBS unavailability
Raw MVDDS transmitter power (*not* EIRP): 0 dBm
MVDDS transmitting antenna: Northpoint large sectoral horn
MVDDS transmitting-antenna boresight: 180° azimuth (S); 0° elevation tilt
MVDDS transmitting antenna 100 meters above horizontal plane
Assumed MVDDS interference scaling factor: 1 dB
Frequency offset between MVDDS and DBS carriers: none
DBS performance measure: VQ6
DBS receiving antenna: 18" single-feed dish
Minimum ratio of DBS EIRP to receiver threshold assumed for each satellite longitude
Baseline rain-induced unavailabilities (*without* MVDDS interference):

101° W:	2.66 hr/yr
110° W:	16.37 hr/yr
119° W:	19.02 hr/yr

Note: For 119° W only, the **second**-weakest satellite was considered from this locale.

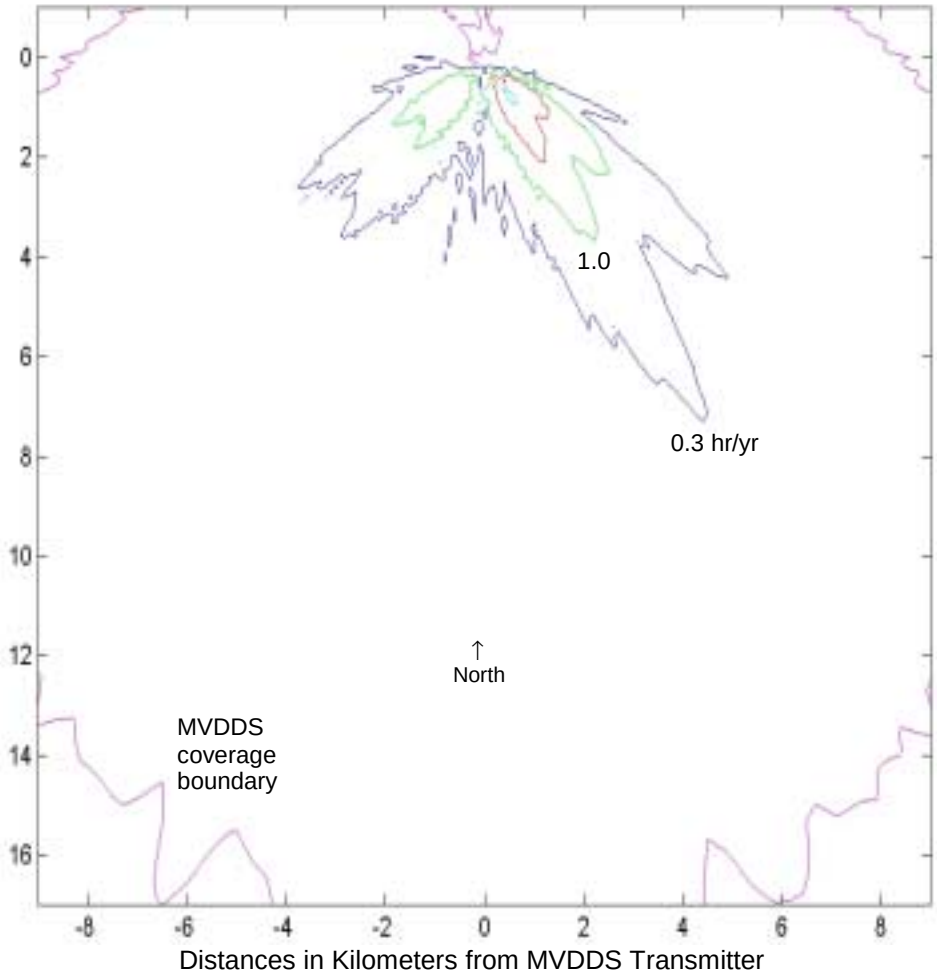

Phoenix, AZ (12.45 GHz)
Maximum absolute increase caused by MVDDS in rain-induced DBS unavailability
Raw MVDDS transmitter power (*not* EIRP): 0 dBm
MVDDS transmitting antenna: Northpoint large sectoral horn
MVDDS transmitting-antenna boresight: 180° azimuth (S); 0° elevation tilt
MVDDS transmitting antenna 100 meters above horizontal plane
Assumed MVDDS interference scaling factor: **0 dB**
Frequency offset between MVDDS and DBS carriers: none
DBS performance measure: VQ6
DBS receiving antenna: 18" single-feed dish
Minimum ratio of DBS EIRP to receiver threshold assumed for each satellite longitude
Baseline rain-induced unavailabilities (*without* MVDDS interference):

101° W:	2.66 hr/yr
110° W:	16.37 hr/yr
119° W:	19.02 hr/yr

Note: For 119° W only, the **second**-weakest satellite was considered from this locale.

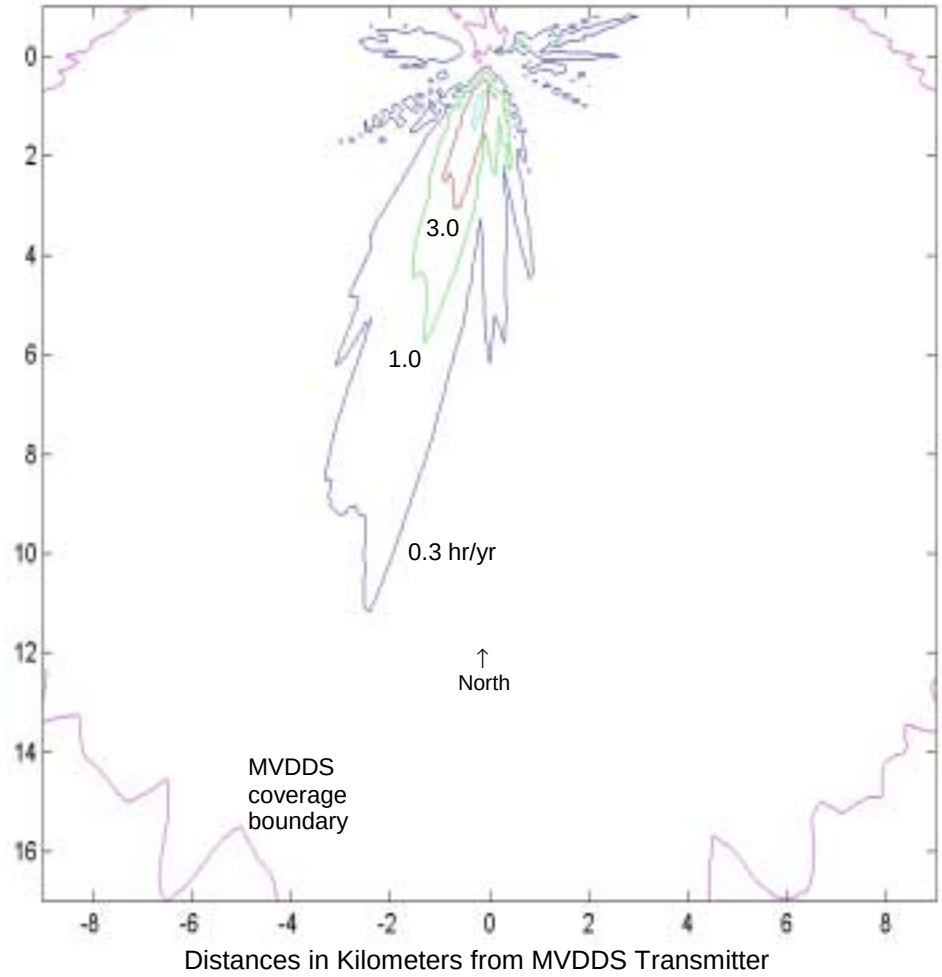

Boston, MA (12.45 GHz)
Maximum absolute increase caused by MVDDS in rain-induced DBS unavailability
Raw MVDDS transmitter power (*not* EIRP): 0 dBm
MVDDS transmitting antenna: Northpoint large sectoral horn
MVDDS transmitting-antenna boresight: 180° azimuth (S); 0° elevation tilt
MVDDS transmitting antenna 100 meters above horizontal plane
Assumed MVDDS interference scaling factor: 1 dB
Frequency offset between MVDDS and DBS carriers: none
DBS performance measure: VQ6
DBS receiving antenna: 18" single-feed dish
Minimum ratio of DBS EIRP to receiver threshold assumed for each satellite longitude
Baseline rain-induced unavailabilities (*without* MVDDS interference):

101° W:	2.92 hr/yr
110° W:	4.77 hr/yr
119° W:	44.63 hr/yr

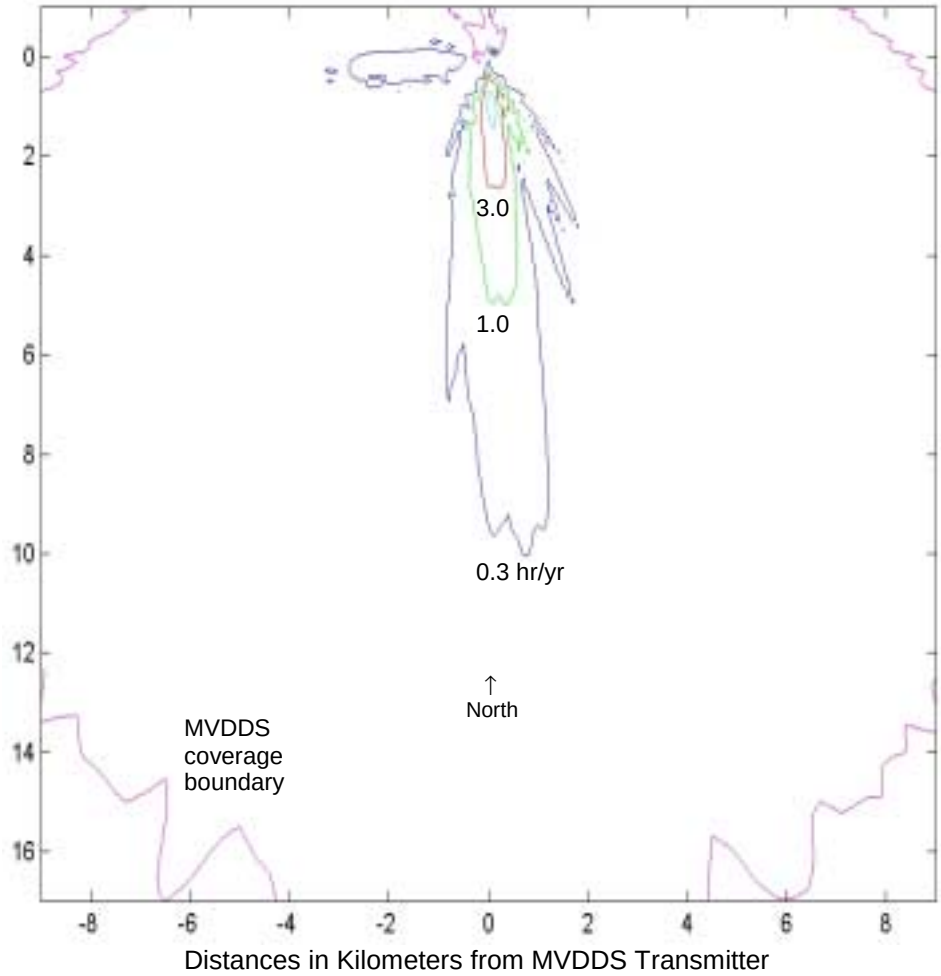

Chicago, IL (12.45 GHz)
Maximum absolute increase caused by MVDDS in rain-induced DBS unavailability
Raw MVDDS transmitter power (*not* EIRP): 0 dBm
MVDDS transmitting antenna: Northpoint large sectoral horn
MVDDS transmitting-antenna boresight: 180° azimuth (S); 0° elevation tilt
MVDDS transmitting antenna 100 meters above horizontal plane
Assumed MVDDS interference scaling factor: 1 dB
Frequency offset between MVDDS and DBS carriers: none
DBS performance measure: VQ6
DBS receiving antenna: 18" single-feed dish
Minimum ratio of DBS EIRP to receiver threshold assumed for each satellite longitude
Baseline rain-induced unavailabilities (*without* MVDDS interference):

101° W:	2.89 hr/yr
110° W:	3.07 hr/yr
119° W:	31.33 hr/yr

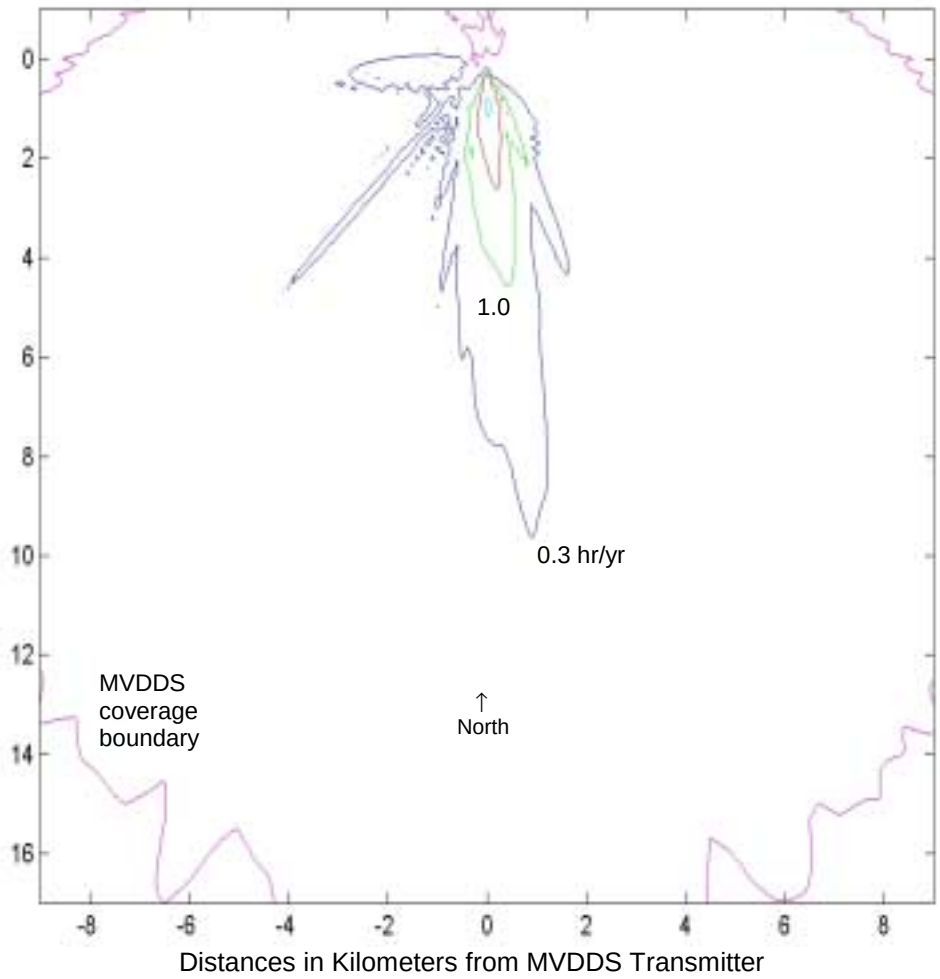

Houston, TX (12.45 GHz)
Maximum absolute increase caused by MVDDS in rain-induced DBS unavailability
Raw MVDDS transmitter power (*not* EIRP): 0 dBm
MVDDS transmitting antenna: Northpoint large sectoral horn
MVDDS transmitting-antenna boresight: 180° azimuth (S); 0° elevation tilt
MVDDS transmitting antenna 100 meters above horizontal plane
Assumed MVDDS interference scaling factor: 1 dB
Frequency offset between MVDDS and DBS carriers: none
DBS performance measure: VQ6
DBS receiving antenna: 18" single-feed dish
Minimum ratio of DBS EIRP to receiver threshold assumed for each satellite longitude
Baseline rain-induced unavailabilities (*without* MVDDS interference):

101° W:	4.48 hr/yr
110° W:	11.65 hr/yr
119° W:	36.55 hr/yr

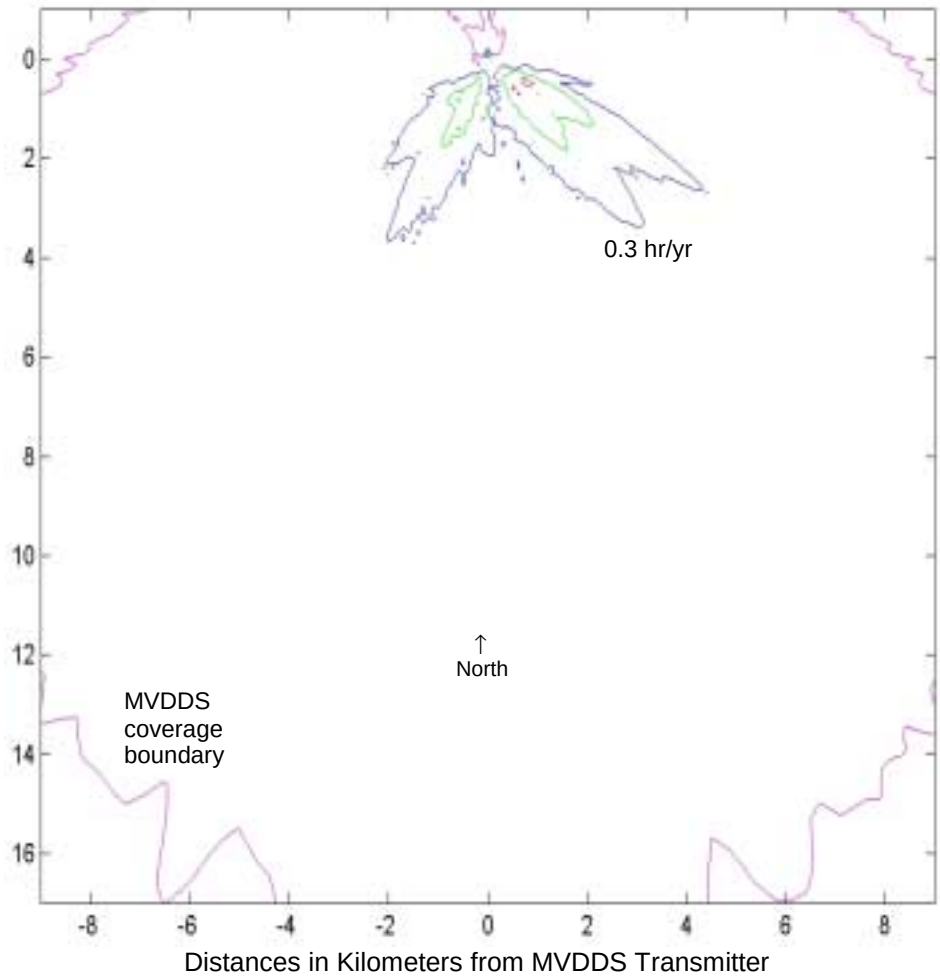

Los Angeles, CA (12.45 GHz)
Maximum absolute increase caused by MVDDS in rain-induced DBS unavailability
Raw MVDDS transmitter power (*not* EIRP): 0 dBm
MVDDS transmitting antenna: Northpoint large sectoral horn
MVDDS transmitting-antenna boresight: 180° azimuth (S); 0° elevation tilt
MVDDS transmitting antenna 100 meters above horizontal plane
Assumed MVDDS interference scaling factor: 1 dB
Frequency offset between MVDDS and DBS carriers: none
DBS performance measure: VQ6
DBS receiving antenna: 18" single-feed dish
Minimum ratio of DBS EIRP to receiver threshold assumed for each satellite longitude
Baseline rain-induced unavailabilities (*without* MVDDS interference):

101° W:	1.42 hr/yr
110° W:	11.69 hr/yr
119° W:	9.29 hr/yr

Note: For 119° W only, the **second**-weakest satellite was considered from this locale.

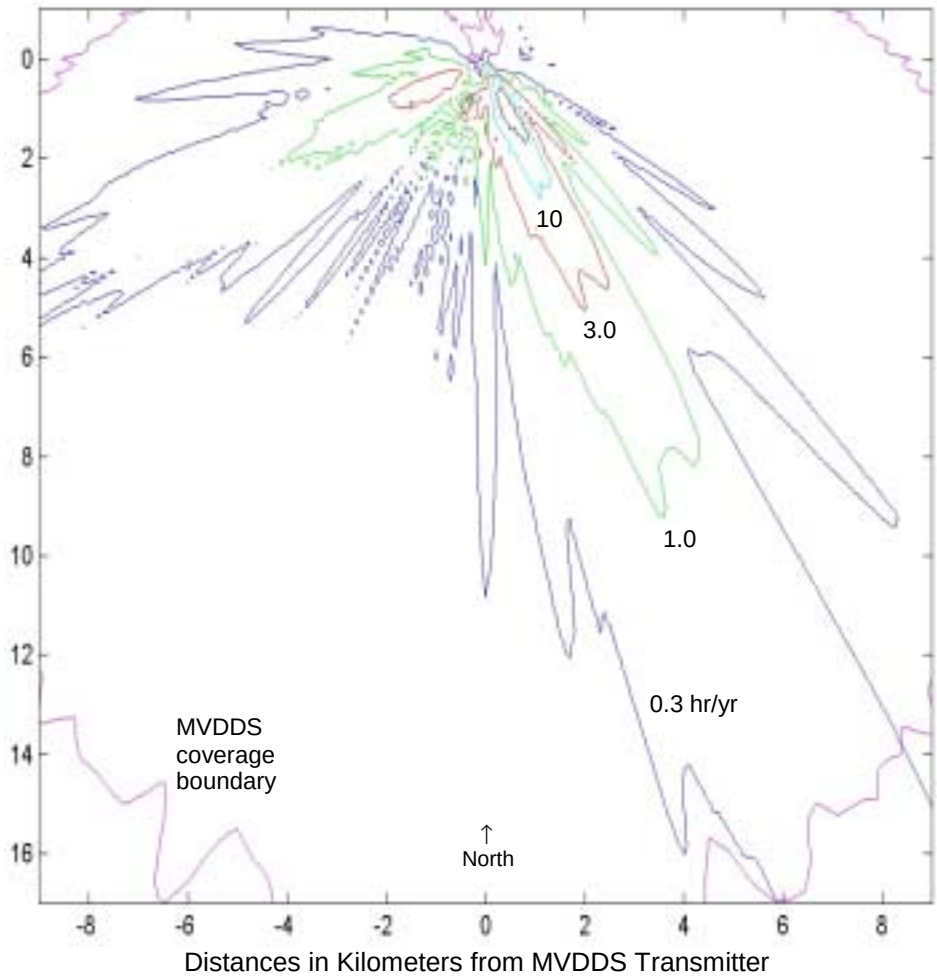

Denver, CO (12.45 GHz)
Maximum absolute increase caused by MVDDS in rain-induced DBS unavailability
Raw MVDDS transmitter power (*not* EIRP): 0 dBm
MVDDS transmitting antenna: Northpoint large sectoral horn
MVDDS transmitting-antenna boresight: 180° azimuth (S); 0° elevation tilt
MVDDS transmitting antenna 100 meters above horizontal plane
Assumed MVDDS interference scaling factor: 1 dB
Frequency offset between MVDDS and DBS carriers: none
DBS performance measure: VQ6
DBS receiving antenna: 18" single-feed dish
Minimum ratio of DBS EIRP to receiver threshold assumed for each satellite longitude
Baseline rain-induced unavailabilities (*without* MVDDS interference):

101° W:	0.79 hr/yr
110° W:	2.22 hr/yr
119° W:	33.25 hr/yr

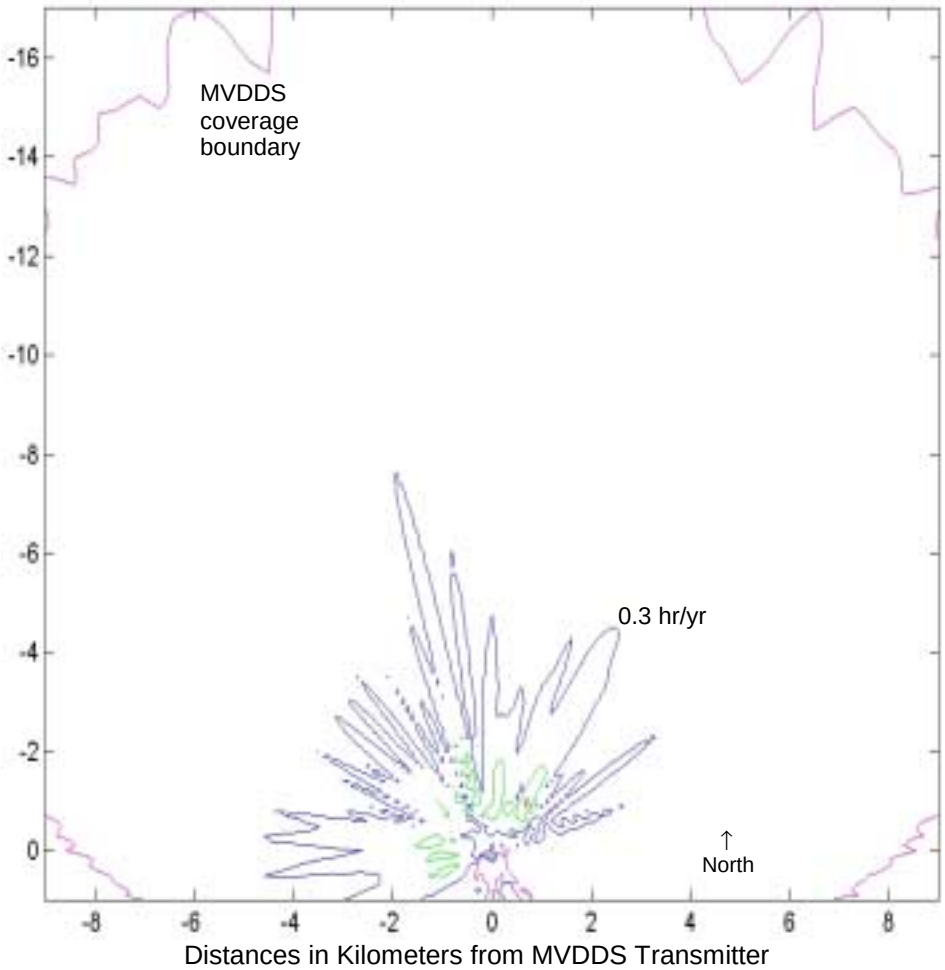

Denver, CO (12.45 GHz)
Maximum absolute increase caused by MVDDS in rain-induced DBS unavailability
Raw MVDDS transmitter power (*not* EIRP): 0 dBm
MVDDS transmitting antenna: Northpoint large sectoral horn
MVDDS transmitting-antenna boresight: **000°** azimuth **(N)**; 0° elevation tilt
MVDDS transmitting antenna 100 meters above horizontal plane
Assumed MVDDS interference scaling factor: 1 dB
Frequency offset between MVDDS and DBS carriers: **7 MHz**
DBS performance measure: VQ6
DBS receiving antenna: 18" single-feed dish
Minimum ratio of DBS EIRP to receiver threshold assumed for each satellite longitude
Baseline rain-induced unavailabilities (*without* MVDDS interference):

101° W: 0.79 hr/yr
110° W: 2.22 hr/yr
119° W: 33.25 hr/yr

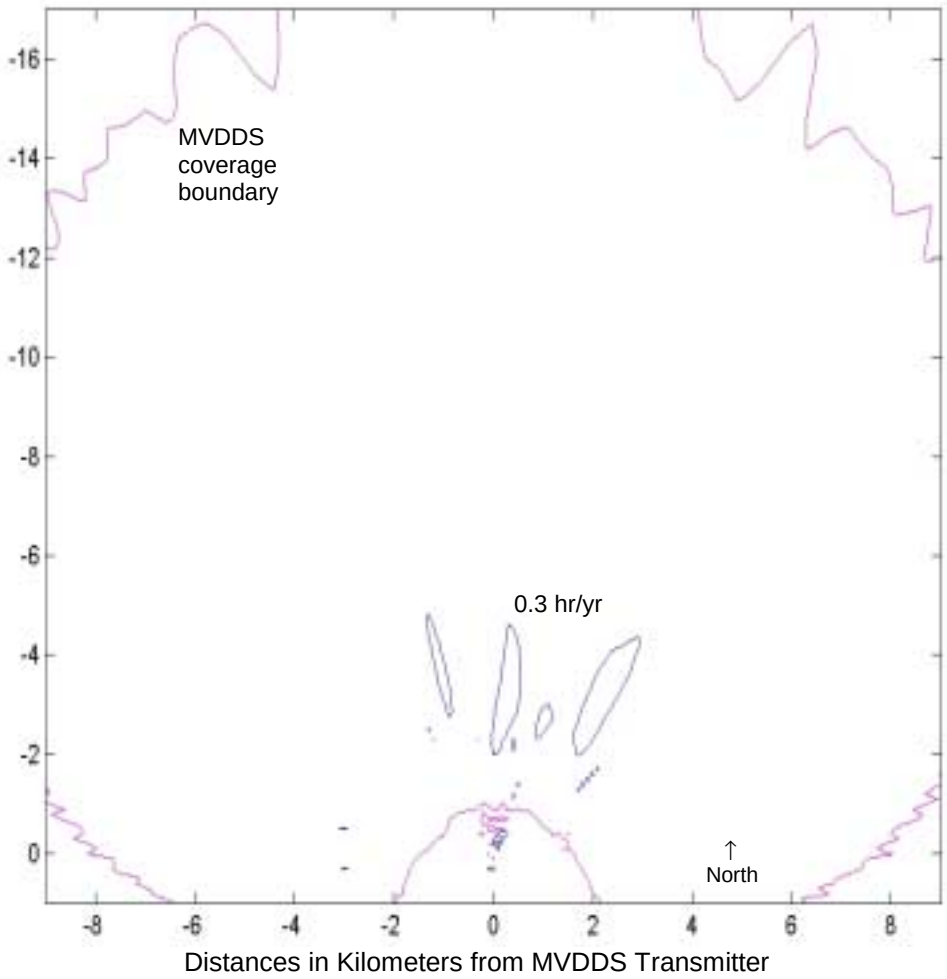

Denver, CO (12.45 GHz)
Maximum absolute increase caused by MVDDS in rain-induced DBS unavailability
Raw MVDDS transmitter power (*not* EIRP): 0 dBm
MVDDS transmitting antenna: Northpoint large sectoral horn
MVDDS transmitting-antenna boresight: **000°** azimuth **(N)**; 0° elevation tilt
MVDDS transmitting antenna **300** meters above horizontal plane
Assumed MVDDS interference scaling factor: 1 dB
Frequency offset between MVDDS and DBS carriers: **7 MHz**
DBS performance measure: VQ6
DBS receiving antenna: 18" single-feed dish
Minimum ratio of DBS EIRP to receiver threshold assumed for each satellite longitude
Baseline rain-induced unavailabilities (*without* MVDDS interference):

101° W:	0.79 hr/yr
110° W:	2.22 hr/yr
119° W:	33.25 hr/yr

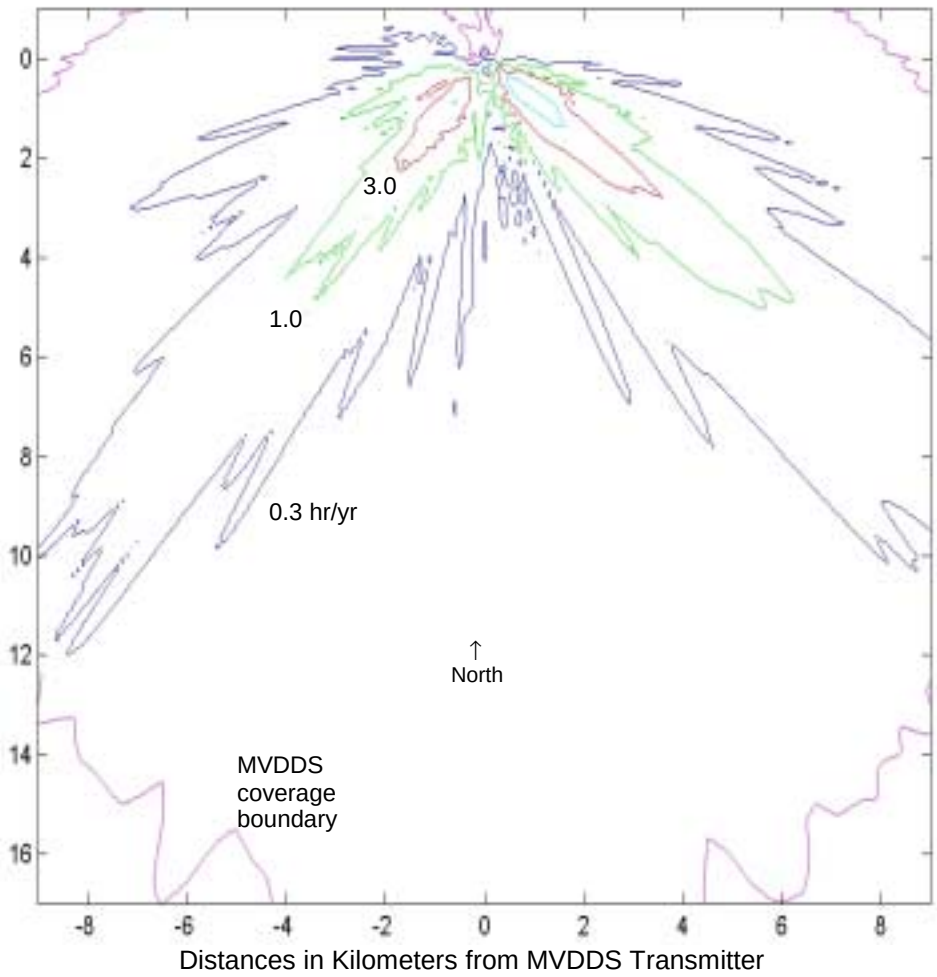

Seattle, WA (12.45 GHz)
Maximum absolute increase caused by MVDDS in rain-induced DBS unavailability
Raw MVDDS transmitter power (*not* EIRP): 0 dBm
MVDDS transmitting antenna: Northpoint large sectoral horn
MVDDS transmitting-antenna boresight: 180° azimuth (S); 0° elevation tilt
MVDDS transmitting antenna 100 meters above horizontal plane
Assumed MVDDS interference scaling factor: 1 dB
Frequency offset between MVDDS and DBS carriers: none
DBS performance measure: VQ6
DBS receiving antenna: 18" single-feed dish
Minimum ratio of DBS EIRP to receiver threshold assumed for each satellite longitude
Baseline rain-induced unavailabilities (*without* MVDDS interference):

101° W:	6.84 hr/yr
110° W:	28.79 hr/yr
119° W:	55.87 hr/yr

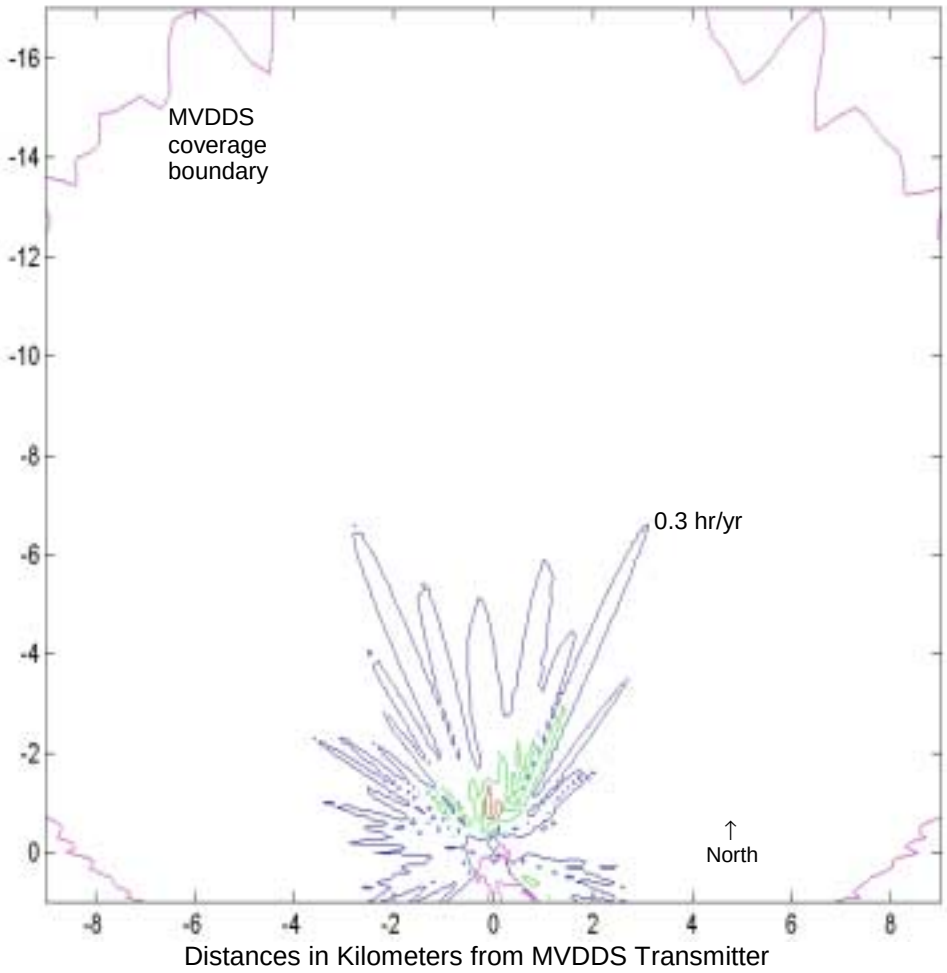

Seattle, WA (12.45 GHz)
Maximum absolute increase caused by MVDDS in rain-induced DBS unavailability
Raw MVDDS transmitter power (*not* EIRP): 0 dBm
MVDDS transmitting antenna: Northpoint large sectoral horn
MVDDS transmitting-antenna boresight: **000°** azimuth **(N)**; 0° elevation tilt
MVDDS transmitting antenna 100 meters above horizontal plane
Assumed MVDDS interference scaling factor: 1 dB
Frequency offset between MVDDS and DBS carriers: **7 MHz**
DBS performance measure: VQ6
DBS receiving antenna: 18" single-feed dish
Minimum ratio of DBS EIRP to receiver threshold assumed for each satellite longitude
Baseline rain-induced unavailabilities (*without* MVDDS interference):

101° W: 6.84 hr/yr
110° W: 28.79 hr/yr
119° W: 55.87 hr/yr

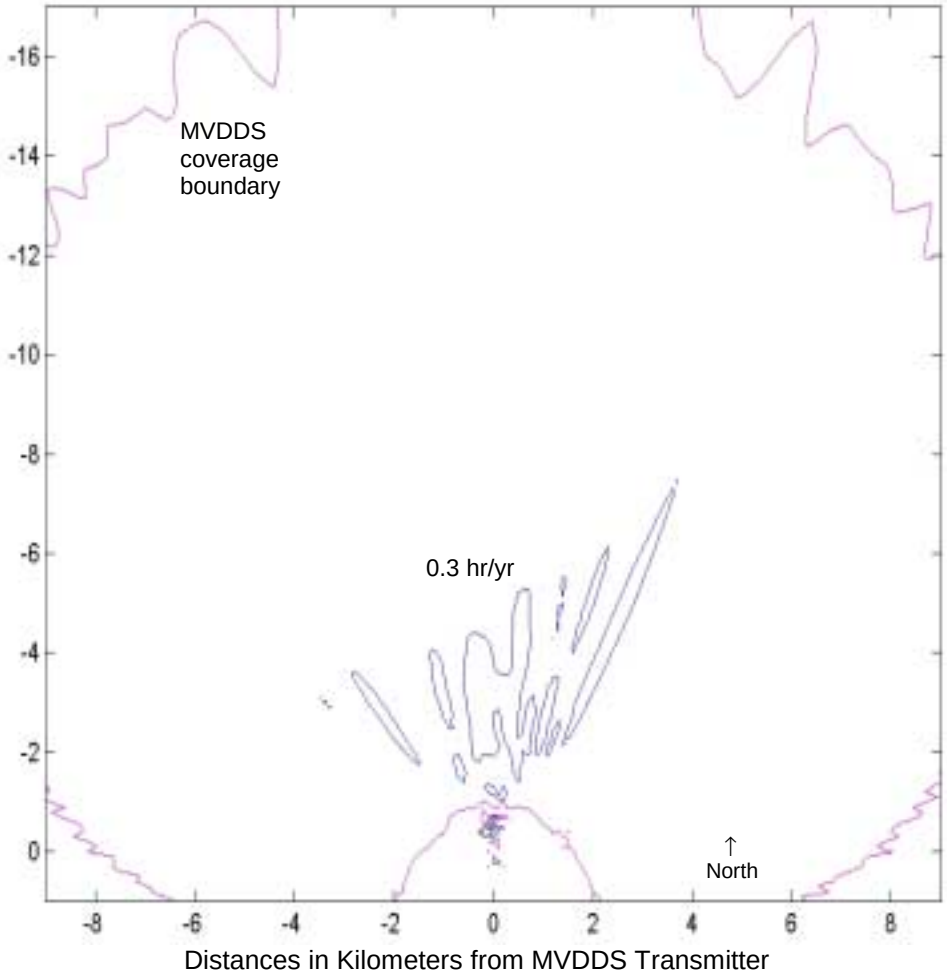

Seattle, WA (12.45 GHz)
Maximum absolute increase caused by MVDDS in rain-induced DBS unavailability
Raw MVDDS transmitter power (*not* EIRP): 0 dBm
MVDDS transmitting antenna: Northpoint large sectoral horn
MVDDS transmitting-antenna boresight: **000°** azimuth **(N)**; 0° elevation tilt
MVDDS transmitting antenna **300** meters above horizontal plane
Assumed MVDDS interference scaling factor: 1 dB
Frequency offset between MVDDS and DBS carriers: **7 MHz**
DBS performance measure: VQ6
DBS receiving antenna: 18" single-feed dish
Minimum ratio of DBS EIRP to receiver threshold assumed for each satellite longitude
Baseline rain-induced unavailabilities (*without* MVDDS interference):

101° W:	6.84 hr/yr
110° W:	28.79 hr/yr
119° W:	55.87 hr/yr

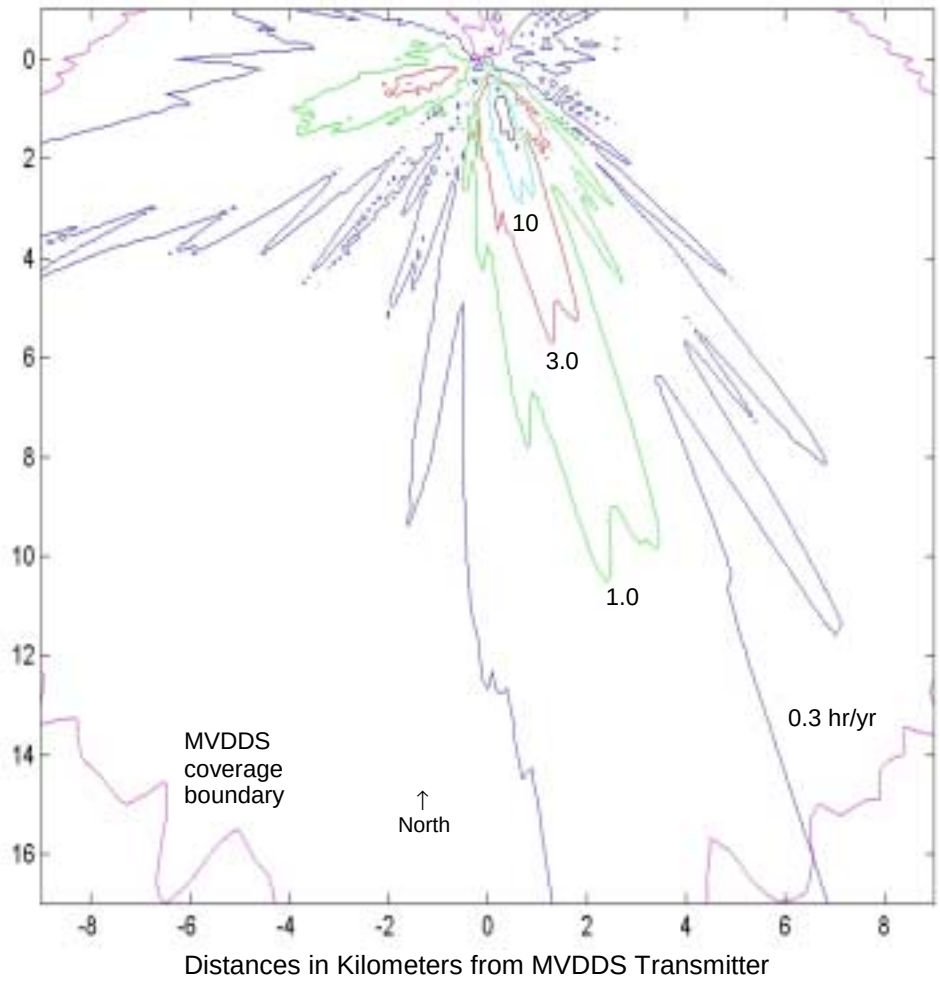

Fargo, ND (12.45 GHz)
Maximum absolute increase caused by MVDDS in rain-induced DBS unavailability
Raw MVDDS transmitter power (*not* EIRP): 0 dBm
MVDDS transmitting antenna: Northpoint large sectoral horn
MVDDS transmitting-antenna boresight: 180° azimuth (S); 0° elevation tilt
MVDDS transmitting antenna 100 meters above horizontal plane
Assumed MVDDS interference scaling factor: 1 dB
Frequency offset between MVDDS and DBS carriers: none
DBS performance measure: VQ6
DBS receiving antenna: 18" single-feed dish
Minimum ratio of DBS EIRP to receiver threshold assumed for each satellite longitude
Baseline rain-induced unavailabilities (*without* MVDDS interference):

101° W: 4.78 hr/yr
110° W: 14.26 hr/yr
119° W: 63.24 hr/yr

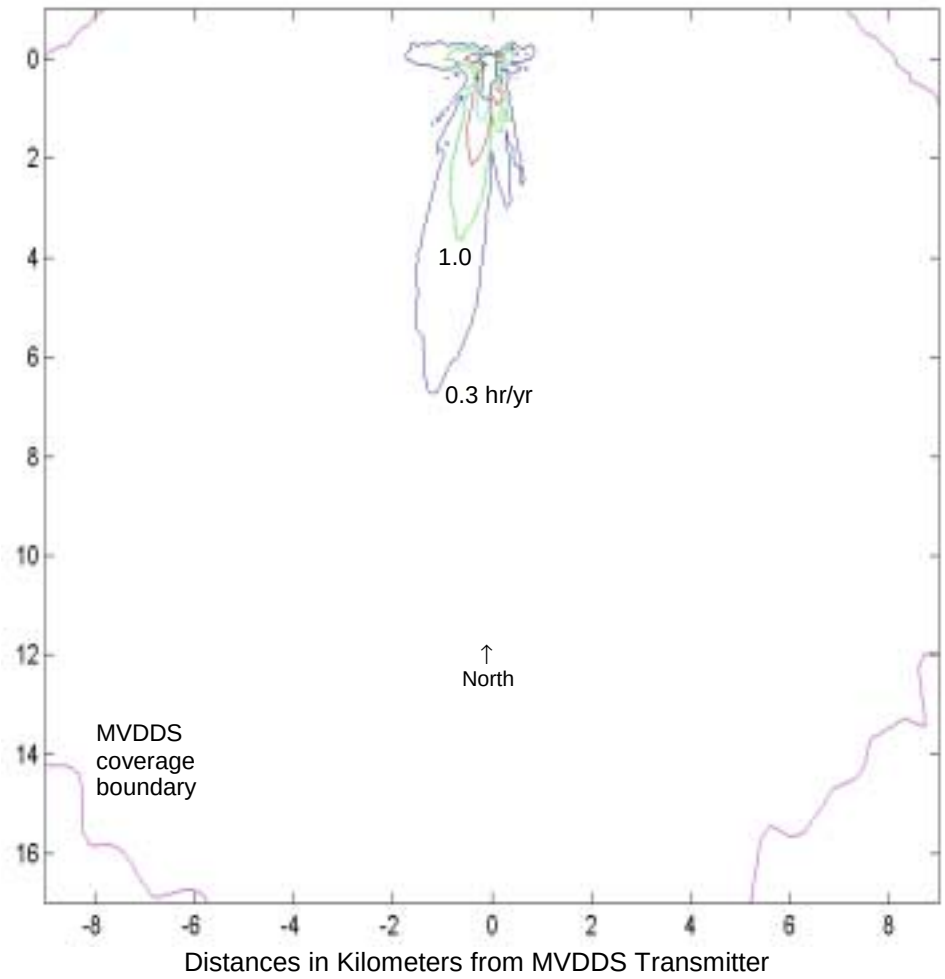

Washington, DC (12.45 GHz)
Maximum absolute increase caused by MVDDS in rain-induced DBS unavailability
Raw MVDDS transmitter power (*not* EIRP): 0 dBm
MVDDS transmitting antenna: **Pegasus** large sectoral horn
MVDDS transmitting-antenna boresight: 180° azimuth (S); 0° elevation tilt
MVDDS transmitting antenna 100 meters above horizontal plane
Assumed MVDDS interference scaling factor: 1 dB
Frequency offset between MVDDS and DBS carriers: none
DBS performance measure: VQ6
DBS receiving antenna: 18" single-feed dish
Minimum ratio of DBS EIRP to receiver threshold assumed for each satellite longitude
Baseline rain-induced unavailabilities (*without* MVDDS interference):

101° W:	2.17 hr/yr
110° W:	3.88 hr/yr
119° W:	24.56 hr/yr

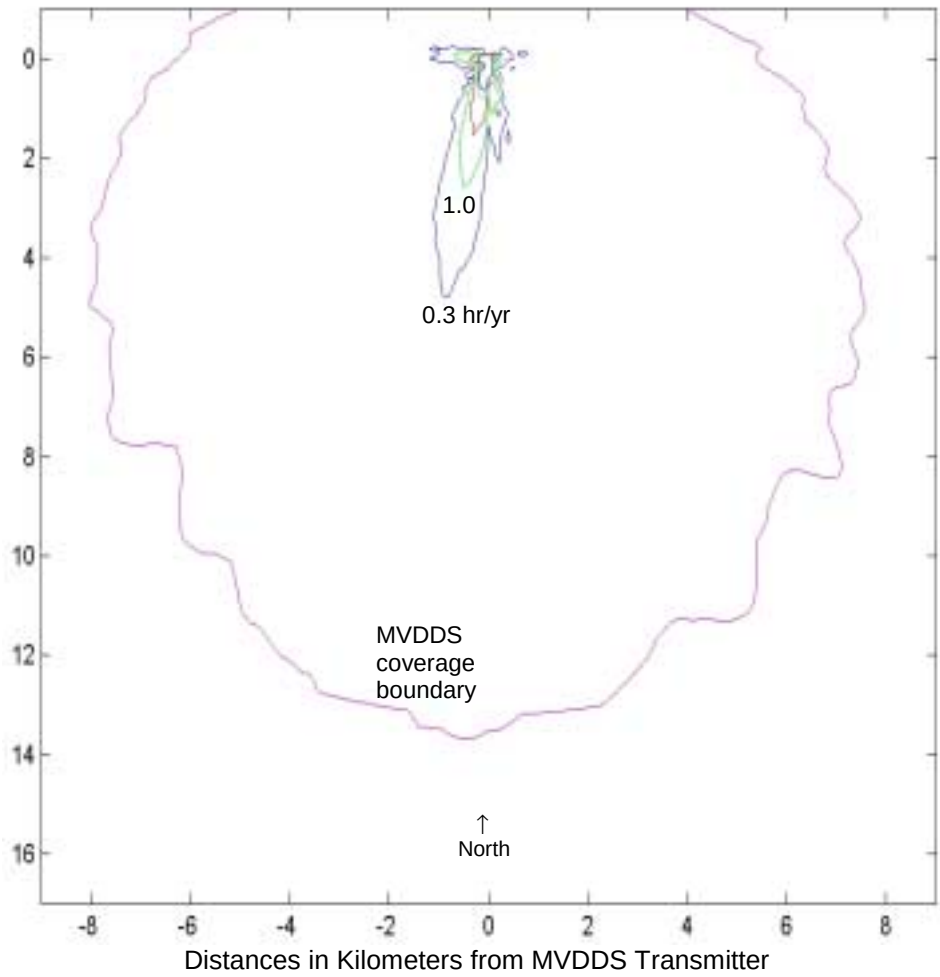

Washington, DC (12.45 GHz)
Maximum absolute increase caused by MVDDS in rain-induced DBS unavailability
Raw MVDDS transmitter power (*not* EIRP): 0 dBm
MVDDS transmitting antenna: **Pegasus small** sectoral horn
MVDDS transmitting-antenna boresight: 180° azimuth (S); 0° elevation tilt
MVDDS transmitting antenna 100 meters above horizontal plane
Assumed MVDDS interference scaling factor: 1 dB
Frequency offset between MVDDS and DBS carriers: none
DBS performance measure: VQ6
DBS receiving antenna: 18" single-feed dish
Minimum ratio of DBS EIRP to receiver threshold assumed for each satellite longitude
Baseline rain-induced unavailabilities (*without* MVDDS interference):

101° W:	2.17 hr/yr
110° W:	3.88 hr/yr
119° W:	24.56 hr/yr

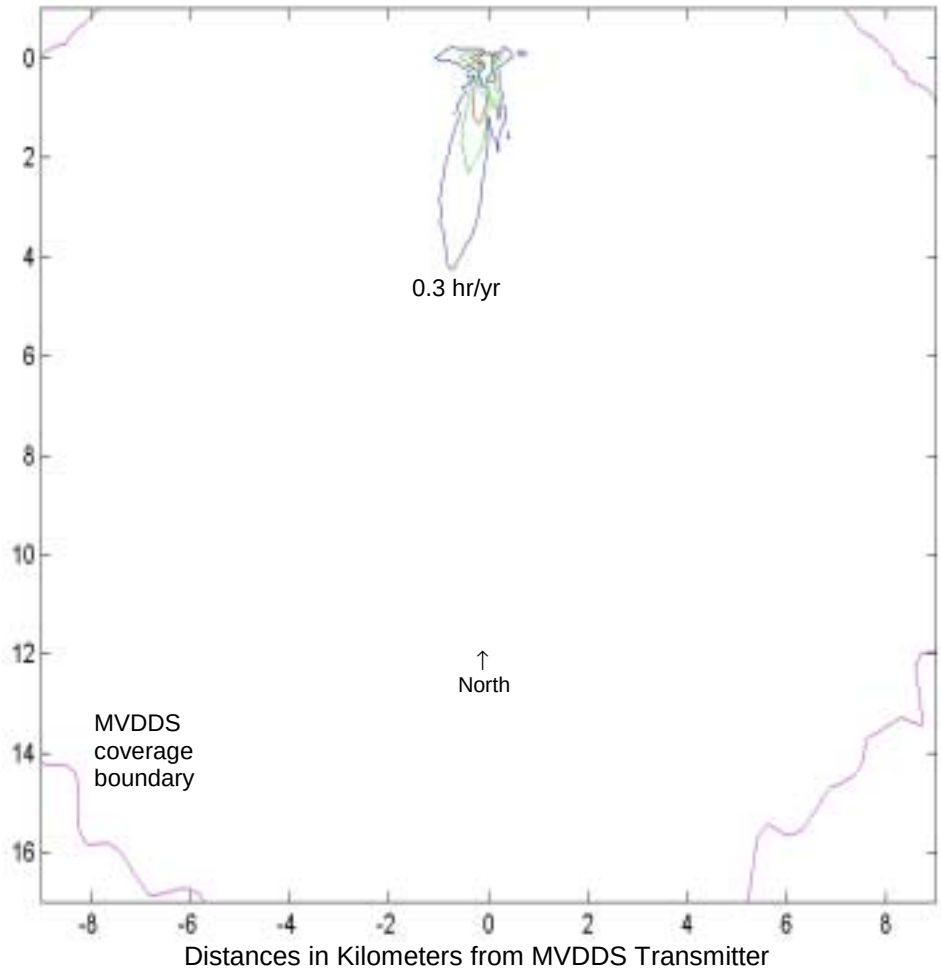

Washington, DC (12.45 GHz)
Maximum absolute increase caused by MVDDS in rain-induced DBS unavailability
Raw MVDDS transmitter power (*not* EIRP): **-4 dBm**
MVDDS transmitting antenna: **Pegasus** large sectoral horn
MVDDS transmitting-antenna boresight: 180° azimuth (S); 0° elevation tilt
MVDDS transmitting antenna 100 meters above horizontal plane
Assumed MVDDS interference scaling factor: 1 dB
Frequency offset between MVDDS and DBS carriers: none
DBS performance measure: VQ6
DBS receiving antenna: 18" single-feed dish
Minimum ratio of DBS EIRP to receiver threshold assumed for each satellite longitude
Baseline rain-induced unavailabilities (*without* MVDDS interference):

101° W:	2.17 hr/yr
110° W:	3.88 hr/yr
119° W:	24.56 hr/yr

Note: Above coverage boundary assumes G/T = **15.2 dB** rather than the usual 11.22 dB.

Glossary

AM	amplitude modulation
AUT	antenna under test
A/V	audiovisual
AWGN	additive White Gaussian noise
AWS	arbitrary waveform synthesizer
BER	bit error rate
BW	bandwidth
C/N	carrier to noise ratio
C/N + I	carrier to noise plus interference ratio
dB	decibel
dBi	db referenced to the gain of an isotropic antenna
dBil	dBi linear
dBic	dBi circular
DBS	Direct Broadcast Satellite
EIRP	effective isotropically radiated power
FCC	Federal Communications Commission
FY	Fiscal Year
GHz	gigahertz
hr/yr	hours per year
IF	intermediate frequency
IMUX	input multiplexer
ITU	International Telecommunications Union
km	kilometer
LHCP	left-hand circular polarization
LNB	low noise block converter
MHz	megahertz
MPEG	Motion Picture Experts Group

MVDDS	Multichannel Video Distribution and Data Service
NPRM	Notice of Proposed Rulemaking
NSI	Nearfield Systems Incorporated
OMUX	output multiplexer
PFD	power flux density
PM	phase modulation
QEF	quasi-error free
QPSK	quadrature phase shift keying
RHCP	right-hand circular polarization
RMS	root mean square
R&O	Report and Order
SMA	sub-miniature A
SPW™	Signal Processing Workstation
TWT	traveling wave tube
TWTA	TWT amplifier
U.S.	United States